UNIVERSITY OF SOUTHAMPTON

QUANTUM CHROMODYNAMICS AND THE NUCLEON LONGITUDINAL STRUCTURE FUNCTION

by

Stephen N Coulson

A Thesis submitted for the degree of

Doctor of Philosophy

Department of Physics

December 1981

CONTENTS

UNIVERSITY OF SOUTHAMPTON

ABSTRACT

FACULTY OF SCIENCE

PHYSICS

Doctor of Philosophy

QUANTUM CHROMODYNAMICS AND THE NUCLEON LONGITUDINAL STRUCTURE FUNCTION

by Stephen Norman Coulson

The phenomenon of asymptotic freedom together with the theoretical tools of the operator product expansion and renormalisation group allow a systematic and reliable application of perturbative quantum chromodynamics (Q.C.D.) to deep inelastic lepton-hadron scattering. In particular one can study the ratio of the longitudinal to transverse cross-section, $R = \sigma_L/\sigma_T$. Leading order Q.C.D. predictions for R are concluded not to give a satisfactory description of the current data at large $X > 0{\cdot}5$.

Here we extend this perturbative analysis to include the next to leading order, $O(g^4)$, Q.C.D. contributions. This involves calculating the fourth order contribution to the flavour non-singlet longitudinal coefficient function that appears in the light cone expansion. A technique that regulates the spurious mass-singularities encountered in a consistent manner is discussed, and its use justified through examples utilising the optical theorem.

The $O(\bar{g}^4 MS)$ Q.C.D. expression for the moments of the flavour non-singlet longitudinal structure function is then inverted using a simple technique, allowing a plot of the next to leading order Q.C.D. corrections to the ratio R . Such corrections are found to be small ($\sim 12\%$ for $X > 0{\cdot}5$) and it is concluded that to this order of perturbation theory a discrepancy between theory and experiment still exists.

ACKNOWLEDGEMENTS

Firstly, I would like to thank Ralph Ecclestone with whom much of this work was done in collaboration. His diligence and care have proved a great asset. I extend these thanks to Professor K J Barnes, together with all the members of the Theory Group who help make Southampton a friendly and stimulating place for research. I am particularly grateful to Drs C Cornelius and D Storey for the generous advice given concerning the numerical problems in this thesis. I also wish to thank Dr R G Roberts for supplying the latest data of the CDHS collaboration at CERN, and Dr D W Duke for his kind co-operation in sending advance notification of his results. Many thanks go to Maria Hayter for speedy and efficient typing.

Finally it is a pleasure to especially thank my supervisor, Dr C T C Sachrajda, for originally suggesting this problem and his continued advice and encouragement towards the completion of this thesis.

Financial support for this work from a Science Research Council studentship is gratefully acknowledged.

INTRODUCTION

0.1 Early Experimental Situation

Photons are ideally suited as tools with which to probe hadronic structure. Their interaction with matter, Quantum Electrodynamics, is one of the most successful physical theories in existence. With the inclusion of the order α^4 radiative corrections the theoretical prediction for the anomalous magnetic moment of the electron [0.1] agrees with the experimental value to one part in 10^7. By using virtual spacelike photons exchanged in electron-hadron scattering we can vary both the 4-momentum transfer, $q^2 (<0)$, and the energy exchanged ν. Large magnetic spectrometers identify and track the scattered electron allowing an accurate determination of these variables.

Early indications of nucleon structure came with the measurement of their magnetic moments. The Dirac theory of point-like spin $\frac{1}{2}$ massive nucleons carrying one unit of electric charge gives

$$\mu_{DIRAC} = \frac{e\hbar}{2Mc} = 1 \text{ n.m.} \qquad \text{(nuclear magneton)} \qquad (0.1)$$

Thus for the proton and neutron

proton : $\mu_{DIRAC} = +1.0$ n.m. $\qquad \mu_{expt.} = +2.79$ n.m.

neutron : $\mu_{DIRAC} = 0$ n.m. $\qquad \mu_{expt.} = -1.91$ n.m.

to be compared with the experimental values as indicated. The anomalous moments indicate that the nucleon has spatial structure. This conclusion was confirmed by experiments at SLAC and DESY measuring

elastic electron-proton scattering [0.2]. The experimental cross-section exhibited a deviation from that predicted by the Dirac theory of an electron scattering off a point proton of spin $\frac{1}{2}$ and magnetic moment $\frac{e\hbar}{2Mc}$.

In the one photon exchange approximation,

$$\left(\frac{d\sigma}{d\Omega}\right)_{DIRAC} = \left(\frac{d\sigma}{d\Omega}\right)_{MOTT} \left\{ 1 + \frac{Q^2}{2M^2} \tan^2\left(\frac{\theta}{2}\right) \right\} \qquad (0.2)$$

where $Q^2 = -q^2$, and $\left(\frac{d\sigma}{d\Omega}\right)_{MOTT}$ is the formula for the scattering of relativistic electrons off spinless point-like protons. The second term in the curly brackets of Eq. (0.2) is the "essential complication" of proton spin, and is called magnetic scattering. It dominates the cross section for large angle and high momentum transfer scattering.

In order to fit the data and take into account the spatial structure of the proton, electric and magentic form factors were introduced by Rosenbluth [0.3].

$$\left(\frac{d\sigma}{d\Omega}\right) = \left(\frac{d\sigma}{d\Omega}\right)_{MOTT} \left\{ \left(\frac{G_E^2 + \tau G_M^2}{1+\tau}\right) + \tau . 2 G_M^2 \tan^2\left(\frac{\theta}{2}\right) \right\} \qquad (0.3)$$

where

$$\tau = \frac{Q^2}{4M^2} \qquad (0.4)$$

with form factors : electric $G_E(Q^2)$

$$\begin{aligned} G_E^p(0) &= +1 \\ G_E^N(0) &= 0 \end{aligned} \qquad (0.5)$$

$$\text{magnetic } G_m(Q^2): \quad G_m^P(0) = \mu_P = +2.79$$
$$G_m^N(0) = \mu_N = -1.91 \qquad (0.6)$$

The form factors are found experimentally to obey the simple approximate relation

$$G_E^N(Q^2) = 0 \qquad (0.7)$$

$$G_E^P(Q^2) = \frac{G_M^P(Q^2)}{|\mu_P|} = \frac{G_M^N(Q^2)}{|\mu_N|} = G(Q^2) \qquad (0.8)$$

where

$$G(Q^2) = \left(1 + \frac{Q^2}{\Lambda^2}\right)^{-2}, \quad \Lambda^2 = 0.71 \text{ Gev}^2 \qquad (0.9)$$

over the range $0 \leq Q^2 \leq 25 \text{ Gev}^2$.

$G(Q^2)$ effectively measures the probability that the proton will recoil elastically, ie. that it will hold together under the momentum transfer Q^2. At $Q^2 = 25 \text{ Gev}^2$ this probability has fallen from 1 to about 10^{-6}. The ratio of actual to point-like elastic cross sections has a very strong dependence on Q^2; it falls roughly as Q^{-6}.

This is in complete contrast to what is observed in inelastic electron-proton scattering [0.4, 0.5].

For low Q^2, there are several peaks in the cross-section corresponding to the production of pion-nucleon resonances. The exclusive quasi-elastic cross section

$$e^- + p \longrightarrow e^- + N^* \begin{pmatrix} 1238\ \text{Mev} \\ 1512 \\ 1688 \\ \vdots \end{pmatrix} \longrightarrow \begin{matrix} \pi^\circ + p \\ \pi^+ + n \end{matrix} \qquad (0.10)$$

behaves much the same as ep elastic scattering. In fact the ratio of the two tends to a constant for $Q^2 > 2\ \text{Gev}^2$.

However, for inclusive ep scattering (in which no attention is paid to the final state hadrons), the cross-section shows no further structure beyond the elastic and quasi-elastic peaks.
In this region, for high Q^2, the proton is being excited into the continuum instead of undergoing transitions to well defined excited states. Here the ratio of actual to point-like cross sections is large and only weakly Q^2 dependent . Analagous to form factors, inelastic structure functions are introduced to parameterize the cross-section. They are now functions of two variables Q^2 and ν (the energy transfer) due to the lack of constraint on the final state hadronic mass. (For a review of elastic and inelastic scattering kinematics, see Fig. 0.1).

Virtual photons, such as those exchanged in electron-proton scattering, are not the only tools available to probe the deep structure of hadrons. One can also use the weak gauge bosons $W^\pm, Z^\circ$ exchanged in neutrino (or anti-neutrino) - hadron scattering together with the 'standard' model [0.6, 0.7, 0.8] of electro-weak interactions incorporating quarks. We shall, however, be dealing exclusively with electromagnetic processes, and so turn to a brief discussion of deep inelastic electroproduction.

Fig 0.1 Kinematics

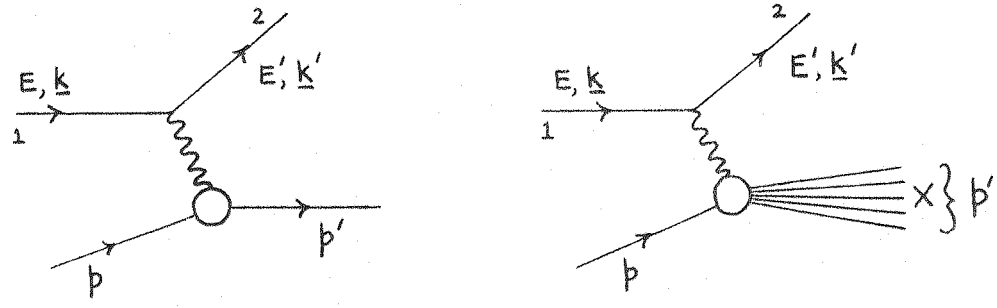

LAB frame, target proton at rest $p^\mu = (m, 0)$

$p.q = M(E-E') \equiv \nu$

$q^\mu = (E-E', \underline{k}-\underline{k}')$

$q^2 = -2kk'(1-\cos\theta)$

(neglecting lepton masses)

$-q^2 = Q^2 = 4kk'\sin^2\left(\frac{\theta}{2}\right)$

$p^2 = p'^2 = M^2 = (p+q)^2$

$\left.\begin{matrix} -q^2 \\ p.q \end{matrix}\right\} \to \infty$

$2p.q = -q^2$

$\underline{2\nu = Q^2}$

Elastic condition, one independent variable.

$G(Q^2)$ form factors

(a)

ELASTIC SCATTERING

$p.q = M(E-E') \equiv \nu$

$p^2 = M^2$

$-q^2 = Q^2 = 4kk'\sin^2\left(\frac{\theta}{2}\right)$

$p'^2 = W^2$ unknown variable

$= (p+q)^2$

$\underline{2\nu = W^2 - M^2 + Q^2}$

two independent variables

$W(\nu, Q^2)$ structure functions

$X = -\frac{q^2}{2\nu}$

$p'^2 = W^2 = (p+q)^2 \geq 0$

$2p.q(1-X) \geq 0$

$\underline{0 \leq X \leq 1}$ Range of X

(b)

INELASTIC SCATTERING

0.2 Deep Inelastic Electro-production

The inelastic ep scattering amplitude, A, (Fig. 0.1(b)) may be written as

$$A = \bar{u}_2(k',s')\gamma_\mu u_1(k,s)\frac{e^2}{q^2}\langle X|J_\mu(0)|p\rangle\,\delta^4(p+q-p') \qquad (0.11)$$

where $\langle X|J_\mu(0)|p\rangle$ is the matrix element of the hadronic current about which nothing specific can be said until we formulate a theory of hadron dynamics.

$$AA^\dagger = (\bar{u}_2\gamma_\mu u_1)^\dagger(\bar{u}_2\gamma_\nu u_1)\left(\frac{e^2}{q^2}\right)^2 \cdot$$

$$\cdot \sum_X \langle p|J_\mu(0)|X\rangle\langle X|J_\nu(0)|p\rangle \cdot \delta^4(p+q-p') \qquad (0.12)$$

for the unpolarised cross-section, summing over electron and proton spins

$$AA^\dagger = \left(\frac{e^2}{q^2}\right)^2 4\pi \cdot \frac{1}{2} \cdot L^{\mu\nu}W_{\mu\nu} \qquad (0.13)$$

where $L^{\mu\nu}$ is the lepton tensor

$$L^{\mu\nu} = \frac{1}{2}\sum_{\text{pol.}}(\gamma_\mu u_2\bar{u}_2\gamma_\nu u_1\bar{u}_1) \qquad (0.14)$$

(neglecting lepton masses)

$$= \frac{1}{2}\cdot\frac{1}{4m^2}\,\mathrm{Tr}[\gamma_\mu \not{k}'\gamma_\nu \not{k}] \qquad (0.15)$$

$$= \frac{1}{4m^2}\cdot 2\left[k'^\mu k^\nu + k'^\nu k^\mu - k\cdot k' g^{\mu\nu}\right] \qquad (0.16)$$

and $W_{\mu\nu}$ is the hadronic tensor

$$W_{\mu\nu} = \sum_{\text{pol.}} \frac{1}{4\pi} \sum_{X} \langle p | J_\mu(0) | X \rangle \langle X | J_\nu(0) | p \rangle \, \delta^4(p+q-p') \qquad (0.17)$$

$$= \frac{1}{4\pi} \int d^4z \, e^{iqz} \langle p | \left[J_\nu^\dagger(z), J_\mu(0) \right] | p \rangle_{\text{spin av.}} \qquad (0.18)$$

On the general grounds of Lorentz invariance and Current Conservation ($q^\mu W_{\mu\nu} = q^\nu W_{\mu\nu} = 0$)

$$W_{\mu\nu} = \left(-g_{\mu\nu} + \frac{q_\mu q_\nu}{q^2} \right) W_1(\nu, Q^2) + \left(p_\mu - \frac{p.q}{q^2} q_\mu \right) \left(p_\nu - \frac{p.q}{q^2} q_\nu \right) W_2(\nu, Q^2) \qquad (0.19)$$

for electroproduction, with independent structure functions $W_{1,2}(\nu, Q^2)$.

In the deep inelastic region $\quad Q^2 = -q^2 \to \infty$

$$\nu = p.q \to \infty \qquad (0.20)$$

But $\quad X = \frac{Q^2}{2\nu}$ $\quad$ kept fixed

then, neglecting lepton masses, and choosing the LAB frame $p^\mu = (M, \underline{0})$ to evaluate the kinematics

$$AA^\dagger = \frac{e^4}{q^4} \frac{4\pi}{4m^2} 2EE' \left[M^2 \cos^2\left(\frac{\theta}{2}\right) W_2 + 2\sin^2\left(\frac{\theta}{2}\right) W_1 \right] \qquad (0.21)$$

Thus, the cross-section:-

$$d\sigma = \frac{1}{4\sqrt{(p.k)^2 - k^2 p^2}} 2m \, 2M \left[AA^\dagger \right] \frac{d^3k'}{(2\pi)^3} \frac{m}{E'} \qquad (0.22)$$

where

$$d^3k' = d\Omega' . dE' . E'^2$$
$$\sqrt{(p.k)^2 - k^2p^2} \approx ME \qquad (0.23)$$

$$\frac{d\sigma}{d\Omega' dE'} = \frac{\alpha^2}{4E^2 \sin^4\left(\frac{\theta}{2}\right)} \left[M^2 \cos^2\left(\frac{\theta}{2}\right) W_2 + 2\sin^2\left(\frac{\theta}{2}\right) W_1 \right] \qquad (0.24)$$

with

$$\alpha = \frac{e^2}{4\pi} \qquad (0.25)$$

or, writing the differential cross-section as $\frac{d\sigma}{dQ^2 d\bar{\nu}}$

where Q^2 = 4-momentum transfer

$\bar{\nu}$ = energy transfer = $E - E' = \frac{\nu}{M}$

$$\frac{d\sigma}{dQ^2 d\bar{\nu}} = \frac{\pi\alpha^2}{4E^2 \sin^4\left(\frac{\theta}{2}\right)} \frac{1}{EE'} \left[M^2 \cos^2\left(\frac{\theta}{2}\right) W_2 + 2\sin^2\left(\frac{\theta}{2}\right) W_1 \right] \qquad (0.26)$$

Relatively large errors are produced when extracting $W_1(\nu, Q^2)$ from the angular distribution of the data due to the scarcity of events at appreciable values of $\sin^2\left(\frac{\theta}{2}\right)$. However, both W_1 and W_2 can be determined and exhibit a remarkable phenomenon in the deep inelastic region. The structure functions, implicitly functions of two variables Q^2 and ν, are said to apprximately scale. They become a function of one variable $X = \frac{Q^2}{2\nu}$ in the limit $Q^2, \nu \to \infty$, but $X = \frac{Q^2}{2\nu}$ fixed.

i.e. $$M W_1(\nu, Q^2) \longrightarrow F_1(X) \qquad (0.27)$$

$$M\nu W_2(\nu, Q^2) \xrightarrow[\substack{Q^2, \nu \to \infty \\ X = \frac{Q^2}{2\nu} \text{ fixed}}]{} F_2(X) \qquad (0.28)$$

Furthermore, empirically

$$F_2(x) \approx 2x F_1(x) \tag{0.29}$$

This behaviour had been predicted by Bjorken [0.9] who considered matrix elements of electromagnetic current commutators at infinite nucleon momentum.

It was out of desire to understand scaling that the simple intuitive framework of the parton model was proposed.

CHAPTER ONE

HADRONS AT SHORT DISTANCES

1.1 Pre-theory : the Parton Model in Deep Inelastic Scattering

In the naive Parton Model introduced by Feynman [1.1], the nucleon is seen as a collection of free point-like constituents called partons. In the Bjorken limit, the lepton-nucleon centre of momentum frame is essentially the frame in which the nucleon has infinite momentum. In this frame the nucleon charge distribution is Lorentz contracted to a disc, and parton motion time dilated. The large momentum transfer 'freezes' any parton interaction and so the virtual photon sees the collection as free. This is the essence of the Impulse Approximation [1.2]. The assumptions involved in this approximation can be justified to some extent by a crude computation in the infinite momentum frame (see Fig. 1.1).

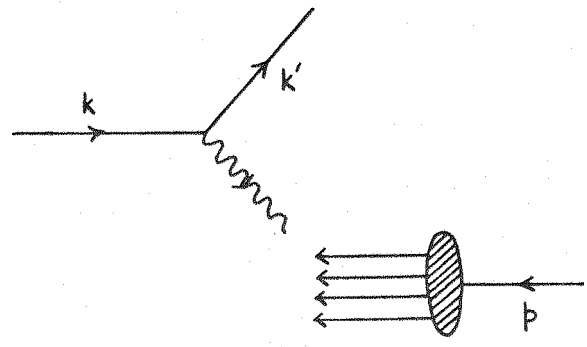

Fig. 1.1 Interpretation of lepton-nucleon scattering via the naive parton model.

Choose the frame

$$p = \left(P + \frac{M^2}{2P} , \; 0 , \; 0 , \; P \right) \tag{1.1}$$

$$q = \left(\frac{2\nu - Q^2}{4P} , \; \underline{q}_\perp , \; - \frac{2\nu + Q^2}{4P} \right) \tag{1.2}$$

and take $P \to \infty$

Thus

$$p^2 = M^2 + O\left(\frac{1}{P^2}\right) \tag{1.3}$$

$$q^2 = - q_\perp^2 + O\left(\frac{1}{P^2}\right) \qquad \text{(spacelike)} \tag{1.4}$$

$$p.q = \nu + O\left(\frac{1}{P^2}\right) \tag{1.5}$$

and so satisfy all the criteria of Fig. 0.1(b) to leading order in P.

We can now compare the typical time τ resolved by the virtual photon with the lifetime T of the intermediate parton states as calculated crudely in old-fashioned perturbation theory.

$$T \approx \frac{1}{\Delta E} = \frac{1}{\sum_i E_i - E_p} \tag{1.6}$$

where E_i is the energy of the ith parton and E_p the proton energy.

If the ith parton has a fraction η_i of the longitudinal momentum P of the proton, mass μ_i and transverse momentum $\underline{p}_{\perp i}$,

$$E_i = \sqrt{(\eta_i P)^2 + p_{\perp i}^2 + \mu_i^2} \tag{1.7}$$

where

$$0 < \eta_i < 1 \tag{1.8}$$

$$\sum_i \eta_i = 1 \tag{1.9}$$

$$\sum_i \underline{p}_{\perp i} = 0 \tag{1.10}$$

and the 4-momentum is written

$$p_i = \left(\eta_i P + \frac{\mu_i^2 + p_{\perp i}^2}{2\eta_i P} , \ \underline{p}_{\perp i} , \ \eta_i P \right) \tag{1.11}$$

Summing over parton energies

$$\sum_i E_i = P + \sum_i \left(\frac{\mu_i^2 + p_{\perp i}^2}{2\eta_i P} \right) = E_p + O\left(\frac{1}{P}\right) \tag{1.12}$$

substituting into Eq. (1.6)

$$T \approx \frac{2P}{\sum_i \left(\frac{\mu_i^2 + p_{\perp i}^2}{\eta_i} \right) - M^2} \tag{1.13}$$

The resolving time of the virtual photon, τ

$$\tau \sim \frac{1}{q^0} = \frac{4P}{2\nu - Q^2} \tag{1.14}$$

Thus for

$$T \gg \tau \tag{1.15}$$

then

$$W^2 = M^2 + 2\nu - Q^2 \gg m^2_{eff.} - M^2 \qquad (1.16)$$

with

$$m^2_{eff.} = 2\sum_i \left(\frac{\mu_i^2 + p_{\perp i}^2}{\eta_i} \right) \qquad (1.17)$$

so providing the partons are light and have small finite transverse momenta, the Impulse approximation holds through Eq. (1.16) at current W^2 as measured by SLAC. The virtual photon resolves the proton on a time scale small enough for the partons to appear to be non-interacting, i.e. free.

It is then assumed that the lepton scatters elastically and incoherently from one of the point-like partons. This last assumption can be justified by similar arguments [1.3], and also leads to an identification of the scaling variable X with the fraction of nucleon longitudinal momentum carried by the struck parton, η as follows

$$X = \frac{Q^2}{2\nu} = \eta \qquad (1.18)$$

Considering elastic lepton-parton scattering as in Fig. 1.2

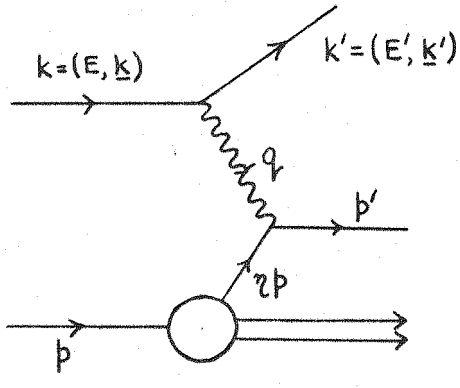

Fig. 1.2 Elastic lepton-parton scattering.

In the phase space integral for this process there is a delta-function which puts the final state parton on shell

$$\delta(p'^2 - m^2) \tag{1.19}$$

by momentum conservation, $p' = \eta p + q$ (1.20)

$$\longrightarrow \quad \delta((\eta p + q)^2 - m^2) \tag{1.21}$$

$$= \delta(\eta^2 M^2 + q^2 + 2\eta p.q - m^2) \tag{1.22}$$

$$= \delta(2\nu(\eta - x) + \eta^2 M^2 - m^2) \tag{1.23}$$

in the Bjorken limit $\nu \to \infty$ the proton and parton mass may be ignored inside the delta-function argument with the result

$$\longrightarrow \quad \frac{1}{2\nu}\,\delta(\eta - x) \tag{1.24}$$

We can now quote the result of calculating Fig. 1.2 for the case of electroproduction. This is the Dirac theory prediction for electrons scattering off point-like spin $\frac{1}{2}$ particles of mass m_i and charge $e_i e$ (assuming partons carry spin $\frac{1}{2}$)

$$\frac{d\sigma^i}{dQ^2 d\bar{\nu}} = \frac{\pi\alpha^2}{4E^2 \sin^4\left(\frac{\theta}{2}\right)} \frac{1}{EE'} \left[e_i^2 \cos^2\left(\frac{\theta}{2}\right) + e_i^2 \frac{Q^2}{4m_i^2} 2\sin^2\left(\frac{\theta}{2}\right)\right] \delta\left(\bar{\nu} - \frac{Q^2}{2m_i}\right) \tag{1.25}$$

where $\bar{\nu} = \dfrac{\eta p.q}{m_i}$ energy transfer as measured in the LAB frame. It is not a free variable but is constrained through the elastic scattering condition in the delta-function of Eq. (1.25). The partons

are assumed to have no intrinsic transverse momentum $p_\perp$, and a γ_μ coupling to the photon (no structure).

This is to be compared with the result for inelastic scattering of electrons off a nucleon (Eq. 0.26).

$$\frac{d\sigma}{dQ^2 d\bar{\nu}} = \frac{\pi\alpha^2}{4E^2 \sin^4\left(\frac{\theta}{2}\right)} \frac{1}{EE'} \left[M^2 \cos^2\left(\frac{\theta}{2}\right) W_2 + 2\sin^2\left(\frac{\theta}{2}\right) W_1 \right] \tag{1.26}$$

To obtain the total electron-nucleon cross-section from Eq. (1.25) it is necessary to sum over parton types, $\sum_i$, found in the nucleon and integrate the fraction of the nucleon longitudinal momentum carried by the parton, η, throughout the allowed range ($0 \leq \eta \leq 1$), weighting the cross-section with the probability for finding a parton of type i and momentum ηp, $f^i(\eta)$.

Recalling that $\eta = X$, the structure functions can be identified from Eq. (1.25) the Bjorken limit as

$$W_2(\bar{\nu}, Q^2) = \sum_i \frac{e_i^2}{M^2} \int_0^1 dX\, f^i(X) \frac{X}{\bar{\nu}} \delta\left(X - \frac{Q^2}{2M\bar{\nu}}\right) \tag{1.27}$$

$$W_1(\bar{\nu}, Q^2) = \sum_i \frac{e_i^2}{M^2} \int_0^1 dX\, f^i(X) \frac{M}{2\bar{\nu}} \delta\left(X - \frac{Q^2}{2M\bar{\nu}}\right) \tag{1.28}$$

or writing in terms of $\nu = M\bar{\nu} = p.q$, and using the delta function to do the X integration

$$\nu W_2(\nu, Q^2) = \sum_i \frac{e_i^2}{M} X f^i(X) \tag{1.29}$$

$$W_1(\nu, Q^2) = \sum_i \frac{e_i^2}{M} \frac{1}{2} f^i(X) \tag{1.30}$$

where

$$X = \frac{Q^2}{2\nu} \tag{1.31}$$

Thus in the Bjorken limit, the structure functions scale exactly

$$M\nu W_2(\nu, Q^2) \longrightarrow F_2(X) \tag{1.32}$$

$$MW_1(\nu, Q^2) \longrightarrow F_1(X) \tag{1.33}$$

$Q^2, \nu \to \infty$
$X = \frac{Q^2}{2\nu}$ fixed

where

$$F_2(X) = 2XF_1(X) \tag{1.34}$$

This last statement is particular to our choice of scattering off spin $\frac{1}{2}$ partons, [1.4] and at presently accessible Q^2 is approximately experimentally verified. If the charged partons are exclusively spin $\frac{1}{2}$ then Eq. (1.34) should be exactly satisfied as the scaling limit is reached, $Q^2 \to \infty$. In the simple parton model, then, exact Bjorken scaling is seen as the result of elastic incoherent scattering off a point-like spin $\frac{1}{2}$ consituent.

Having already determined that charged partons carry spin $\frac{1}{2}$, it is interesting to ask what other quantum numbers the partons may carry; in particular to explore the consequences of identifying partons as quarks. This step leads to a number of experimentally testable sum rules.

The $f^i(x)$ of the previous analysis now become quark distribution functions. The label i now runs over the number of different quark flavours. In what follows we will consider only up, down and strange distributions. However, it is straightforward to extend the subsequent Parton Model formulae to include contributions from charmed, top, bottom etc quarks. Specifically, for the proton there are six distributions

$u(x)$ = number of up quarks in the proton with momentum fraction between x and $x+dx$

with similar distributions for the down quarks $d(x)$, strange quarks $s(x)$ and the corresponding antiparticles $\bar{u}(x), \bar{d}(x), \bar{s}(x)$.

Thus for the proton

$$F_2^{ep}(x) = \sum_i e_i^2 x f^i(x) = \sum_i e_i^2 x \left[q_i(x) + \bar{q}_i(x) \right] \qquad (1.35)$$

$$\frac{1}{x} F_2^{ep}(x) = \frac{4}{9}\left(u(x)+\bar{u}(x)\right) + \frac{1}{9}\left(d(x)+\bar{d}(x)\right) + \frac{1}{9}\left(s(x)+\bar{s}(x)\right) \qquad (1.36)$$

with the standard charge assignments

$$(u, d, s) = \left(\frac{2}{3}, -\frac{1}{3}, -\frac{1}{3}\right) \qquad (1.37)$$

and the constraints (coming from the total charge, isospin and strangeness quantum numbers of the proton)

$$\int_0^1 dx \left(u(x) - \bar{u}(x)\right) = 2 \qquad (1.38)$$

$$\int_0^1 dx \left(d(x) - \bar{d}(x)\right) = 1 \qquad (1.39)$$

$$\int_0^1 dx \left(s(x) - \bar{s}(x)\right) = 0 \qquad (1.40)$$

These are just the number of valence quarks to be found in the proton from the simple quark model.

Also, by isospin symmetry the number of up quarks in a proton is equivalent to the number of down quarks in a neutron

$$u^p(x) = d^n(x) \equiv u(x) \qquad (1.41)$$

$$d^p(x) = u^n(x) \equiv d(x) \qquad (1.42)$$

and so

$$\frac{1}{x} F_2^{en}(x) = \frac{4}{9}\left(d(x) + \bar{d}(x)\right) + \frac{1}{9}\left(u(x) + \bar{u}(x)\right) + \frac{1}{9}\left(s(x) + \bar{s}(x)\right) \qquad (1.43)$$

Assuming $q_i(x) \geq 0$ then the ratio of neutron to proton structure functions νW_2 in the scaling limit is [1.5, 1.6]

$$\frac{1}{4} \leq \frac{F_2^{en}(x)}{F_2^{ep}(x)} \leq 4 \qquad (1.44)$$

This inequality is not in conflict with the experimental result [1.7], although for large $x \sim 0{\cdot}8$ the data are very close to the lower bound of $\frac{1}{4}$.

Various other sum rules expressing charge or baryon number conservation in neutrino processes may also be derived, for example

$$\int_0^1 dx\ \frac{1}{x}\left(F_2^{\bar{\nu}p}(x) - F_2^{\nu p}(x)\right) = 2 \qquad \text{(Adler [1.8])} \qquad (1.45)$$

$$\int_0^1 dx\ \left(F_1^{\bar{\nu}p}(x) - F_1^{\nu p}(x)\right) = 1 \qquad \text{(Bjorken [1.9])} \qquad (1.46)$$

Finally, the fraction of the total momentum carried by each quark flavour is

$$U \equiv \int_0^1 dx\ x\left[u(x) + \bar{u}(x)\right] \qquad (1.47)$$

$$D \equiv \int_0^1 dx\ x\left[d(x) + \bar{d}(x)\right] \qquad (1.48)$$

$$S \equiv \int_0^1 dx\ x\left[s(x) + \bar{s}(x)\right] \qquad (1.49)$$

The conservation of momentum requires

$$1 - \varepsilon = U + D + S \qquad (1.50)$$

where ε is the fraction of total momentum carried by objects other than charged quarks. The right hand side of Eq. (1.50) can be written in terms of experimentally measured combinations of structure functions as

$$1-\varepsilon = \int_0^1 dx\ \frac{9}{2}\left(F_2^{ep}(x) + F_2^{en}(x)\right) - \frac{3}{4}\left(F_2^{\nu p}(x) + F_2^{\nu n}(x)\right) \qquad (1.51)$$

Inserting the known [1.10, 1.11] experimental values of the integrals

$$1-\varepsilon = \frac{9}{2}\left(0.28 \pm 0.004\right) - \frac{3}{4}\left(\geq 1.08 \pm 0.27\right) \qquad (1.52)$$

to give

$$\varepsilon \geq 0.52 \pm 0.38 \qquad (1.53)$$

Thus on the basis of momentum conservation all partons cannot be quarks. The electrically neutral partons are conventionally identified as the vector gluons of Q.C.D.

In conclusion, the naive parton model predicts exact Bjorken scaling as the result of elastic incoherent lepton-parton scattering. The data supports the idea of charged spin $\frac{1}{2}$ partons and severely restricts the amount of charged spin 0 admixture. The charged partons $\equiv$ quarks hypothesis yields many experimentally testable sum rules which are not in conflict with data but none of which provide compelling evidence for these partons to carry quark quantum numbers. Momentum conservation forces the existence of electrically neutral partons which account for roughly half of the protons' longitudinal momentum. Parton model ideas have since been successfully extended to other physical processes including e^+e^- annihilation into hadrons, massive lepton-pair production (Drell-Yan processes) and the inclusive production of particles with large transverse momenta.

Despite these successes the simple parton model does not give a satisfactory explanation of the data. Although scaling works well in the region $0{\cdot}15 < X < 0{\cdot}25$ (for Q^2 in the range of $2 \rightarrow 100\,\text{Gev}^2$), for $X > 0{\cdot}25$ a definite pattern of scaling violations emerges, [1.12, 1.13] and $F_L(X) \equiv F_2(X) - 2X F_1(X)$ is reported to have a value different from zero [1.14]. Thus we have to go beyond the simple parton model, and extensions of parton model ideas have been investigated. In particular, endowing the partons with form factors (and so implying the existence of yet another sub-structure) does avoid the problem of exact Bjorken scaling despite being an unimaginative solution [1.15].

A more interesting line of approach is to explore the possibility that the parton model is a first approximation to some underlying Quantum Field Theory that describes the strong interactions, especially as this appears to be the only way to reliably calculate dynamical quantities. There is now a wealth of qualitative evidence [1.16] that this theory is Quantum Chromodynamics (Q.C.D.). A brief review of the theory and its salient features will be given in the next section, but for the sake of clarity it is perhaps better to state the main results that emerge now. Q.C.D. has the unique property of asymptotic freedom. Its momentum dependent effective quark-gluon coupling constant decreases for increasing Q^2, allowing the application of perturbation theory to hard scattering processes. This provides an explanation of Bjorken scaling and its violation in agreement with the observed experimental results. Because the effective coupling constant goes to zero as $\left[\ln(Q^2)\right]^{-1}$ then, likewise, many of the previous parton model results (sum rules, scaling etc) are violated only logarithmically in Q^2. Extrapolated to low Q^2, the effective coupling increases without limit, therefore allowing possibility of quark and gluon confinement.

1.2 The theory :- Quantum Chromodynamics and its asymptotic behaviour

Quantum Chromodynamics (Q.C.D.) [1.16, 1.17] is a non-abelian gauge field theory in which coloured spin $\frac{1}{2}$ quarks are coupled to gluons; the coloured spin 1 gauge bosons. The Lagrangian which describes this quark-gluon interaction is

$$\mathcal{L} = -\frac{1}{4} G^A_{\mu\nu} G^A_{\mu\nu} + i \bar{\psi}_i \left(\gamma^\mu D_{ij\mu} + i m \delta_{ij} \right) \psi_j \qquad (1.54)$$

where there are f (for f flavours) quark colour triplets coupled to one colour octet of gluons. A sum over repeated indices and flavours is understood, and the indices run from

$$i, j = 1, 2, 3$$
$$A = 1, 2, \text{----} 8$$

The field strength $G^A_{\mu\nu}$ is given by

$$G^A_{\mu\nu} = \partial_\mu G^A_\nu - \partial_\nu G^A_\mu + g f^{ABC} G^B_\mu G^C_\nu \tag{1.55}$$

and the covariant derivative $D_{\mu ij}$

$$D_{\mu ij} = \partial_\mu \delta_{ij} - i g T^A_{ij} G^A_\mu \tag{1.56}$$

The matrices T^A_{ij} are the generators of the colour group $SU(3)_c$ and are related to the Gell-Mann matrices λ^A_{ij} as

$$T^A_{ij} = \frac{\lambda^A}{2}{}_{ij} \tag{1.57}$$

and satisfy the commutation relations

$$\left[T^A, T^B\right] = i f^{ABC} T^C \tag{1.58}$$

where f^{ABC} are the structure constants of $SU(3)_c$.

Finally, the ψ_i and G^A_μ are the quark and gluon fields respectively, with the strong coupling constant g (dimensionless). The Q.C.D. Lagrangian Eq. (1.54) is invariant under the (simultaneous) local gauge transformation

$$\begin{cases} \psi_i \rightarrow e^{ig\theta^A(x)T^A_{ij}}\psi_j & (1.59) \\ G^A_\mu \rightarrow G^A_\mu + \partial_\mu\theta^A(x) - gf^{ABC}\theta^B(x)G^C_\mu & (1.60) \end{cases}$$

In order to compute the Feynman rules for this theory two additional terms must be included in the Lagrangian. These are

(i) $-\frac{1}{\alpha}Tr\left[(\partial^\mu G_\mu)^2\right]$ - a gauge fixing term with a gauge parameter α, necessary in order to uniquely determine the gluon propagator

(ii) $+\bar{\eta}^A\partial^\mu\left[\partial_\mu\delta^{AC}+gf^{ABC}G^B_\mu\right]\omega^C$ a Fadeev-Popov ghost lagrangian essential in order to preserve unitarity and prevent unphysical degrees of freedom in the gauge bosons from propagating.

The Feynman rules for this complete Lagrangian are shown in Fig. 1.3. An immediate problem is encountered though when computing Feynman diagrams beyond tree level. In many one loop diagrams the integral over the loop momentum which has to be performed formally diverges and yields infinity. This problem is not specific to Q.C.D. but is a general feature of any renormalizable Quantum Field Theory (or indeed, in one form or another, of any interacting theory). Its solution and the process by which finite physically meaningful answers are extracted from perturbation theory is called the Renormalization Program [1.18]. For an illustration of its application take as an example a massive ϕ^4 scalar field theory described by the lagrangian density.

Fermion Propagator

$$+\frac{i}{\not p - m + i\varepsilon}\,\delta_{ij}$$

Gluon Propagator

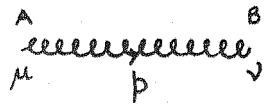

$$-\frac{i\,\delta^{AB}}{p^2+i\varepsilon}\left[\,g_{\mu\nu}-(1-\alpha)\,\frac{p_\mu p_\nu}{p^2+i\varepsilon}\,\right]$$

Ghost Propagator

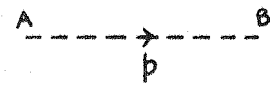

$$+\frac{i\,\delta^{AB}}{p^2+i\varepsilon}$$

Fermion vertex

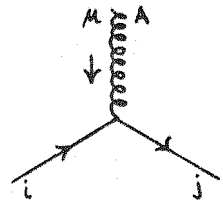

$$+\,ig\left(\frac{\lambda^A}{2}\right)_{ji}\gamma_\mu$$

Triple vertex

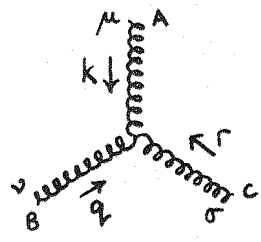

$$+g f_{ABC}\left[\,g_{\mu\nu}(k-q)_\sigma + g_{\nu\rho}(q-r)_\mu + g_{\sigma\mu}(r-k)_\nu\,\right]$$

Quartic vertex

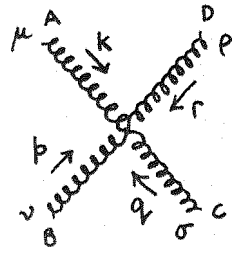

$$-ig^2\Big[f_{ABE}f_{CDE}\left(g_{\mu\sigma}g_{\nu\rho}-g_{\mu\rho}g_{\nu\sigma}\right) + f_{ACE}f_{BDE}\left(g_{\mu\nu}g_{\sigma\rho}-g_{\mu\rho}g_{\nu\sigma}\right) + f_{ADE}f_{CBE}\left(g_{\mu\sigma}g_{\nu\rho}-g_{\mu\nu}g_{\sigma\rho}\right)\Big]$$

Ghost vertex

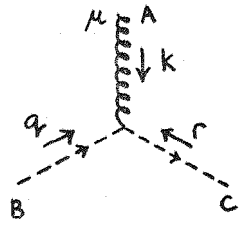

$$+\,g f_{ABC}\,r_\mu$$

-1 for closed loop of fermions or ghosts

Diagrams related by the exchange of external fermion lines have a relative minus sign.

Fig. 1.3 Feynman rules for Q.C.D. Lagrangian of Eq. (1.54)

$$\mathcal{L}_0 = \tfrac{1}{2}(\partial_\mu \phi_0)(\partial_\mu \phi_0) - \tfrac{1}{2} m_0^2 \phi_0^2 - \frac{g_0}{4!} \phi_0^4 \qquad (1.61)$$

The label 0 refers to 'bare' quantities. The physically measurable quantities are shifted from these bare parameters by the self-interactions generated in perturbation theory. To see this let us compute the physical mass, m^2, defined as the pole in the full two point Greens function, $G^{(2)}(q^2)$

The bare two-point Greens function is

$$G_0^{(2)}(q^2) = \frac{i}{q^2 - m_0^2} = \quad q \qquad (1.62)$$

The proper self energy, $-i\Sigma(q)$, is defined as the sum of all one particle irreducible graphs (graphs that cannot be separated by cutting through one propagator)

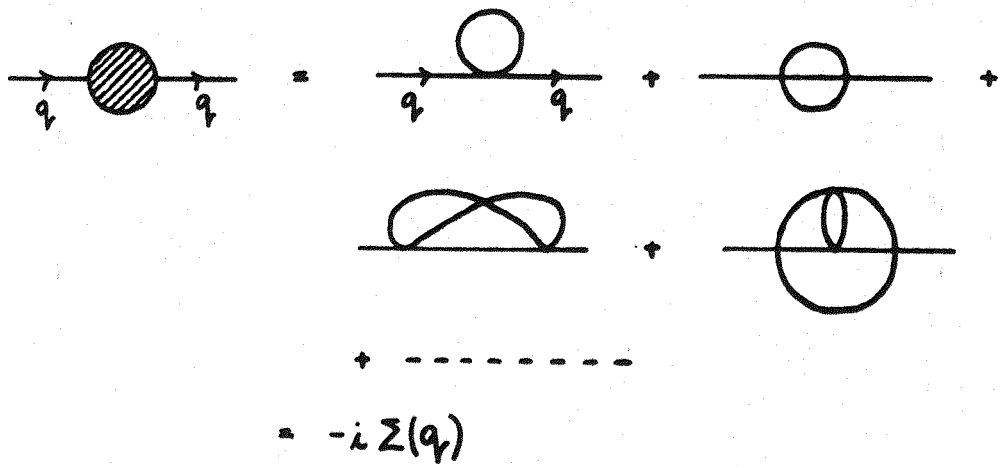

(1.63)

So the full two point Greens function is generated by successive iterations of the proper self energy

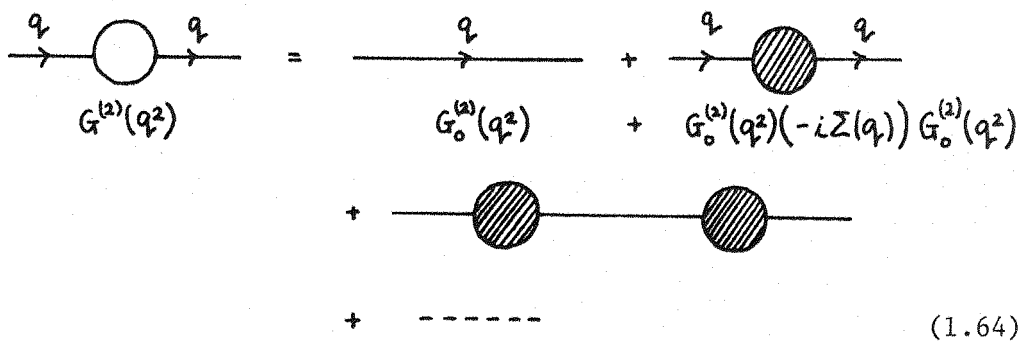

(1.64)

The resulting geometrical series can be summed to give

$$G^{(2)}(q^2) = \frac{G_0^{(2)}(q^2)}{1 + i\,\Sigma(q)\,G_0^{(2)}(q^2)} \tag{1.65}$$

using Eq. (1.62) for $G_0^{(2)}(q^2)$ to arrive at

$$G^{(2)}(q^2) = \frac{i}{q^2 - m_0^2 - \Sigma(q)} \equiv \frac{i}{q^2 - m_R^2} \tag{1.66}$$

with the physical mass occurring as the pole in the full propagator

$$m_R^2 = m_0^2 + \Sigma(q) \tag{1.67}$$

Thus, if we wish to identify m^2 as the physical mass in the lagrangian then

$$m_0^2 = m_R^2 - \delta m^2$$

where the counterterm δm^2 must be chosen order by order in perturbation theory to precisely cancel the shifts produced in the parameters of the lagrangian by self interactions. As well as this mass renormalization, there is also a coupling constant and wavefunction renormalization. The bare lagrangian

$$\mathcal{L}_0 = \tfrac{1}{2}(\partial_\mu \phi_0)(\partial_\mu \phi_0) - \tfrac{1}{2} m_0^2 \phi_0^2 - \frac{g_0}{4!}\phi_0^4 \tag{1.68}$$

may be written

$$\mathcal{L}_0 = \tfrac{1}{2}(1+A)(\partial_\mu \phi_R)(\partial_\mu \phi_R) - \frac{m_R^2}{2}(1+B)\phi_R^2 - \frac{g_R}{4!}(1+C)\phi_R^4 \tag{1.69}$$

where the counterterms A, B, C are to be determined to each order of perturbation theory by three arbitrary constraints

$$\Gamma^{(2)}(p)\Big|_{p^2=-\mu^2} = -\mu^2 - m^2 \tag{1.70}$$

$$\frac{\partial}{\partial p^2}\Gamma^{(2)}(p)\Big|_{p^2=-\mu^2} = -i \tag{1.71}$$

$$\Gamma^{(4)}(p_1 p_2 p_3 p_4)\Big|_{\substack{p_i^2=-\mu^2 \\ s=t=u=-\frac{4}{3}\mu^2}} = -ig \tag{1.72}$$

with $\Gamma^{(n)}$ being the n-particle proper vertex functions, and $-\mu^2$ some arbitrary space-like momentum. Of course, physical results cannot depend upon the point at which the theory is renormalised, $-\mu^2$. The expression of this fact results in the Renormalization group equation to be discussed shortly. So far no mention of infinities has been made. However, the proper self energy $\Sigma(q)$ can be expanded perturbatively in successive powers of the coupling constant g_0 as in Eq. (1.63). The leading contribution is

$-i\Sigma_1(q) =$

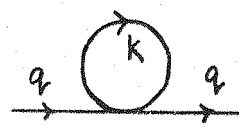

$$= -ig_0 \int_{-\infty}^{\infty} \frac{d^4k}{(2\pi)^4} \frac{i}{(k^2 - m_0^2)} \tag{1.73}$$

which, for large k

$$\sim \int^{\Lambda} \frac{d^4k}{k^2} \sim \Lambda^2 \qquad (1.74)$$

The integral diverges quadratically as $\Lambda \to \infty$. This is precisely where the infinities of Quantum Field theory arise. In order to determine the (infinite) counterterms that must be added to the lagrangian to cancel these shifts from perturbation theory, the formally divergent loop integrals must be regulated in some manner. Clearly one way to achieve this is to enforce an ultraviolet cut-off, Λ, in the loop integral. After adding the appropriate counterterms to the lagrangian, we could then successfully take the limit $\Lambda \to \infty$. This procedure is not applicable to the renormalization of gauge theories, as the counterterms do not respect the gauge invariance of the lagrangian. A simple method that survives this test is the dimensional regularization scheme [1.19] in which Feynman diagrams are calculated in an arbitrary integer number of space-time dimensions, D, and the results analytically continued to any real or complex value of D. Specifically if $D = 4 - 2\varepsilon$ then the ultra-violet (large k) divergences manifest themselves as poles in $\frac{1}{\varepsilon}$, $\frac{1}{\varepsilon^2}$ etc. This is the scheme that will be adopted later to regulate Feynman diagrams.

Note that the bare Lagrangian

$$\mathcal{L}_0 = \tfrac{1}{2}(1+A)(\partial_\mu \phi_R)(\partial_\mu \phi_R) - \frac{m_R^2}{2}(1+B)\phi_R^2 - \frac{g_R}{4!}(1+C)\phi_R^4 \qquad (1.75)$$

which comprises the renormalised parameters plus the counterterms is equivalent to

$$\mathcal{L}_0 = \tfrac{1}{2}(\partial_\mu \phi_0)(\partial_\mu \phi_0) - \tfrac{1}{2} m_0^2 \phi_0^2 - \frac{g_0}{4!} \phi_0^4 \tag{1.76}$$

together with the following re-definition of the quantities

$$\phi_0 = Z_\phi^{\frac{1}{2}} \phi_R \tag{1.77}$$

$$m_0 = Z_m^{\frac{1}{2}} m_R \tag{1.78}$$

$$g_0 = Z_g g_R \tag{1.79}$$

and the Z's, the multiplicative renormalization constants, are related to the counter-terms as

$$Z_\phi^{\frac{1}{2}} = \sqrt{1+A} \tag{1.80}$$

$$Z_m^{\frac{1}{2}} = \sqrt{\frac{1+B}{1+A}} \tag{1.81}$$

$$Z_g = \frac{1+C}{(1+A)^2} \tag{1.82}$$

Thus the Z's can be calculated to any order of perturbation theory and will be functions of the cut off Λ (or ε) diverging as $\Lambda \to \infty$ (or $\varepsilon \to 0$). The bare quantities are infinite and unobservable; however, the divergence can be factored into multiplicative renormalization constants leaving finite observable parameters [1.20].

The precise method by which this is achieved is called the subtraction scheme. Illustrated above is subtraction at $p^2 = -\mu^2$ in which the Z's are determined by specifying simple properties of Greens functions at some arbitrary space-like momentum μ^2. In this procedure the Z's are generally complicated expressions involving finite terms as well as functions of the regulator (Λ or ε). There exist many other

schemes though, some of which are particularly simple to implement such as the minimal subtraction scheme (MS) proposed by 't Hooft. Here one chooses the Z's to remove only the ultra-violet divergences and no finite terms, so they take the simple form of a power series in $\frac{1}{\varepsilon}$. However, in the MS scheme, the renormalized Greens functions now no longer have any simple properties at $p^2 = -\mu^2$. The arbitrary mass scale μ^2 is encountered in order to keep the coupling constant dimensionless in $D = 4 - 2\varepsilon$ dimensions, the space in which the theory is now formulated. Specifically, g^2 is scaled to $g^2\mu^{2\varepsilon}$.

If the perturbation expansion is summed to all orders then the dependence of the physical quantity on μ^2 vanishes as it must do. It is then irrelevant what subtraction scheme each term in the renormalised expansion is calculated in, as long as the same scheme is used consistently throughout. However, the coefficients of successive terms become increasingly difficult to calculate with increasing order, so in practice only the first few (i.e. at most four) terms in the perturbation expansion are determined. Having truncated the series thus, we are now left with renormalization scheme dependent predictions, a fact which plagues practical application of perturbative QCD. The same problem occurs in principle in QED, but here there exists a physically 'obvious' choice of subtraction procedure known as mass shell subtraction. In this method the renormalization constants are determined by requiring the two primitively divergent Greens functions of the theory to take a simple form on mass shell. For example, the constant $\tilde{Z}_1$ that renormalizes the photon-electron bare coupling e_o is chosen order by order in perturbation theory such that at $q^2 = 0$ and $p^2 = M_e^2$ this coupling is just e_R. Perturbative predictions for QED processes then take the form of an expansion in $\frac{e_R^2}{4\pi} = \alpha$, a quantity which must ult-

imately be taken from experiment (i.e. the low energy limit of Thomson scattering). Indeed, α appears to be a 'good' expansion parameter in the sense that it is accompanied by small coefficients, as is the case for the anomalous magnetic moment of the electron a_e

$$a_e = \left(\frac{g_e - 2}{2}\right) = \frac{1}{2}\left(\frac{\alpha}{\pi}\right) - 0.328478966\ldots\left(\frac{\alpha}{\pi}\right)^2 + 1.1835\left(\frac{\alpha}{\pi}\right)^3 + \ldots \qquad (1.83)$$

For Q.C.D. no such 'natural' definition of the renormalised quark-gluon coupling occurs since there are no physical on-shell quarks and gluons available. Once again all renormalization schemes are equally valid, although there clearly exist 'best' choices (in the sense above) of scheme and μ^2 . MS, although theoretically easy to work with, appears not to be a good choice of subtraction scheme as it leads almost universally to large corrections. However, having calculated a process as an expansion in α_s defined in one scheme there exists a well defined method for translating the expansion to that in $\tilde{\alpha}_s$ defined in any other scheme [1.21].

Up to now we have merely stated that these constants are calculable perturbatively, but to render a theory sensible, in the sense of being predictive, more than this is needed. Clearly if more counterterms are needed to cancel an increasing proliferation of divergences for higher orders of perturbation theory then ultimately after renormalization the lagrangian will depend on an infinite set of arbitrary parameters leaving it devoid of predictive content. This leads to the question of renormalizability [1.22]. A theory is said to be renormalizable if there are only a finite number of primitively divergent Greens functions requiring only a finite set of counterterms. This translates into

a statement concerning the momentum dimensions of the coupling constant.

In general if

$$g \sim [p]^a \tag{1.84a}$$

then the theory is renormalizable if $a \geq 0$

and is non-renormalizable if $a < 0$

An intuitive reason for this power counting statement can be seen by expanding any Greens function in perturbation theory. For example the two point Greens function discussed previously

$$G^{(2)}(q^2) = G_0^{(2)}(q^2)\left[1 + g^2\{\int\} + g^4\{\int\} + \cdots\right] \tag{1.84b}$$

where $\{\int\}$ represents some integral over loop momenta.

If $a > 0$, then the momentum dimensions of the loop integral(s) must decrease with more powers of g in order to keep the total dimension fixed (and equal to $G^{(2)}(q^2)$). The integrals are becoming more convergent for large loop momenta with higher order. Conversely if $a < 0$, the situation reverses and the loop integrals grow increasingly divergent, requiring the introduction of more counterterms.

For the ϕ^4 theory under consideration $\mathcal{L} \sim [p]^4$ in 3 + 1 dimensions, hence from the kinetic term in the lagrangian density $\phi \sim [p]^1$ and so the coupling

$$g \sim [p]^0 \tag{1.85}$$

The theory is renormalizable as $a = 0$.

So to recap, the Renormalization Program consists of two distinct steps. The first is concerned with regularizing the formally divergent integrals encountered, while the second consists of the systematic calculation of the renormalization constants, and is known as the subtraction scheme.

We now turn to the question of the arbitrary scale μ introduced in the implementation of this program. Because the choice of renormalization point μ is completely free, changes in μ cannot affect any physical predictions. Therefore, the other parameters of the theory must change in order to compensate for the variations in μ. In order to study the asymptotic behaviour of Greens functions for large space-like momenta, mass terms in the Lagrangian are ignored in the belief that massless and massive theories have the same asymptotic limit. Now a change in μ is equivalent to a change in the scale of momenta since μ is the only dimensionful parameter in the theory (the coupling constant is dimensionless). The renormalization group relates Greens functions for one set of momenta and coupling constant to Greens functions with a scaled set of momenta and different value of the coupling constant. Specifically one can relate the asymptotic form of Greens functions to those for fixed momenta and an effective coupling constant. The asymptotic value of this effective coupling constant is given by the positions of the zeros of a perturbatively calculable function. These zeros are known as the fixed points of the renormalization group.

For convenience, we work with the renormalised one particle irreducible (1PI) truncated vertex functions defined as

$$\Gamma_R^{(N_F,N_G)} = \frac{G_R^{(N_F,N_G)}(1PI)}{\prod_{N_F} G_R^{(2,0)} \prod_{N_G} G_R^{(0,2)}} \tag{1.86}$$

where the renormalised Greens functions are given by

$$G_R^{(N_F,N_G)} = \langle 0|T(\psi_1 \cdots \psi_{N_F} G_1 \cdots G_{N_G})|0\rangle \tag{1.87}$$

with N_F and N_G corresponding to the number of external fermion and gluon legs respectively. The unrenormalized and renormalized vertex functions are related to each other via the multiplicative renormalization constants. If by analogy with the ϕ^4 example we define

$$\psi_i^0 = Z_F^{\frac{1}{2}} \psi_i^R \tag{1.88}$$

$$(G_\mu^A)^0 = Z_G^{\frac{1}{2}} (G_\mu^A)^R \tag{1.89}$$

$$g_0 = Z_g g_R \tag{1.90}$$

then

$$\Gamma_R^{(N_F,N_G)}(p_i, g, \mu) = Z_F^{\frac{N_F}{2}} Z_G^{\frac{N_G}{2}} \Gamma_u^{(N_F,N_G)}(p_i, g_0, \Lambda) \tag{1.91}$$

The Z's depend on the ultra-violet cut-off Λ but are dimensionless and so functions only of the ratio $\frac{\Lambda}{\mu}$

i.e. $$Z_F^{\frac{N_F}{2}}\left(g_0, \frac{\Lambda}{\mu}\right) \tag{1.92}$$

The arbitrariness of the scale μ implies

$$\mu \frac{d}{d\mu}\left(\Gamma_u^{(N_F,N_G)}(p_i, g_0, \Lambda)\Big|_{\text{fixed } g_0, \Lambda} \right) = 0 \tag{1.93}$$

or equivalently that

$$\left[\mu\frac{\partial}{\partial\mu} + \beta(g,\alpha)\frac{\partial}{\partial g} - N_F\gamma_F(g,\alpha) - N_G\gamma_G(g,\alpha) + \delta(g,\alpha)\frac{\partial}{\partial\alpha}\right]\Gamma_R^{(N_F,N_G)} = 0 \qquad (1.94)$$

where α is the gauge parameter

$$\beta(g,\alpha) = \mu\frac{\partial g}{\partial\mu} \qquad (1.95)$$

$$\gamma_F(g,\alpha) = \mu\frac{\partial}{\partial\mu}\ln\sqrt{Z_F} \qquad (1.96)$$

$$\gamma_G(g,\alpha) = \mu\frac{\partial}{\partial\mu}\ln\sqrt{Z_G} \qquad (1.97)$$

$$\delta(g,\alpha) = \mu\frac{\partial\alpha}{\partial\mu} \qquad (1.98)$$

Eq. (1.94) is known as the Renormalization Group equation [1.23] and it is the functions β, γ, δ that give the precise compensating changes in the parameters of the lagrangian for variations in μ. They depend on the theory and not the vertex functions. Due to the fact that the longitudinal part of the vector propagator is not renormalised

$$\alpha_0 = Z_G\alpha_R \qquad (1.99)$$

so

$$\delta(g,\alpha) = -\frac{\alpha_0}{Z_G^2}\mu\frac{\partial Z_G}{\partial\mu} \qquad (1.100)$$

$$= -2\alpha_R\gamma_G(g,\alpha) \qquad (1.101)$$

Hence the R.G.E. takes on a particularly simple form in the Landau gauge $\alpha = 0$, explicitly

$$\left[\mu\frac{\partial}{\partial\mu} + \beta(g)\frac{\partial}{\partial g} - N_F\gamma_F(g) - N_G\gamma_G(g)\right]\Gamma_R^{(N_F,N_G)} = 0 \qquad (1.102)$$

The γ_F and γ_G are known as the anomalous dimensions of the fermion and gluon fields respectively. It is the function $\beta(g)$ that governs the momentum dependence of the effective coupling constant. All these quantitites can be systematically calculated in perturbation theory.

Due to the lack of any dimensionful parameters to set the momentum scale in the lagrangian, one might expect vertex functions to scale according to naive dimensional analysis when all the momenta are transformed $p_i \to \lambda p_i$ so that

$$\Gamma_R^n(\lambda p_i, g, \mu) = [\lambda]^D \Gamma_R^n\left(p_i, g, \frac{\mu}{\lambda}\right) \qquad (1.103)$$

where D is the physical dimension of Γ_R^n. However, the existence of a hidden dimension-full parameter μ in the theory spoils this behaviour. We can use the R.G.E. to relate vertex functions evaluated at momenta p_i to those evaluated at rescaled momenta λp_i if

$$\lambda = e^t \qquad (1.104)$$

then

$$\Gamma_R^{(N_F,N_G)}(e^t p_i, g, \mu) =$$

$$\exp\left[Dt - \int_g^{\bar{g}(t)} dg' \frac{N_F\gamma_F(g') + N_G\gamma_G(g')}{\beta(g')}\right]\Gamma_R^{N_F,N_G}(p_i, \bar{g}(t), \mu) \qquad (1.105)$$

where the effective coupling constant $\bar{g}(t)$ satisfies the equation

$$\frac{d\bar{g}^2}{dt} = \bar{g}\beta(\bar{g}) \qquad (1.106)$$

with the boundary condition

$$\bar{g}(t=0) = g \tag{1.107}$$

From Eq. (1.105) we can see that once the vertex function is known at some specific value of t, then we can use this equation to calculate it for any subsequent t.

We are now in a position to explore the interesting asymptotic region of $t \to +\infty$. Suppose that in this limit the effective coupling constant converges to some fixed value, g^*

$$\lim_{t\to+\infty} \bar{g}(t) = g^* \tag{1.108}$$

These fixed points (there may be more than one) are determined by the zeros of the β function. If the convergence to this fixed value g^* is sufficiently rapid (determined by the properties of the β function) then

$$\lim_{t\to+\infty} \int_0^t dt \left[N_F \gamma_F(\bar{g}(t)) + N_G \gamma_G(\bar{g}(t)) \right] \tag{1.109}$$

$$\approx \lim_{t\to+\infty} \left[N_F \gamma_F(g^*) + N_G \gamma_G(g^*) \right] \int_0^t dt \tag{1.110}$$

and so in the asymptotic limit the canonical scaling of the vertex function given by dimensional analysis is spoiled by extra powers of λ

$$\Gamma_R^{(N_F,N_G)}(\lambda p_i, g, \mu) = [\lambda]^{D - N_F\gamma_F(g^*) - N_G\gamma_G(g^*)} \Gamma_R^{(N_F,N_G)}(p_i, \bar{g}, \mu) \tag{1.111}$$

and hence the identification of γ with anomalous dimensions.

Thus we can imagine the following possible form for the β function with fixed points occurring at g_1^*, g_2^* and g_3^* (see Fig. 1.4). Because it can be expanded perturbatively in $\bar{g}$, there is always a zero of $\beta(\bar{g})$ at the origin.

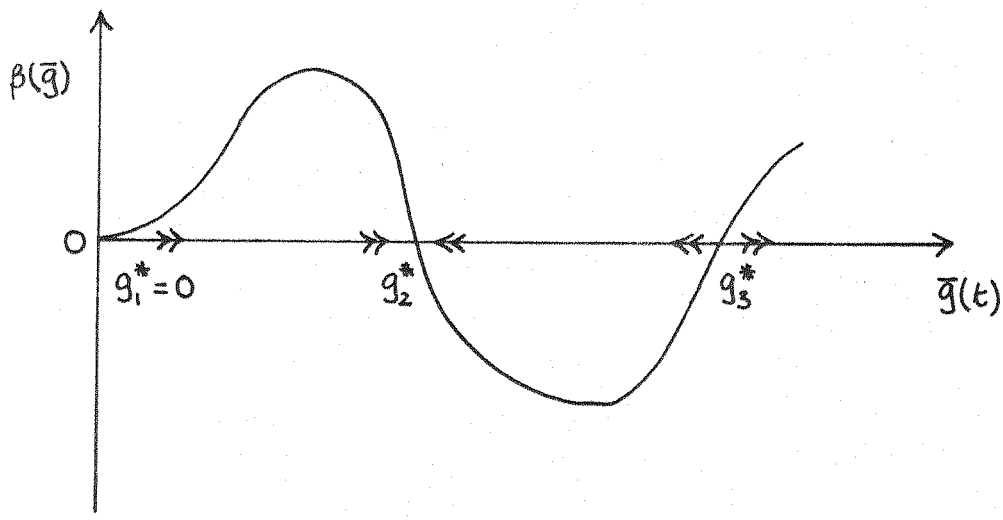

Fig. (1.4) Possible form for a β function:- arrows indicate movement of the coupling constant as $t \to +\infty$.

If $\beta(\bar{g})$ has a simple zero at $\bar{g} = g_2^*$, then we can expand around this point

$$\beta(\bar{g}) = \beta(g_2^*) + (\bar{g} - g_2^*) \left.\frac{\partial \beta(\bar{g})}{\partial \bar{g}}\right|_{\bar{g} = g_2^*} + O(\bar{g} - g_2^*)^2 \qquad (1.112)$$

But $\beta(g_2^*) = 0$, and using Eq. (1.106) to obtain

$$\frac{d\bar{g}(t)}{dt} \approx (\bar{g} - g_2^*) \left.\frac{\partial \beta(\bar{g})}{\partial \bar{g}}\right|_{\bar{g} = g_2^*} + \cdots\cdots \qquad (1.113)$$

Consider the point $g = g_2^*$. From Fig. 1.4 it is evident that

$$\left.\frac{\partial \beta(\bar{g})}{\partial \bar{g}}\right|_{\bar{g}=g_2^*} < 0 \qquad (1.114)$$

so if

$$(\bar{g} - g_2^*) > 0 \qquad (1.115)$$

then

$$\frac{d\bar{g}}{dt} < 0 \qquad (1.116)$$

and $\bar{g}(t)$ will decrease as t increases until it approaches g_2^* in asymptopia (i.e. $t \to +\infty$) . g_2^* is said to be an ultra-violet stable fixed point. For the opposite sign of the gradient of the β function at the fixed point, as is the case for $\bar{g} = g_3^*$, then $\bar{g}(t)$ is forced away as $t \to +\infty$, and the fixed point is ultra-violet unstable. However for $t \to -\infty$ (or $\lambda \to 0$) $\bar{g}(t)$ is attracted to such points and so they are known as infra-red stable. The actual behaviour of $\bar{g}(t)$ will depend on which domain contains $\bar{g}(t=0) = g$.

If $g^* = 0$ is an ultra-violet stable fixed point then the theory is known as Asymptotically Free. For large space-like momenta the effective coupling goes to zero, and the theory approaches free-field like behaviour.

The β function can be calculated perturbatively for Q.C.D.

$$\beta(g) = -\beta_0 \frac{g^3}{(4\pi)^2} - \beta_1 \frac{g^5}{(4\pi)^4} - \beta_2 \frac{g^7}{(4\pi)^6} + \cdots \qquad (1.117)$$

The lowest order coefficient of the fermion anomalous dimension

$$\gamma_F = \gamma_F^0 \frac{g^2}{(4\pi)^2} + \gamma_F^1 \frac{g^4}{(4\pi)^4} + \cdots \quad (1.118)$$

γ_F^0 can be evaluated directly from the lowest order fermion self energy graph of Fig. 1.5

$$\gamma_F^0 = \frac{4}{3}\alpha \quad (1.119)$$

in an arbitrary covariant gauge α. Similarly for the gluon field, the sum of the diagrams of Fig. 1.6 yields, where

$$\gamma_G = \gamma_G^0 \frac{g^2}{(4\pi)^2} + \gamma_G^1 \frac{g^4}{(4\pi)^4} + \cdots \quad (1.120)$$

$$\gamma_G^0 = -\left[\left(\frac{13}{6} - \frac{\alpha}{2}\right)3 - \frac{2}{3}f \right] \quad (1.121)$$

with f being the number of fermion flavours.

Finally to evaluate $\beta(g)$ to $O(g^3)$ one considers either the diagrams of Fig. 1.7 or those of Fig. 1.8. The calculation determines β_0 as [1.24, 1.25]

$$\beta_0 = 11 - \frac{2}{3}f \qquad \text{(gauge invariant)} \quad (1.122)$$

so for the number of flavours $f<16$ the lowest order coefficient of the β function is negative, having the consequence that Q.C.D. is asymptotically free providing the β function does become positive before $\bar{g}(t=0) = g$. The two and three loop parameters β_1 [1.26] and β_2 [1.27] have now been calculated with the result (for β_2 in the minimal subtraction scheme and Feynman gauge $\alpha = 1$).

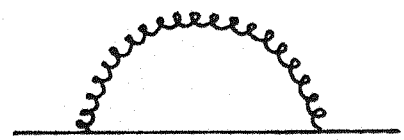

Fig 1. 5 Lowest order fermion self energy

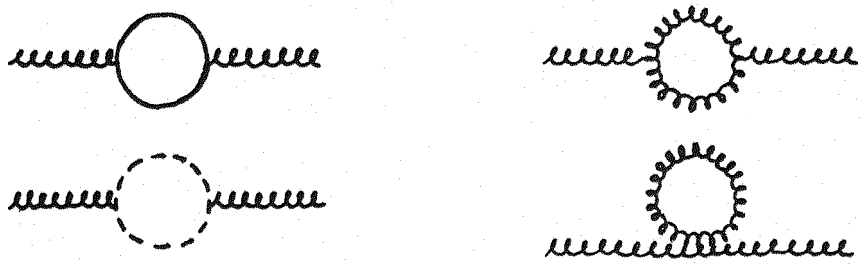

Fig 1. 6 Lowest order gluon self energy

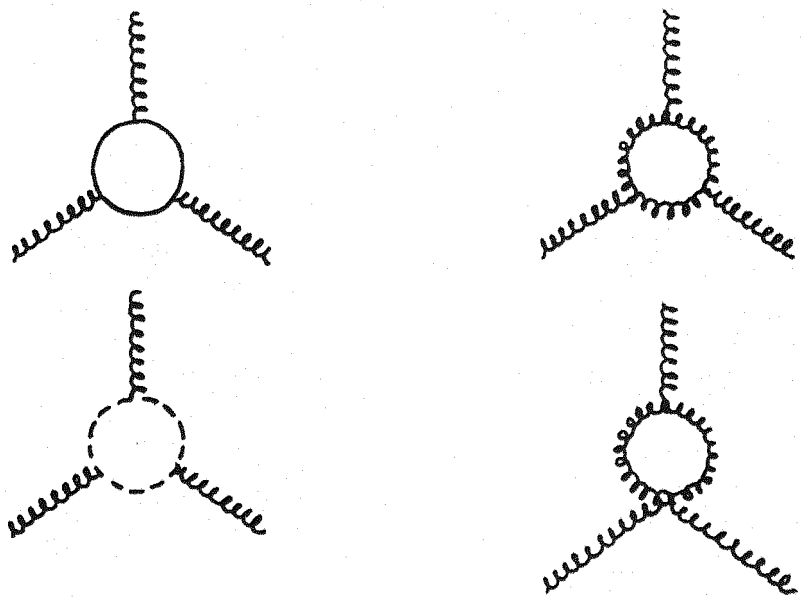

Fig 1. 7 Lowest order corrections to the three-gluon coupling

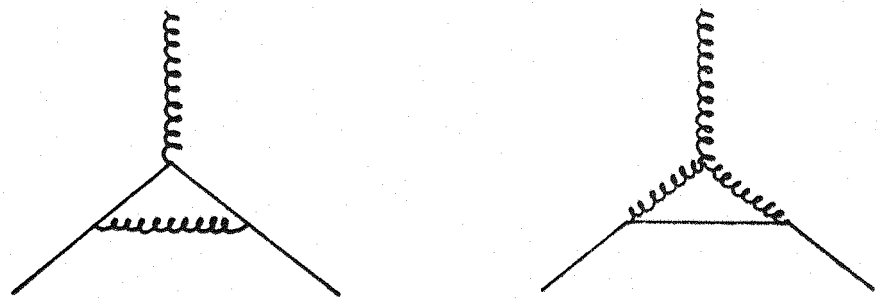

Fig 1. 8 Lowest order corrections to the quark-gluon coupling

$$\beta_1 = 102 - \frac{38}{3} f \tag{1.123}$$

$$\beta_2 = \frac{2857}{2} - \frac{5033}{18} f + \frac{325}{54} f^2 \tag{1.124}$$

lending further support for the consequence of asymptotic freedom. The class of theories in which this phenomenon can occur appears to be very limited. It has been proved that no theory which is not a non-Abelian gauge field theory can be asymptotically free [1.28].

Knowing the first few terms of the β function allows an approximate solution for the explicit momentum dependence of the effective coupling constant to be constructed. The β function is defined by Eq. (1.95)

$$\frac{d\bar{g}^2}{dt} = \bar{g}\beta(\bar{g}) \tag{1.125}$$

with the boundary condition

$$\bar{g}(t=0) = g \tag{1.126}$$

and

$$t = \ln\left(\frac{Q^2}{\mu^2}\right) \tag{1.127}$$

Keeping the first term in the expansion Eq. (1.117)

Then

$$2\bar{g}\frac{d\bar{g}}{dt} = -\beta_0 \frac{\bar{g}^4}{(4\pi)^2} \tag{1.128}$$

which can be integrated incorporating the condition (Eq. 126) as

$$-\frac{32\pi^2}{\beta_0}\int_g^{\bar{g}(Q^2)}\frac{d\bar{g}}{\bar{g}^3} = \int_0^t dt \tag{1.129}$$

$$\frac{1}{\bar{g}^2(Q^2)} - \frac{1}{g^2} = \frac{\beta_0}{16\pi^2}\ln\left(\frac{Q^2}{\mu^2}\right) \tag{1.130}$$

thus

$$\bar{g}^2(Q^2) = \frac{g^2}{1+\frac{g^2}{16\pi^2}\beta_0\ln\left(\frac{Q^2}{\mu^2}\right)} \tag{1.131}$$

or

$$\bar{g}^2(Q^2) = \frac{16\pi^2}{\beta_0\ln\left(\frac{Q^2}{\Lambda^2}\right)} \tag{1.132}$$

with

$$\Lambda^2 = \mu^2 \exp\left[-\frac{16\pi^2}{g^2\beta_0}\right] \tag{1.133}$$

from Eq. (1.132) it is evident that $\bar{g}(Q^2)\to 0$ as $Q^2\to\infty$ logarithmically.

For higher order calculations, the effective coupling constant can be solved for using the two loop expansion (β_1) of the β function. The result is

$$\bar{g}^2(Q^2) = \bar{g}_0^2(Q^2)\left[1 - \frac{\beta_1}{\beta_0}\frac{1}{16\pi^2}\bar{g}_0^2(Q^2)\ln\ln\left(\frac{Q^2}{\Lambda^2}\right) + O(\bar{g}_0^4)\right] \tag{1.134}$$

where

$$\bar{g}_0^2(Q^2) = \frac{16\pi^2}{\beta_0\ln\left(\frac{Q^2}{\Lambda^2}\right)} \tag{1.135}$$

and Λ has been chosen so that no more terms of $O\left[\frac{1}{\ln^2\left(\frac{Q^2}{\Lambda^2}\right)}\right]$ appear in the expansion

$$\Lambda^2 = \mu^2 \exp\left[-\frac{16\pi^2}{g^2\beta_0}\right]\left(\frac{\beta_0}{16\pi^2}\cdot\frac{g^2}{1+\frac{\beta_1}{\beta_0}\frac{1}{16\pi^2}g^2}\right)^{-\frac{\beta_1}{\beta_0}} \qquad (1.136)$$

which is different from the leading order Λ of Eq. (1.133)

The hope of asymptotic freedom then is that for processes which involve some large momentum transfer Q^2, the effective coupling constant at these scales is small enought to allow a reliable application of perturbation theory. In this spirit we now turn to the classic application of Q.C.D. perturbation theory to Deep Inelastic lepton-hadron scattering

1.3 Asymptotic Freedom in Deep Inelastic Scattering

In this section we give a brief review of how, utilising the techniques of the Operator Product Expansion and Renormalization Group, asymptotic freedom predictions can be calculated for deep inelastic processes to an arbitrary order of Q.C.D. perturbation theory [1.29]. Despite the complexity of the mathematical machinery involved, the results still have a simple intuitive interpretation to that of the Parton Model.

It is interesting to see the kinematic region explored by the deep inelastic Bjorken limit

$$Q^2 = -q^2 \to \infty \tag{1.137}$$

$$\nu = p.q \to \infty \tag{1.138}$$

with $$X = \frac{Q^2}{2\nu} \quad \text{fixed} \quad (0 \leq X \leq 1)$$

The relevant region of integration of the electromagnetic current commutator of Eq. (0.18) occurs when the exponential $e^{iq.z}$ is stationary. All other regions become wiped out by rapid oscillation of the exponential. writing

$$q.z = \left(\frac{q_0 + q_3}{\sqrt{2}}\right)\left(\frac{z_0 - z_3}{\sqrt{2}}\right) + \left(\frac{q_0 - q_3}{\sqrt{2}}\right)\left(\frac{z_0 + z_3}{\sqrt{2}}\right) - \underline{q}_\perp \cdot \underline{z}_\perp \tag{1.139}$$

Then, in the target rest frame of

$$p = (m_H, 0, 0, 0) \tag{1.140}$$

$$q = \frac{1}{m_H}\left(\nu, 0, 0, \sqrt{\nu^2 + m_H^2 Q^2}\right) \tag{1.141}$$

The Bjorken limit implies

$$q_0 + q_3 \approx \frac{2\nu}{m_H} \to \infty \tag{1.142}$$

$$q_0 - q_3 \approx m_H X \tag{1.143}$$

The relevant regions of z-space integration are, therefore, expected to be

$$z_0 - z_3 \approx \frac{m_H}{2\nu} \tag{1.144}$$

$$z_0 + z_3 \approx \frac{1}{m_H X} \tag{1.145}$$

Now as

$$z^2 = (z_0 - z_3)(z_0 + z_3) - z_\perp^2 \tag{1.146}$$

and causality forces the current commutator to vanish outside the light cone, i.e. $z^2 \geq 0$, then

$$z^2 \leq \left(\frac{m_H}{2\nu}\right)\left(\frac{1}{m_H x}\right) \approx O\left(\frac{1}{Q^2}\right) \tag{1.147}$$

Thus the Bjorken limit probes the product of currents near the light cone.

In field theory, many Greens functions are singular in this region, the simplest example being the free scalar field propagator

$$\Delta_F(z, m^2) = -i\langle 0|T[\phi(z)\phi(0)]|0\rangle \tag{1.148}$$

$$= -\int \frac{d^4k}{(2\pi)^4} \frac{e^{ik\cdot z}}{k^2 - m^2 + i\varepsilon} \tag{1.149}$$

$$\Delta_F(z, m^2) \underset{z^2 \to 0}{\approx} \frac{i}{(4\pi)^2} \frac{1}{-z^2 + i\varepsilon} + \cdots \tag{1.150}$$

For deep inelastic processes, the dominant contribution will come from the highest divergence near the light cone in products of operators of the underlying field theory [1.30]. The operator product expansion (O.P.E.) provides a method of categorizing these divergences allowing the leading singularity to be identified.

For convenience we choose to work with the forward elastic Compton scattering amplitude $T_{\mu\nu}$, where

$$T_{\mu\nu}(\nu, Q^2) = i\int d^4z\, e^{iq\cdot z}\langle p|T\left[J_\mu^\dagger(z)J_\nu(0)\right]|p\rangle \text{ spin averaged} \qquad (1.151)$$

This is related by the Optical Theorem to the deep inelastic hadron tensor $W_{\mu\nu}$ Eq. (0.18) as (see Fig. 1.9)

$$W_{\mu\nu} = \frac{1}{2\pi}\,\mathrm{Im}(T_{\mu\nu}) \qquad (1.152)$$

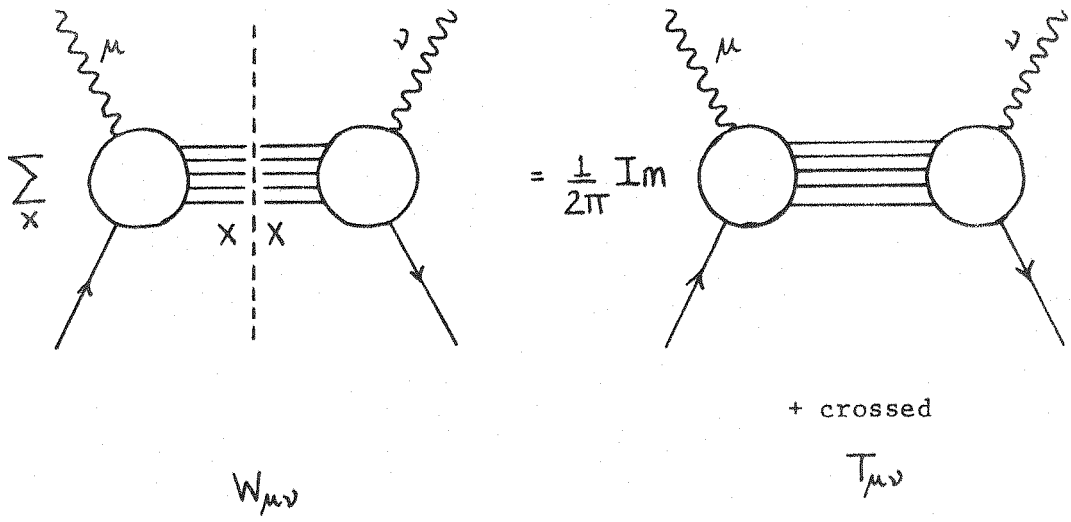

Fig. 1.9 Schematic illustration of the Optical Theorem.

As an illustration of the main features of the O.P.E. we will consider products of spinless currents. The generalization to vector currents carrying spin is reasonably straightforward. The physical idea behind the O.P.E. is that for small distances (compared to some characteristic length scale of the problem) a product of local operators should itself behave as a local operator [1.31]. These ideas may be extended to light cone expansions, [1.32] so we can write

$$i\,T[J(z)J(0)] \underset{\substack{z^2\to 0\\ z^\mu\neq 0}}{\approx} \sum_{i=0}^{M}\sum_{n=0}^{\infty} C_{i,n}(z)\, z^{\mu_1\cdots\mu_n}\, O^n_{i\,\mu_1\cdots\mu_n} \tag{1.153}$$

where the $O^n_{i\,\mu_1\cdots\mu_n}$ are an infinite set of regular (finite) local operators the label i referring to the quantum numbers admissible by the symmetries of the theory. The coefficients are in general c-number singular functions. In free field theory their degree of divergence is given by naive power counting of Eq. (1.153). Thus if

$$C_{i,n}(z) \sim \left(\frac{1}{z^2}\right)^{\frac{d_{C_{i,n}}}{2}} \tag{1.154}$$

then

$$2d_J = d_{C_{i,n}} - n + d_{O^n_i} \tag{1.155}$$

with $d_{O^n_i}$ the dimension of the local operator of spin n. So, the degree of divergence (in a free field theory)

$$d_{C_{i,n}} = 2d_J - (d_{O^n_i} - n) \tag{1.156}$$

Hence the most singular coefficients multiply those operators having the lowest value of

$$(d_{O^n_i} - n) \equiv \tau = \text{Twist} \tag{1.157}$$

In field theory one constructs local operators from scalar fields ϕ, fermion fields ψ and gauge fields G_μ which all have twist $\tau = 1$; together with derivatives ∂_ρ. The addition of these derivative

terms can only increase or leave unchanged the operator twist. Since we are interested in operators that are bi-linear in the fundamental fields it follows that the operators having lowest twist will be those of $\tau=2$. These operators take the form

for scalar field theory

$$O^{n}_{\mu_1\cdots\mu_n} = \phi^* \overleftrightarrow{\partial}_{\mu_1}\cdots\overleftrightarrow{\partial}_{\mu_n}\phi \tag{1.158}$$

for Q.C.D.

$$O^{n,K}_{NS\,\mu_1\cdots\mu_n} = S\left[\bar{\psi}_\alpha \lambda^K_{\alpha\beta}\gamma_{\mu_1}\overleftrightarrow{D}_{\mu_2}\cdots\overleftrightarrow{D}_{\mu_n}\psi_\beta\right] \tag{1.159}$$

$$O^{F}_{\mu_1\cdots\mu_n} = S\left[\bar{\psi}_\alpha \gamma_{\mu_1}\overleftrightarrow{D}_{\mu_2}\cdots\overleftrightarrow{D}_{\mu_n}\psi_\beta\right] \tag{1.160}$$

$$O^{G}_{\mu_1\cdots\mu_n} = S\left[G_{\mu_1\nu}\overleftrightarrow{D}_{\mu_2}\cdots\overleftrightarrow{D}_{\mu_{n-1}}G_{\mu_n\nu}\right] \tag{1.161}$$

where S denotes symmetrization over all Lorentz indices, and $\lambda^K_{\alpha\beta}$ is a flavour group generator. The O_{NS} are the fermion flavour non-singlet operators, whereas O^F and O^G are the flavour singlet fermion and gluon operators respectively. Their asymptotic freedom analysis is complicated by the fact that they carry the same quantum numbers and so mix under renormalization. All the above operators have dimension $n+2$, spin n and so are twist $\tau=2$.

Taking matrix elements of (1.153) between hadronic target states of momentum p , then Fourier transforming to obtain

$$T(\nu,Q^2) = i\int d^4z\, e^{iq\cdot z}\langle p|T\left[J^\dagger(z)J(0)\right]|p\rangle_{\text{spin av.}} \tag{1.162}$$

$$= \sum_{i=0}^{M}\sum_{n=0}^{\infty}\langle p|O^n_{i\,\mu_1\cdots\mu_n}(0)|p\rangle_{\text{sp.av.}}\, q^{\mu_1\cdots\mu_n}\,\tilde{C}_{i,n}(q^2) \tag{1.163}$$

where

$$\int d^4z\, e^{iq\cdot z}\, z^{\mu_1\cdots\mu_n}\, C_{n,i}(z) \equiv q^{\mu_1\cdots\mu_n}\, \tilde{C}_{i,n}(q^2) \tag{1.164}$$

If naive dimensional counting were correct, then

$$C_{n,i}(z) \sim \left(\frac{1}{z^2}\right)^{\frac{d_{C_{i,n}}}{2}} \tag{1.165}$$

with

$$d_{C_{i,n}} = 2d_J - \tau \tag{1.166}$$

This implies that

$$\tilde{C}_{i,n}(q^2) \sim \left(\frac{1}{q^2}\right)^{\frac{d_{\tilde{C}_{i,n}}}{2}} \tag{1.167}$$

where

$$d_{\tilde{C}_{i,n}} = 2n + 4 + \tau - 2d_J \tag{1.168}$$

In the scalar case $J(x) = :\phi^2(x):$ where the colons denote normal ordering.

Hence

$$d_J = 2 \tag{1.169}$$

If we define a reduced singular coefficient function $\overline{C}_{i,n}$ through

$$\tilde{C}_{i,n}(q^2) = \left(\frac{1}{q^2}\right)^{n+\frac{\tau}{2}} \overline{C}_{i,n}(q^2) \tag{1.170}$$

then the singularity structure of $\bar{C}_{i,n}(q^2)$ will express the deviation from free-field behaviour.

Writing the spin-averaged matrix elements as

$$\langle p| O^n_{i\,\mu_1\cdots\mu_n}(0)|p\rangle_{sp.av.} = A^n_i(\mu^2)\, p_{\mu_1}\cdots p_{\mu_n} \quad - \text{traces} \qquad (1.171)$$

The trace terms involve contractions of $\mu_i\mu_j$ and so are corrections of $O\left(\frac{p^2}{q^2}\right)$. For the moment they are neglected, although we shall mention them later.

Thus

$$T(\nu,Q^2) = \sum_{i=0}^{M}\sum_{n=0}^{\infty} \frac{(p\cdot q)^n}{(q^2)^{n+\frac{\tau}{2}}}\, A^n_i(\mu^2)\,\bar{C}_{i,n}(q^2) \qquad (1.172)$$

from which it is easy to see that the higher twist components of an operator of given spin n are suppressed by powers of $\frac{1}{q^2}$. Keeping only lower twist $\tau=2$, we can write

$$T(\nu,Q^2) = \sum_{i=0}^{M}\sum_{n=0}^{\infty} \frac{1}{q^2}\frac{1}{(-2)^n}\frac{1}{x^n}\, A^n_i(\mu^2)\,\bar{C}_{i,n}(q^2)\left[1 + O\left(\frac{1}{q^2}\right)+\cdots\right] \qquad (1.173)$$

where the $O\left(\frac{1}{q^2}\right)$ corrections represent contributions from both higher twist operators and neglected trace terms in Eq. (1.171). These corrections are assumed negligible in the scaling limit. The analyticity properties of the full elastic Compton amplitude will be dealt with specifically in the next chapter; however, here it is sufficient to note that there are cuts in $T(\nu,Q^2)$ for

$$\nu = -\frac{q^2}{2} \longrightarrow +\infty \qquad (1.174)$$

and

$$\nu = + \frac{q^2}{2} \longrightarrow - \infty \qquad (1.174)$$

corresponding to the (massless) intermediate states propagating on shell. This is equivalent in the complex X plane (keeping q^2 fixed) to a cut between $X = \pm 1$. This analytic structure enables us to construct a dispersion relation in X relating the amplitude at some unphysical value of $X (|X| > 1)$ to the imaginary part along physical $X' \leq 1$. This where the moments of the deep inelastic structure functions arise naturally. Specifically,

$$T(X,Q^2) = -\frac{1}{\pi}\int_{-1}^{+1} dX' \frac{1}{X'} \sum_{n=0}^{\infty} \left(\frac{X'}{X}\right)^n \mathrm{Im}\left[T(X',Q^2)\right] \qquad (1.175)$$

we can now use this dispersion relation together with the optical theorem (1.152) to identify the coefficient of X^n in Eq. (1.173) arrive at

$$\int_0^1 dx\, x^{n-1} W(x,Q^2) = -\frac{1}{q^2} \frac{1}{(-2)^{n+2}} \sum_{i=0}^{M} A_i^n(\mu^2)\, \overline{C}_{i,n}(q^2) \qquad (1.176)$$

Thus, the moments of the deep inelastic structure functions have a Q^2 dependence in the asymptotic region given by that of the coefficient functions appearing in the Operator product expansion. The sum in Eq. (1.176) is over twist $\tau = 2$, spin n operators. For the scalar case considered there is only one such operator, that of Eq. (1.158).

A few remarks are necessary in order to extend this analysis to the product of vector currents as is required for the singular behaviour of light-cone Q.C.D. Firstly, the operator product expansion

is richer due to the independent Lorentz covariant tensor structures that can be constructed. There are five independent tensors

$$g_{\mu\nu} \quad g_{\mu\mu_1} z_\nu \quad z_\mu g_{\nu\mu_1} \quad g_{\mu\mu_1} g_{\nu\mu_2} \quad z_\mu z_\nu \tag{1.177}$$

But for electroproduction there exist only two linearly independent Lorentz covariant structures. This is equivalent to the statement there are only two independent tensorial decompositions of $T_{\mu\nu}$ (or $W_{\mu\nu}$). Thus for vector currents

$$i\,T[J_\mu(z)\,J_\nu(0)] \underset{\substack{z^2\to 0 \\ z^\mu \neq 0}}{\approx} \sum_{i=0}^{M}\sum_{n=0}^{\infty}\Bigg[\left(g_{\mu\nu}\Box - z_\mu z_\nu\right)\frac{z_{\mu_1}z_{\mu_2}}{z^2+i\varepsilon z_0}\,C^i_{1,n}(z)$$

$$-\left(g_{\mu\mu_1}g_{\nu\mu_2}\Box - g_{\mu\mu_1}\partial_\nu\partial_{\mu_2} - \partial_\mu g_{\nu\mu_1}\partial_{\mu_2} + g_{\mu\nu}\partial_{\mu_1}\partial_{\mu_2}\right)C^i_{2,n}(z)\Bigg] z_{\mu_3}\cdots z_{\mu_n}\,O_i^{n\,\mu_1\cdots\mu_n} \tag{1.178}$$

With this added complication we can now proceed as for the scalar case and arrive at the generic result

$$\int_0^1 dx\, x^{n-2} F_k(x,Q^2) = M_k(n,Q^2) = \sum_{i=0}^{n} A_i^n(\mu^2)\, C^i_{k,n}\left(\frac{Q^2}{\mu^2}, g^2\right) \tag{1.179}$$

where in the deep inelastic limit the structure functions approach

$$\nu W_k(\nu,Q^2) \longrightarrow F_k(x,Q^2) \qquad k = 1,2,3 \tag{1.180}$$

$$W_1(\nu,Q^2) \longrightarrow F_1(x,Q^2) \tag{1.181}$$

$$\nu W_L = \nu W_2 - 2x W_1 \tag{1.182}$$

The sum in Eq. (1.179) is over the twist $\tau=2$ spin n operators of Eq's (1.159) to (1.161). The effects of the operator O_{NS} can be isolated by looking at flavour non-singlet combinations of structure functions such as $\nu W_2^{e\text{-proton}} - \nu W_2^{e\text{-neutron}}$

A second comment concerns the terms neglected in the Bjorken limit in this analysis. There were two sources of these terms, one being the (infinitely many) higher twist operators for a given spin n, and the other the trace terms encountered when taking matrix elements of local operators. There are at present no techniques available for the calculation of higher twist effects; however, we saw that these were suppressed by powers of $\left(\frac{1}{q^2}\right)$.

The trace terms of Eq. (1.171) are of order $\left(\frac{m_H^2}{q^2}\right)$ where m_H is the mass of the hadronic target. At infinite Q^2 they are not present and so the simple moments of Eq. (1.179) arise from operators of fixed spin n and leading twist $\tau=2$. At finite Q^2 all operators of spin $\leq n$ contribute to these simple moments. It is possible however, to re-define the moments such that for the $n-2$ moment, operators of spin n only contribute, as is the case for a massless target (or infinite Q^2). These moments take the following form [1.33]

$$M_i(n,Q^2) = \int_0^1 dx \; \frac{f^{n+1}}{x^k} \; K_i(n,x;Q^2) \; F_i(x,Q^2) \qquad (1.183)$$

where for say $i=2$, then $k=3$ and

$$K_2(n,x,Q^2) = \frac{n^2+2n+3 \; +3(n+1)\sqrt{1+4x^2\frac{m_H^2}{Q^2}} \; +(n+2)nx^2\frac{m_H^2}{Q^2}}{(n+2)(n+3)} \qquad (1.184)$$

and

$$\xi = \frac{2x}{1+\sqrt{1+4x^2\frac{m_H^2}{Q^2}}} \tag{1.185}$$

for $Q^2 \to \infty$ these Nachtmann moments reduce to the simple moments

$$M_2(n,Q^2) = \int_0^1 dx\ x^{n-2} F_2(x,Q^2) \tag{1.186}$$

The correction factors K_i are designed to account for target mass effects present in the experimental structure functions $F_i(x,Q^2)$. So with their inclusion one can relate directly the experimental distributions to the asymptotic freedom predictions for moments calculated in the massless case $M_i(n,Q^2)$.

An alternative (but theoretically equivalent) approach is to work directly with the structure functions relating the experimentally measured quantities $\nu W_k(\nu,Q^2)$ to those obtained by inverting the asymptotic freedom moment predictions, $F_k(x,Q^2)$.

in the massless case for $k=2$

$$\nu W_2(x,Q^2) = F_2(x,Q^2) \tag{1.187}$$

With the inclusion of target mass corrections [1.34]

$$\nu W_2(x,Q^2) = \frac{1}{\left(1+4x^2\frac{m_H^2}{Q^2}\right)^{\frac{3}{2}}}\frac{x^2}{\xi^2}F_2(\xi,Q^2)$$

$$+ 6\frac{m_H^2}{Q^2}\frac{x^3}{\left(1+4x^2\frac{m_H^2}{Q^2}\right)^2}\int_{\xi}^{\xi'_{max}} d\xi' \frac{F_2(\xi',Q^2)}{\xi'^2}$$

$$+ 12\frac{m_H^4}{Q^4}\frac{x^4}{\left(1+4x^2\frac{m_H^2}{Q^2}\right)^{\frac{5}{2}}}\int_{\xi}^{\xi'_{max}} d\xi' \int_{\xi'}^{\xi''_{max}} d\xi'' \frac{F_2(\xi'',Q^2)}{\xi''^2} \qquad (1.188)$$

where

$$M_2(n,Q^2) = \int_0^{\xi_{max}} d\xi\ \xi^{n-2} F_2(\xi,Q^2) \qquad (1.189)$$

and

$$\xi_{max} = \xi'_{max} = \xi''_{max} = \frac{2}{1+\sqrt{1+4\frac{m_H^2}{Q^2}}} \qquad (1.190)$$

the kinematic limit. Similar expressions exist for $W_{1,3,L}$.
The inclusion of target mass effects, then, represents only one source of $O(\frac{1}{q^2})$ corrections, and so alone they are of limited quantitative value. However, if they are large then it seems unlikely that the twist $\tau=4$ contributions would be any less significant. All these comments are to be considered in the context of perturbation theory. There is, or course, no guarantee that when summed to all orders of perturbation theory the higher twist operators destroy the dominance

of those of twist $\tau=2$.

To summarize, the operator product expansion gives the general form for the moments of structure functions as

$$M_k(n,Q^2) = \sum_{i=0}^{M} A_i^n(\mu^2)\, C_{k,n}^i\left(\frac{Q^2}{\mu^2}, g^2\right) \qquad (1.191)$$

The utility of this technique lies in the fact that the coefficient functions $C_{k,n}^i$ are independent of the target states. They are defined through the expansion Eq. (1.178) and can be calculated perturbatively. The reduced matrix elements of local operators A_i^n are beyond perturbation theory and must be ultimately eliminated by experiment. The O.P.E. has allowed us to identify and separate out the (presently) incalculable contributions to the moments.

The asymptotic behaviour of the coefficient functions (and so of the moments themselves) can be calculated by a straightforward application of the Renormalization Group Equation (R.G.E.). The moments are physical observables and consequently cannot depend on any (arbitrary) renormalisation point μ^2 .

i.e. $$\mu \frac{d}{d\mu} M_k(n,Q^2) = 0 \qquad \text{for each } n \qquad (1.192)$$

Choosing non-singlet (NS) combinations of structure functions this is equivalent to

$$\mu \frac{d}{d\mu}\left[C_{k,n}^{NS}\, O_{NS}^n \right] = 0 \qquad (1.193)$$

the label k refers to which structure function $k = 1,2,3,L$ is under consideration. As the R.G.E holds for each k separately, it will be dropped.

Assuming the multiplicative renormalization of the bare operator $O^{0,n}_{NS}$ is given by

$$O^{0,n}_{NS} = Z^n_{NS}\, O^n_{NS} \tag{1.194}$$

and so

$$\mu \frac{d}{d\mu}\left[O^{0,n}_{NS}\right] = 0 \tag{1.195}$$

Eq. (1.193) can be written

$$\frac{1}{Z^n_{NS}} O^{0,n}_{NS}\, \mu \frac{d}{d\mu}\left[C^{NS}_n\right] + C^{NS}_n O^{0,n}_{NS}\, \mu \frac{d}{d\mu}\left[\frac{1}{Z^n_{NS}}\right] = 0 \tag{1.196}$$

or

$$\mu \frac{d}{d\mu}\left[C^{NS}_n\right] = C^{NS}_n \gamma^n_{NS}(g) \tag{1.197}$$

where

$$\gamma^n_{NS}(g) = \mu \frac{d}{d\mu}\left[\ln Z^n_{NS}\right] \tag{1.198}$$

In the Landau gauge ($\alpha = 0$) in which there is no renormalization of the gauge parameter α, this leads immediately to

$$\left[\mu \frac{\partial}{\partial \mu} + \beta(g)\frac{\partial}{\partial g} - \gamma^n_{NS}(g)\right] C^{NS}_{k,n}\left(\frac{Q^2}{\mu^2}, g^2\right) = 0 \tag{1.199}$$

As mentioned previously the flavour singlet operators O_F, O_G carry the same quantum numbers and so mix under renormalization. They satisfy a matrix R.G.E.

$$\sum_b \left[\left(\mu \frac{\partial}{\partial \mu} + \beta(g) \frac{\partial}{\partial g} \right) \delta_{ab} - \gamma^n_{ab}(g) \right] C^b_n\left(\frac{Q^2}{\mu^2}, g^2\right) = 0 \qquad (1.200)$$

where the 2 × 2 anomalous dimension matrix

$$\gamma^n_{ab}(g) = \left(\mu \frac{\partial}{\partial \mu} \ln Z \right)_{ab} \qquad (1.201)$$

and

$$O^{0,n}_a = \sum_b (Z^n)_{ab} \, O^n_b \qquad (1.202)$$

Since this thesis is not concerned with singlet combinations of structure functions we will not consider flavour singlet operators further but refer the reader to a review by Buras [1.29] for a thorough treatment.

Eq. (1.199) can be solved to give (analagous to Eq. (1.105))

$$C^{NS}_{k,n}\left(\frac{Q^2}{\mu^2}, g^2\right) = C^{NS}_{k,n}\left(1, \bar{g}^2\right) \exp\left[- \int_{\bar{g}(\mu^2)}^{\bar{g}(Q^2)} dg' \, \frac{\gamma^n_{NS}(g')}{\beta(g')} \right] \qquad (1.203)$$

where the 1 means evaluated at $Q^2 = \mu^2$.

Thus for non-singlet moments

$$M^{NS}_k(n, Q^2) = A^{NS}_n\left(\frac{p^2}{\mu^2}, g^2\right) C^{NS}_{k,n}\left(1, \bar{g}^2\right) \exp\left[- \int_{\bar{g}(\mu^2)}^{\bar{g}(Q^2)} dg' \, \frac{\gamma^n_{NS}(g')}{\beta(g')} \right] \qquad (1.204)$$

Since we cannot calculate the moments up to an overall normalization (this reflects ignorance of the size of matrix elements of local operators) then the normalization of $C^{NS}_{k,n}$ and A^{NS}_n are chosen such that

$$C^{0,NS}_{k,n} = A^{0,NS}_n = 1 \tag{1.205}$$

we then have perturbative expansions as follows:-

$$A^{NS}_n\left(\frac{p^2}{\mu^2}, g^2\right) = \tilde{A}^{NS}_n\left[1 + \left(\frac{g}{4\pi}\right)^2\left(\tfrac{1}{2}\gamma^n_{NS}\ln\left(\frac{-p^2}{\mu^2}\right) + A^{2,NS}_n\right) + \cdots\right] \tag{1.206}$$

(1.207)

$$C^{NS}_{k,n}\left(1, \bar{g}^2\right) = \begin{cases} \delta^k_{NS}\left(1 + \left(\frac{\bar{g}}{4\pi}\right)^2 B^{1,NS}_{k,n} + \cdots\right) & k = 1,2,3 \\ \delta^L_{NS}\left(0 + \left(\frac{\bar{g}}{4\pi}\right)^2 B^{1,NS}_{L,n} + \left(\frac{\bar{g}}{4\pi}\right)^2 B^{2,NS}_{L,n} + \cdots\right) & k = L \end{cases} \tag{1.208}$$

$$\gamma^n_{NS}(g) = \left(\frac{g}{4\pi}\right)^2 \gamma^{0,n}_{NS}(g) + \left(\frac{g}{4\pi}\right)^4 \gamma^{1,n}_{NS}(g) + \cdots \tag{1.209}$$

The perturbative expansion for $\beta(g)$ was given in Eq. (1.117). δ^k_{NS} are constants that depend on the weak and electromagnetic charges. For electron-proton or electron-neutron scattering $\delta^k_{NS} = \delta^L_{NS} = \frac{1}{6}$.

In order to calculate matrix elements of local operators, effective Feynman rules for the insertion of lowest twist operators are needed. These are found by introducing into the Lagrangian a source term

$$\Delta_{\mu_1} \cdots \Delta_{\mu_n} O_i^{\mu_1 \cdots \mu_n} \tag{1.210}$$

with Δ_μ an arbitrary light-like four vector $\Delta^2 = 0$. For the calculation of non-singlet matrix elements, this leads to the Feynman rules shown in figure 1.10, where the crosses represent an operator insertion [1.24].

The quantity Γ^n_{NS} is determined by calculating the coefficient of the pole term of the diagrams in Fig. 1.11 (this is true only at one loop level), but now there exists a choice of procedure to follow. One can either:

(a) calculate all diagrams of Fig. 1.11, in which case one must include diagrams involving external fermion leg renormalizations when computing the coefficient functions. In this case

$$r^n_{NS} = \gamma^{0,n}_{NS} \tag{1.211}$$

(b) Ignore diagrams (d) and (e) of Fig. 1.11 and the corresponding diagrams with external fermion leg renormalisations contributing to the coefficient functions. Now one must add in by hand the previously calculated anomalous dimension of the fermion field. then

$$r^n_{NS} = \gamma^{0,n}_{NS} - 2\gamma^0_F \tag{1.212}$$

As option (b) reduces the number of diagrams to be evaluated by four, this is the procedure we shall adopt.

The lowest order non-singlet anomalous dimensions are found to be

$$\gamma^{0,n}_{NS} = 2C_2(R)\left[1 - \frac{2}{n(n+1)} + 4\sum_{j=2}^{n}\frac{1}{j}\right] \tag{1.213}$$

with $C_2(R) = \frac{4}{3}$ for $SU(3)$.

We now have all the necessary ingredients in order to extract the leading order Q.C.D. result for the moments of non-singlet structure functions.

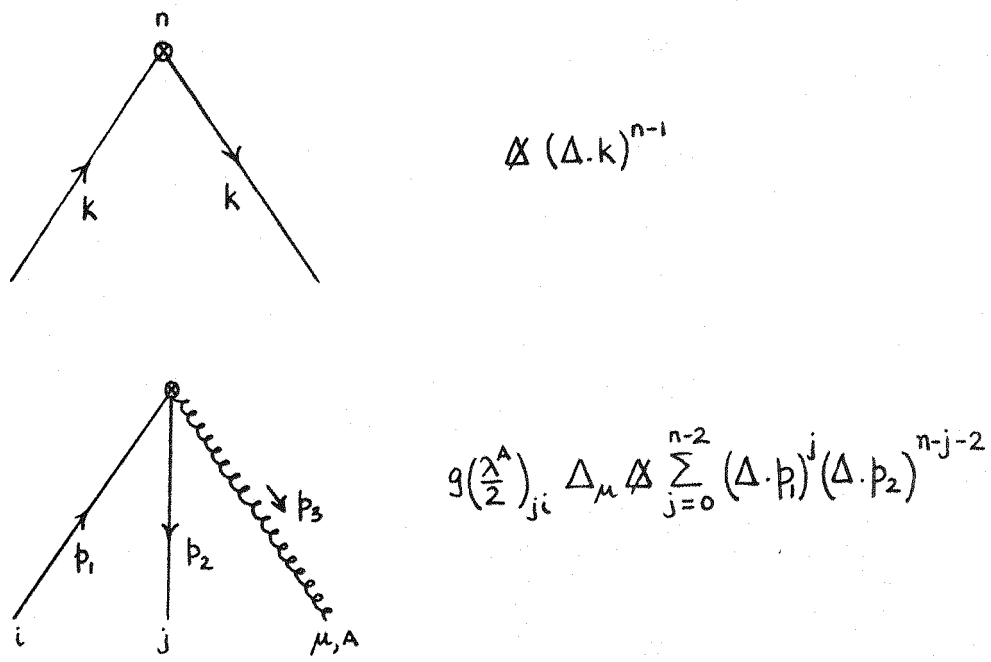

Fig 1.10 Feynman rules necessary for the calculation of non-singlet matrix elements

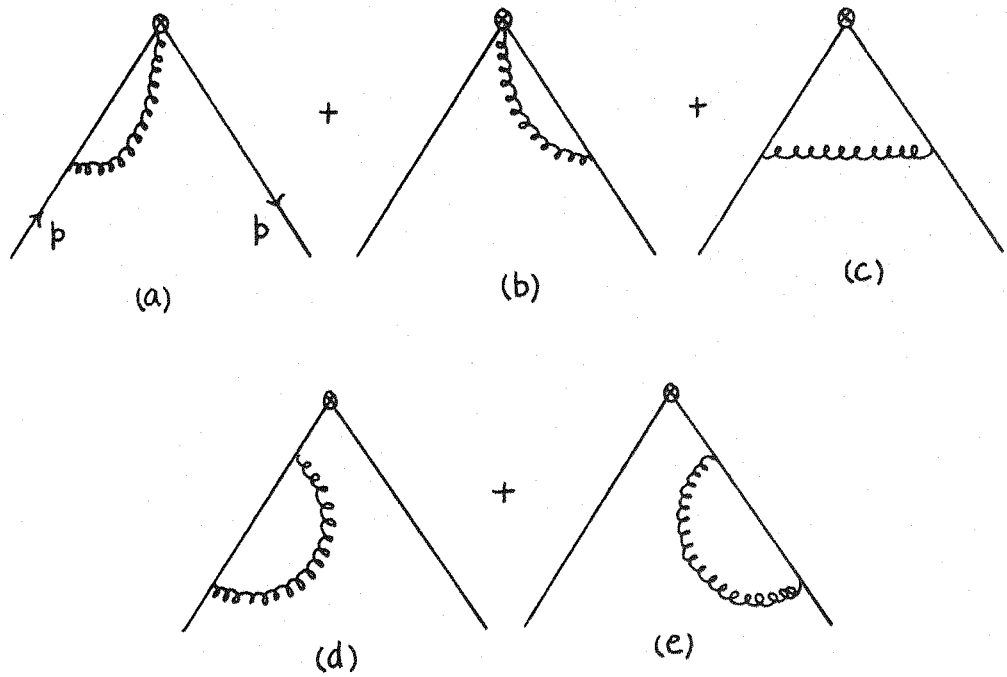

Fig 1.11 Diagrams entering in the calculation of $\gamma_{NS}^{0,\,n}$

Keeping only lowest order terms in the expansion of γ^n_{NS} and $\beta(g)$, the exponential in Eq. (1.203) can be integrated explicitly to give

$$\exp\left[-\int_{\bar{g}(\mu^2)}^{\bar{g}(Q^2)} dg' \frac{\gamma^n_{NS}(g')}{\beta(g')}\right] \sim \left[\frac{\bar{g}(Q^2)}{\bar{g}(\mu^2)}\right]^{d^n_{NS}} \tag{1.214}$$

where

$$d^n_{NS} = \frac{\gamma^{0,n}_{NS}}{2\beta_0} \tag{1.215}$$

Using the form of the effective coupling constant obtained from the one loop β function, and setting $\mu^2 = Q_0^2$ some reference momentum (still large enough for the application of perturbation theory) then we arrive at

$$\int_0^1 dx\, x^{n-2} F_k(x,Q^2) = \begin{cases} A^{NS}_n \delta^k_{NS} \left[\dfrac{\ln\left(\frac{Q^2}{\Lambda^2}\right)}{\ln\left(\frac{Q_0^2}{\Lambda^2}\right)}\right]^{-d^n_{NS}} & k=1,2,3 \qquad (1.216) \\ 0 & k=L \qquad (1.217) \end{cases}$$

$\tilde{A}^{NS}_n$ is an overall (unknown) normalisation constant that can be found from the moments at Q_0^2 taken from experiment. Hence, leading order Q.C.D. necessarily involves a logarithmic (in Q^2) violation of Bjorken scaling, the strength of the effect, Λ, being an unknown free parameter of the theory to be fitted to experiment. The comparison of this leading order result with the scaling violations seen at SLAC for νW_2 can be seen in Fig. 1.13. The best value of the fitted value of Λ is found to be [1.35]

$$\Lambda \sim 0.3 \text{ Gev} \tag{1.218}$$

To leading order in Q.C.D. all parton model sum rules remain unchanged. The only difference introduced is that now the parton distributions depend on both x and Q^2 in a calculable manner. At higher orders, we expect a violation of these sum rules. Using the fitted value of Λ, we can determine the size of the effective coupling constant from

$$\alpha_s(Q^2) = \frac{1}{\beta_0 \ln\left(\frac{Q^2}{\Lambda^2}\right)} \tag{1.219}$$

for 4 flavours $\beta_0 = \frac{25}{3}$, thus

$$\alpha_s(Q^2 = 10\,\text{Gev}^2) \sim 0.3 \tag{1.220}$$

This is still a reasonably large expansion parameter at accessible values of Q^2 and so it is important to check the significance of higher order corrections.

To go beyond leading order involves the computation of the next terms in the expansion for $\gamma^n_{NS}(g)$, $\beta(g)$ and $C^{NS}_{k,n}(1, g^2)$. The two loop contribution to the anomalous dimensions of twist 2 non-singlet operators $\gamma^{1,n}_{NS}$, has been calculated [1.36]. Recall that

$$\gamma^n_{NS}(g) = \mu \frac{\partial}{\partial \mu}\left(\ln Z^n_{NS}\right) \tag{1.221}$$

then, in the minimal subtraction scheme (MS)

$$\gamma^n_{NS} = -g^2 \frac{\partial Z^n_1}{\partial g^2} \tag{1.222}$$

where

$$Z^n_{NS} = 1 + \sum_{i=1}^{\infty} \frac{Z^n_i(g^2)}{\varepsilon^i}, \quad D = 4 - 2\varepsilon \tag{1.223}$$

Thus to determine $\gamma^{1,n}_{NS}$ it is necessary to evaluate the coefficient of $\frac{1}{\epsilon}$ (the sub-leading ultra-violet divergence) in all of the two loop diagrams that renormalize O^n_{NS}. A summary of the techniques needed to calculate these diagrams together with the results of the calcualtion can be found in ref. [1.36]. As mentioned previously, the coefficient of the two loop β function, β_1, has been calculated by a similar method to that above. Again recall

$$\beta(g) = \mu \frac{\partial}{\partial \mu} g \tag{1.224}$$

in the MS scheme with $D = 4-2\epsilon$, then

$$\beta(g) = \epsilon g + g^3 \frac{\partial Z^1_g}{\partial g^2} \tag{1.225}$$

where

$$g_0 = Z_g g_R \tag{1.226}$$

and

$$Z_g = 1 + \sum_{i=1}^{\infty} \frac{Z^i_g}{\epsilon^i} \tag{1.227}$$

So β_1 can be determined by calculating the coefficient of $\frac{1}{\epsilon}$ in all of the two loop diagrams that renormalise the coupling constant g.

The result [1.26] is

$$\beta_1 = 102 - \frac{38}{3} f \tag{1.228}$$

with f being the number of fermion flavours.

Finally, the next term in the expansion of the coefficient function $B^{1,NS}_{k,n}$ can be determined by the following procedure. Using the fact that the coefficient functions are independent of the states

between which we sandwich the currents we may choose the most convenient states and calculate deep inelastic scattering on a quark of space-like momentum p. In this case the lowest order contribution is due to elastic quark scattering, leading to a structure function of $\delta(1-x)$. Thus all lowest order moments are normalised to 1. Beyond leading order we calculate all the one loop corrections to the elastic Compton Amplitude (see Fig. 1.12) for unphysical Bjorken $x(>1)$ and express the answer as a power series in $\frac{1}{x}$. A dispersion relation states that the coefficient of $\left(\frac{1}{x}\right)^n$ is proportional to the nth moment of the deep inelastic structure function. Next we expand the right hand side of Eq. (1.204) in terms of $\bar{g}(\mu^2) = g$ to obtain

$$1 + \left(\frac{g}{4\pi}\right)^2 \left[-\frac{\gamma_{NS}^{0,n}}{2} \ln\left(\frac{q^2}{p^2}\right) + M_{k,n}^{1,NS} \right]$$

$$= \left[1 + \left(\frac{g}{4\pi}\right)^2 \left(\frac{\gamma_{NS}^{0,n}}{2} \ln\left(\frac{-p^2}{\mu^2}\right) + A_n^{2,NS} \right) \right] \delta_{NS}^k \left[1 + \left(\frac{g}{4\pi}\right)^2 B_{k,n}^{1,NS} \right] \cdot$$

$$\cdot \left[1 - \left(\frac{g}{4\pi}\right)^2 \frac{\gamma_{NS}^{0,n}}{2} \ln\left(\frac{-q^2}{\mu^2}\right) \right] \qquad (1.229)$$

The only unknown in the above equation is $B_{k,n}^{1,NS}$.

The Q.C.D. result including next to leading order contributions can be found by re-expanding Eq. (1.204) in terms of the effective coupling constant $\bar{g}(Q^2)$. The general form is (for $\mu^2 = Q_0^2$)

$$M_k^{NS}(n,Q^2) = \tilde{A}_n^{NS} \delta_{NS}^k \left[\frac{\ln\left(\frac{Q^2}{\Lambda^2}\right)}{\ln\left(\frac{Q_0^2}{\Lambda^2}\right)} \right]^{-d_{NS}^n} \left[1 + \left(\frac{\bar{g}_0(Q^2)}{4\pi}\right)^2 \left(E_n^k + F_n + G_n(Q^2) \right) \right] \qquad (1.230)$$

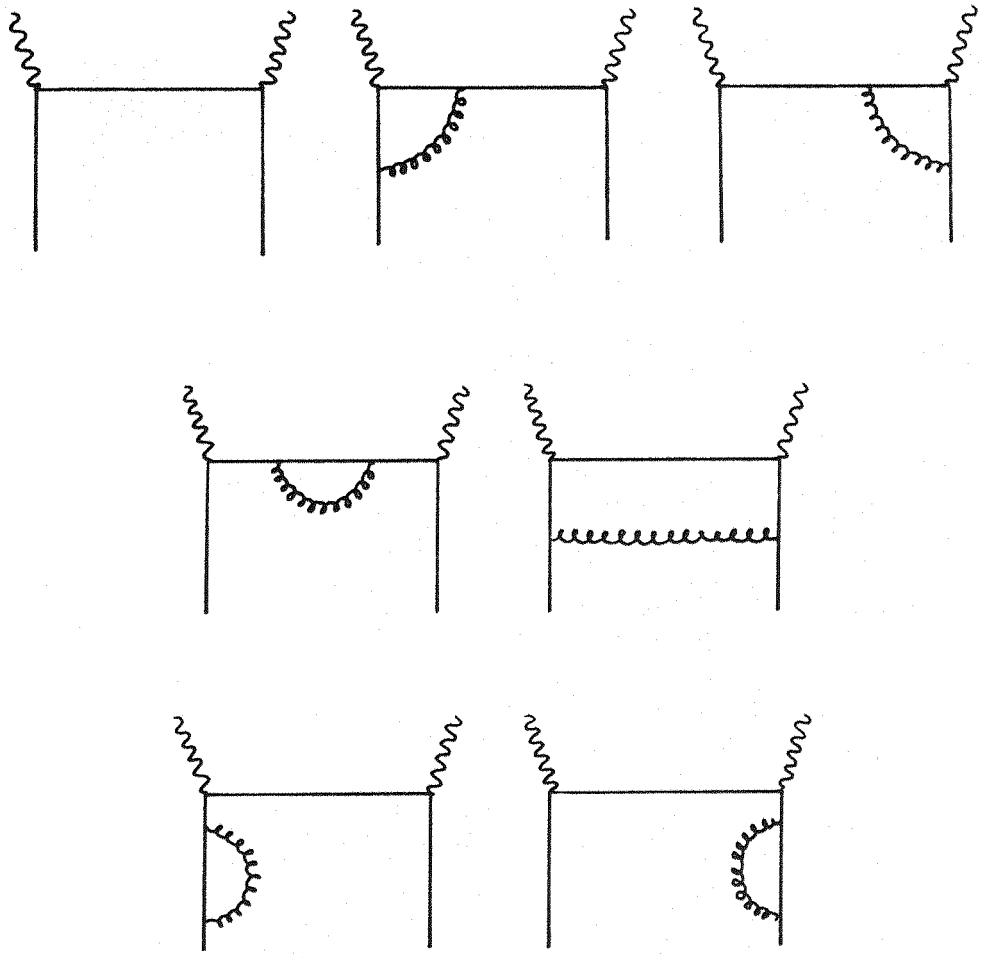

Fig. 1.12 Diagrams of the elastic Compton amplitude to $O(g^2)$ necessary to determine the coefficient functions

where

$$\bar{g}_0(Q^2) = \frac{16\pi^2}{\beta_0 \ln\left(\frac{Q^2}{\Lambda^2}\right)} \tag{1.231}$$

$$E_n^K = B_{K,n}^{1,NS} \tag{1.232}$$

$$F_n = \frac{\gamma_{NS}^{1,n}}{2\beta_0} - \frac{\gamma_{NS}^{0,n}\beta_1}{2\beta_0^2} \tag{1.233}$$

$$G_n(Q^2) = -\frac{\gamma_{NS}^{0,n}\beta_1}{2\beta_0^2} \ln\ln\left(\frac{Q^2}{\Lambda^2}\right) \tag{1.234}$$

A few technical comments are in order. If all renormalization is carried out in the MS scheme, then the gauge dependence of the virtual compton amplitude and the matrix elements of local operators are the same and cancel, leaving $C_{K,n}^{NS}(1,\bar{g}^2)$ a gauge invariant quantity [1.37]. It remains renormalization prescription dependent; however, this dependence is cancelled by that of the two loop anomalous dimensions [1.36]. All other perturbative quantities are both guage and renormalization prescription independent, resulting in a physical answer for the moments. Of course, there still exists an overall prescription dependence due to the definition of the coupling g. The actual numerical value of the higher order corrections looks significant. If, as for the leading order

$$\frac{\alpha_s}{4\pi}(Q^2 = 10\,\text{Gev}^2) \sim 2\% \tag{1.235}$$

Then

$$\left.\frac{\bar{g}_0^2(Q^2)}{(4\pi)^2}\left(E_n + F_n + G_n(Q^2)\right)\right|_{Q^2=10\text{Gev}^2} \gtrsim 50\% \quad \text{for } n=4 \tag{1.236}$$

and increasing for increasing n .

However, these corrections become almost entirely incorporated [1.35] into a re-fitted $\Lambda = 0.346$ Gev and lead to no further improvement on the agreement between theory and experiment. The inclusion of target mass corrections does provide such an improvement, and gives the optimum value of $\Lambda = 0.474$ Gev. For an illustration of the comparison between theory and the experimental results for $\nu W_2(x,Q^2)$ (non-singlet) see Fig. (1.13).

The general results of the application of perturbative Q.C.D. to deep inelastic processes may be summarized by saying that the parton distributions acquire a (perturbatively) calculable Q^2 dependence roughly in agreement with that observed. To leading order, all parton model sum rules remain unchanged, and are violated logarithmically in Q^2 at higher orders. For example the Bjorken sum rule of Eq. (1.46) becomes [1.37, 1.38]

$$\int_0^1 dx \left[F_1^{\bar{\nu}p}(x) - F_1^{\nu p}(x) \right] = 1 - \frac{8}{3} \cdot \frac{1}{\beta_0 \ln\left(\frac{Q^2}{\Lambda^2}\right)} \qquad (1.237)$$

Some insight into the Q^2 dependence of the structure functions can be gained by considering the following intuitive argument [1.39] . By increasing the Q^2 of the virtual photon (or weak boson) one imagines that the beam is probing smaller and smaller distances. Thus at higher Q^2, a quark is resolved into a quark and soft gluon, and a gluon into a quark-anti-quark pair or two gluons. In such a picture, parton distributions are then naturally Q^2 dependent.

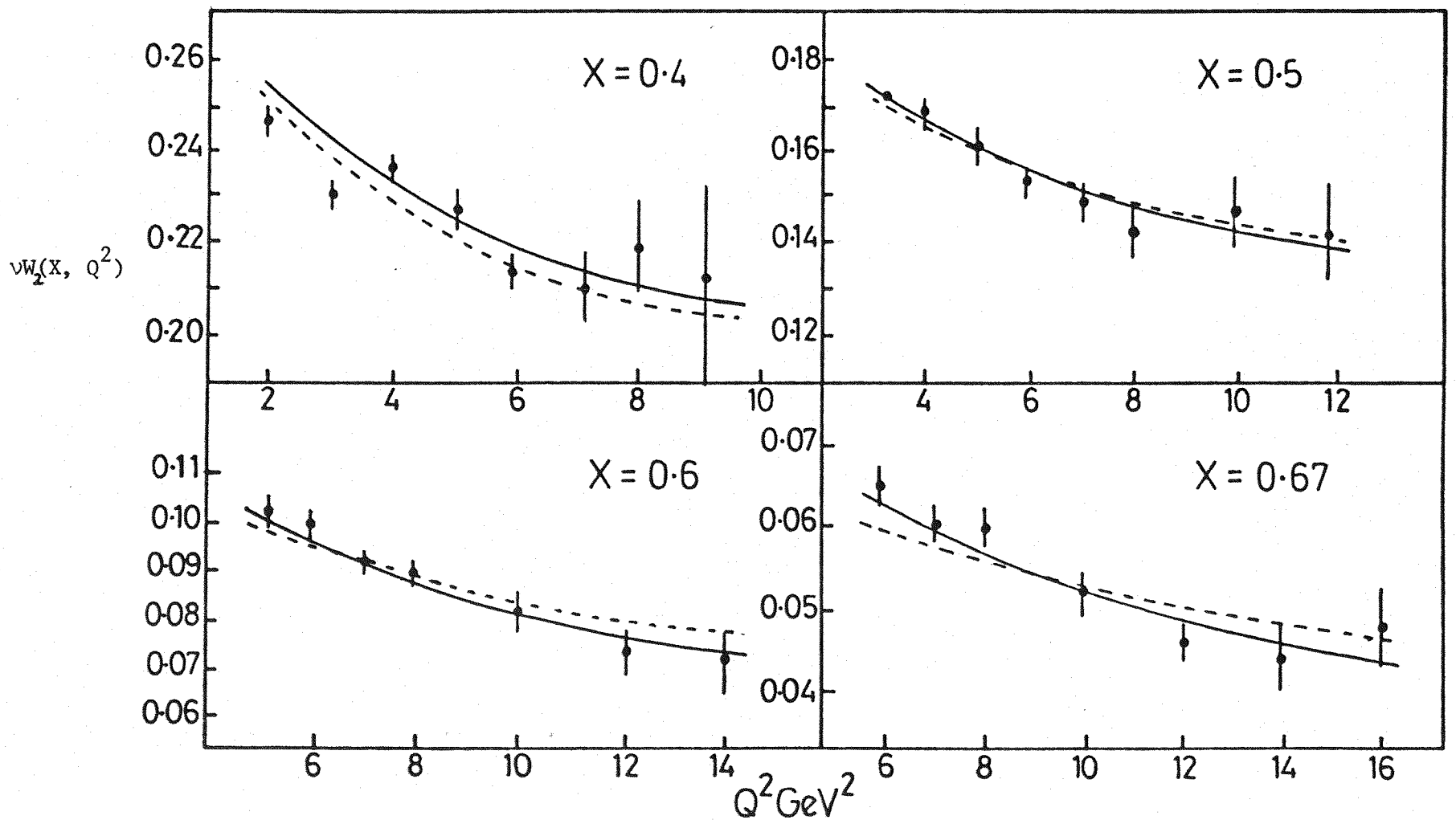

Fig 1.13

------ leading order QCD

——— next to leading order QCD + target mass corrections

If $t = \ln\left(\frac{Q^2}{Q_o^2}\right)$ then the leading order Q.C.D. result for the moments of non-singlet structure functions Eq. (1.216) can be written

$$M_k(n,t) = M_k(n,0)\left[\frac{\alpha_s(t)}{\alpha_s(0)}\right]^{d_{NS}^n} \tag{1.238}$$

with

$$\alpha_s(t) = \frac{1}{\frac{4\pi}{g^2} + \frac{\beta_0}{4\pi}t} \tag{1.239}$$

Thus

$$\frac{d}{dt}M_k(n,t) = -\frac{\gamma_{NS}^{o,n}}{8\pi}\alpha_s(t)\,M_k(n,t) \tag{1.240}$$

The convolution theorem states that the moment of the convolution of two functions is equal to the product of the separate moments of the functions.

Thus if

$$H_1(x) = \int_x^1 \frac{dy}{y} H_2(y) H_3\left(\frac{x}{y}\right) \tag{1.241}$$

Then

$$M_1(n) = M_2(n).\,M_3(n) \tag{1.242}$$

where

$$M_i(n) = \int_0^1 dx\; x^{n-1} H_i(x) \tag{1.243}$$

So if we can define a function whose moments are $\gamma_{NS}^{o,n}$ then Eq. (1.240) can be inverted

let

$$\int_0^1 dz\, z^{n-1}\, P_{qq}(z) \;=\; -\frac{\gamma_{NS}^{0,n}}{4} \tag{1.244}$$

Now inverting (1.240) we arrive at

$$\frac{d}{dt}\Delta_{ij}(x,t) \;=\; \frac{\alpha(t)}{2\pi}\int_x^1 \frac{dy}{y}\,\Delta_{ij}(y,t)\,P_{qq}\left(\frac{x}{y}\right) \tag{1.245}$$

with Δ_{ij} being some non-singlet combination of structure functions occurring in a process labelled by i and j (for example $\Delta_{ep}(x,t)$ $\Delta_{en}(x,t)$). Similarly, the evolution equations for the flavour singlet $\Sigma(x,t)$ and gluon $G(x,t)$ distributions can be constructed as

$$\frac{d}{dt}\Sigma(y,t) \;=\; \frac{\alpha(t)}{2\pi}\int_x^1 \frac{dy}{y}\left[\Sigma(y,t)\,P_{qq}\left(\frac{x}{y}\right) + 2f\,G(y,t)\,P_{qG}\left(\frac{x}{y}\right)\right] \tag{1.246}$$

$$\frac{d}{dt}G(y,t) \;=\; \frac{\alpha(t)}{2\pi}\int_x^1 \frac{dy}{y}\left[\Sigma(y,t)\,P_{Gq}\left(\frac{x}{y}\right) + G(y,t)\,P_{GG}\left(\frac{x}{y}\right)\right] \tag{1.247}$$

These equations are coupled due to the fact that gluons can convert into $q\bar{q}$ pairs in a flavour invariant way.

The 'splitting functions' [1.40] $P_{qq}(z)$ etc are interpreted as probability functions in the following way. $P_{qq}\left(\frac{y}{x}\right)$ gives the probability of finding a quark of momentum fraction y in a quark of momentum fraction x. They are defined through the vertices of Fig. (1.14) and have moments proportional to the entries in the anomalous dimension matrix $\tilde{\gamma}^{0,n}$

$$\tilde{\gamma}^{0,n} \;=\; \begin{pmatrix} \gamma_{FF}^{0,n} & \gamma_{FG}^{0,n} \\ \gamma_{GF}^{0,n} & \gamma_{GG}^{0,n} \end{pmatrix} \tag{1.248}$$

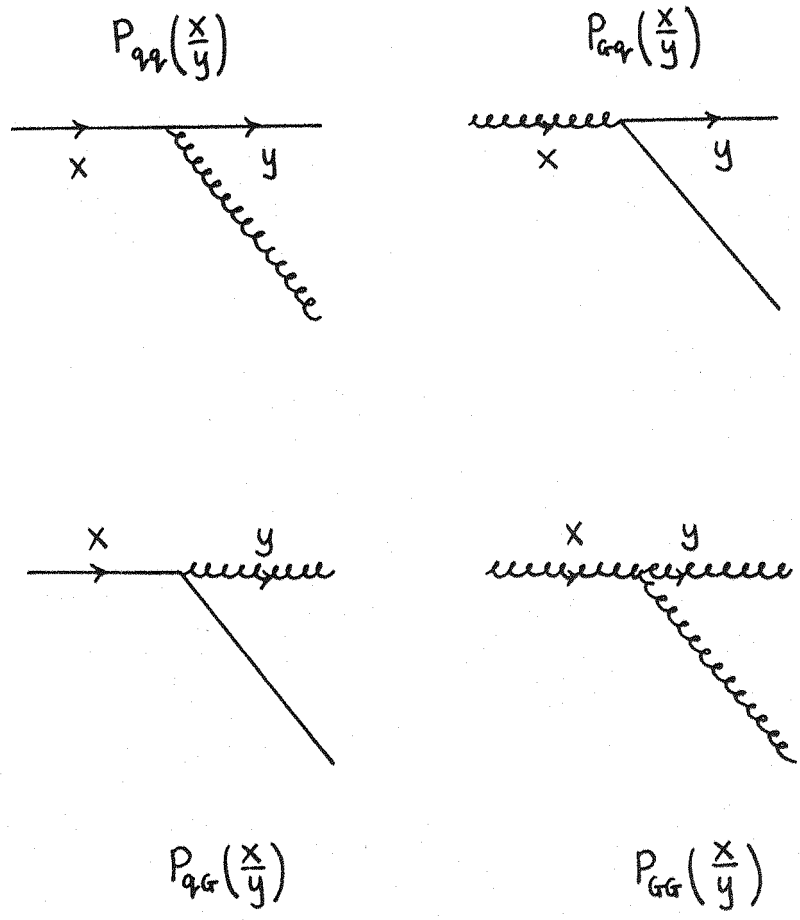

Fig. 1.14 Vertices defining the splitting functions

with

$$\gamma_{FF}^{0,n} = \gamma_{NS}^{0,N} = \frac{8}{3}\left(1 - \frac{2}{n(n+1)} + 4\sum_{j=2}^{n}\frac{1}{j}\right) = -4\int_0^1 dz\, z^{n-1} P_{qq}(z) \tag{1.249}$$

$$\gamma_{FG}^{0,n} = -4f\,\frac{n^2+n+2}{n(n+1)(n+2)} = -8f\int_0^1 dz\, z^{n-1} P_{qG}(z) \tag{1.250}$$

$$\gamma_{GF}^{0,n} = -\frac{16}{3}\,\frac{n^2+n+2}{n(n^2-1)} = -4\int_0^1 dz\, z^{n-1} P_{Gq}(z) \tag{1.251}$$

$$\gamma_{GG}^{0,n} = 6\left[\frac{1}{3} - \frac{4}{n(n-1)} - \frac{4}{(n+1)(n+2)} + 4\sum_{j=2}^{n}\frac{1}{j}\right] + \frac{4}{3}f$$

$$= -4\int_0^1 dz\, z^{n-1} P_{GG}(z) \tag{1.252}$$

The $P_{\alpha\beta}(z)$ are thus given explicitly in Q.C.D. as

$$P_{qq}(z) = \frac{4}{3}\left[\frac{1+z^2}{(1-z)_+} + \frac{3}{2}\delta(1-z)\right] \tag{1.253}$$

$$P_{qG}(z) = \frac{1}{2}\left[z^2 + (1-z)^2\right] \tag{1.254}$$

$$P_{Gq}(z) = \frac{4}{3}\left[\frac{1+(1-z)^2}{z}\right] \tag{1.255}$$

$$P_{GG}(z) = 6\left[\frac{z}{(1-z)_+} + \frac{(1-z)}{z} + z(1-z) + \left(\frac{11}{12} - \frac{f}{18}\right)\delta(1-z)\right] \tag{1.256}$$

where the distribution $\frac{1}{(1-z)_+}$ is defined through

$$\int_0^1 dz\,\frac{f(z)}{(1-z)_+} \equiv \int_0^1 dz\,\frac{f(z)-f(1)}{(1-z)} \tag{1.257}$$

with $f(z)$ any function regular at its endpoints.

Thus the probabilistic type framework of the parton model has been retained in the context of perturbative Q.C.D. It must be remarked however, that there is no unique definition of parton distributions beyond leading order.

Finally, it is important to note that the use of the Operator Product Expansion is not the only approach to deep inelastic processes. A completely equivalent analysis [1.41] has been carried out by studying the Feynman diagrams that describe the process and identifying their dominant contribution at some large momentum transfer Q^2. The criterion used to perform this identification is known as the Leading Logarithmn Approximation (L.L.A.) in which one keeps all terms of the form

$$\left[\alpha_s \ln\left(\frac{Q^2}{\mu^2}\right)\right]^n \tag{1.258}$$

but neglects contributions of the type

$$(\alpha_s)^k \left[\alpha_s \ln\left(\frac{Q^2}{\mu^2}\right)\right]^m \qquad k \geq 1 \tag{1.259}$$

where μ^2 is some typical parton virtualness (i.e. 4-momenta squared) at which perturbation theory is assumed valid

$$\frac{\alpha_s(\mu^2)}{4\pi} \ll 1 \tag{1.260}$$

It follows that μ^2 must be at least comparable to the average momentum of valence quarks in a nucleon

$$\mu^2 \gtrsim (300\,\text{Mev})^2 \gtrsim 0{\cdot}1\ \text{Gev}^2 \tag{1.261}$$

Thus the L.L.A. requires selecting those Feynman diagrams that give the maximum power of $\ln(Q^2)$ to a given order of perturbation theory. An analysis of the lowest order graph of Fig. (1.15) shows that the principal contribution (i.e. $\sim \alpha_s \ln\left(\frac{Q^2}{\mu^2}\right)$) comes from the region where

$$\mu^2 \sim p^2 \ll |k|^2 \sim k_\perp^2 \ll Q^2 \tag{1.262}$$

and

$$\mu^2 \ll M'^2 = (k+q)^2 \ll Q^2 \tag{1.263}$$

This is the region where the initial parton struck by the virtual photon, and the final parton are not very virtual (i.e. far off shell) with respect to the large momentum transfer Q^2. These are the basic assumptions of Feynman's parton model although in a somewhat weaker sense since here the parton $k_\perp^i$ do grow with increasing Q^2. This result can be extended to the nth order perturbation theory ladder type diagram of Fig. (1.16) to yield the dominant kinematic region as

$$\mu^2 \sim p^2 \ll k_1^2 \sim k_{1\perp}^2 \ll k_2^2 \cdots\cdots \ll k_{n-1}^2 \sim k_{n-1_\perp}^2 \ll k_n^2 \sim k_{n_\perp}^2 \ll Q^2 \tag{1.264}$$

with

$$1 \geq \rho_1 \geq \rho_2 \cdots\cdots \geq \rho_{n-1} \geq \rho_n \sim X \tag{1.265}$$

where ρ_i is the fraction of longitudinal momentum of the original parton carried by the ith parton up the ladder.

These ladder diagrams constitute the dominant contribution to deep inelastic scattering if one deals solely with the emission of real physical gluons [1.42]. This amounts to choosing a physical transverse gauge (such as the axial or planar gauges) in which the unphysical spurious degrees of freedom of the gluon do not propagate by virtue of

$$k^\mu \varepsilon_\mu = 0 \tag{1.266}$$

with k_μ and ε_μ being the gluon 4-momentum and polarisation 4-vector respectively. Although these gauges are ghost-less, they are in general

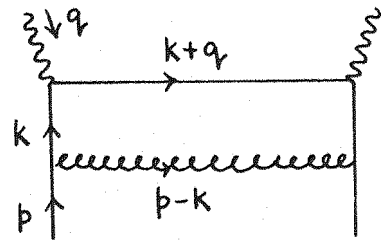

Fig 1.15 Lowest order ladder diagram in the leading logarithm approximation giving the leading contribution to deep inelastic scattering

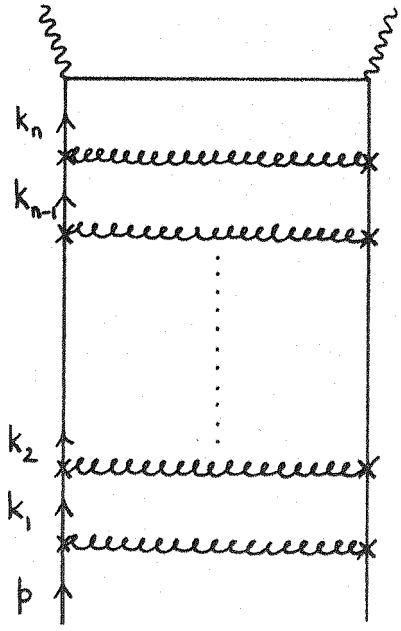

Fig 1.16 The dominant diagram for deep inelastic scattering in the leading logarithm approximation at nth order perturbation theory. The X's represent self energy and vertex insertions.

cumbersome to work in. However, in such gauges all crossed diagrams are suppressed by powers of $\ln(Q^2)$ relative to the ladder diagrams.

Both the transverse and longitudinal momentum integrals up the ladder can be performed and the result summed to all orders of perturbation theory to reproduce the standard leading order expression for the moments of structure functions from the operator product expansion

$$M(n,Q^2) \sim \left[\ln\left(\frac{Q^2}{\Lambda^2}\right)\right]^{-\frac{\gamma^{0,n}_{NS}}{2\beta_0}} \qquad (1.267)$$

The great advantage of this Feynman diagram analysis is that it may be extendable to other hard processes (i.e. those in which the distances probed are small compared to typical hadronic dimensions of 10^{-15} m), where there exist no light-cone techniques. Such processes are, for example, massive lepton pair production and the inclusive production of hadrons with large $p_\perp$.

In conclusion, we have seen in this chapter how a simple model of parton dynamics failed to explain adequately the experimental data. We have also witnessed the emergence of a theory of quark (= parton?) - gluon dynamics in which the observed logarithmic scaling violations are seen as a consequence of a logarithmic approach of the dynamics to that of a free field theory; a phenomenon labelled as Asymptotic Freedom. All results so far predicted by the theory, Quantum Chromodynamics, are in qualitative agreement with those events observed. However due to the inherent largeness of the effective quark-gluon coupling constant, there is as yet no precise 'g-2' type quantitative test of Q.C.D.

The experimental lack of evidence for free quarks and gluons is taken as support for the idea that these states are permanently confined to the interior of hadrons. The theory at present admits this possibility with the breakdown of perturbation theory at low energies; however, it still remains an outstanding challenge to prove quark confinement within the context of Q.C.D. Some degree of success along this direction has been achieved by numerical studies of gauge theories on the lattice.

Having briefly discussed the application of Asymptotic Freedom to deep inelastic scattering we now continue to look in detail at the predictions for the longitudinal structure function of the nucleon.

CHAPTER TWO

NUCLEON LONGITUDINAL STRUCTURE

In this chapter we shall begin a study of the subject of this thesis, the longitudinal structure function of a nucleon. Recall that in deep inelastic lepton-hadron scattering the amplitude squared for the process may be written as $L^{\mu\nu}W_{\mu\nu}$ where $L^{\mu\nu}$ is the leptonic tensor calculable within the framework of Q.E.D. (for electroproduction) or the standard model (for $\nu, \bar{\nu}$ scattering), and $W_{\mu\nu}$ is the hadronic tensor. As previously discussed, $W_{\mu\nu}$ can be decomposed on the general grounds of Lorentz invariance and current conservation as [2.1]

$$W_{\mu\nu} = \frac{1}{4\pi}\int d^4z\, e^{iq\cdot z} \langle p|\left[J_\mu^\dagger(z) J_\nu(0)\right]|p\rangle \quad \text{spin averaged} \qquad (2.1)$$

$$= \left(-g_{\mu\nu} + \frac{q_\mu q_\nu}{q^2}\right) W_1(\nu, Q^2) + \left(p^\mu - \frac{p\cdot q}{q^2} q^\mu\right)\left(p^\nu - \frac{p\cdot q}{q^2} q^\nu\right) \cdot W_2(\nu, Q^2)$$

$$- i\varepsilon_{\mu\nu\alpha\beta} \frac{p^\alpha p^\beta}{\nu} \cdot \nu W_3(\nu, Q^2) \qquad (2.2)$$

$$= \left(g_{\mu\nu} - \frac{q_\mu q_\nu}{q^2}\right) \frac{\nu}{2X} W_L(\nu, Q^2)$$

$$+ \left(\frac{p_\mu q_\nu + p_\nu q_\mu}{\nu} - \frac{p_\mu p_\nu}{\nu^2} q^2 - g_{\mu\nu} \right) \frac{\nu}{2X} W_2(\nu, Q^2)$$

$$- i\varepsilon_{\mu\nu\alpha\beta} \frac{p^\alpha p^\beta}{\nu} \cdot \nu W_3(\nu, Q^2) \qquad (2.3)$$

where

$$\nu W_L = \nu W_2 - 2X W_1 \qquad (2.4)$$

and $W_3 = 0$ for electromagnetic processes

The $|p\rangle$ are hadronic target states and we are interested in the limit

$$-q^2 = Q^2 \to \infty$$

$$p.q = \nu \to \infty$$

with the ratio $X = \frac{Q^2}{2\nu}$ kept fixed

and p^2 is a fixed mass (which we shall neglect here).

In order to deal exclusively with W_L we need to construct a projection operator for $W_{\mu\nu}$ that projects out only this part; such an operator [2.2] is $p^\mu p^\nu$ where (for $p^2 = 0$).

$$p^\mu p^\nu W_{\mu\nu} = \left(\frac{\nu}{2X}\right)^2 W_L(\nu, Q^2) \qquad (2.5)$$

Thus we may begin a systematic study of the longitudinal structure function W_L order by order in Q.C.D. perturbation theory.

2.1 Zeroth order Q.C.D. :- The Parton Model.

In the naive Parton Model the nucleon is seen as an assemblage of free on-mass-shell, point-like constituents called partons. These are tentatively identified as the quarks of Q.C.D. and it is in this sense that zeroth order Q.C.D. is equivalent to the Parton model. Clearly this is not a realistic picture; how for instance are the non-interacting partons constrained to stay within the interior of hadrons? However, the impulse approximation does provide some justification for neglecting parton-parton interactions at high enough Q^2.

We may study either the inelastic cross section directly, or the imaginary (absorbetive) part of the corresponding forward elastic compton amplitude, as the two are related via the optical theorem (see Fig. 2.1(a)).

The amplitude to this order of perturbation theory may be written

$$A = -ie_i \bar{u}_\beta(p',s')(\gamma_\mu)_{\alpha\beta} u_\alpha(p,s) \tag{2.6}$$

where A is related to the S-Matrix element as

$$S = 1 + iT \tag{2.7}$$

$$\langle f|T|i\rangle = \delta^4(p_f - p_i)\,|A|^2 \tag{2.8}$$

So

$$|A|^2 = AA^\dagger \tag{2.9}$$

$$= e_i^2 \bar{u}_\beta(p',s')(\gamma_\mu)_{\beta\alpha} u_\alpha(p,s) \bar{u}_\delta(p,s)(\gamma_\nu)_{\delta\varepsilon} u_\varepsilon(p',s') \tag{2.10}$$

Now perform the quark spin sum $\frac{1}{2}\sum_{ss'}$ and use

$$\sum_s u_\alpha(p,s)\bar{u}_\delta(p,s) = (\not{p})_{\alpha\delta} \tag{2.11}$$

for massless fermions

Thus

$$|A|^2 = \tfrac{1}{2} e_i^2 \,\mathrm{Tr}\left[\gamma_\mu \not{p} \gamma_\nu (\not{p}+\not{q})\right] \tag{2.12}$$

where we have set $p' = p+q$ through the momentum conserving delta function of (2.8).

Performing the Trace using Appendix A1 , we obtain

$$|A|^2 = \tfrac{1}{2} e_i^2 \, 4\left[(p+q)_\mu p_\nu + (p+q)_\nu p_\mu - p\cdot(p+q)\, g_{\mu\nu}\right] \tag{2.13}$$

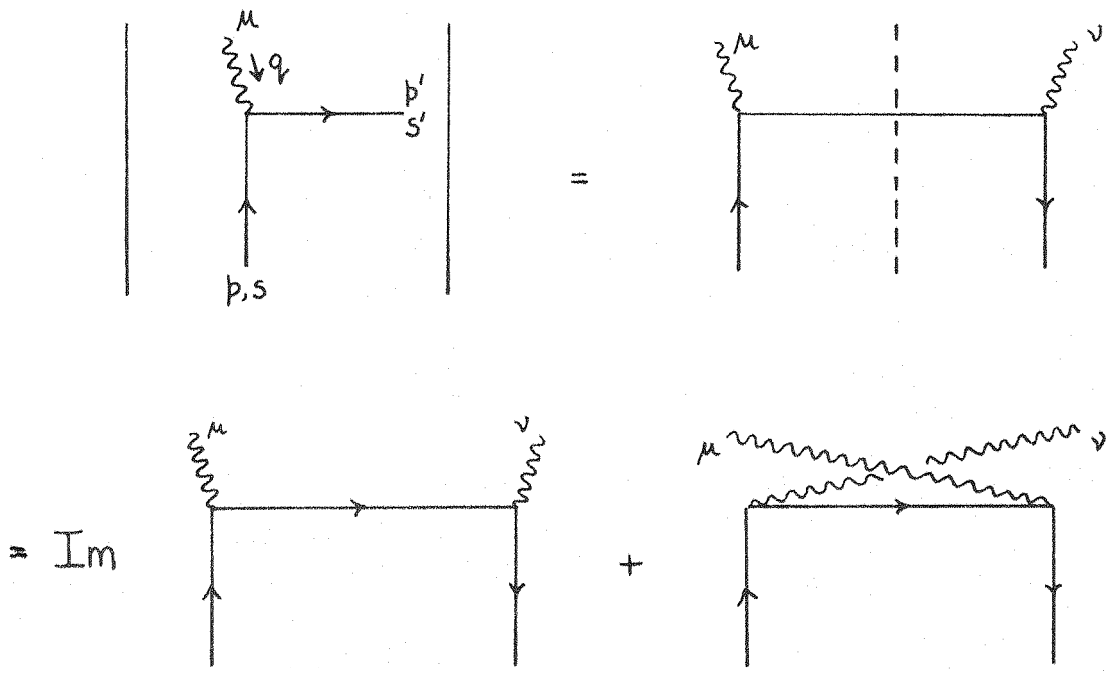

Fig 2.1(a)

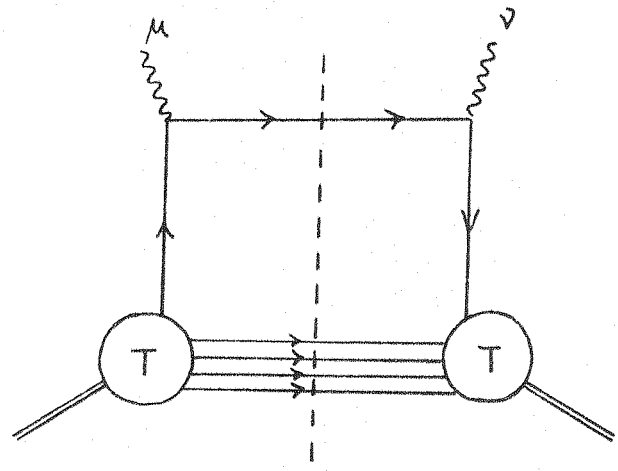

Fig 2.1(b)

and using the elastic condition

$$2p.q = 2\nu = Q^2 \tag{2.14}$$

$$|A|^2 = 2e_i^2 \nu \left[\frac{p_\mu q_\nu + p_\nu q_\mu}{\nu} - \frac{p_\mu p_\nu q^2}{\nu^2} - g_{\mu\nu} \right] \sim W_{\mu\nu} \tag{2.15}$$

Thus we can see that for massless, on-shell quarks the tensor structure that accompanies the longitudinal structure function W_L is not present. The squared amplitude admits a non-zero W_2 only.

Thus the parton-model result is

$$W_L = 0 \tag{2.16}$$

and consequently the ratio

$$R = \frac{\sigma_L}{\sigma_T} = 0 \tag{2.17}$$

One can also build Parton models with less stringent assumptions such as that of Landshoff and Polkinghorne [2.3] where the partons are taken not to be free, but nonetheless not far from mass shell. The use of free parton spinors to describe the incoming state is now forbidden and one has to work with a general matrix $(T)_{\alpha\delta}$ in Dirac spinor indices (see Fig. 2.1(b)). This matrix can be expanded in a Γ^r matrix basis (as they form a complete set) and it is possible to show that the only tensor structure is $(\not{p})_{\alpha\delta}$, thus yielding results identical to those above.

Some physical insight into the meaning of these results can be gained if we go into the Breit frame (the frame in which the parton just reverses its direction of 3 momentum).

We know that for massless fermions the γ_μ coupling conserves helicity because the amplitude for a massless fermion to flip its helicity through a γ_μ coupling is zero. The helicity projection operators for massless fermions are

$$\tfrac{1}{2}(1 \pm i\gamma_5) \tag{2.18}$$

So the helicity flip amplitude

$$\sim \overline{(1-i\gamma_5)u}\ \gamma_\mu\ (1+i\gamma_5)u \tag{2.19}$$

$$= \bar{u}\,(1+i\gamma_5)\,\gamma_\mu\,(1+i\gamma_5)\,u \tag{2.20}$$

But since

$$\{\gamma_\mu, \gamma_5\} = 0 \tag{2.21}$$

the above

$$= \bar{u}\,\gamma_\mu(1-i\gamma_5)(1+i\gamma_5)\,u = 0 \tag{2.22}$$

as

$$(i\gamma_5)^2 = 1$$

This same argument can be extended to weak processes such as those involved in νp scattering, where the only complication is the additional axial vector coupling $\gamma_\mu\gamma_5$. It is obvious through the above analysis that

$$\overline{(1-i\gamma_5)u}\ \gamma_\mu\gamma_5\ (1+i\gamma_5)u = 0 \tag{2.23}$$

Thus, in the Breit frame, consider massless fermions scattering off both transverse and longitudinally polarised photons.

for transverse helicity γ_T, $\lambda = \pm 1$

hence

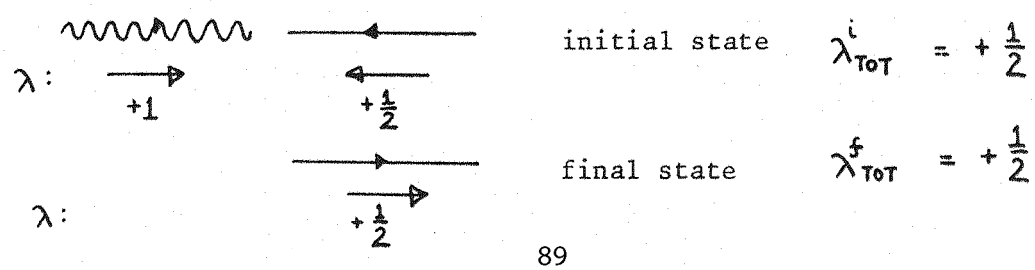

so we can see that total angular momentum $\lambda^i_{TOT} = \lambda^f_{TOT}$ is conserved and $\sigma_T \neq 0$.

γ_L longitudinal helicity $\lambda = 0$

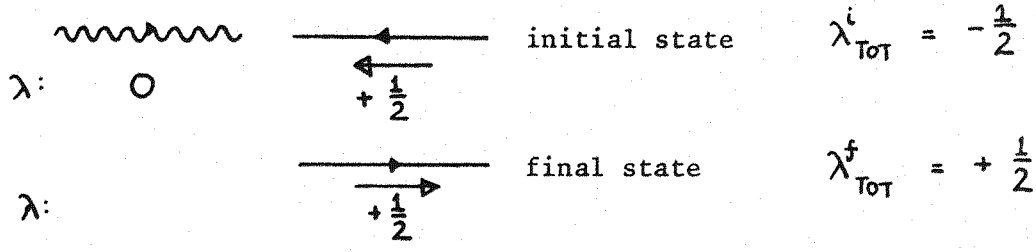

The only way that total angular momentum can be conserved is for the final state fermion to flip its helicity through the γ_μ coupling, but we know the amplitude for this process to be zero. Hence $\sigma_L = 0$ for massless fermions.

and $$R = \frac{\sigma_L}{\sigma_T} = 0$$

These simple helicity arguments may be repeated for the case of polarised photons scattering off scalar partons, with the result that $\sigma_T = 0$, $\sigma_L \neq 0$

and

$$R = \frac{\sigma_L}{\sigma_T} = \infty \qquad \text{for scalar partons} \qquad (2.24)$$

so the measurement of R provides a direct test as to what spin quantum numbers the partons carry.

Both these predictions are in disagreement with the small but non-zero value of R seen in ep scattering [2.4]. In order to explain the data, we clearly need to go beyond the simple parton model, and the preceeding arguments suggest now this could be done. We can either give the partons a small mass explicity, in which case the helicity projection operators are

$$\frac{1}{2}\left(1 \pm i\gamma_5 \frac{\not{p}\not{s}}{m}\right) \qquad (2.25)$$

S_μ is some arbitrary 4-vector

where $S.p = 0$

and $S^2 = -1$

which in general will not commute with γ_μ and so leads to $\sigma_L \neq 0$. Or, we can switch on the Q.C.D. interaction through lowest order perturbation theory. Now a massless parton (= quark) can brehmstrahlung a coloured gluon and go off shell thus allowing its helicity to flip through a γ_μ coupling.

Feynman [2.5] has calculated R where the partons have a mass m and transverse momentum $k_\perp$. Assuming the partons stay close to mass-shell in the initial and final state, he finds for large Q^2

$$R = \frac{4(k_\perp^2 + m^2 + \Delta)}{Q^2} \tag{2.26}$$

where Δ is a binding energy factor (unknown) to correct for using free parton masses in the formula.

From observations of the average $p_\perp$ of pions seen in hadronic collisions (which seems to be energy independent), $k_\perp^2$ is estimated as $\approx 250\ (\text{MeV})^2$ and assumed to be X independent. Naive arguments based on the Uncertainty Principle and the localisation of partons within hadronic radii of $\approx$ 1 fm support this number

Thus for $k_\perp^2 \approx m^2 \approx 250\,(\text{Mev})^2$

and $Q^2 \sim 8\ \text{Gev}^2$

which is a typical value of Q^2 for which data exists, we find

$$R \sim 0{\cdot}25 \pm 0{\cdot}5\,\Delta \tag{2.27}$$

This is to be compared with the quoted value of R (in ep scattering) averaged over a Q^2 range of $2 \rightarrow 16$ Gev^2 as

$$R = 0{\cdot}14$$

The errors are too large in the data to determine variation of R with Q^2, but an important test of future experiments is to verify that R does approach zero as $Q^2 \rightarrow \infty$. Only this will justify the assumption that charged partons are spin $\frac{1}{2}$.

However, to see what sort of test R can afford a theory of hadronic interactions rather than a constructed model, we can continue to study R in the context of Q.C.D. perturbation theory. To do this we use the standard techniques of the Operator Product expansion and Renormalization Group as outlined in the previous chapter.

2.2 σ_L to order g^2 in Q.C.D. - Preliminaries

To calculate the longitudinal coeffcient function that appears in the Operator Product expansion to $O(g^2)$, we need to calculate the imaginary part of the $p^\mu p^\nu$ projected Feynman diagrams appearing in Fig. 2.2. Alternatively, one could expand the inelastic amplitude A to $O(g^2)$ and obtain the matrix elements $AA^\dagger$ by coherently summing over identical final states (see Fig. 2.3). The resulting matrix elements are then integrated over the corresponding one or two-body massless phase space. These two approaches are equivalent by the Optical Theorem. As an illustration, we shall use both approaches to calculate $C^{NS}_{L,n}(1, \bar{g}^2)$ to one loop in the next section.

A few preliminary remarks are necessary about the first method. The contributions of diagrams 2.2(f) and (g) (the type where the fermions receive an external leg renormalization) may be neglected

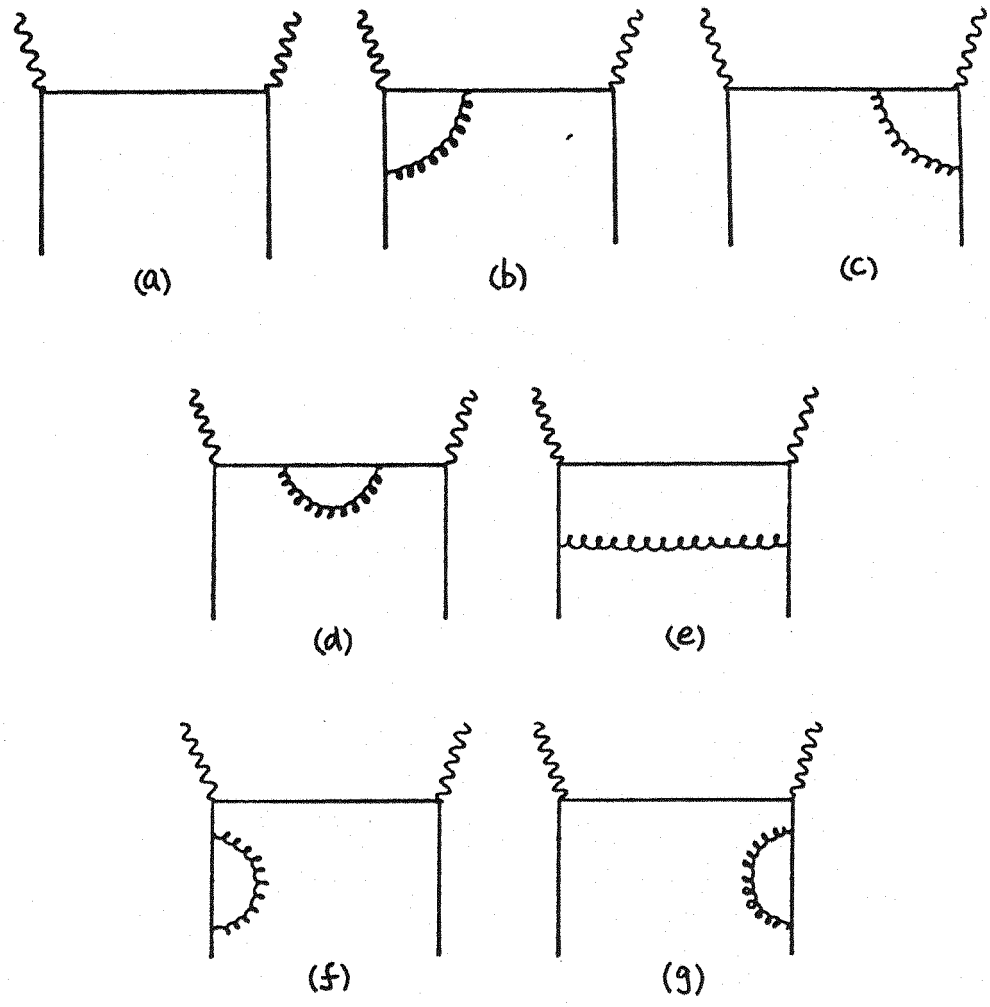

Fig. (2.2) Diagrams of the elastic Compton amplitude to $O(g^2)$ necessary to determine the coefficient functions

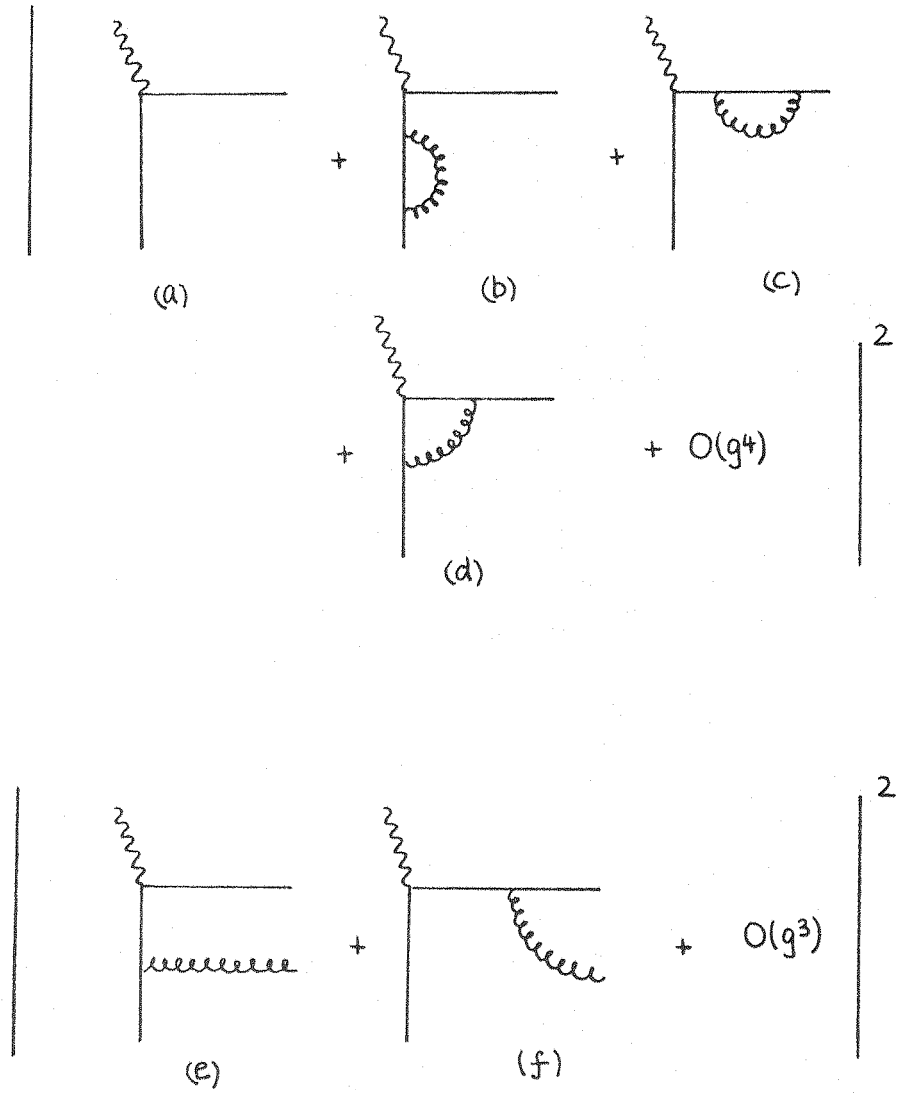

Fig 2.3 Inelastic amplitudes to $O(g^2)$ contributing to σ_L

providing the corresponding diagrams that occur in calculating the matrix elements of local operators are also ignored. This is a process independent statement. Also, the contribution of diagrams 2.2(b), (c) and (d) to σ_L is zero because these involve a massless fermion flipping helicity through a γ_μ coupling. (It is easy to see that this property will reduce greatly the number of diagrams contributing to σ_L at two loops). Thus we are left with just the diagram 2.2(e) to calculate. At this point, it is convenient to consider the analytic structure of the forward elastic compton amplitude. The spin averaged amplitude.

$$T_{\mu\nu}(\nu,Q^2) = i\int d^4z\, e^{iq\cdot z}\langle p|\, T\left[J_\mu^\dagger(z)\, J_\nu(0)\right]|p\rangle_{\text{spin av.}} \tag{2.28}$$

which may be decomposed as

$$T_{\mu\nu}(\nu,Q^2) = \left(g_{\mu\nu} - \frac{q_\mu q_\nu}{q^2}\right) T_L(\nu,Q^2) + \left(\frac{p_\mu q_\nu + p_\nu q_\mu}{\nu} - \frac{p_\mu p_\nu q^2}{\nu^2} - g_{\mu\nu}\right) T_2(\nu,Q^2) - i\varepsilon_{\mu\nu\alpha\beta}\frac{p^\alpha p^\beta}{\nu} T_3(\nu,Q^2) \tag{2.29}$$

The Optical Theorem states

$$W_{\mu\nu} = \frac{1}{2\pi}\,\mathrm{Im}\left[T_{\mu\nu}\right] \tag{2.30}$$

hence

$$\frac{1}{2\pi}\,\mathrm{Im}\left[T_L(\nu,Q^2)\right] = \frac{\nu}{2x} W_L(\nu,Q^2) \tag{2.31}$$

The full elastic Compton Amplitude

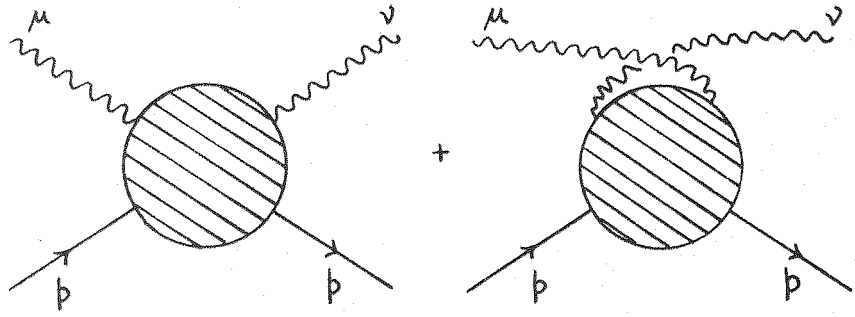

Fig. 2.4

has a branch point in the centre of mass energy variable, S, whenever threshold energy for the production of intermediate states is achieved (and at subsequent multiples of this value). These singularities in Perturbation Theory arise from virtual particles being allowed to go on their mass-shell and thus propagating over arbitrarily large distances. For massless intermediate states, there is a cut in $T_{\mu\nu}$ for $S \geq 0$. In terms of $X = \frac{-q^2}{2p.q}$ this analytic structure translates into a cut strung between $X = \pm 1$ (see Fig. 2.5).

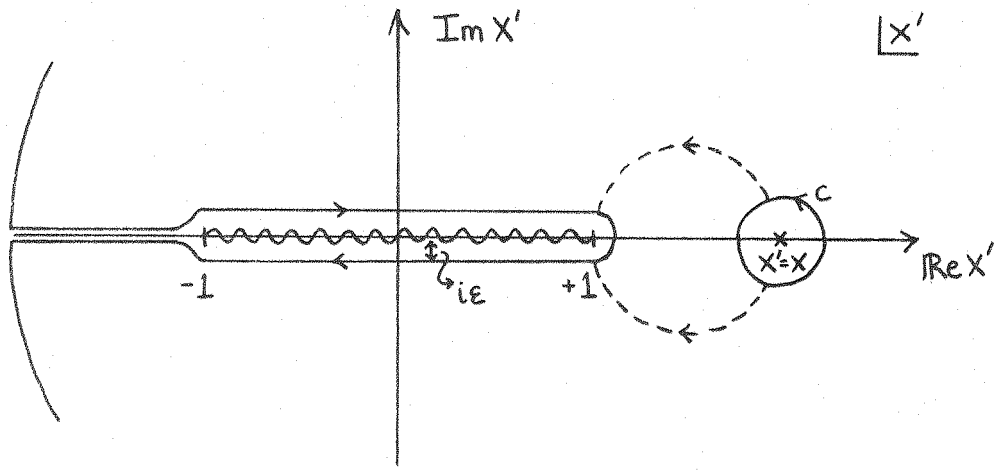

Fig. 2.5

So by Cauchy's Theorem

$$T_{\mu\nu}(X,Q^2) = \frac{1}{2\pi i}\int_C \frac{T_{\mu\nu}(X',Q^2)}{X'-X}\,dX' \tag{2.32}$$

Assuming

i) $T_{\mu\nu}(X',Q^2)$ is everywhere analytic except on the cut for $|X'|\leq 1$

ii) $T_{\mu\nu}(X',Q^2) \to 0$ as $|X'| \to \infty$

Then the contour C can be expanded as shown and all contributions to the integral vanish apart from

$$T_{\mu\nu}(X,Q^2) = \lim_{\varepsilon\to 0}\frac{1}{2\pi i}\int_{-1}^{+1} \frac{T_{\mu\nu}(X'+i\varepsilon,Q^2) - T_{\mu\nu}(X'-i\varepsilon,Q^2)}{X'-X}\,dX' \tag{2.33}$$

By Schwarz's Reflection Principle $f(z^*) = f^*(z)$

Then

$$T_{\mu\nu}(X'-i\varepsilon) = T^*_{\mu\nu}(X'+i\varepsilon) \tag{2.34}$$

$$T_{\mu\nu}(X,Q^2) = \frac{1}{\pi}\int_{-1}^{+1} \frac{\mathrm{Im}\,T_{\mu\nu}(X',Q^2)}{X'-X}\,dX' \tag{2.35}$$

Expanding

$$\left(1-\frac{X'}{X}\right)^{-1} = \sum_{n=0}^{\infty}\left(\frac{X'}{X}\right)^n \tag{2.36}$$

$$T_{\mu\nu}(X,Q^2) = -\frac{1}{\pi}\int_{-1}^{+1}\frac{1}{X}\sum_{n=0}^{\infty}\left(\frac{X'}{X}\right)^n \mathrm{Im}\left[T_{\mu\nu}(X',Q^2)\right]dX' \tag{2.37}$$

where $X>1$ unphysical

and $X'<1$ physical Bjorken X

If we take the $p^\mu p^\nu$ projection of Eq. (2.37) and use Eq. (2.29)

$$p^\mu p^\nu T_{\mu\nu}(x,Q^2) = -\frac{1}{\pi}\int_{-1}^{+1}\frac{1}{x}\sum_{n=0}^{\infty}\left(\frac{x'}{x}\right)^n \frac{\nu}{2x'}\,\mathrm{Im}\left[T_L(x',Q^2)\right]\,dx' \qquad (2.38)$$

and now use the Optical theorem Eq. (2.30), then

$$p^\mu p^\nu T_{\mu\nu}(x,Q^2) = -\sum_{n=0}^{\infty}\left(\frac{1}{x}\right)^n \frac{\nu}{2x}\int_{-1}^{+1} dx'\,x'^{n-2}\,\nu W_L(x',Q^2) \qquad (2.39)$$

from the crossing properties of

$$W_L(x',Q^2) = -W_L(-x',\ Q^2) \qquad (2.40)$$

Then

$$p^\mu p^\nu T_{\mu\nu}(x,Q^2) = -\sum_{n=0}^{\infty}\left(\frac{1}{x}\right)^n \frac{\nu}{2x}\,2M_L(n,Q^2) \qquad (2.41)$$

where

$$M_L(n,Q^2) = \int_0^1 dx'\,x'^{n-2}\,\nu W_L(x',Q^2) \qquad (2.42)$$

Now as an expansion in g^2, the effective Q.C.D. coupling at the renormalization point μ^2, the moments of the non-singlet longitudinal structure function

$$M_L^{NS}(n,Q^2) = \delta_L^{NS}\left(\frac{g}{4\pi}\right)^2 B_{L,n}^{1,NS} + O(g^4) \qquad (2.43)$$

where $\delta_L^{NS} = e_i^2$ the quark charge

and $B_{L,n}^{1,NS}$ is the first term in the expansion of the coefficient function

$$C^{NS}_{L,n}(1,\bar{g}^2) = \delta^{NS}_L \left[0 + \left(\frac{\bar{g}}{4\pi}\right)^2 B^{1,NS}_{L,n} + O(\bar{g}^4) \right] \qquad (2.44)$$

So to $O(g^2)$

$$p^\mu p^\nu T_{\mu\nu}(X,Q^2) = -\sum_{n=0}^{\infty} \left(\frac{1}{X}\right)^n \frac{\nu}{2X}\, 2\delta^{NS}_L \left(\frac{g}{4\pi}\right)^2 B^{1,NS}_{L,n} \qquad (2.45)$$

Thus we can see that in order to calculate the first term in C^{NS}_L we must calculate diagram 2.2(e) for unphysical $X>1$ (hence there are no singularities in the amplitude) and express the answer as a power series in $\frac{1}{X^n}$. $B^{1,NS}_{L,n}$ can be read off from the coefficient of $\left(\frac{1}{X}\right)^n$. This calculation is outlined in the next section.

The second of the approaches mentioned previously does not involve the use of any disperion theory, but is concerned with the direct evaluation of the inelastic cross-section from the squared amplitudes of Fig. 2.3 integrated over massless two body phase space. The moments can then be taken explicitly for all integer n in contrast to the above technique which yields information on the moments for even n only. The only graph of Fig. 2.3 that contributes to σ_L (including all the interference diagrams) is the squared amplitude of Fig. 2.3(e). By the Optical Theorem, this is just proportional to the Imaginary part of the oneloop graph (Fig. 2.2(e)). The calculation of this inelastic cross-section is presented in the next section.

2.3 σ_L to order g^2 in Q.C.D. - Calculation

We wish to calculate the $p^\mu p^\nu$ projection of diagram 2.2(e). We work in a space-time dimension $D=4-2\varepsilon$ where the ultra-violet divergences of the theory appear as poles in $\frac{1}{\varepsilon}, \frac{1}{\varepsilon^2}$ etc. We will also evaluate 2.2(e) through to $O(\varepsilon)$ as this will be useful in

determining counter-terms for some two loop graphs later on.

Using the Feynman Rules of Fig. (1.3), 2.2(e) may be written (in the Feynman gauge) as

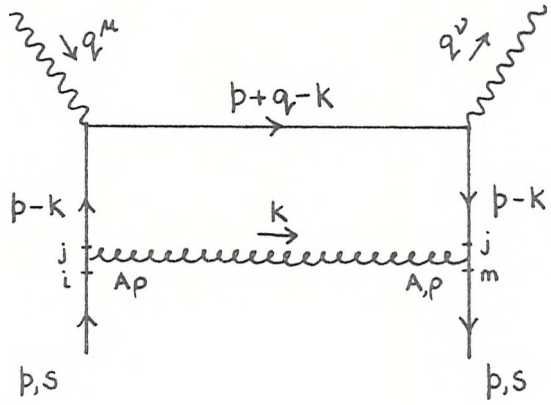

$$= \sum_A \int_{-\infty}^{+\infty} d^D k \; \bar{u}(p,s)\, i g \left(\frac{\lambda^A}{2}\right)_{mj} \gamma^\rho \frac{i}{\not p - \not k} (-i e_i \gamma_\nu) \frac{i}{\not p + \not q - \not k} (-i e_i \gamma_\mu)$$

$$\frac{i}{\not p - \not k}\, i g \left(\frac{\lambda^A}{2}\right)_{ji} \gamma_\rho\, u(p,s) \left(-\frac{i}{k^2}\right) \tag{2.46}$$

perform the Quark spin sum

Quark colour sum

$$= -C_2(R)\, g^2 e_i^2 \int d^D k \; \frac{\mathrm{Tr}\left[(\not p + \not q - \not k)\gamma_\mu (\not p - \not k)\gamma_\rho \not p \gamma^\rho (\not p - \not k)\gamma_\nu\right]}{k^2 (p-k)^4 (p+q-k)^2} \tag{2.47}$$

(all propagators with $+i\varepsilon$ understood)

Evaluating the Trace in D dimensions and setting $p^2 = 0$ for massless fermions (note : in general, great care must be taken in setting $p^2 = 0$ in the numerator as sometimes the coefficient of p^2, which itself is an integral, yields a factor $\frac{1}{p^2}$ thus giving a

finite contribution as $p^2 \to 0$. One can show this effect is not present in this diagram though)

$$p^\mu p^\nu \, Tr \;\longrightarrow\; 16(2-D)(p.k)^2 \, p.(p+q-k) \tag{2.48}$$

We use the standard Feynman parameterization of the propagators (Appendix A.1)

$$\underset{(\alpha)\ (\beta)\quad(\gamma)}{\frac{1}{k^2(p-k)^4(p+q-k)^2}} = \Gamma(4)\int_0^1 d\gamma d\beta \; \frac{\theta(1-\beta-\gamma)\,\gamma}{\left[\hat{k}^2 - M^2\right]^4} \tag{2.49}$$

where

$$M^2 = 2\gamma\beta\, p.(p+q) - \beta(1-\beta)(p+q)^2 - \gamma(1-\gamma)p^2 \tag{2.50}$$

and

$$k = \hat{k} + \beta(p+q) + \gamma p \tag{2.51}$$

This shift of origin in the Trace yields

$$Tr \;\to\; 16(2-D)\,(p.q)^3\,\beta^2(1-\beta) \tag{2.52}$$

So far

$$T = -e_i^2 q^2 C_2(R)\,\tfrac{1}{2}\cdot 16(2-D)(p.q)^3\,\Gamma(4)\cdot \int_0^1\int_0^1 d\beta d\gamma\,\theta(1-\beta-\gamma)\,\beta^2(1-\beta)\,\gamma \int_{-\infty}^{\infty} d^D\hat{k}\;\frac{1}{\left[\hat{k}^2 - M^2\right]^4} \tag{2.53}$$

Performing the loop integral (Appendix A1) and choosing $D = 4-2\varepsilon$

$$\int_{-\infty}^{\infty} d^D\hat{k}\;\frac{1}{\left[\hat{k}^2 - M^2\right]^4} = \frac{i}{(4\pi)^{2-\varepsilon}}\,\frac{\Gamma(2+\varepsilon)}{\Gamma(4)}\,\frac{1}{(M^2)^{2+\varepsilon}} \qquad \text{U.V. finite} \tag{2.54}$$

scale $g^2 \to g^2\mu^{2\varepsilon}$ to keep the coupling constant dimensionless in $D = 4-2\varepsilon$,

$$T = +\frac{i}{(4\pi)^2} e_c^2 g^2 C_2(R)\, 16 (p.q)^3\, \Gamma(2+\varepsilon)\Gamma(1-\varepsilon)(4\pi)^{\varepsilon}\mu^{2\varepsilon}$$

$$\int_0^1\int_0^1 d\gamma\, d\beta\, \frac{\theta(1-\gamma-\beta)\ \gamma\beta^2(1-\beta)}{\left[2\gamma\beta\, p.(p+q) - \beta(1-\beta)(p+q)^2 - \gamma(1-\gamma)p^2\right]^{2+\varepsilon}} \qquad (2.55)$$

Now we can see that in the numerator there are enough powers of β to kill all the powers of β that result from $(M^2)^{2+\varepsilon}$ if we drop p^2, leaving only β^{ε} integrable singularities.

This is a reflection of the fact that there are no mass singularities in the $p^\mu p^\nu$ projection of this diagram. As $k_p \to 0$, the propagator $\frac{1}{(p-k)^2} \to \frac{1}{p^2-0}$ which is a potential divergence regulated by p^2. For the contribution of this diagram to νW_2 this effect would produce a $\ln(-p^2)$. However, for the contribution to νW_L there is a compensating effect. As $k_p \to 0$ the longitudinal photon 'sees' the fermion as massless in the limit $p^2 \to 0$ and hence de-couples from it. This is enough to kill the $\ln(-p^2)$ singularity, leaving a finite answer. Thus the structure of the numerator in the σ_L process helps to simplify some of the integrals encountered.

Consider $\int_0^1 d\gamma\, d\beta$ only. Dropping p^2 in M^2 gives

$$\int_0^1\int_0^1 d\gamma\, d\beta\ \theta(1-\gamma-\beta)\ \frac{\gamma\beta^2(1-\beta)}{\beta^2\beta^{\varepsilon}\left[M'^2\right]^{2+\varepsilon}} \qquad (2.56)$$

where
$$M'^2 = 2p.q\,\gamma - (1-\beta)(p+q)^2 \qquad (2.57)$$

$$= -q^2(1-\beta)\left[1 - \left(\frac{1-\beta-\gamma}{1-\beta}\right)\frac{1}{X}\right] \qquad (2.58)$$

Change variables

$$\beta \to 1-\beta \tag{2.59}$$

$$\frac{\beta-\gamma}{\beta} \to \gamma' \tag{2.60}$$

Then

$$T = + \frac{i}{(4\pi)^2} e_i^2 g^2 C_2(R)\, 16 \frac{(p.q)^3}{(-q^2)^2} \Gamma(2+\varepsilon)(1-\varepsilon)(4\pi)^{\varepsilon} \mu^{2\varepsilon} (-q^2)^{-\varepsilon}$$

$$\int_0^1 d\beta \frac{\beta}{(\beta(1-\beta))^{\varepsilon}} \int_0^1 d\gamma' \frac{(1-\gamma')}{\left(1-\frac{\gamma'}{X}\right)^{2+\varepsilon}} \tag{2.61}$$

Consider

$$\int_0^1 d\gamma' \, (1-\gamma')\left(1-\frac{\gamma'}{X}\right)^{-2-\varepsilon} \tag{2.62}$$

and expand binomially.

Note, as γ' takes values in the range $0 \to 1$, this expansion requires $X > 1$ to be valid. This corresponds to the condition of calculating this diagram for unphysical Bjorken X thus avoiding the threshold singularity at $\gamma' = X$.

$$(1+Y)^n = \sum_{j=0}^{n} \frac{n!}{j(n-j)!} Y^j \tag{2.63}$$

The general term for $n = -(2+\varepsilon)$ is

$$\sum_{j=0}^{\infty} \frac{(-1)^j (2+\varepsilon)(3+\varepsilon) \cdots\cdots (2+\varepsilon+j-1)}{j!} \left(-\frac{\gamma'}{X}\right)^j \tag{2.64}$$

expanding this term to $O(\varepsilon)$

$$\sum_{j=0}^{\infty} \left(\frac{\gamma'}{X}\right)^j \left[\frac{(j+1)!}{j!} + \varepsilon \frac{(j+1)!}{j!} \left(\frac{1}{2} + \frac{1}{3} + \frac{1}{4} + \cdots \frac{1}{j+1} \right) \right] \tag{2.65}$$

$$= \sum_{j=0}^{\infty} \left(\frac{\gamma'}{X}\right)^j (j+1) \left[1 + \varepsilon \left(S_1(j+1) - 1 \right) \right] \tag{2.66}$$

where $$S_1(n) = \sum_{k=1}^{n} \frac{1}{k} \tag{2.67}$$

Substitute back and expand Eq (2.61) to $O(\varepsilon)$ using the recursion relation in Appendix A.1 for $\Gamma(2+\varepsilon)$ to arrive at

$$T = + \frac{i}{(4\pi)^2} e_i^2 g^2 C_2(R) \frac{16 (p.q)^3}{(-q^2)^2} \int_0^1 d\beta\, \beta \int_0^1 d\gamma' \sum_{j=0}^{\infty} \left(\frac{\gamma'}{X}\right)^j (j+1)(1-\gamma').$$

$$\left\{ 1 + \varepsilon \left[\ln(4\pi) - \gamma_E - \ln\left(\frac{-q^2}{\mu^2}\right) - \ln(\beta(1-\beta)) + S_1(j+1) - 1 \right] \right\} \tag{2.68}$$

Both the Feynman parameter integrals are now straight-forward to do, yielding

$$T = + \frac{i}{(4\pi)^2} e_i^2 g^2 C_2(R) \frac{8 (p.q)^3}{(-q^2)^2} \sum_{j=0}^{\infty} \left(\frac{1}{X}\right)^j \frac{1}{(j+2)} \left[1 + \varepsilon \left(\gamma + S_1(j+1) + 1 \right) \right] \tag{2.69}$$

where $$\gamma = \ln(4\pi) - \gamma_E - \ln\left(\frac{-q^2}{\mu^2}\right) \tag{2.70}$$

relabelling $$j+1 = n \tag{2.71}$$

and using $$\frac{(p.q)^3}{(-q^2)^2} = \frac{\nu}{2X} \frac{1}{2X} \tag{2.72}$$

$$T = +ie_i^2\left(\frac{g}{4\pi}\right)^2 \frac{\nu}{2X}\, 4C_2(R) \sum_{n=1}^{\infty} \left(\frac{1}{X}\right)^n \frac{1}{(n+1)} \left\{ 1 + \varepsilon\left(S_1(n) + 1 + \gamma\right) \right\} \qquad (2.73)$$

Thus we see we have the answer for T in the desired form; a power series expansion in unphysical Bjorken $X > 1$. The effect of the crossed diagram is to change

$$q^\mu \rightarrow -q^\mu \qquad (2.74)$$

and so

$$X \rightarrow -X \qquad (2.75)$$

This introduces a factor 2 for n even and knocks out the n odd terms in the expansion $\left(\frac{1}{X}\right)^n$.

So knowing $p^\mu p^\nu T_{\mu\nu} = iT$

and using the dispersion relation Eq (2.41) together with Eq (2.43) and Eq (2.73), we deduce that [2.6, 2.7]

$$B_{L,n}^{i,NS} = \frac{4\, C_2(R)}{n+1} \qquad (2.76)$$

For comparison, we now present the alternative method of calculating the coefficient function. This involves the evaluation of the inelastic cross-section from the squared amplitude of Fig. 2.3(e). Again, all ultra violet divergences are regulated by calculating the amplitude in a space-time of dimension $D = 4 - 2\varepsilon$. To order g^2 the amplitude is U.V. finite; however, we will still evaluate it through to $O(\varepsilon)$ in D dimensions as this will be useful in determining counterterms for some one loop amplitudes later on. All phase space integration is carried out in $D = 4$ dimensions.

Using the Feynman Rules of Fig. 1.3, Fig. 2.3(e) may be written as

$$A_{\mu\nu} = A_\mu (A_\nu)^\dagger$$

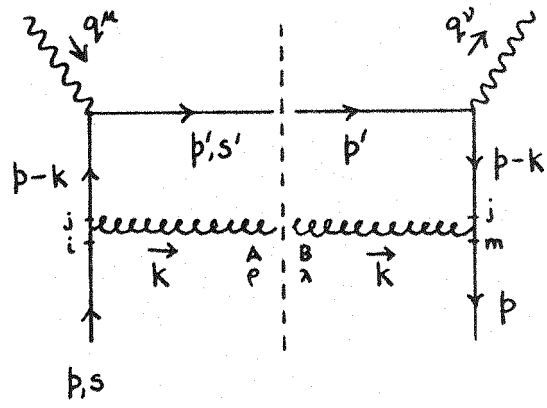

Fig. (2.7)

with all real massless particles being on-shell

$$p'^2 = (p+q-k)^2 = 0 \qquad (2.77)$$

$$p^2 = \quad k^2 \quad = 0 \qquad (2.78)$$

(This particular amplitude is infra-red finite, as we shall see shortly, so there are no divergences introduced by the above statements. A discussion of infra-red regularization techniques for more complicated amplitudes will be given in the next chapter).

Thus

$$A_\mu = \bar{u}(p',s')(-ie_i\gamma_\mu)\frac{i}{\not p - \not k} ig(\tfrac{\lambda^A}{2})_{ji}\,\gamma_\rho\, u(p,s)\,\varepsilon^{\rho,A}_\sigma \qquad (2.79)$$

So $A_{\mu\nu} = A_\mu (A_\nu)^\dagger$

$$= \sum_A e_i^2 g^2 (\tfrac{\lambda^A}{2})_{ji}(\tfrac{\lambda^A}{2})_{mj}\;\bar{u}(p',s')\,\gamma_\mu \frac{1}{\not p - \not k}\gamma_\rho\, u(p,s)\,\bar{u}(p,s)\,.$$

$$\gamma_\lambda \frac{1}{\not p - \not k}\gamma_\nu\, u(p',s')\;\varepsilon^{\rho,A}_\sigma \left(\varepsilon^{\lambda,B}_\sigma\right)^\dagger \qquad (2.80)$$

Performing the gluon colour and polarisation sums

$$\sum_A \left(\frac{\lambda^A}{2}\right)_{mj}\left(\frac{\lambda^A}{2}\right)_{ji} = C_2(R)\,\delta_{mi} \qquad C_2(R) = \frac{4}{3} \text{ for } SU(3) \tag{2.81}$$

$$\sum_\sigma \varepsilon^{p,A}_\sigma \varepsilon^{\lambda,B\,\dagger}_\sigma = -g^{p\lambda}\delta^{AB} \tag{2.82}$$

and the quark spin sum

$$\sum_s u(p,s)\,\bar{u}(p,s) = \not{p} \tag{2.83}$$

We obtain

$$A_{\mu\nu} = -e_i^2 g^2 C_2(R)\,\frac{1}{2}\,\mathrm{Tr}\left[\gamma_\mu(\not{p}-\not{k})\gamma^\lambda \not{p}\,\gamma_\lambda(\not{p}-\not{k})\gamma_\nu \not{p}'\right] \Big/ (p-k)^4 \tag{2.84}$$

We now project out the contribution of this graph to the longitudinal cross-section σ_L using the projector $p^\mu p^\nu$, $p^\mu p^\nu A_{\mu\nu} \equiv A^2$ (2.85)

$$p^\mu p^\nu \mathrm{Tr} = \mathrm{Tr}\left[\not{p}(\not{p}-\not{k})\gamma^\lambda \not{p}\,\gamma_\lambda(\not{p}-\not{k})\not{p}\not{p}'\right] \tag{2.86}$$

We evaluate the trace in $D=4-2\varepsilon$ dimensions and set $p^2=0$. (In general, care must be taken with this last step as it is possible to miss finite contributions of the form $\frac{p^2}{p^2}$. This is not the case for this diagram though).

$$p^\mu p^\nu \mathrm{Tr} = 16(2-D)(p.k)^2\, p.p' \tag{2.87}$$

The factor of $(p.k)^2$ kills both the propagators in the denominator as

$$p.k = -\tfrac{1}{2}(p-k)^2 + O(p^2,k^2) \tag{2.88}$$

hence

$$A^2 = -e_i^2 g^2 C_2(R)\, 2(2-D)\, p.p' \tag{2.89}$$

This squared amplitude must now be integrated over massless two body phase space.

$$\bar{A}^2 = \int [d\!\!^{-}k][d\!\!^{-}p']\, \delta^4(p+q-k-p')\, A^2 \tag{2.90}$$

where the Lorentz invariant volume element

$$[d\!\!^{-}k] = d\!\!^{-4}k\, \delta(k^2-m^2)\, \theta(k^\circ) \tag{2.91}$$

$$d\!\!^{-4}k = \frac{d^4k}{(2\pi)^4} \tag{2.92}$$

and

$$\delta(k^2-m^2) = 2\pi\, \delta(k^2-m^2) \tag{2.93}$$

The p' integrals can be done immediately with the 4 dimensional delta function with the result

$$p' = p+q-k \tag{2.94}$$

So

$$\bar{A}^2 = -e_i^2 g^2 C_2(R)\, 2(2-D)$$

$$\int d\!\!^{-4}k\, \delta(k^2)\, \theta(k^\circ)\, \delta[(p+q-k)^2]\, \theta(p^\circ+q^\circ-k^\circ)\; p.(q-k) \tag{2.95}$$

In order to do the remaining phase-space integrals we choose a particular kinematic frame, say the quark-photon centre of momentum frame, and align it along the z direction.

Thus

$$p^\mu = (E, 0, 0, \underline{p}) \quad \text{with} \quad E = \underline{p} \tag{2.96}$$

$$q^\mu = (q^0, 0, 0, -\underline{p}) \tag{2.97}$$

$$k^\mu = (\omega, \underline{k}) \tag{2.98}$$

in this frame the centre of momentum energy

$$S = (p+q)^2 = (E+q^0)^2 \tag{2.99}$$

and

$$(p+q).k = (E+q^0)\omega = \sqrt{S}\omega \tag{2.100}$$

Thus

$$\bar{A}^2 = -e_c^2 g^2 C_2(R)\, 2(2-D)$$
$$\frac{1}{(2\pi)^2}\int_0^\infty d\omega \int_{-\infty}^{\infty} d^3\underline{k}\; \delta(\omega^2 - |\underline{k}|^2)\, \delta(S - 2\sqrt{S}\omega)\, \theta(\omega)\, p.(q-k) \tag{2.101}$$

Now

$$d^3\underline{k} = k^2\, dk\, d\phi\, d(\cos\theta) \tag{2.102}$$

So in d^4k we can do the energy $(d\omega)$ and modulus of 3-vector (dk) integrals using the two delta functions, leaving the two angle integrals yet to do

$$\bar{A}^2 = -e_c^2 g^2 C_2(R)\, 2(2-D)$$
$$\frac{1}{(2\pi)^2}\frac{1}{2\sqrt{S}}\frac{1}{\sqrt{S}}\frac{S}{4}\int_0^{2\pi} d\phi \int_{-1}^{+1} d(\cos\theta)\; p(q-k) \tag{2.103}$$

where

$$\omega = |\underline{k}| = \frac{\sqrt{s}}{2} \tag{2.104}$$

and

$$p.k = E\omega - |\underline{p}||\underline{k}|\cos\theta \tag{2.105}$$

$$= E\frac{\sqrt{s}}{2}(1-\cos\theta) \tag{2.106}$$

With no azimuthal dependence in the integrand, the ϕ integral may be done trivially.

Choosing $D = 4-2\varepsilon$

$$\bar{A}^2 = +e_i^2 g^2 C_2(R)(1-\varepsilon) \frac{E\sqrt{s}}{2}\frac{4}{(2\pi)}\frac{1}{8}\int_{-1}^{+1} dz\,(1-z) \tag{2.107}$$

using

$$p.(p+q) = E\sqrt{s} = p.q \tag{2.108}$$

then finally

$$\bar{A}^2 = e_i^2\left(\frac{g}{4\pi}\right)^2 C_2(R)\, 4\pi\, p.q\,(1-\varepsilon) \tag{2.109}$$

Now

$$p^\mu p^\nu W_{\mu\nu} = \frac{1}{4\pi}\bar{A}^2 = \left(\frac{\nu}{2x}\right)^2 W_L(\nu, Q^2) \tag{2.110}$$

in the scaling limit

$$\nu W_L(\nu, Q^2) \rightarrow F_L(x, Q^2) \tag{2.111}$$

The Operator product expansion now gives the moments of non-singlet structure functions as

$$M_L^{NS}(n, Q^2) = \int_0^1 dx\, x^{n-2} F_L^{NS}(x, Q^2) = A_n^{NS}\left(\frac{p^2}{\mu^2}, g^2\right) C_{L,n}^{NS}\left(\frac{Q^2}{\mu^2}, g^2\right) \tag{2.112}$$

expanding the right hand side as a power series in g we have

$$M_L^{NS}(n, Q^2) = \delta_L^{NS}\, B_{L,n}^{1,NS}\left(\frac{g}{4\pi}\right)^2 + O(g^4) \tag{2.113}$$

with $\delta_L^{NS} = e_i^2$ for deep inelastic scattering on a quark.

Combining Eqs. (2.109 - 2.112) we obtain

$$e_i^2\left(\frac{g}{4\pi}\right)^2 C_2(R) \int_0^1 dx\; x^{n-2}\, 4x^2 = e_i^2\left(\frac{g}{4\pi}\right)^2 B_{L,n}^{1,NS} \tag{2.114}$$

from which

$$B_{L,n}^{1,NS} = \frac{4}{(n+1)} C_2(R) \tag{2.115}$$

in agreement with the result from the previous method.

Thus in this section we have presented two equivalent methods of calculating the coefficient functions appearing in the Operator Product Expansion to one loop. Even at this order of perturbation theory it appears that the second of the two techniques outlined above is the simpler. For this reason, we shall adopt this as our approach to the two loop calculation to be discussed in detail in Chapters 3 and 4.

During the closing stages of this work, however, it was brought to our attention that a similar calculation had been recently performed utilizing the first of the two techniques and a Monte-Carlo numerical integration routine to evaluate some of the more difficult integrals. The status of the agreement between the two calculations will be discussed subsequently.

2.4 σ_L to order g^2 in Q.C.D. - phenomenology.

In this section we give a brief discussion of the phenomenology of the order g^2 contribution to σ_L from Q.C.D. perturbation theory. Although much of the material found here is discussed in greater detail in Chapter 5, it is appropriate to consider the one loop corrections now because the result will serve as further motivation to go to higher orders of perturbative Q.C.D.

We can now use the techniques of the Operator Product expansion and Renormalization Group to re-write the Q.C.D. predictions for the moments of structure functions as an expansion in the effective (running) strong coupling constant.

For non-singlet combinations of structure functions

$$M_L^{NS}(n,Q^2) = A_n^{NS}\left(\frac{p^2}{\mu^2}, g^2\right) C_{L,n}^{NS}\left(\frac{Q^2}{\mu^2}, g^2\right) = \int_0^1 dx\, x^{n-2} F_L^{NS}(x,Q^2) \qquad (2.116)$$

where A_n^{NS} is the (Q^2 independent) reduced matrix element of the fermion non-singlet operator

$$\langle p | O_{NS}^{\mu_1 \cdots \mu_n} | p \rangle = A_n^{NS}\left(\frac{p^2}{\mu^2}, g^2\right) p^{\mu_1 \cdots \mu_n} - \text{traces} \qquad (2.117)$$

and $C^{NS}_{L,n}$ are the Q^2 dependent coefficient functions calculable in perturbation theory. The Renormalization Group expresses the invariance of physically measurable quantities, such as the moments of structure functions, under changes of the arbitrary mass scale μ^2 ; the Renormalization point. In particular we can relate the coefficient functions at some arbitrary scale μ^2 , to those at $Q^2 = \mu^2$ and an effective coupling $\bar{g}(Q^2)$.

$$C^{NS}_{L,n}\left(\frac{Q^2}{\mu^2}, g^2\right) = C^{NS}_{L,n}(1, \bar{g}^2)\, exp\left\{ -\int_{\bar{g}(\mu^2)}^{\bar{g}(Q^2)} dg' \; \frac{\gamma_n^{NS}(g')}{\beta(g')} \right\} \qquad (2.118)$$

Inserting Eqs (2.117) and (2.118) into Eq. (2.116) and expanding everything in powers of $\bar{g}_o^2(Q^2)$ the one loop running coupling constant, then for $\mu^2 = Q_o^2$

$$M^{NS}_L(n, Q^2) = \bar{A}^{NS}_n \, \delta^L_{NS} \, B^{1,NS}_{L,n} \left[\frac{\bar{g}_o^2(Q^2)}{(4\pi)^2} + O(g_o^4) \right] \left[\frac{\bar{g}_o^2(Q^2)}{\bar{g}_o^2(Q_o^2)} \right]^{\frac{\gamma_n^{0,NS}}{2\beta_o}} \qquad (2.119)$$

the unknown $\bar{A}^{NS}_n$ may be eliminated through the moments of the non-singlet combination of νW_2 at Q_o^2 (since the data are more accurate for νW_2) giving

$$M^{NS}_L(n, Q^2) = M^{NS}_2(n, Q_o^2)\, B^{1,NS}_{L,n} \, \frac{\bar{g}_o^2(Q^2)}{(4\pi)^2} \left[\frac{\bar{g}_o^2(Q^2)}{\bar{g}_o^2(Q_o^2)} \right]^{\frac{\gamma_n^{0,NS}}{2\beta_o}} \qquad (2.120)$$

$$\frac{g_o^2(Q^2)}{(4\pi)^2} = \frac{1}{\beta_o \ln\left(\frac{Q^2}{\Lambda^2}\right)} \qquad (2.121)$$

where

$$\Lambda^2 = \mu^2 \exp\left[-\frac{16\pi^2}{g^2\beta_0}\right] \tag{2.122}$$

is the one free parameter of the theory to be determined by the magnitude of the scaling violations of νW_2.

So after measuring the moments of νW_2 at some $Q_0^2 < Q^2$ (but still large enough to justify the use of perturbation theory, i.e. $Q_0^2 >$ few GeV^2) Q.C.D. predicts exactly the Q^2 dependence of the moments of νW_L.

Expressions similar to Eq. (2.120) can also be derived for the moments of νW_2 to $O(\bar{g}^2)$. Here the equations are more complex due to the fact that the Parton Model result for νW_2 does not vanish.

In order to obtain the structure function $F_L(x, Q^2)$, Eq. (2.120) must be inverted. As the n dependence is fairly complicated this cannot be done easily (if at all) analytically. It is usual to employ one of the standard inversion techniques described in Chapter 5.

Having determined

$$F_L(x, Q^2) = F_2(x, Q^2) - 2x F_1(x, Q^2) \tag{2.123}$$

and

$$F_2(x, Q^2) \tag{2.124}$$

one can find $F_1(x, Q^2)$ and so plot a graph of

$$R(x, Q^2) = \frac{\sigma_L}{\sigma_T} = \frac{F_L(x, Q^2)}{2x F_1(x, Q^2)} \tag{2.125}$$

The resulting plot of R and its comparison to the data can be seen in Fig. (2.7).

In Eq. (2.125) we have neglected contributions of order $\frac{m^2_{proton}}{Q^2}$; the target mass corrections. These reflect the fact that we are not measuring the moments at the scaling limit $Q^2 \to \infty$, but in the region of $Q^2 = 2 \to 20\,GeV^2$. In this region

$$\nu W_L(x,Q^2) \neq F_L(x,Q^2) \tag{2.126}$$

$$= F_L(x,Q^2) + O\left(\frac{m^2_{proton}}{Q^2}\right) \tag{2.127}$$

These corrections are known and have been discussed in Chapter 1. They are included in Fig. 2.7 and tend to improve agreement with the data.

Although the error bars on the data are large in Fig. 2.7, one can conclude [2.7, 2.8] that, even with target mass corrections, the $O(g^2)$ Q.C.D. prediction lies consistently below the best experimental fit, especially at large X. Clearly this cannot be seen as a satisfactory description of the data.

2.5 σ_L to order g^4 : A preliminary look

We have seen in the previous section that the leading order Q.C.D. corrections for σ_L do not provide a satisfactory explanation of the data for $X > 0.5$. There may be many reasons for this discrepancy. It could be due to some (presently) incalculable non-perturbative contribution of the neglected higher twist operators.

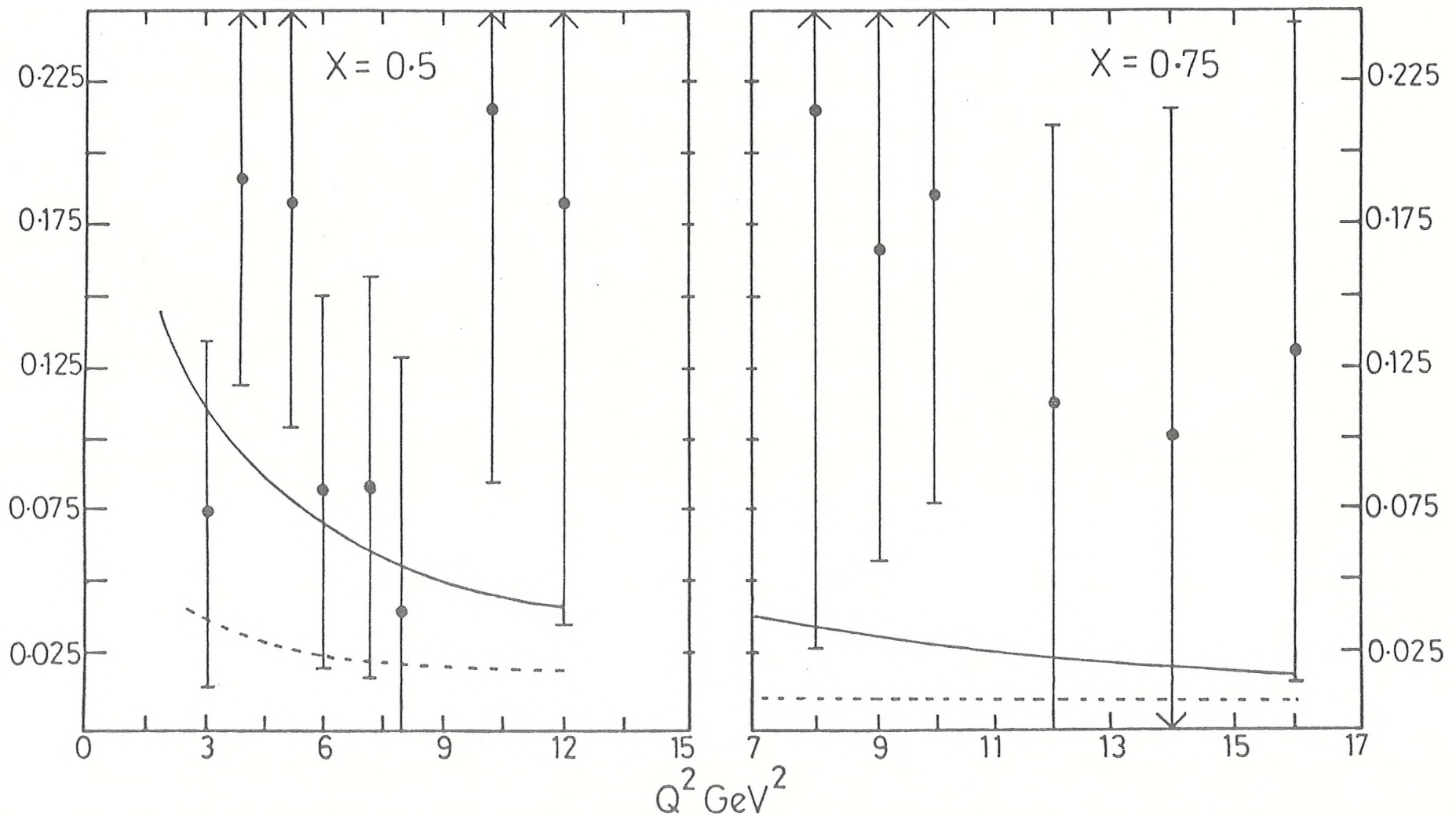

Fig 2.7

——— leading order QCD + target mass corrections

------ leading order QCD

This statement is counter-productive in the sense that it exchanges one problem for another. However Schmidt et al [2.9] have considered non-scaling contributions to $F_L(x,Q^2)$ from scattering off di-quark systems within a proton and conclude that they could become significant as $x \to 1$.

The discrepancy could also be the result of truncating the Q.C.D. perturbation expansion after only the second term. It is important, therefore, to look at the next highest order correction, the $O(g^4)$ term to try and understand how reliable the leading order calculation is.

There are interesting theoretical questions as to the nature of this order g^4 term though. It may make no sense at all to construct a perturbation theory where asymptotic states are taken to be objects which do not seem to appear in the physical spectrum of the theory, namely quarks and gluons. This is a problem that requires mathematical proof or dis-proof. The relative size of the order g^4 to order g^2 term however, may at least provide a check as to whether Q.C.D. is self consistant as a perturbative expansion - does the series appear to converge? The answer to this question is by no means clear in view of some of the recent perturbative corrections computed [2.10]. Finally, if the Q.C.D. prediction for σ_L is fitted to the data in order to obtain a value for the one free parameter of the theory Λ, then this value is meaningless unless the Q.C.D. expansion contains the order g^4 term [2.11]. This is easily seen if we consider the two loop β function solution of the running coupling constant.

$$\alpha_s(Q^2) = \frac{\bar{g}_0^2(Q^2)}{4\pi} = \frac{4\pi}{\beta_0 \ln\left(\frac{Q^2}{\Lambda^2}\right)} \qquad (2.128)$$

Then

$$\bar{\alpha}_s = \alpha_s(Q^2) - \frac{\beta_1}{\beta_0}\frac{1}{4\pi}\alpha_s^2(Q^2)\ln\ln\left(\frac{Q^2}{\Lambda^2}\right) + O(\alpha_s^3) \qquad (2.129)$$

now let $\bar{\alpha}_s'$ be a running coupling constant with a different Λ', then

$$\bar{\alpha}_s' = \bar{\alpha}_s + K\bar{\alpha}_s^2 + \cdots\cdots \qquad (2.130)$$

where

$$K = \frac{\beta_0}{4\pi}\ln\left(\frac{\Lambda'^2}{\Lambda^2}\right) \qquad (2.131)$$

Thus to leading order $\bar{\alpha}_s' = \bar{\alpha}_s$ and Λ is left as an entirely free parameter. In the same spirit, when making comparisons of theory to data the coefficient of the $\bar{\alpha}_s^2$ term must be known in order to attach any significance to the value of Λ obtained.

In order to calculate the order g^4 Q.C.D. correction for the moments of the longitudinal structure function (non-singlet), we must calculate the order g^4 term in the expansion of the longitudinal coefficient function $C_{L,n}^{NS}(1, \bar{g}^2)$. All other perturbatively calculable quantities, namely the two loop beta function and anomalous dimensions of fermion non-singlet operators, have been calculated previously. Thus we are faced with calculating the cross-sections given by the squared amplitudes of Fig. 2.8 integrated over the corresponding two or three body massless phase space, or equivalently the imaginary parts of the elastic amplitudes in Fig. 2.9. (Again we ignore graphs corresponding to external leg renormalizations).

The remainder of this thesis will be devoted to a discussion of the techniques used and results obtained in calculating these graphs.

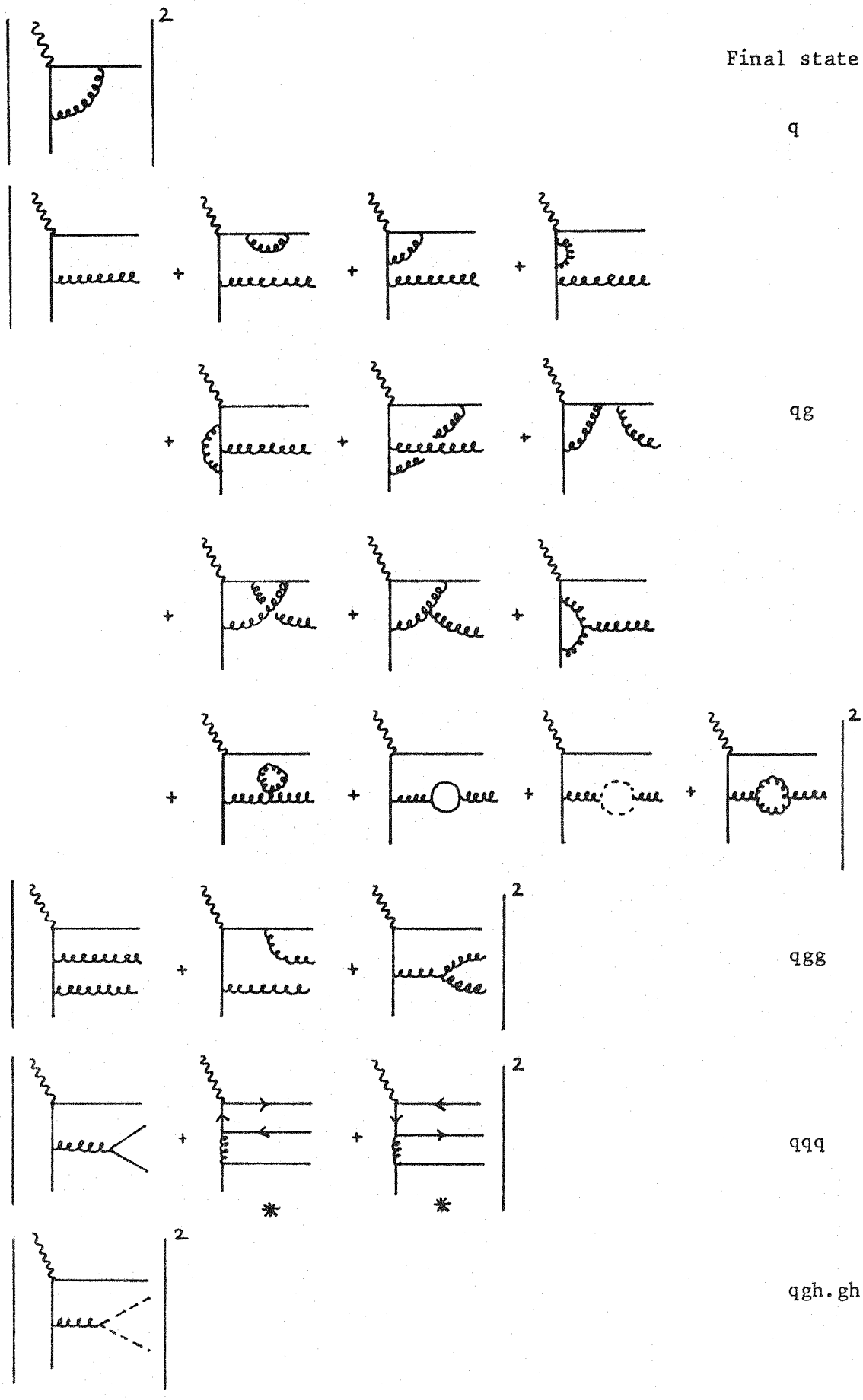

Fig. 2.8

* these are flavour singlet amplitudes, but they can interfere with flavour non singlet amplitudes to give a contribution to σ_L .

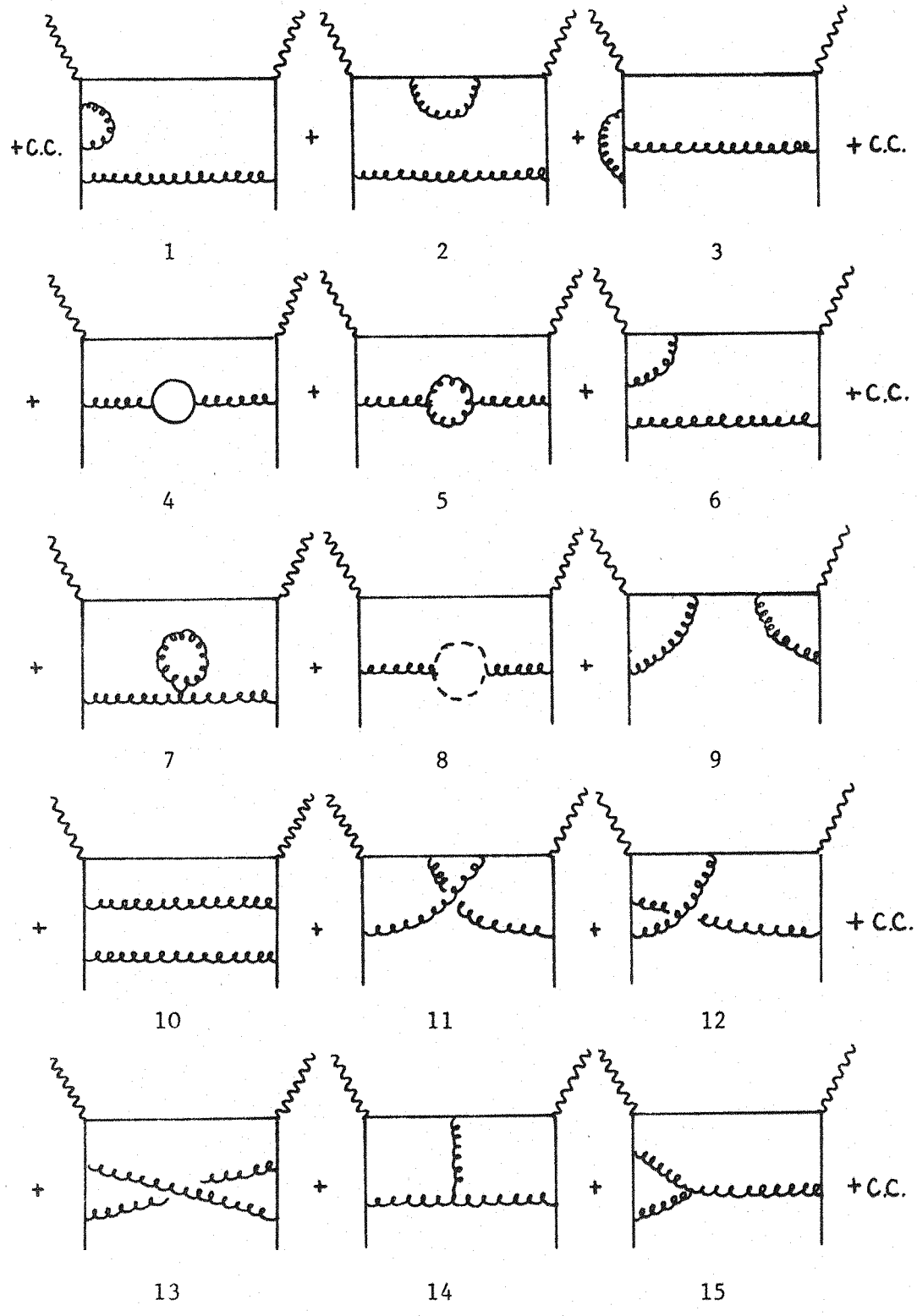

Fig. 2.9

(Crossed diagrams are understood)

Two loop elastic amplitudes contributing to σ_L

CHAPTER THREE

INFRA-RED REGULARISATION

3.1 Bloch-Nordsieck Mechanism for QED and the KLN Theorem

We have already encountered ultra-violet divergences in Quantum Field theory and briefly discussed how the Renormalization Program was set up in order to extract finite, physically sensible predictions.

In theories containing massless particles however, there exists a new class of divergences originating from the low momentum region of loop integrations, and so known as infra-red divergences [3.1]. Thus they are sensitive to the values of the external momenta of a Greens function and cannot be simply renormalised away. As an illustration, consider the purely electromagnetic process of $e^+e^- \to \mu^+\mu^-$ calculated in successive orders of QED perturbation theory. The lowest order diagram of Fig 3.1 is straight-forward to evaluate and yields

$$\sigma_0 = \frac{4\pi\alpha^2}{3Q^2} \tag{3.1}$$

with

$$\alpha = \frac{e^2}{4\pi} \tag{3.2}$$

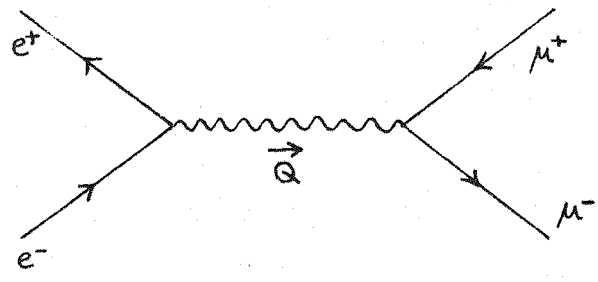

Fig 3.1 Lowest order Feynman diagram for $e^+e^- \to \mu^+\mu^-$

If we continue the perturbation expansion in α for this process, the diagrams to be calculated at one loop level are illustrated in Fig 3.2. Consider separately the $\mu^+\mu^-\gamma$ vertex correction depicted in Fig 3.3. Using the Feynman Rules for QED, it can be written in the Feynman gauge $\alpha = 1$ as

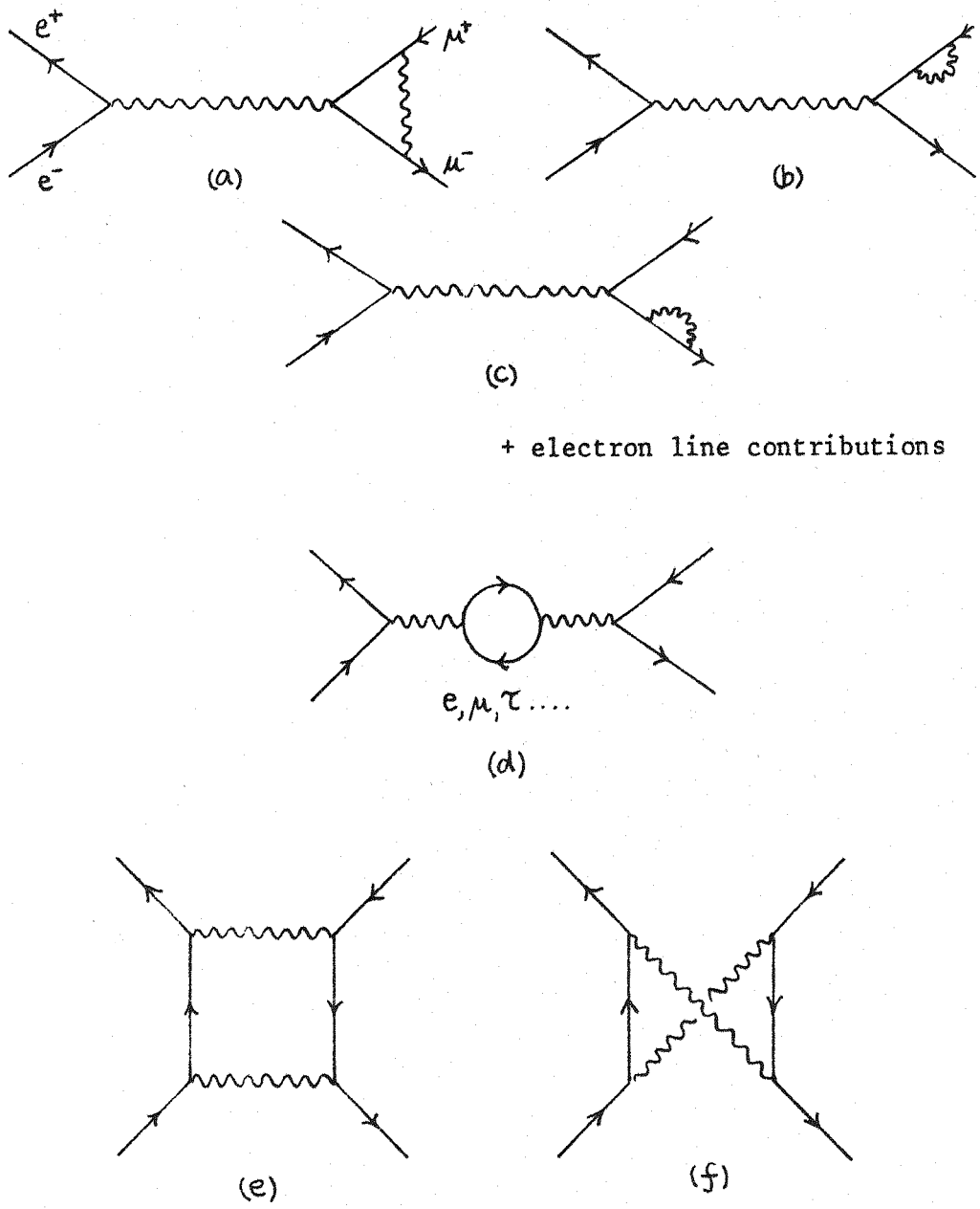

Fig 3.2 One-loop virtual corrections to $e^+e^- \to \mu^+\mu^-$

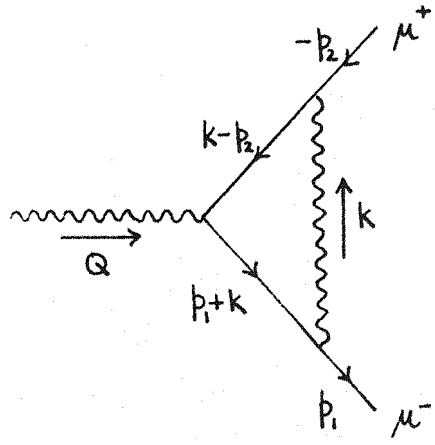

Fig 3.3 Vertex correction

$$V_\mu = -ie\,\bar{u}(p_1)\,\Lambda_\mu\,u(-p_2) \tag{3.3}$$

with $$\Lambda_\mu = (-ie)^2\int_{-\infty}^{\infty} d^Dk\ \gamma^\lambda \frac{i(\not p+\not k+m)}{[(p_1+k)^2-m^2+i\varepsilon]}\,\gamma_\mu \frac{i(-\not p_2+\not k+m)}{[(-p_2+k)^2-m^2+i\varepsilon]}\,\gamma_\lambda \frac{(-i)}{(k^2+i\varepsilon)} \tag{3.4}$$

For massive on-shell final state fermions

$$p_1^2 = p_2^2 = m^2 \tag{3.5}$$

then the loop integral above as $k \to 0$

$$\sim \int d^Dk\ \frac{\text{constant}}{k^4} \tag{3.6}$$

which is logarithmically divergent for small (IR) k in D = 4 dimensions. Notice that for off shell fermions, the infra-red divergence vanishes as now the behaviour for small k is

$$\sim \int d^Dk\ \frac{\text{constant}}{k^2} \tag{3.7}$$

In order to calculate the coefficient of this IR divergence, the numerator of V_μ can be re-arranged using the equations of motion

$$(\not{p}_2 + m)\, u(-p_2) = 0 \tag{3.8}$$

$$\bar{u}(p_1)(\not{p}_1 - m) = 0 \tag{3.9}$$

to take the form in the limit of $k \to 0$

$$ie^2 4p_1 \cdot p_2 \; (-ie)\; \bar{u}(p_1)\gamma_\mu u(-p_2) \tag{3.10}$$

which is proportional to the Dirac structure associated with the lowest order vertex, V_μ^o

$$V_\mu^o = -ie\, \bar{u}(p_1)\, \gamma_\mu\, u(-p_2) \tag{3.11}$$

Thus $V_\mu^{IR} = V_\mu^o I$ for small k (3.12)

where

$$I = ie^2 4p_1 \cdot p_2 \int d^D k \; \frac{1}{(k^2+i\varepsilon)(2p_1 \cdot k + k^2 + i\varepsilon)(-2p_2 \cdot k + k^2 + i\varepsilon)} \tag{3.13}$$

The divergent integral, I, can now be regulated by one of the following two procedures.

Either a) Introduce a photon "mass" λ^2 so that the photon propagator

$$\frac{1}{k^2 + i\varepsilon} \longrightarrow \frac{1}{k^2 - \lambda^2 + i\varepsilon} \tag{3.14}$$

This substitution will now modify a previously divergent Feynman Parameter integral

$$\int_0^1 d\alpha \, \frac{1}{\alpha} \rightarrow \int_0^1 d\alpha \, \frac{1}{\alpha + O\left(\frac{\lambda^2}{Q^2}\right)} \sim \ln\left(\frac{\lambda^2}{Q^2}\right) \tag{3.15}$$

λ^2 is not a mass in the formal sense of A_μ now being a Proca field, but rather a small dimensionful parameter introduced by hand in order to render some Greens functions finite. All Greens functions are then considered as the limit as $\lambda^2 \rightarrow 0$.

Or b) Use the previously discussed technique of dimensional regularization [3.2] to evaluate the diagram away from 4 dimensions. In particular if $D = 4 - \varepsilon$ then what was a divergent Feynman parameter integral will now yield a $\frac{1}{\varepsilon}$ pole.

$$\int_0^1 d\alpha \, \frac{1}{\alpha} \rightarrow \int_0^1 d\alpha \, \alpha^{-1-\varepsilon} = -\frac{1}{\varepsilon} \tag{3.16}$$

Choosing the second of these regularization methods, the divergent integral, I, can be evaluated in a straight-forward manner to give (for $Q^2 > 4m^2$)

$$I = \frac{e^2}{16\pi^2} \frac{4}{\varepsilon} \frac{\left(1 - \frac{2m^2}{Q^2}\right)}{\sqrt{1 - \frac{4m^2}{Q^2}}} \ln\left(\frac{1 + \sqrt{1 - \frac{4m^2}{Q^2}}}{1 - \sqrt{1 - \frac{4m^2}{Q^2}}} \right) \tag{3.17}$$

To calculate the cross-section for $e^+e^- \rightarrow \mu^+\mu^-$ to $O(\alpha^3)$, the diagrams of Fig 3.2 have to be interfered with the lowest order graph of Fig 3.1 and integrated over the corresponding two particle phase space. From the above we can see that the contribution of Fig 3.2(a) will contain an infra-red divergent term with a coefficient

$$\sigma_a^{IR} = \frac{\alpha}{\pi}\frac{1}{\varepsilon}\frac{\left(1-\frac{2m^2}{Q^2}\right)}{\sqrt{1-\frac{4m^2}{Q^2}}}\ln\left(\frac{1+\sqrt{1-\frac{4m^2}{Q^2}}}{1-\sqrt{1-\frac{4m^2}{Q^2}}}\right)\sigma_0 \qquad (3.18)$$

This contribution is not cancelled by any of the other infra-red divergent terms arising from the remaining diagrams of Fig 3.2.

Thus we are faced once again with the dilemma of perturbation theory supplying infinite corrections to cross-sections beyond leading order.

The resolution of this problem was realised long ago by Bloch and Nordsieck [3.3]. They argued that in any physical measurement of the cross-section $e^+e^- \to \mu^+\mu^-$ the final state detection apparatus is not perfect and so will have an energy resolution Δ. Therefore it is impossible to specify the final state completely as the detection equipment will miss any number of soft photons with combined energy $< \Delta$ produced with the muon pair. Thus physical experiments do not measure strictly exclusive processes, but rather suitably defined inclusive reactions.

To the order of perturbation theory considered above, the amplitudes for the production of $\mu^+\mu^-\gamma$ are shown in Fig 3.4. In order to calculate the cross-section, the resulting squared amplitudes are integrated over the corresponding three-body phase space. The photon energy, ω, is integrated over all values missed by the detection equipment, i.e. from zero to Δ. This integral is found to diverge as $\omega \to 0$ for $D = 4$ dimensions. Considering Fig 3.4a only, the coefficient of this infra-red divergence can be calculated by evaluating the phase space integrals in $D = 4 - \varepsilon$ dimensions.

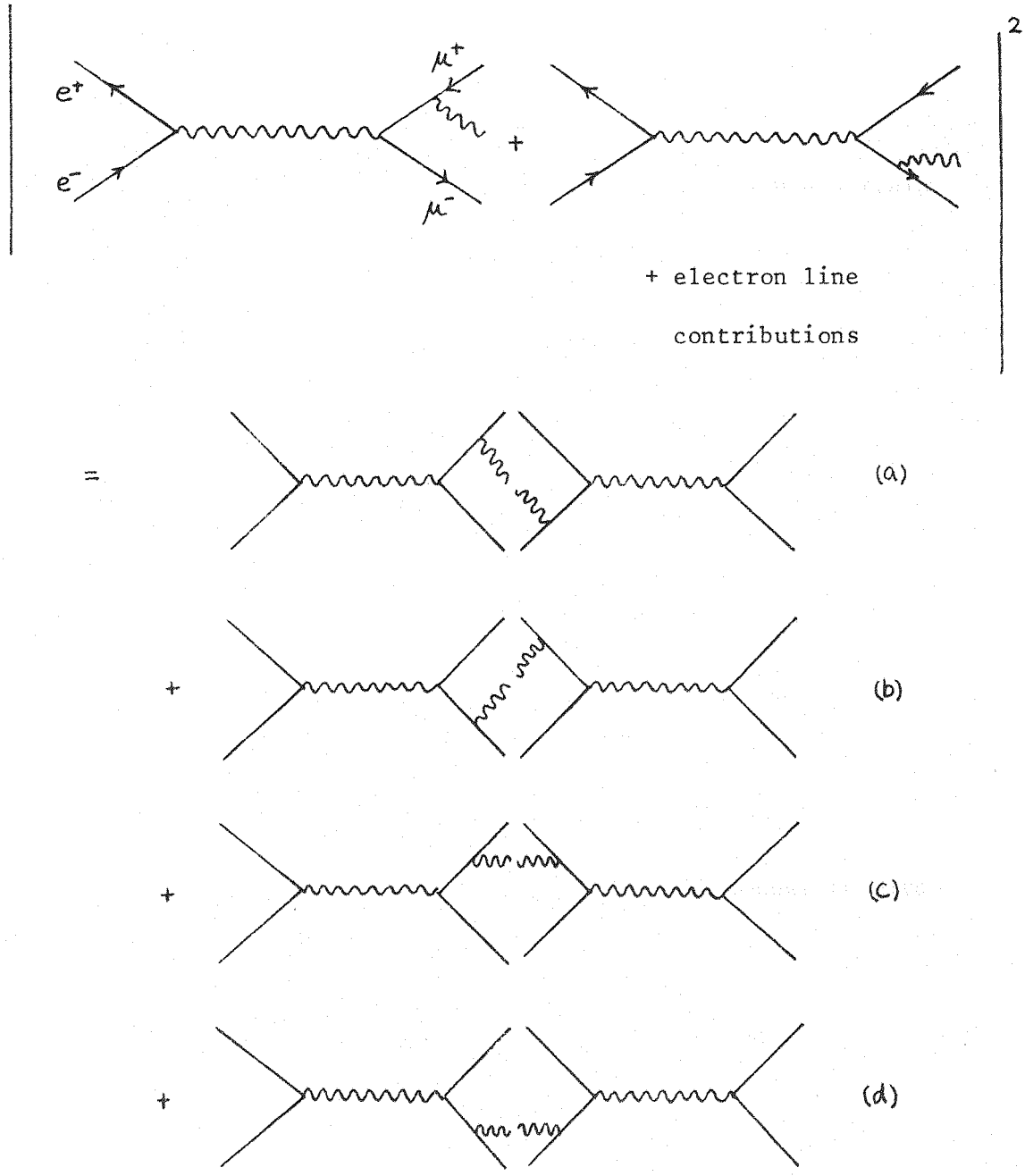

Fig 3.4 Lowest order diagrams for the process $e^+e^- \to \mu^+\mu^-\gamma$

Specifically

$$\tilde{\sigma}_a^{IR} = -\frac{\alpha}{\pi}\frac{1}{\varepsilon}\frac{1-\frac{2m^2}{Q^2}}{\sqrt{1-\frac{4m^2}{Q^2}}}\ln\left(\frac{1+\sqrt{1-\frac{4m^2}{Q^2}}}{1-\sqrt{1-\frac{4m^2}{Q^2}}}\right)\sigma_o \qquad (3.19)$$

This term precisely cancels the infra-red divergence of Fig 3.2a above. Further cancellations take place between diagrams of Fig 3.2b, c and those of Fig 3.4c, d, rendering the total physically measurable cross-section for $e^+e^- \to \mu^+\mu^-$ + soft photon infra-red finite to $O(\alpha^3)$.

The proof that a cancellation of this type takes place to all orders of QED perturbation theory was subsequently given by Yennie, Frautschi and Suura [3.4].

For theories that contain coupled massless particles such as QCD and massless QED, there exist further divergences known as mass singularities. These arise from the simple fact that two collinear massless particles have a total invariant mass of zero. An indication of this extra divergence can be gained by trying to take the $m_\mu \to 0$ limit of the coefficient of the infra-red divergence previously calculated in $e^+e^- \to \mu^+\mu^-$. For the deep inelastic scattering amplitude of Fig 3.5

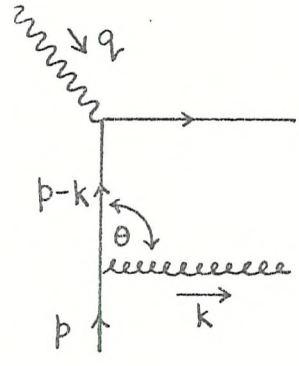

Fig 3.5

Consider the propagator $\frac{1}{(p-k)^2}$ where the (massless) quark and gluon are both on mass shell

$$p^2 = k^2 = 0 \tag{3.20}$$

Then if $p^\mu = (E, \underline{p})$ and $k^\mu = (\omega, \underline{k})$ the mass-shell condition implies $E = |\underline{p}|$ and $\omega = |\underline{k}|$. Thus

$$\frac{1}{(p-k)^2} \rightarrow \frac{1}{-2E\omega(1-\cos\theta)} \tag{3.21}$$

where $\omega \rightarrow 0$ represents the infra-red divergence, and $\cos\theta \rightarrow 1$, the endpoint of the angular phase space integral, is the new mass (collinear) singularity. Notice that it occurs independent of the value of ω.

If we regulate this mass singularity by taking the initial quark slightly off shell and space-like

$$p^2 < 0 \tag{3.22}$$

But, with

$$q^2 \gg p^2 \tag{3.23}$$

then

$$\frac{1}{(p-k)^2} \rightarrow \frac{1}{p^2 - 2E\omega\left[1 - \frac{|\underline{p}|}{E}\cos\theta\right]} \tag{3.24}$$

But

$$E^2 - \underline{p}^2 = p^2 \tag{3.25}$$

therefore

$$\frac{|\underline{p}|}{E} = 1 - \frac{p^2}{2E^2} \tag{3.26}$$

and so

$$\frac{1}{(p-k)^2} \rightarrow \frac{1}{p^2 - 2E\omega\left[1-(1-\frac{p^2}{2E^2})\cos\theta\right]} \tag{3.27}$$

It is now clear that there is no infra-red divergence as $\omega \rightarrow 0$, and the $\cos\theta \rightarrow 1$ limit produces terms in the propagator of $O(p^2)$. The angular integration thus gives a $\ell n \left(\frac{p^2}{q^2}\right)$.

The KLN theorem [3.5, 3.6] is concerned with the cancellation of these mass-singularities for suitably defined inclusive cross sections. They prove that if quark and gluon masses are introduced in order to calculate a cross-section from some initial to final state, $\sigma_{i\rightarrow f}$, then the quantity

$$\sum_{D(E_i)} \sum_{D(E_f)} \sigma_{i\rightarrow f} \tag{3.28}$$

is mass finite as $m_q, m_g \rightarrow 0$. The sums are over states degenerate with the initial and final states as $m_q, m_g \rightarrow 0$ (for example a quark + any number of soft massless gluons). This theorem assures that the cross-section for $e^+e^- \rightarrow \mu^+\mu^- X$ is finite even in the limit of both the muon and photon masses approaching zero.

3.2 Off mass-shell regularization

For deep inelastic scattering on a quark the KLN theorem asserts that all mass-singularities associated with the final states must cancel. This is because we are calculating the inclusive cross-section

$$\gamma^* + q \rightarrow q + X \tag{3.29}$$

The mass singularities due to the initial quark remain but it can be shown that they factorise to all orders of perturbation theory leaving a calculable Q^2 dependence. This structure supports the use of the Operator Product expansion in deep inelastic scattering, and the assumption that hard scattering cross sections can be written as a convolution of some process-independent soft hadronic wavefunction (sensitive to large distances) and hard sub-process involving only quarks and gluons amenable to perturbation theory.

In order to regulate the collinear divergences, we shall follow the previous example and take the initial quark slightly off shell and space-like. Generally we would expect a diagram such as Fig 3.5 to contain a factor of $\ell n \left(\frac{p^2}{q^2}\right)$ and, as both gluons go collinear with the initial quark in Fig 3.6, a $\ell n^2 \left(\frac{p^2}{q^2}\right)$.

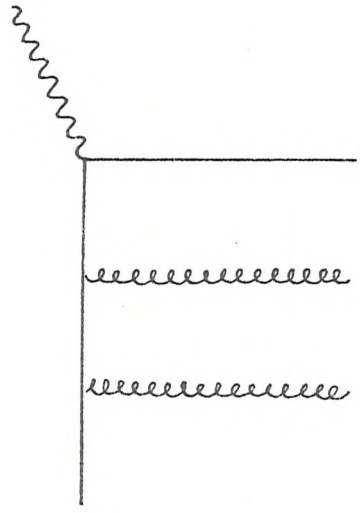

Fig 3.6

This is not found when calculating the contributions of these diagrams to σ_L however due to the extra "helicity suppression" previously discussed in the context of the parton model. Effectively, when calculating σ_L the numerator factors using the $p^\mu p^\nu$ projector always arrange to cancel one power of naive logarithmic collinear divergence. Thus for σ_L Fig 3.5 is mass finite, and Fig 3.6 yields only one power of $\ell n \left(\frac{p^2}{q^2} \right)$. Although this type of off mass shell regularization has the advantage that one can clearly see which are the singular regions of phase space integration and how $p^2 < 0$ regulates these would-be divergences, in general great care must be taken when implementing the second of the conditions on p^2, that of

$$2p.q > -q^2 \gg -p^2 \tag{3.30}$$

It is not sufficient to simply set $p^2 = 0$ in the numerator of some Feynman diagram. This action carries the possibility of missing finite contributions as in some cases the coefficient of p^2 (itself an integral) is so divergent that it gives a $\frac{1}{p^2}$. Out of all the two loop amplitudes of Fig 2.9 this effect was found to be present only in diagram, 2.9(10). This fact is again probably due to the special structure of the σ_L process, for out of all the inteferences of the inelastic amplitudes of Fig 2.8, the s-channel cut of Fig 2.9(10) is the only one in which one gluon can go collinear with the initial quark and put two propagators simultaneously on shell without decoupling from the σ_L process. This produces a $\frac{1}{p^4}$ pole in the integrand which is converted into a $\frac{1}{p^2}$ after the phase space integral. This, of course, must be cancelled by an overall factor of p^2 appearing in the numerator, and indeed is. All other potential $\frac{1}{p^4}$ poles are suppressed by the numerator killing one power of divergence of the

propator $\frac{1}{(p - k_1)^4}$. Thus all other $\ell n\ (p^2)$ terms arise from regions of phase space where only one propagator is put on shell producing just a $\frac{1}{p^2}$ pole in the integrand. For this degree of divergence, it is safe to drop p^2 in the numerator.

We now extend this technique in order to regulate the collinear divergences associated with the final state particles of Fig 2.8. The KLN theorem states that the sum of these divergences is zero, but the optical theorem can provide a stronger constraint than that. If we consider an arbitrary two loop amplitude as shown in Fig 3.7, and calculate it

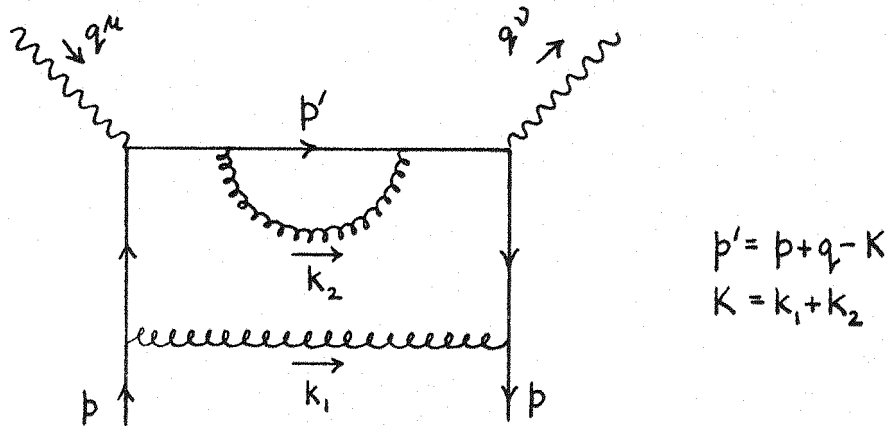

Fig 3.7 Two loop amplitude contributing to σ_L

for massless off-shell quarks $p^2 < 0$ then it has no infra-red divergences due to the virtual gluons being soft. All mass singularities are regulated by p^2. The optical theorem relates the imaginary part of this amplitude to the corresponding inelastic

cross-section, the imaginary part being the sum of all the physical s-channel cuts illustrated in Fig 3.8

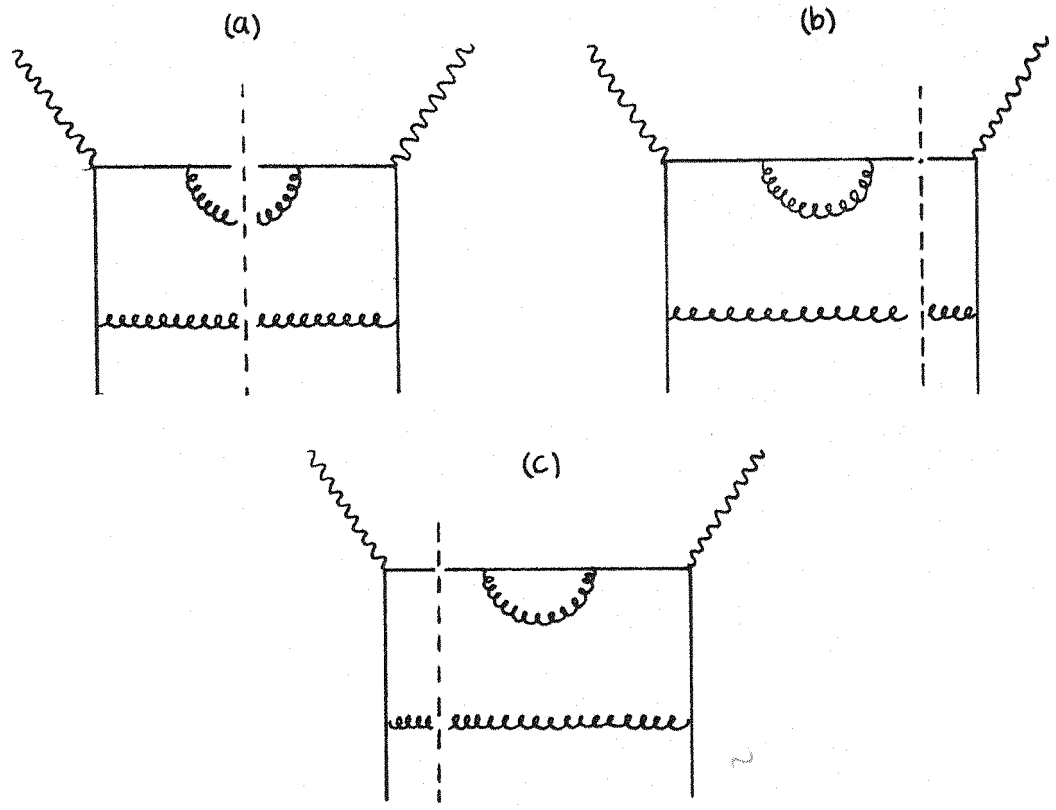

Fig 3.8 S-channel cuts of a two loop amplitude contributing to σ_L. Cut lines are on mass-shell

These three cuts separately have mass singularities associated with the emission of real and virtual gluons almost parallel to the final state quark. By virtue of the optical theorem, the sum of these divergences must be zero due to the absence of any such divergence in the imaginary part of the two loop amplitude. Thus we have a diagram by diagram implementation of the KLN theorem at two loop amplitude level.

All final state mass singularities of the three cuts of Fig 3.7 can be regularized in each case by taking the final state quark slightly off shell and time-like. Thus for the cut of Fig 3.8(a) if, in the massless three body phase space integral, $\delta(p'^2)$ is replaced by $\delta(p'^2 - \lambda^2)$ then this diagram will yield a $\ell n \left(\frac{\lambda^2}{Q^2}\right)$. However, we could have also regulated the divergence giving the gluon a "mass" by taking

$$\delta(k_2^2) \rightarrow \delta(k_2^2 - \lambda^2) \tag{3.31}$$

or by introducing a mass into the propagator

$$\frac{1}{\not p + \not q - \not k_1 + i\varepsilon} \rightarrow \frac{1}{\not p + \not q - \not k_1 - \lambda + i\varepsilon} \tag{3.32}$$

Each of these three prescriptions will provide (as they must) the same leading divergence of $\ell n \left(\frac{\lambda^2}{Q^2}\right)$, but will give in general different finite parts. Thus it is important to realise that the assignment of regulators λ^2 is not arbitrary. In order to calculate the correct finite part for the sum of the three cuts a), b) and c) the regulator λ^2 must be assigned in a consistent manner to each cut [3.7]. A clue to how this is achieved is again provided by the optical theorem. At the two loop amplitude level we choose one internal propagator, which by the introduction of a small regulator λ^2, will render all physical cuts finite and calculable. Using the same labelling system this guarantees that the correct regulator assignment is followed for each separate physical cut. The procedure obviously generalises to any number of regulators required at the elastic amplitude level such that all physical cuts are finite.

To illustrate the method consider again the two loop amplitude of Fig 3.7. It is clear that the introduction of a small regulator to any of the propagators of the top fermion rung will regularise all the s-channel cuts of Fig 3.8. We will therefore choose the central propagator and take

$$\frac{1}{\not{p}'+i\varepsilon} \longrightarrow \frac{1}{\not{p}'-\lambda+i\varepsilon} \tag{3.33}$$

For the physical cuts, this implies that:-

for Fig 3.8(a) the final state quark p', is taken off-shell and time-like by an amount λ^2.

$$\delta(p'^2) \rightarrow \delta(p'^2-\lambda^2) \tag{3.34}$$

All other propagators in the diagram are massless.

for Figs 3.8 b), c) the final state quark $\tilde{p}'$ is on shell, $\tilde{p}'^2 = 0$, but a small regulator λ is introduced into the propagator

$$\frac{1}{\not{p}'+i\varepsilon} \longrightarrow \frac{1}{\not{p}'-\lambda+i\varepsilon} \tag{3.35}$$

All other propagators in the diagram are massless.

In order to check this procedure, we performed the following calculation working, as usual, in $D = 4 - 2\varepsilon$ dimensions and using the minimal subtraction procedure.

Firstly we calculated directly the imaginary part of the renormalised two loop amplitude shown in Fig 3.9. This involved the use of the dispersion relation techniques discussed in the previous chapter to evaluate the contribution of this renormalised two loop amplitude to the longitudinal coefficient function.

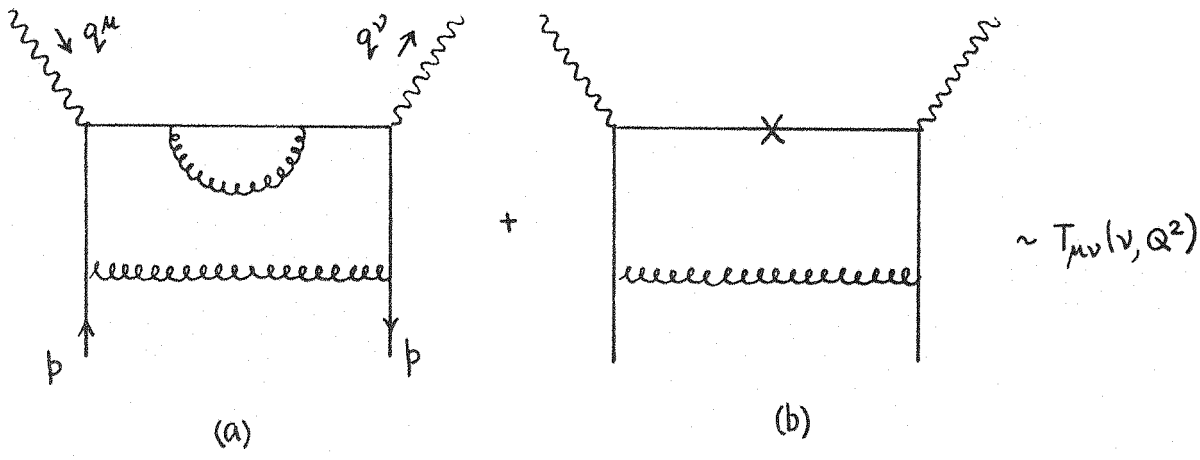

Fig 3.9 A renormalised two loop amplitude contributing to σ_L. The inclusion of crossed photon diagrams is understood.

In the previous notation

$$p^\mu p^\nu T_{\mu\nu}(x,Q^2) = -\frac{\nu}{2x}\sum_{n=0}^{\infty}\left(\frac{1}{x}\right)^n 2M_L(n,Q^2) \quad \text{n even only} \qquad (3.36)$$

The calculation proceeds much as that of the one loop diagram outlined in chapter two. We find for the contribution of the above diagrams to $M_L(n, Q^2)$ (all contributions are to be multiplied by a common factor of $e_c^2 C_2^2(R)\left(\frac{g}{4\pi}\right)^4 \frac{4}{n+1}$)

$$M_L^a(n,Q^2) = \left\{-\frac{1}{\varepsilon} - \frac{1}{2} - 2\left(S_1(n) + 1 + \gamma\right)\right\} \qquad (3.37)$$

$$M_L^b(n,Q^2) = \left\{\frac{1}{\varepsilon} + \left(S_1(n) + \gamma + 1\right)\right\} \qquad (3.38)$$

where

$$\gamma = \ln(4\pi) - \gamma_E - \ln\left(\frac{-q^2}{\mu^2}\right) \qquad (3.39)$$

$$S_1(n) = \sum_{j=1}^{n} \frac{1}{j} \tag{3.40}$$

This leads to a total renormalised contribution of

$$M_L^{a+b}(n,Q^2) = \left\{ -\gamma - \frac{3}{2} - S_1(n) \right\} \qquad \text{n even only} \tag{3.41}$$

Alternatively we can calculate the inelastic cross-section and determine $F_L(X, Q^2)$ by using

$$p^\mu p^\nu W_{\mu\nu}(X,Q^2) = \frac{\nu}{2X} \cdot \frac{1}{2X} F_L(X,Q^2) \tag{3.42}$$

and then evaluate the contribution to the moments by explicitly performing the integral over x

$$M_L(n,Q^2) = \int_0^1 dX \; X^{n-2} F_L(X,Q^2) \tag{3.43}$$

This necessitates calculating the squared amplitudes of Fig 3.10 integrated over phase space using the regularisation technique described above. The methods employed to do the three body phase space integrals of Fig 3.10a are to be discussed in the next chapter.

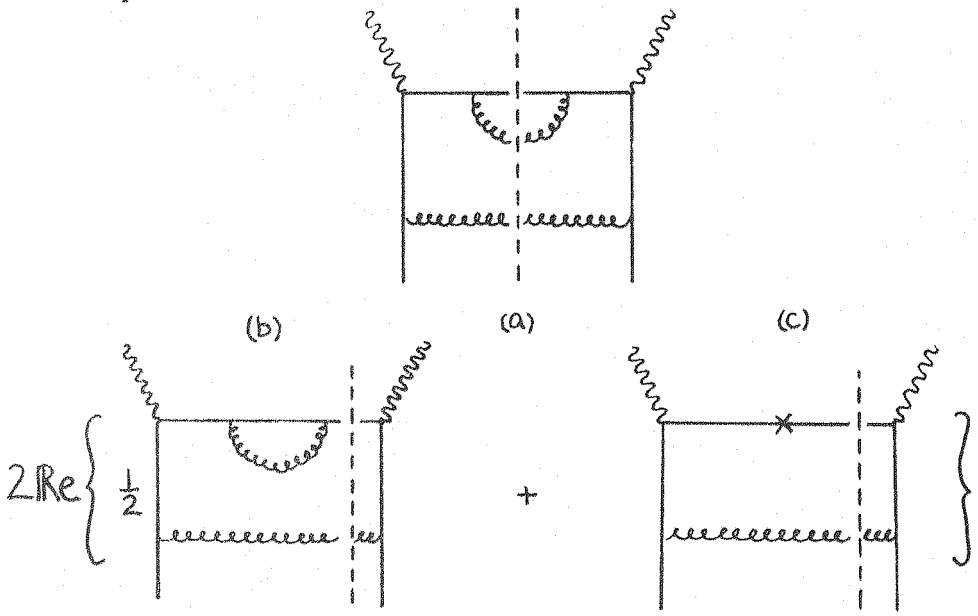

Fig 3.10 Interfered amplitudes contributing to σ_L to $O(g^4)$

The contributions are found to be (all diagrams are to be multiplied by a common factor of $e_c^2 C_2^2(R)\left(\frac{9}{4\pi}\right)^4 \frac{4}{n+1}$

$$M_L^a(n,Q^2) = \left\{-1 - \ln\left(\frac{\lambda^2}{S}\right)\right\} \tag{3.44}$$

$$M_L^b(n,Q^2) = \left\{-\frac{1}{\varepsilon} - \gamma + \ln\left(\frac{\lambda^2}{S}\right) - S_1(n) + \frac{1}{2}\right\} \tag{3.45}$$

$$M_L^c(n,Q^2) = \left\{\frac{1}{\varepsilon} - 1\right\} \tag{3.46}$$

with $S = (p + q)^2$ the centre of momentum energy. These lead to a total renormalised contribution of

$$M_L^{a+b+c}(n,Q^2) = \left\{-\gamma - \frac{3}{2} - S_1(n)\right\} \text{ for all } n \geq 1 \tag{3.47}$$

which is identical to that found before in Eq (3.41), and so verifies the use of the proposed scheme to regulate mass singularities.

As a final check to illustrate that it is irrelevant which propagator at two loop amplitude level is chosen for the introduction of the small regulator λ, consider the diagram of Fig 3.11

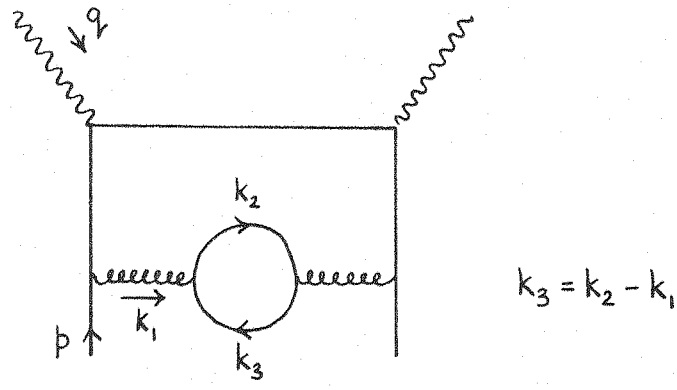

Fig 3.11 Two loop amplitude contributing to σ_L

Mass divergences are encountered in the physical s-channel cuts of this diagram when the massless fermions that propagate round the loop become parallel and so put the gluon propagator on shell. This happens for both real or virtual fermions (see Fig 3.12)

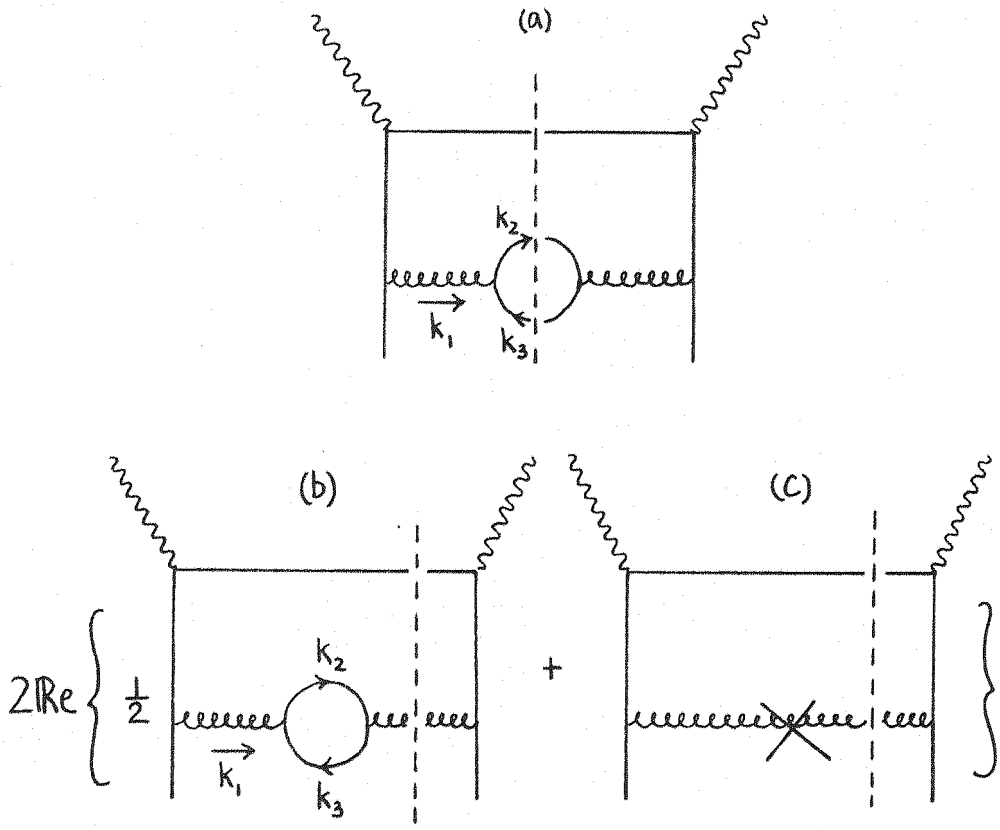

Fig 3.12 Interfered amplitudes contributing to σ_L to $O(g^4)$

These collinear divergences can be controlled using either of the following regulator assignments.

(i) evaluate the graphs of Fig 3.12 with a gluon propagator

$$\frac{-i}{k_1^2 + i\varepsilon} \longrightarrow \frac{-i}{k_1^2 + \lambda^2 + i\varepsilon} \tag{3.48}$$

The use of a space-like regulator, $\lambda^2 > 0$, avoids the possibility of further divergences due to the production of real massless fermions in the loop of Fig 3.12(b).

(ii) give the loop fermions a small mass, λ^2, such that for Fig 3.12(a) $k_2^2 = k_3^2 = \lambda^2$, whereas in Fig 3.12(b) the fermion propagators become

$$\frac{i}{\not{k}_{2,3} + i\varepsilon} \longrightarrow \frac{i}{\not{k}_{2,3} - \lambda + i\varepsilon} \tag{3.49}$$

with the final state gluon on shell $k_1^2 = 0$.

We present here the results of these calculations. Quoted are the $O(g^4)$ contributions to the structure function, $F_L(X, Q^2)$ as an expansion in g. We work directly in X space with all diagrams to be multiplied by a common factor of $e_i^2 \left(\frac{g}{4\pi}\right)^4 C_2(R)\, T(R)\, 4$

For method (i)

$$F_L^a(X,Q^2) = \frac{4}{3}\left\{ \frac{1}{X} - \frac{5}{2} - 2\ln x + \ln(1-X) - \ln\left(-\frac{\lambda^2}{q^2}\right)\right\} \tag{3.50}$$

$$F_L^b(X,Q^2) = \frac{4}{3}\left\{ -\frac{1}{\varepsilon} + \gamma - \frac{2}{3} + \ln\left(-\frac{\lambda^2}{q^2}\right)\right\} \tag{3.51}$$

$$F_L^c(X,Q^2) = \frac{4}{3}\left\{ \frac{1}{\varepsilon} - 1\right\} \tag{3.52}$$

Together these three quantities give a total renormalised contribution of

$$F_L^{a+b+c}(X,Q^2) = \frac{4}{3}\left\{ -\gamma + \frac{1}{X} - \frac{25}{6} - 2\ln x + \ln(1-X)\right\} \tag{3.53}$$

for method (ii) the diagrams are found to give

$$F_L^a(X,Q^2) = \frac{4}{3}\left\{ \frac{1}{X} - \frac{25}{6} - 2\ln x + \ln(1-X) - \ln\left(\frac{-\lambda^2}{q^2}\right)\right\} \tag{3.54}$$

$$F_L^b(x,Q^2) = \frac{4}{3}\left\{-\frac{1}{\varepsilon} - \gamma + 1 + \ln\left(\frac{\lambda^2}{q^2}\right)\right\} \tag{3.55}$$

$$F_L^c(x,Q^2) = \frac{4}{3}\left\{\frac{1}{\varepsilon} - 1\right\} \tag{3.56}$$

resulting in a renormalised contribution

$$F_L^{a+b+c}(x,Q^2) = \frac{4}{3}\left\{-\gamma + \frac{1}{x} - \frac{25}{6} - 2\ln x + \ln(1-x)\right\} \tag{3.57}$$

in agreement with the previous value of Eq (3.53).

Having demonstrated and justified the scheme by which collinear divergences are regularized, we now proceed to present an example calculation of a two loop amplitude contributing to σ_L.

CHAPTER FOUR

FOURTH ORDER CALCULATION OF σ_L:- DETAILS

At the end of chapter two, we gave a preliminary survey of the fourth order calculation of σ_L, and identified the relevant Feynman diagrams to be evaluated. In this chapter we outline how the calculation was performed and present an example calculation utilising the salient techniques for evaluating the phase space integrals. The final results are given diagram by diagram.

4.1 Calculational techniques

We calculate the squared amplitudes of Fig 2.8 integrated over the corresponding two or three body phase space. By the optical theorem this is equivalent to determining the s-channel discontinuities of the two loop amplitudes of Fig 2.9, including the crossed photon diagrams. In most cases, it is obvious how this identification works. Take for example the amplitude of Fig 2.9 (14), then the physical s-channel cuts are illustrated in Fig 4.1.

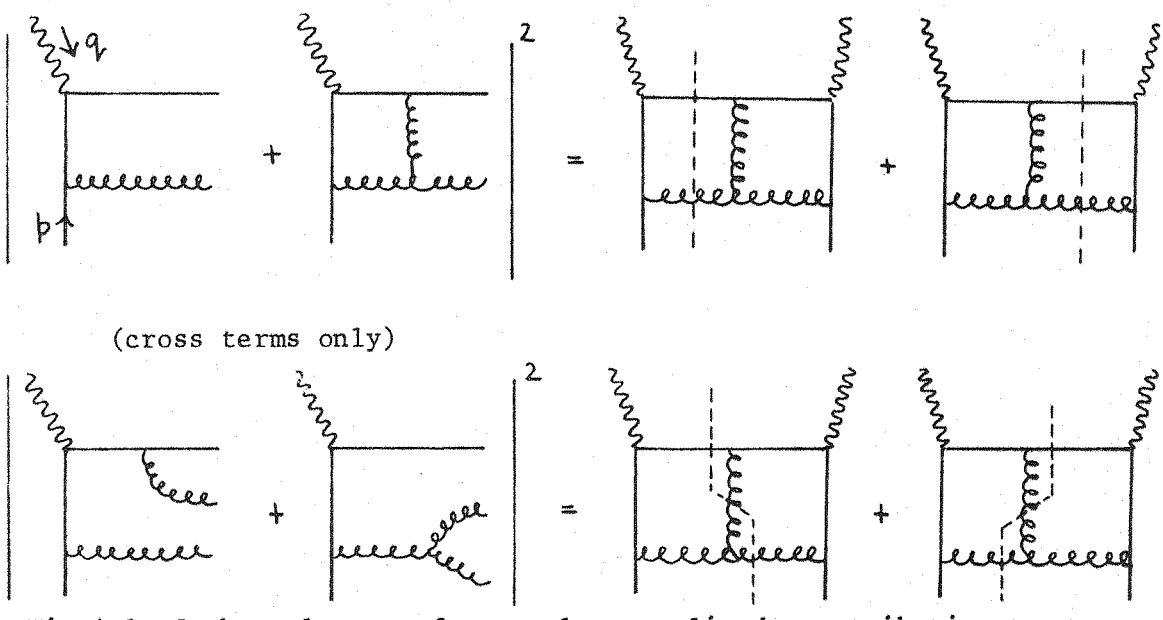

Fig 4.1 S-channel cuts of a two loop amplitude contributing to σ_L

The crossed photon diagram has no s-channel cut. This is true for all planar two loop amplitudes contributing to σ_L.

The situation for non-planar amplitudes is more complicated. The uncrossed amplitudes have a $u = (p - q)^2$ channel cut, and so the crossed photon amplitudes do indeed have s-channel discontinuities. These 'extra' cuts correspond to interferences of the flavour singlet amplitudes drawn when calculating the flavour non-singlet inelastic cross section, and are shown in Fig 4.2.

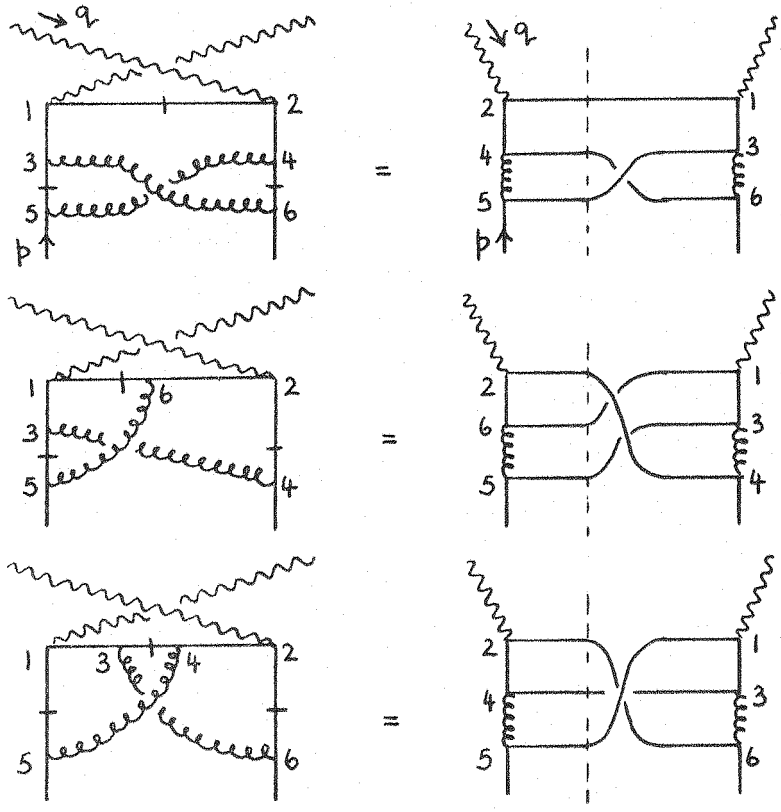

Fig 4.2 $S = (p + q)^2$ channel discontinuities of crossed photon non-planar two loop amplitudes contributing to σ_L

We found that we could not do some of the phase space integrals encountered in calculating these cuts totally analytically. It was

thus necessary to determine them by numerical methods, more about which will be mentioned later. In any case, the contribution of these integrals to the longitudinal coefficient function was small. The largest effect occured for n = 2 and was less then 7% of the total value in the MS scheme.

The cut amplitudes fall into one of two main categories, although all have spurious mass singularities arising from regions of phase space where massless final states are becoming parallel.

Some cuts consist of squared inelastic amplitudes containing a one loop integral and integrated over two body phase space. In these cases all the mass divergence is contained in the loop integral, leaving simple massless two body phase space to do. The loop is integrated using the standard techniques of Feynman parameterisation.

The rest of the cuts require the integration of three body phase-space in which are buried the mass divergences. The final state consists always of a quark of momentum p', together with a pair of either quarks, gluons or ghosts of momenta k_1 and k_2. All three final states are nominally massless. The general technique employed was to pair up the two momenta k_1 and k_2 using the identity

$$1 = \int_{-\infty}^{+\infty} d^4K \, \delta^4(K - k_1 - k_2) \tag{4.1}$$

This reduces the three body phase space integral

$$\int [dk_1][dk_2][dp'] \, \delta^4(p + q - k_1 - k_2 - p') \tag{4.2}$$

into two coupled quasi - two body phase space integrals

$$\int [d^4p'][d^4K]\, \delta^4(p+q-K-p') \int [d^4k_1][d^4k_2]\, \delta^4(K-k_1-k_2) \tag{4.3}$$

The regulator assignment was chosen such that in the three body phase space integrals, all final state divergences were then regularised by giving the final state quark of momentum p' a small mass

$$p'^2 = m^2$$

and by introducing a small regulator into the propagator

$$\frac{1}{K^2+i\varepsilon} \rightarrow \frac{1}{K^2+\lambda^2+i\varepsilon} \tag{4.4}$$

Only one amplitude (that of Fig 2.9(14)) required the simultaneous introduction of both these regulators and even here it would have been possible to abandon this assignment totally, choosing another gluon to make massive and so uniquely regularise all the divergences. We elected to continue using this choice though, as by this stage many of the familiar integrals appearing were tabulated.

All phase space and loop integrals were evaluated in the limit of

$$\lim_{-q^2, pq \rightarrow \infty} \lim_{\substack{\text{regulators} \\ -p^2, \lambda^2, m^2 \rightarrow 0}} I(p, q, m^2, \lambda^2) \tag{4.5}$$

and nowhere were we forced to make decisions about the relative sizes of the regulators, i.e. logs of the form $\ell n\ (m^2 + \lambda^2)$ do not occur.

The phase space integrals done numerically were evaluated using two different techniques. The first consisted of a straightforward application of the Gaussian integration formula

$$\int_{-1}^{+1} dx\, f(x) = \sum_{i=1}^{n} \omega_i f(x_i) + E_n \qquad (4.6)$$

where x_i, ω_i are the abscissas and weight factors tabulated [4.1] for some chosen value of n. The use of this formula technically requires the existence of the first 2n derivatives of the integrand f(x) throughout the integration region for finite error E_n

$$E_n = \frac{2^{2n+1}(n!)^4}{(2n+1)[(2n)!]^3} f^{(2n)}(\xi) \qquad (-1 < \xi < 1) \qquad (4.7)$$

As we were integrating functions with logarithmic end-point singularities this may appear an unreasonable approach to take. However, we found that for n = 32 the method could satisfactorily cope with integrable logarithmic singularities to an accuracy of ± 0.1%.

The second, and more reliable method, was to use an assisted Monte-Carlo integrating package known as VEGAS. Basically, this technique consists of evaluating the integrand at randomly generated points in the integration range. The program then looks for regions of maximum variation of the integrand, and saturates them with points in subsequent iterations. The program is iterated until it settles down to a consistent answer. This, of course, never occurs for singular integrals.

Both techniques could handle up to ten dimensional integrals although we used them to integrate functions of only three variables. The two methods were also of comparable efficiency, taking on the order of 30 seconds of processor time to evaluate one of the many three dimensional integrals.

4.2 Example calculation

We now present an example calculation of the s-channel discontinuities of a two loop amplitude contributing to σ_L, that of Fig 2.9(**6**). The two physical s channel cuts are shown in Fig 4.3

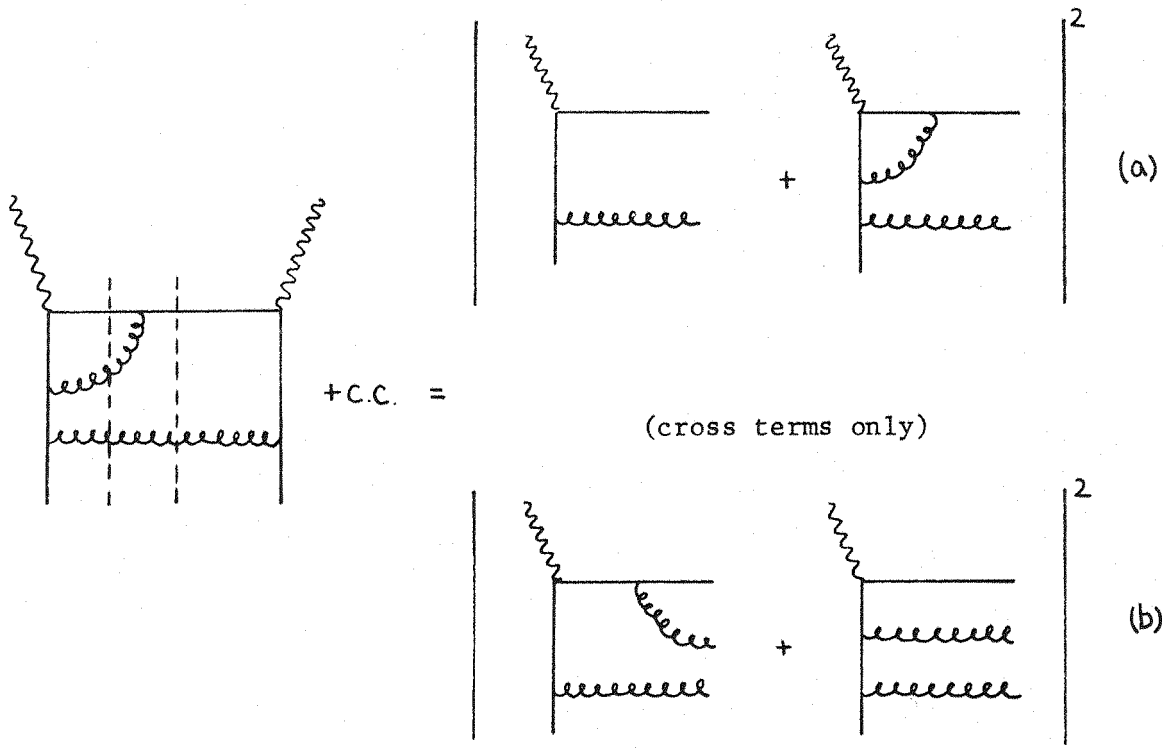

Fig 4.3 s-channel cuts of a two loop amplitude contributing to σ_L.

Again there are no s-channel cuts of the crossed photon amplitude. As previously discussed, both of these cuts (a) and (b) have spurious mass singularities associated (in this case) with real and virtual emission of gluons parallel to the final state quark. We shall choose to regulate these divergences by giving the final state quark of the inelastic amplitudes in (b) a small mass $p'^2 = m^2$.

Thus we commence by calculating the two body cut (a). In order to regularise the ultra-violet divergences of this cut we work in $D = 4 - 2\varepsilon$ dimensions and perform the D dimensional Dirac Algebra using the identities of Appendix A.1. From the Feynman rules of chapter 1, the cut (a) can be written as (see Fig 4.4(i))

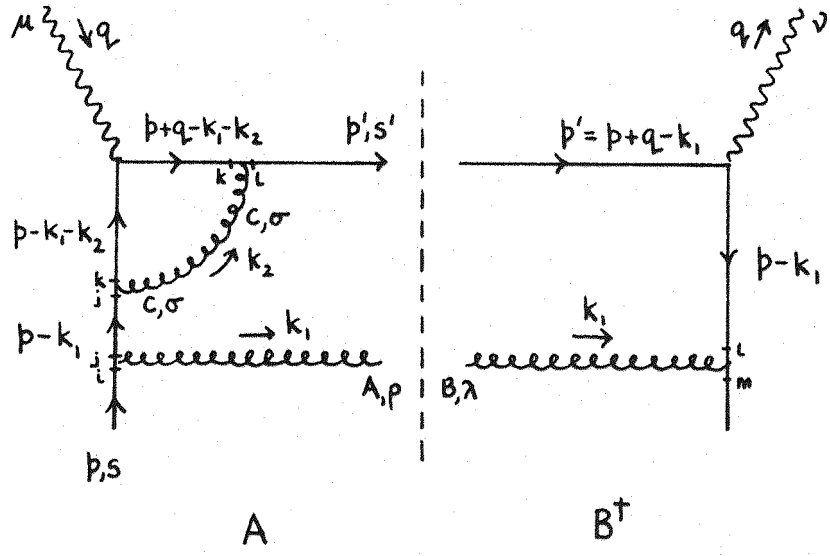

Fig 4.4(i) Two body s-channel cut (a)

$$A = -e_i g^3 \sum_c \left(\frac{\lambda^c}{2}\right)_{lk}\left(\frac{\lambda^c}{2}\right)_{kj}\left(\frac{\lambda^A}{2}\right)_{ji} \int_{-\infty}^{+\infty} d^D k_2 \; \bar{u}(p',s')\,\gamma^\sigma \frac{1}{(\not p' - \not k_2)}\gamma_\mu \frac{1}{(\not p - \not k_1 - \not k_2)} \cdot$$

$$\cdot \gamma_\sigma \frac{1}{(\not p - \not k_1)}\gamma_\rho\, u(p,s)\, \varepsilon_\kappa^{A,\rho}\, \frac{1}{k_2^2} \qquad (4.8)$$

$$B^\dagger = +ie_i^2 g \left(\frac{\lambda^B}{2}\right)_{ml} \bar{u}(p,s)\gamma^\lambda \frac{1}{(\not p - \not k_1)}\gamma_\nu\, u(p',s')\, \varepsilon_\kappa^{B,\lambda\dagger} \qquad (4.9)$$

Take the product $AB^\dagger$, and perform

i) the quark spin sum $\frac{1}{2}\sum_{ss'} \longrightarrow \frac{1}{2}\,\mathrm{Tr}$

ii) the gluon colour sum $\sum_{A,C}$

iii) the gluon polarisation sum

$$\sum_{\chi} \varepsilon_{\chi}^{A,\rho} \varepsilon_{\chi}^{B,\lambda\,\dagger} = -\delta^{AB} g^{\rho\lambda} \tag{4.10}$$

Then

$$AB^{\dagger} = +ie_i^2 g^4 C_2^2(R) \frac{1}{2} \cdot \int_{-\infty}^{\infty} d^D k_2 \; \frac{\mathrm{Tr}\left[\gamma^{\sigma}(\not{p}'-\not{k}_2)\gamma_{\mu}(\not{p}-\not{k}_1-\not{k}_2)\gamma_{\sigma}(\not{p}-\not{k}_1)\gamma_{\rho}\not{p}\gamma^{\rho}(\not{p}-\not{k}_1)\gamma_{\nu}\not{p}'\right]}{(p'-k_2)^2(p-k_1-k_2)^2(p-k_1)^2 k_2^2} \tag{4.11}$$

To calculate the contribution of this diagram to σ_L we apply the projection operator $p^{\mu}p^{\nu}$, then setting $p^2 = p'^2 = k_1^2 = 0$,

$$p^{\mu}p^{\nu}\,\mathrm{Tr} = (2-D)2p.k_1\left[\gamma^{\sigma}(\not{p}'-\not{k}_2)\not{p}(\not{p}-\not{k}_1-\not{k}_2)\gamma_{\sigma}\not{k}_1\not{p}\not{p}'\right] \tag{4.12}$$

$$= (2-D)2p.k_1\left[(i)+(ii)+(iii)+(iv)\right] \tag{4.13}$$

where

$$(i) = -4p.(p'-k_2)\,\mathrm{Tr}\left[(\not{p}-\not{k}_1-\not{k}_2)\not{k}_1\not{p}\not{p}'\right] \tag{4.14}$$

$$= -16p.(p'-k_2)\left[k_1.(p-k_2)p.p' + p'.(p-k_1-k_2)p.k_1 + p'.k_1\,p.(k_1+k_2)\right] \tag{4.15}$$

$$(ii) = +4p.k_1\,\mathrm{Tr}\left[(\not{p}-\not{k}_1-\not{k}_2)(\not{p}'-\not{k}_2)\not{p}\not{p}'\right] \tag{4.16}$$

$$= +16p.k_1\left[(p'-k_2).(p-k_1-k_2)p.p' + p'.(p-k_1-k_2)\,p.(p'-k_2) - p.(k_1+k_2)p'.k_2\right] \tag{4.17}$$

Both (iii) and (iv) are multiplied by an overall factor of 2ε, so the only contributions come from the UV divergent terms of these Traces, i.e. the $O(k_2^2)$ terms.

$$(iii) = (4-D)\,8p.k_2\left[p.p'k_1.k_2 + p'.k_2\,p.k_1 - p.k_2\,p'.k_1\right] \tag{4.18}$$

$$(iv) = -(4-D)\,8p.k_1\,p.p'\,k_2^2 \tag{4.19}$$

Now combine denominators using the standard Feynman parameterisation of Appendix A.1, and introduce a small 'mass' m^2 into the propagator $(p' - k_2)^2$ to regulate any mass singularities.

$$\frac{1}{k_2^2\left[(p'-k_2)^2-m^2\right](p-k_1-k_2)^2} = 2!\int_0^1 \frac{d\alpha d\beta d\gamma\ \delta(1-\alpha-\beta-\gamma)}{\left[\gamma k_2^2 + \alpha(p'-k_2)^2 - \alpha m^2 + \beta(p-k_1-k_2)^2\right]^3} \tag{4.20}$$

Doing the γ integral

$$= 2\int_0^1 d\alpha d\beta\ \frac{\theta(1-\alpha-\beta)}{\left[\hat{k}_2^2 - M^2\right]^3} \tag{4.21}$$

where
$$\hat{k}_2 = k_2 - \left(\alpha p' + \beta(p-k_1)\right) \tag{4.22}$$

and
$$M^2 = 2\alpha\beta p'.(p-k_1) + \alpha m^2 - \beta(1-\beta)(p-k_1)^2 \tag{4.23}$$

inserting this shift of origin into the Traces

$$p^\mu p^\nu\,Tr \equiv N = p.k_1\,p.p'\left(C_1 + C_2\hat{k}_2^2\right) \tag{4.24}$$

with

$$C_1 = -32(1-\beta)(1-\alpha)\, p'\!\cdot\! k_1 \tag{4.25}$$

$$C_2 = \frac{8}{D}(D-2)^2 \tag{4.26}$$

Thus, so far

$$p^\mu p^\nu [AB^\dagger] = i e_i^2 g^4 C_2^2(R) \int_0^1 d\alpha\, d\beta\, \theta(1-\alpha-\beta)\, \frac{2(p\cdot k_1)^2}{(p-k_1)^4}\, p\cdot p'(2-D) \cdot \int d^D\hat{k}_2 \quad \frac{C_1 + C_2 \hat{k}_2^2}{[\hat{k}_2^2 - M^2]^3} \tag{4.27}$$

performing the loop integrals using Appendix A.1, choosing $D = 4 - 2\varepsilon$, scaling $g^2 \to g^2\, \mu^{2\varepsilon}$ and expanding the whole result in powers of ε we arrive at

$$p^\mu p^\nu [AB^\dagger] = +e_i^2 g^4 C_2^2(R)\, \frac{1}{(4\pi)^2}\, p\cdot p' \cdot \iint_0^1 d\alpha\, d\beta\, \theta(1-\alpha-\beta) \left\{ \frac{16(1-\beta)(1-\alpha)\, p'\!\cdot\! k_1}{M^2} + 8\left(\frac{1}{\varepsilon} + \ln(4\pi) - \gamma_E - 3 - \ln\left(\frac{M^2}{\mu^2}\right)\right) \right\} \tag{4.28}$$

$$M^2 = 2\alpha\beta\, p'\!\cdot\!(p-k_1) + \alpha m^2 - \beta(1-\beta)(p-k_1)^2 - i\varepsilon \tag{4.29}$$

There are now two sets of Feynman parameter integrals to be done. Consider first

$$I_1 = \int_0^1 d\alpha\,(1-\alpha) \int_0^{1-\alpha} d\beta\, \frac{1-\beta}{a\beta^2 + b\beta + c} \tag{4.30}$$

where

$$a = (p-k_1)^2 < 0$$

$$b = 2\alpha p'(p-k_1) - (p-k_1)^2 > 0$$
$$c = \alpha m^2 - i\varepsilon > 0 \qquad (4.31)$$

The denominator is a quadratic in β with roots r_1 and r_2 given by

$$r_1 = \frac{-b+\sqrt{b^2-4ac}}{2a} \qquad (4.32)$$

Expanding the square root around the small quantity c, then

$$r_1 = -\frac{c}{b} + O(m^4) \quad < 0 \qquad (4.33)$$

As can easily be seen, if $m^2 = 0$ then the β integral is infinite.

Similarly

$$r_2 = -\frac{b}{a} + O(m^2) \quad > 0 \qquad (4.34)$$

Now

$$p' = p+q-k_1 \qquad (4.35)$$

So

$$b = 2\alpha(p.q-(p+q).k_1) + 2p.k_1(1-\alpha) \qquad (4.36)$$

But

$$p'^2 = 0, \quad \therefore 2p.q-(p+q).k_1 = q^2 \qquad (4.37)$$

$$\therefore r_2 = -\frac{\alpha q^2}{2p.k_1} + (1-\alpha) > (1-\alpha) \qquad (4.38)$$

Thus we see that the two roots of the quadratic in β lie outside the range of the β integral. So the $i\varepsilon$ in the denominator can be dropped and the β integral performed straightforwardly to yield

$$I_1 = \int_0^1 d\alpha\,(1-\alpha)\Big[\ \frac{1}{a}\Big(\ell n\Big(\frac{b}{e}\Big) - \ell n\alpha\Big) + \frac{1}{b}\Big(2\ell n\Big(\frac{b}{e}\Big) - 2\ell n\alpha + \ell n(1-\alpha) - \ell n\Big(\frac{m^2}{e}\Big)\Big)\Big] \qquad (4.39)$$

with $e = 2p'\cdot(p-k_1) - (p-k_1)^2$ independent of α.

Notice at this stage that the mass singularity is manifest in $\ell n(m^2)$. The α integrals present no problem aside from tedium. Since b is linear in α it is plausible that the result will contain dilogarithmns due to the presence of $\ell n\ \alpha$ and $\ell n(1-\alpha)$ terms in the numerator. The result is

$$I_1 = \frac{1}{d^2}\Big[\ \frac{3d}{2} + d\,\ell n\Big(\frac{m^2}{e}\Big) + \Big\{d - \frac{5}{2}a + e\,\ell n\Big(\frac{m^2}{e}\Big) + e\,\ell n\Big(\frac{d}{e}\Big)\Big\}\ell n\Big(-\frac{a}{e}\Big) - 2ef\Big(-\frac{e}{a}\Big) + ef\Big(\frac{d}{e}\Big) - ef(0) - e\,\ell n^2\Big(-\frac{a}{e}\Big)\Big] \qquad (4.40)$$

where

$$a = (p-k_1)^2$$
$$d = 2p'\cdot(p-k_1)$$
$$e = d-a \qquad (4.41)$$

and

$$f(x) = \int_1^x \frac{\ell n t}{1-t}\,dt \qquad (4.42)$$

One novel feature is that in the later phase space integrals to be done, d can vanish. This may seem catastrophic as I_1 has an overall factor of $\frac{1}{d^2}$, but as will be shown later, in this region the numerator $\sim O(d^2)$ yielding a finite result. The appearance of these fake 'poles' in the phase space integrals turned out to be a common occurrence in the calculation of many diagrams.

The other set of Feynman parameter integrals are much simpler due to the fact that they contain only integrable logarithmic singularities in the limit of $m^2 \to 0$. Thus m^2 does not act as a regulator here. Consider

$$I_2 = \int_0^1 d\alpha \int_0^{1-\alpha} d\beta \left\{ \frac{1}{\varepsilon} + \ln(4\pi) - \gamma_E - 3 - \ln\beta - \ln\left(\frac{2\alpha p'(p-k_1) - (1-\beta)(p-k_1)^2}{\mu^2} \right) \right\} \tag{4.43}$$

in the previous notation, the β integral gives

$$I_2 = \int_0^1 d\alpha \quad (1-\alpha)\left(\frac{1}{\varepsilon} + \ln(4\pi) - \gamma_E - 2 - \ln(1-\alpha) \right)$$

$$- \frac{1}{a}\left(\alpha e \ln\left(\frac{\alpha e}{\mu^2}\right) - a(1-\alpha) - b\ln\left(\frac{b}{\mu^2}\right) \right)$$

with

$$b = \alpha 2p'(p-k_1)^2 - (p-k_1)^2 \tag{4.44}$$

The α integrals are straightforwardly done as the denominator is α independent with the result

$$I_2 = \frac{1}{2}\left[\frac{1}{\varepsilon} + \ln(4\pi) - \gamma_E + \frac{e}{d}\ln\left(-\frac{a}{e}\right) - \ln\left(-\frac{a}{\mu^2}\right) \right] \tag{4.45}$$

Assembling the answer before the final phase space integrals we arrive at

$$p^\mu p^\nu [AB^\dagger] = +e_i^2 g^4 C_2^2(R) \frac{\perp}{(4\pi)^2} 8 p.p' \left[2p'.k_1 I_1 + I_2 \right] \tag{4.46}$$

The final state phase space integral is given by

$$W = \int [d\!\!\!^{-}p'][d\!\!\!^{-}K]\, \delta^4(p+q-K-p') \left[p^\mu p^\nu AB^\dagger \right] \tag{4.47}$$

with $[d\!\!\!^{-}\ell] = d^4\ell\, \delta(\ell^2 - m^2)\Theta(\ell^\circ)$ the Lorentz invariant volume element for a final state of four momentum ℓ and mass m.

The most convenient frame in which to determine the phase space integrals is the p, q centre of momentum frame. Thus

$$p = (E, 0, 0, \underline{p}) \tag{4.48}$$

$$q = (q^\circ, 0, 0, -\underline{p}) \tag{4.49}$$

and if

$$k_1 = (\omega, \underline{k}) \tag{4.50}$$

Then

$$(p+q).k_1 = \omega\sqrt{s} \tag{4.51}$$

$$(p+q).p = E\sqrt{s} \tag{4.52}$$

where $S = (p + q)^2$ the centre of momentum energy.

For no azimuthal (ϕ) dependence of the matrix element, as is the case above, the two body phase space reduces in this frame to

$$W = \frac{1}{8(2\pi)}\int_{-1}^{+1} dz\, [p^\mu p^\nu A B^\dagger] \tag{4.53}$$

with

$$\omega = |\underline{k}| = \frac{\sqrt{s}}{2} \tag{4.54}$$

and

$$p.k_1 = \tfrac{1}{2} p.q \left[1 - \left(1 - \frac{p^2}{2E^2}\right) z\right] \tag{4.55}$$

the only angle (z) dependent quantity.

Consider the contributions to W from I_1 and I_2 separately and re-write the phase space integral in terms of the variable

$$y = -\frac{q}{e} = \frac{(p-k_1)^2}{q^2} \tag{4.56}$$

Thus from I_1

$$W_1 = -e_c^2 g^4 C_2^2(R) \left(\frac{1}{4\pi}\right)^2 \frac{x}{\pi}\frac{s}{2} \cdot \int_{\frac{p^2}{q^2}x}^{\frac{1}{x}} dy \left[\left(\frac{x-1}{x}\right)\frac{1}{(1-y)^2} - \frac{1}{(1-y)}\right]\left[\frac{3}{2}(1-y) + (1-y)\ln\left(\frac{m^2}{-q^2}\right)\right.$$

$$+\left(-\tfrac{3}{2}(1-y) + \tfrac{5}{2} + \ln\left(\tfrac{m^2}{-q^2}\right)\right)\ln y$$

$$\left. - 2f\left(\tfrac{1}{y}\right) - f(y) - \ln^2 y \right] \tag{4.57}$$

where

$$x = -\frac{q^2}{2p.q} \tag{4.58}$$

As previously remarked, the 'pole' at y = 1 is a fake. This can be seen easily by expanding the numerator around y = 1 - δ using

$$f\left(\tfrac{1}{y}\right) = -\tfrac{1}{2}\ln^2 y - f(y) \tag{4.59}$$

and

$$f(1-\delta) = \sum_{k=1}^{\infty} \frac{\delta^k}{k^2} \quad , \quad |\delta| < 1 \tag{4.60}$$

Also, there are only integrable logarithmic divergences as $y \to 0$ reflecting the fact that this cut is insensitive to p^2, the 'off-shellness' of the incoming quark.

The y integrals can now be evaluated separately taking care with the region near y = 1 to give

$$\begin{aligned} W_1 = {} & +e_i^2\left(\frac{g}{4\pi}\right)^4 C_2^2(R)\, 4\pi p.q\; 4(1-X). \\ & \Big[\; 3 + 3\ln X + \ln\left(\tfrac{1-X}{X}\right) + \ln X \ln\left(\tfrac{1-X}{X}\right) \\ & + \left(3X - \tfrac{3}{2}\right) f\left(\tfrac{1}{X}\right) + \left(\tfrac{1}{2} - 3X\right) f(0) \\ & + X \ln\left(\tfrac{1-X}{X}\right)\left(f\left(\tfrac{1}{X}\right) - f(0)\right) + \tfrac{X}{2}[\mathcal{D}] \\ & + \ln\eta \left\{ 1 + \ln X + X\left(f\left(\tfrac{1}{X}\right) - f(0)\right)\right\} \;\Big] \end{aligned} \tag{4.61}$$

where

$$\eta = \frac{m^2}{S} \tag{4.62}$$

$$[\mathcal{D}] = 2\zeta(3) + 2\ln\left(\tfrac{X}{1-X}\right) f\left(\tfrac{1}{X}\right) + \ln X \ln^2\left(\tfrac{X}{1-X}\right) + g\left(\tfrac{1-X}{X}\right) \tag{4.63}$$

$$g(x) = \int_0^x \frac{\ln^2 t}{1+t}\, dt \tag{4.64}$$

Similarly from I_2

$$W_2 = +e_i^2 g^4 C_2^2(R) \frac{1}{(4\pi)^2} \frac{\times q_\perp^2}{4\pi} \cdot$$
$$\int_{\frac{p^2}{q^2}x}^{\frac{1}{x}} dy \,(y-\tfrac{1}{x})\left[\tfrac{1}{\varepsilon} + \ln(4\pi) - \gamma_E - \ln\left(\frac{-q_\perp^2}{\mu^2}\right) - \ln y + \frac{\ln y}{1-y}\right] \tag{4.65}$$

Again, there are only logarithmic integrable singularities as $y \to 0$ which means p^2 can be neglected to give as a result of doing the y integrals

$$W_2 = +e_i^2 \left(\frac{g}{4\pi}\right)^4 C_2^2(R)\, 4\pi p.q \cdot$$
$$\Big[\ \tfrac{1}{\varepsilon} + \ln(4\pi) - \gamma_E - \ln\left(\frac{-q_\perp^2}{\mu^2}\right)$$
$$-\tfrac{3}{2} - 2x + (1-2x)\ln x$$
$$+ 2x(1-x)\left(f(\tfrac{1}{x}) - f(0)\right) \Big] \tag{4.66}$$

Thus, the total contribution from this cut of the amplitude (including the corresponding cut of the complex conjugate elastic amplitude i.e. $[\ BA^\dagger\ ]$) is

$$W^{(a)} = 2(W_1 + W_2) \tag{4.67}$$

$$W^{(a)} = +e_c^2\left(\frac{g}{4\pi}\right)^4 C_2^2(R)\,4\pi p.q\,.$$

$$8x(1-x)\Big[\,3+3\ln x+\ln\left(\frac{1-x}{x}\right)+\ln x\ln\left(\frac{1-x}{x}\right)$$
$$+\left(3x-\frac{3}{2}\right)f\left(\frac{1}{x}\right)+\left(\frac{1}{2}-3x\right)f(0)$$
$$+x\ln\left(\frac{1-x}{x}\right)\left\{f\left(\frac{1}{x}\right)-f(0)\right\}+\frac{x}{2}[0]$$
$$+\ln\eta\left\{1+\ln x+x\left(f\left(\frac{1}{x}\right)-f(0)\right)\right\}\Big]$$

$$+\Big[2\left(\frac{1}{\epsilon}+\ln(4\pi)-\gamma_E-\ln\left(\frac{-q^2}{\mu^2}\right)\right)+3-4x+(2-4x)\ln x$$
$$+4x(1-x)\left(f\left(\frac{1}{x}\right)-f(0)\right)\Big] \qquad (4.68)$$

As can be seen $W^{(a)}$ is UV divergent and requires renormalization. Due to its theoretical simplicity, we choose the minimal subtraction scheme (MS). At one loop, this scheme consists of removing only the $\frac{1}{\epsilon}$ divergence. At two loops however, one must subtract with this divergence a finite part that can be determined by evaluating the lowest order (one loop) diagram through to $O(\epsilon)$. This was done in chapter two. Thus for the counterterm, $W^{(c)}$, we have (see Fig 4.4(ii))

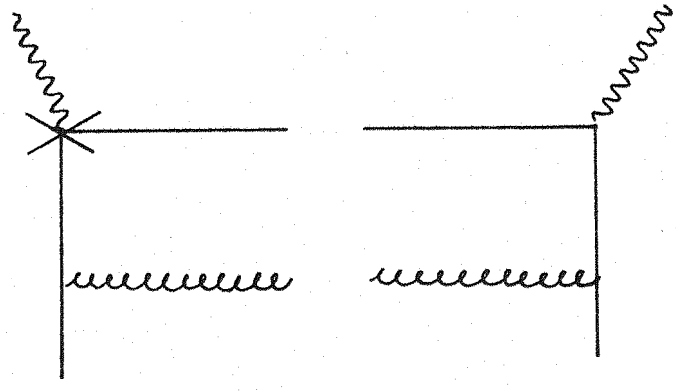

Fig 4.4(ii) Counterterm for the cut (a) of Fig 2.9(6)

$$W^{(c)} = -e_c^2\left(\frac{g}{4\pi}\right)^2 C_2^2(R)\,4\pi p.q\cdot\frac{2}{\epsilon}(1-\epsilon) \qquad (4.69)$$

Having thus determined the renormalised two body cut (a), we now turn to the calculation of the three body cut (b) illustrated in Fig 4.5. This cut is UV finite and so all Dirac algebra is evaluated in D = 4 dimensions. Again there are spurious mass singularities (which must cancel with those of cut (a)) associated with the real emission of a gluon parallel to the final state quark. A regulator assignment consistent with that of cut (a) is to give the final state quark of Fig 4.5 a small 'mass' $p'^2 = m^2$.

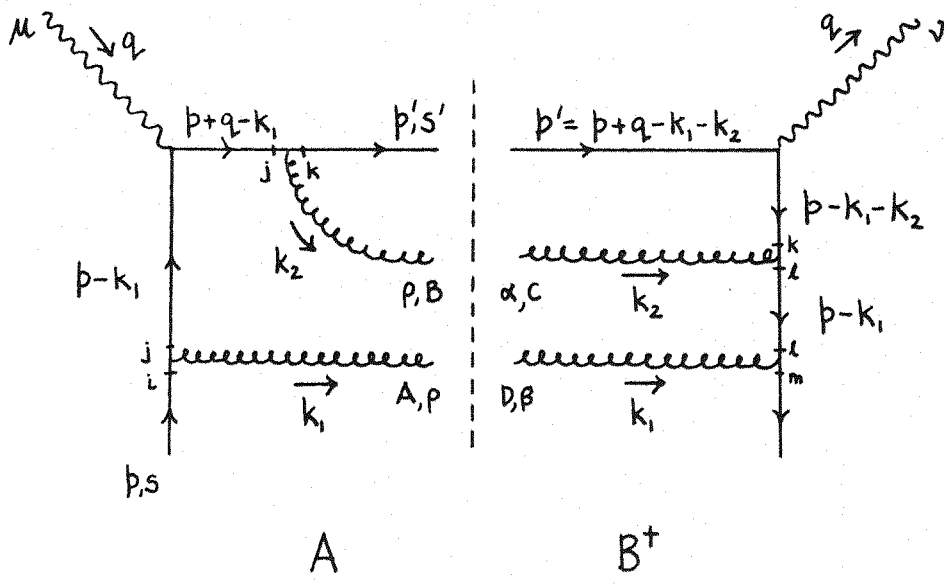

Fig 4.5 Three body s-channel cut (b)

$$A = +ie_i^2 g^2 \left(\frac{\lambda^B}{2}\right)_{kj}\left(\frac{\lambda^A}{2}\right)_{ji} \cdot$$

$$\bar{u}(p',s')\gamma_\rho \frac{1}{\not p+\not q-\not k_1}\gamma_\mu \frac{1}{\not p-\not k_1}\gamma_\lambda u(p,s)\,\varepsilon_x^{\rho,B}\,\varepsilon_y^{\lambda,A} \qquad (4.70)$$

$$B^\dagger = -ie_i^2 \left(\frac{\lambda^C}{2}\right)_{\ell k}\left(\frac{\lambda^D}{2}\right)_{m\ell} \cdot$$

$$\bar{u}(p,s)\gamma_\beta \frac{1}{(\not p-\not k_1)}\gamma_\alpha \frac{1}{\not p-\not k_1-\not k_2}\gamma_\nu u(p',s')\,\varepsilon_x^{C,\alpha\dagger}\,\varepsilon_y^{D,\beta\dagger} \qquad (4.71)$$

Take the product $AB^\dagger$ and perform

i) The quark spin sum $\frac{1}{2}\sum_{s,s'} \rightarrow \frac{1}{2}\mathrm{Tr}$

ii) The gluon polarisation sum

$$\sum_x \varepsilon_x^{\rho,B}\varepsilon_x^{c,a\dagger}\sum_y \varepsilon_y^{\lambda,A}\varepsilon_y^{D,\beta\dagger} = \delta^{B}\delta^{AD}g^{\rho\alpha}g^{\lambda\beta} \tag{4.72}$$

Then

$$AB^{\dagger} = +e_i^2 g^4 C_2^2(R)\tfrac{1}{2}\cdot$$

$$\mathrm{Tr}\left[\gamma_\rho(\not p+\not q-\not k_1)\gamma_\mu(\not p-\not k_1)\gamma_\lambda \not p\gamma^\lambda(\not p-\not k_1)\gamma^\rho(\not p-\not k_1-\not k_2)\gamma_\nu \not p'\right] \tag{4.73}$$
$$\overline{(p-k_1)^4(p+q-k_1)^2(p-k_1-k_2)^2}$$

The three body phase space integral is written as

$$W = \int[d\not p'][d\not K]\delta^4(p+q-K)\int[d\not k_1][d\not k_2]\,\delta^4(K-k_1-k_2)\left[p^\mu p^\nu AB^{\dagger}\right] \tag{4.74}$$

So, doing the k_2 integral with the delta-function setting

$$K = k_1 + k_2 \tag{4.75}$$

then

$$p^\mu p^\nu \mathrm{Tr} = \mathrm{Tr}\left[\gamma_\rho(\not p+\not q-\not k_1)\not p(\not p-\not k_1)\gamma_\lambda \not p\gamma^\lambda(\not p-\not k_1)\gamma^\rho(\not p-\not K)\not p\not p'\right] \tag{4.76}$$

setting $p^2 = k_1^2 = 0$ in the Trace. (One can show strictly that terms of the form $\frac{p^2}{p^2}$ do not occur in the phase space integrals thus justifying such an approximation).

$$p^\mu p^\nu \mathrm{Tr} = 64(p.k_1)^2\left[p.p'k_1.K - p'.q\,p.K + p'.k_1 p.K - p.k_1 p'.K - p.p'p.K + p.q\,p'.K\right]$$

$$-64\,p.k_1\,p.p'\left[-k_1.K\,p.K + k_1.K\,p.q - p'.k_1\,p.K\right] \tag{4.77}$$

The first part of the phase space integral

$$\int d^4k_1\,\delta(k_1^2)\,\theta(k_1^\circ)\,\delta\left((k_1-K)^2\right)\theta(k_1^\circ-K^\circ)\left[p^\mu p^\nu AB^{\dagger}\right] \tag{4.78}$$

is evaluated in the k_1, k_2 centre of momentum frame, i.e. the K rest system. Then

$$W = +e_c^2 g^4 C_2^2(R) \tfrac{1}{2} \int [d\bar{p}'][dK]\, \delta^4(p+q-K-p') \frac{1}{(p-K)^2}$$

$$\frac{8}{(2\pi)^2} \int_{-1}^{+1} d(\cos\theta) \int_0^{2\pi} d\phi \cdot \quad \frac{1}{4}\left[\frac{C_1 + C_2\, p.K_1 + C_3\, p'.K_1}{(p+q-k_1)^2} \right]$$

$$+ \frac{1}{2}\left[\frac{C_4 + C_5\, p'.K_1}{(p-k_1)^2 (p+q-k_1)^2} \right] \tag{4.79}$$

with

$$C_1 = \tfrac{1}{2} K^2 p.p' - p'.q\, p.K - p.p'\, p.K + p.q\, p'.K$$

$$C_2 = -p'.K$$

$$C_3 = +p.K$$

$$C_4 = \tfrac{1}{2} K^2 p.p' (pq - p.K)$$

$$C_5 = -p.p'\, p.K \tag{4.80}$$

All the coefficients have no dependence on the angles θ and ϕ. These angular integrals over one and two propagators are tabulated in Appendix A.2, but a few points are worth mentioning here concerning the choice of Lorentz frames in which they are done. For those integrals over one propagator $(p + q - k_1)^2$, it is obvious that they

will be easier if ϕ dependence can be avoided in the denominator. This requires choosing $\underline{p} + \underline{q}$ to point in the z direction making $(p + q).k_1$ a function of cos θ only, and putting all ϕ dependence into the product $p.k_1$. The ϕ integral is now a trivial polynomial in cos ϕ. From these arguments, it is clear that ϕ dependence in the denominator cannot be avoided if it contains two independent propagators. For these integrals, we chose $\underline{p}$ to point up the z axis making $p.k_1$ a function of cos θ only and $(p + q).k_1$ ϕ dependent. With such a choice, the rôle of p^2 as a regulator of potential mass singularities associated with the incoming quark was easy to identify.

Collecting all the separate factors together after the angle integrals

$$W = +e_i^2 g^4 C_2^2(R) \tfrac{1}{2}\int [d\not{p}'][dK]\, \delta^4(p+q-K-p') \frac{1}{(p-K)^2} \cdot$$

$$\left(\frac{8}{(2\pi)^2}\right)\Bigg[\frac{\pi}{4B}\left(-2C_2 b - 2C_3 K^\circ \not{p}'\right)$$

$$+ \frac{\pi}{4B} ln_0 \left(2C_1 + C_2\left(p.K + b\frac{A}{B}\right) + C_3\left(\not{p}'\not{K} + K^\circ \not{p}'\frac{A}{B}\right)\right)$$

$$+ \frac{\pi}{2}\frac{C_5}{p.K} ln_1$$

$$- \frac{\pi}{2}\frac{\left[C_5\left((p+q)^2 - K^2\right) + 2C_4\right]}{\left[(p+q)^2 p.K - K^2 p.q\right]}\left(ln_1 + ln_2\right) \Bigg] \tag{4.81}$$

where

$$A = (p+q_1)^2 - K.(p+q_1) \tag{4.82}$$

$$B = \sqrt{(K.(p+q_1))^2 - K^2(p+q_1)^2} = K^\circ p' = \sqrt{(K.p')^2 - K^2 p'^2} \tag{4.83}$$

$$b = \frac{p.K\, p'K - K^2 p.p'}{B} \tag{4.84}$$

$$\ell n_0 = \ell n\left(\frac{A+B}{A-B}\right) \tag{4.85}$$

$$\ell n_1 = \ell n\left(\frac{2p.K}{-p^2\left(1 - \frac{K^2}{2p.K}\right)}\right) \tag{4.86}$$

$$\ell n_2 = \ell n\left(\frac{\left[(p+q_1)^2 - \frac{K^2}{p.K} p.q_1\right]^2}{(p+q_1)^2 p'^2}\right) \tag{4.87}$$

Now outside the arguments of the logs, we can make the approximation of $p'^2 = 0$ since the mass divergence is manifest in the logs themselves at this stage (in the limit of $p'^2 \to 0$, then A = B so a mass singularity is buried in ℓn_0 somewhere). This is a sketchy argument though, and the full implications of setting $p'^2 = 0$ will be discussed at a later stage.

In the limit of $p^2 \to 0$, then the coefficient of $\ell n_1 \to 0$ and all mass divergence associated with the incoming quark drops out of this

cut as expected. Thus

$$W = +e_i^2 g^4 C_2^2(R) \frac{1}{2} \int [d^4p'][d^4K]\, \delta^4(p+q-K-p') \frac{1}{(p-K)^2}$$

$$\cdot \frac{8}{(2\pi)^2} \frac{\pi}{4} \left(2p.q - K^2 + (p-K)^2\right) \left[-\frac{K^2}{p'.K} + \frac{(p+q).K}{p'.K} \ell n_0 + \ell n_2 \right] \qquad (4.88)$$

The second part of the phase space integral is now most conveniently done in the p, q centre of momentum system. Then

$$\int [d^4p'][d^4K]\, \delta^4(p+q-K-p') \rightarrow \frac{1}{8(2\pi)^2} S \int_0^1 dv \int_{-(1-v)}^{+(1-v)} dz \qquad (4.89)$$

with

$$S = (p+q)^2$$

$$K^2 = sv$$

$$p.q = \frac{as}{2} \quad , \quad a \geq 1$$

$$p.K = \frac{as}{4}(1+v-z)$$

$$p' = p+q-K \qquad (4.90)$$

Thus both $(p - K)^2$ and ℓn_2 are z dependent, whereas $p'.K$ and ℓn_0 are not.

The results of the more difficult z integrals are

$$\int_{-(1-v)}^{(1-v)} dz \frac{1}{(p-K)^2} = \frac{2}{as} \ell n \left(\frac{v(a-1)}{a-v} \right) \equiv \frac{2}{as} \ell n_3 \qquad (4.91)$$

$$\int_{-(1-v)}^{+(1-v)} dz \frac{1}{(p-K)^2} \ln_2 = \frac{4}{as}\left[-\frac{1}{2}\ln\eta \ln_3 + f(a) - f\left(\frac{a}{v}\right) - f\left(\frac{a-v}{v(a-1)}\right) + \ln_3 \ln\left(\frac{a(1-v)}{v}\right) \right] \tag{4.92}$$

where again

$$\eta = \frac{m^2}{s} \tag{4.93}$$

Assembling the final integral to be done, we obtain

$$W = +e_i^2 g^4 C_2^2(R) S \frac{1}{(2\pi)^4} \frac{\pi}{8} \cdot \int_0^1 dv \left[-4v + 8v\ln v + 2(1+v)\ln_0 - 2(1-v)\ln\eta \right.$$
$$- \frac{4}{a}\frac{v(a-v)}{(1-v)} \ln\left(\frac{v(a-1)}{a-v}\right) + \frac{2}{a}(a-v)\left(\frac{1+v}{1-v}\right)\ln\left(\frac{v(a-1)}{a-v}\right)\ln_0$$
$$+ \frac{4}{a}(a-v)\left[f(a) - f\left(\frac{a}{v}\right) - f\left(\frac{a-v}{v(a-1)}\right) \right.$$
$$\left. -\frac{1}{2}\ln\eta \ln\left(\frac{v(a-1)}{a-v}\right) \right.$$
$$\left. \left. + \ln\left(\frac{a(1-v)}{v}\right)\ln\left(\frac{v(a-1)}{a-v}\right) \right] \right] \tag{4.94}$$

$$\ln_0 = 2\ln(1-v) - \ln\eta \tag{4.95}$$

As can be seen, any potential divergence as $v \to 1$ (the region in phase space where the gluons go back-to-back) is suppressed by a logarithm and rendered integrable.

These final integrals can be done without too much difficulty to give the total contribution of this three body cut of the amplitude (including the corresponding cut of the complex conjugate amplitude) to be

$$W^{(b)} = 2W \tag{4.96}$$

$$\begin{aligned} W^{(b)} = {} & + e_i^2 \left(\frac{g}{4\pi}\right)^4 C_2^2(R)\, 4\pi p.q \\ & 2(1-x)\Big[-14 + \left(\frac{5}{1-x} - 14\right)\ln x + (-6+14x) f(0) \\ & - (2+14x) f\left(\tfrac{1}{x}\right) + 4x[0] \\ & + 4\ln\eta \left\{ -1 - \ln x - x\left(f\left(\tfrac{1}{x}\right) - f(0)\right)\right\} \Big] \end{aligned} \tag{4.97}$$

Finally, a further comment about the approximations made in setting $p'^2 = 0$ outside of the logarithms. With care and effort this final part of the phase space integral can be done for finite $p'^2 = m^2$. For $\eta = \frac{m^2}{s}$, the approximations are equivalent to the statements

$$\lim_{\eta\to 0} \int_{2\sqrt{\eta}}^{1+\eta} du\, \frac{\eta}{u^2-4\eta} \ln\left(\frac{u-\sqrt{u^2-4\eta}}{u+\sqrt{u^2-4\eta}}\right) = 0 \tag{4.98}$$

which can be proved exactly, and

$$\lim_{\eta\to 0} \int_{2\sqrt{\eta}}^{1+\eta} du\, \frac{\eta}{u^2-4\eta} \ln\left(\frac{u-\sqrt{u^2-4\eta}}{u+\sqrt{u^2-4\eta}}\right) F(u,\eta) = 0 \tag{4.99}$$

$$F(u,\eta) = \frac{1}{\sqrt{u^2-4\eta}} \ln\left(\frac{2\left(\frac{a-1}{a}\right)(1-u)+u-\frac{2\eta}{a}-\sqrt{u^2-4\eta}}{2\left(\frac{a-1}{a}\right)(1-u)+u-\frac{2\eta}{a}+\sqrt{u^2-4\eta}}\right) \qquad (4.100)$$

which is true, because in the dangerous region of $u \sim 2\sqrt{\eta}$

$F(u,\eta)\Big|_{u=2\sqrt{\eta}}$ is finite. In fact F(u, η) is finite throughout the range of integration apart from an integrable divergence due to the argument of the logarithm approaching zero as $u \to 1 + \eta$. This divergence is not controlled in any way by η. Indeed

$\int_0^1 du\, F(u,\eta=0)$ is finite.

Approximations in dropping final state 'masses' in the three body phase space integrals of other diagrams reduced to the same or simpler statements than those of above.

We can now add up all the s-channel discontinuities of the renormalised two loop amplitude of Fig 2.9(6) (+ its complex conjugate) and see that the spurious mass singularities, ℓn η, do indeed cancel. Furthermore this amplitude has no collinear divergence associated with incoming quark of momentum p as expected from more general discussions on the structure of the σ_L process.

$$W_6 = W^{(a)} + W^{(b)} + W^{(c)} \qquad (4.101)$$

$$W_6 = +e_i^2\left(\frac{g}{4\pi}\right)^4 C_2^2(R)\, 4\pi p.q \cdot$$

$$\Big[\, 2\left(\ln(4\pi) - \gamma_E - \ln\left(-\frac{q^2}{\mu^2}\right)\right)$$

$$+1 + 8X\ln X + 8(1-X)\left(\ln(1-X) - f(0) - 2f\left(\tfrac{1}{X}\right)\right)$$

$$+ 8(1-X)\ln X \ln\left(\frac{1-X}{X}\right)$$

continued overleaf

$$+8x(1-x)\ln\left(\frac{1-x}{x}\right)\left(f\left(\frac{1}{x}\right)-f(0)\right)$$

$$+12x(1-x)\left[2\ell(3)+2\ln\left(\frac{x}{1-x}\right)f\left(\frac{1}{x}\right)+\ln^2\left(\frac{x}{1-x}\right)\ln x + g\left(\frac{1-x}{x}\right)\right] \qquad (4.102)$$

The s-channel discontinuities of the other amplitudes (including the crossed photon amplitudes) are calculated by techniques similar to those outlined above. A compendium of some of the final three body phase space integrals used is given in Appendix A3 .

4.3 Diagram by Diagram results

Given below are the $O(g^4)$ contributions to the non-singlet quark longitudinal structure function $F_L^{NS}(X, Q^2)$ when expanded in terms of g, the effective QCD coupling constant at the renormalisation point μ^2. The contributions are given diagram by diagram as the sum of the s-channel cuts of the two loop elastic amplitudes of Fig 2.9. Contributions from the crossed photon diagrams are included, and all ultra-violet divergent diagrams are renormalised in the MS scheme.

If the sum of all contributions is written as

$$W = \sum_i W_i \qquad (4.103)$$

then

$$\frac{1}{4\pi}W = \frac{\nu}{4x^2}F_L^{NS}(x,Q^2) \qquad (4.104)$$

All expressions are to be multiplied by a factor of $+e_i^2\left(\frac{g}{4\pi}\right)^4 C_2(R)4\pi p.q$

Factors common to many of the contributions are:-

SU(N) Colour factors

$$T(R) = \tfrac{1}{2} f \text{ , for f flavours}$$
$$C(G) = N$$
$$C_2(R) = \frac{N^2-1}{2N} \tag{4.105}$$

$$\gamma = \ln(4\pi) - \gamma_E - \ln\left(-\frac{q^2}{\mu^2}\right) \tag{4.106}$$

$$[\textcircled{0}] = 2\zeta(3) + 2\ln\left(\frac{x}{1-x}\right) f\left(\frac{1}{x}\right) + \ln^2\left(\frac{x}{1-x}\right)\ln x + g\left(\frac{1-x}{x}\right) \tag{4.107}$$

where

$$f(x) = \int_1^x \frac{\ln t}{1-t}\, dt, \qquad f(0) = \frac{\pi^2}{6} \tag{4.108}$$

$$g(x) = \int_0^x \frac{\ln^2 t}{1+t}\, dt \tag{4.109}$$

and finally,

$$h(x) = \int_0^x \frac{\ln(x-t)\ln t}{(1-t)}\, dt \tag{4.110}$$

If the contribution resulting from Fig 2.9(i) is labelled W_i, then

$$W_1 = C_2(R)\left[-2\gamma - 5 - 2\ln x\right] \tag{4.111}$$

$$W_2 = C_2(R)\left[-\gamma - \tfrac{3}{2} + \ln\left(\frac{1-x}{x}\right)\right] \tag{4.112}$$

$$W_3 = \left(C_2(R) - \frac{C(G)}{2}\right)\left[2\gamma + \frac{16}{x} - 19 + \left(\frac{8}{x} - 6\right)\ln x + \left(\frac{4}{x} - 8\right)\ln\left(\frac{p^2}{q^2}\right)\right] \tag{4.113}$$

$$W_4 = T(R)\left[-\frac{4}{3}\gamma - \frac{50}{9} + \frac{4}{3X} - \frac{8}{3}\ln X + \frac{4}{3}\ln(1-X) \right] \quad (4.114)$$

$$W_5 + W_8 = C(G)\left[\frac{5}{3}\gamma + \frac{137}{18} - \frac{5}{3X} + \frac{10}{3}\ln X - \frac{5}{3}\ln(1-X) \right] \quad (4.115)$$

$$\begin{aligned} W_6 = C_2(R)\Big[& 2\gamma + 1 + 8X\ln X + 8(1-X)\ln(1-X) \\ & - 8(1-X)f(0) - 16(1-X)f\left(\tfrac{1}{X}\right) + 12X(1-X)[\phi] \\ & + 8(1-X)\ln X \ln\left(\frac{1-X}{X}\right) \\ & + 8X(1-X)\ln\left(\frac{1-X}{X}\right)\left(f\left(\tfrac{1}{X}\right) - f(0)\right) \Big] \end{aligned} \quad (4.116)$$

$W_7 = 0$ in dimensional regularisation (4.117)

$$W_9 = C_2(R)\left[2\ln\left(\frac{1-X}{X}\right)\right] \quad (4.118)$$

$$W_{10} = C_2(R)\left[9 - \frac{9}{X} - \left(3 + \frac{4}{X}\right)\ln X - 3\ln^2 X + \left(2 - \frac{2}{X} - 2\ln X\right)\ln\left(\frac{p^2}{q^2}\right) \right] \quad (4.119)$$

$$W_{11} = \left(C_2(R) - \frac{C(G)}{2}\right)\Big[-\frac{3}{2} + 8\zeta(3) + 14x + 14x\ln x$$
$$+ (12 - 8f(0))\ln(1-x) + (4x + 14x^2)\left(f\left(\tfrac{1}{x}\right) - f(0)\right)$$
$$+ 8\ln x\, f\left(\tfrac{1}{x}\right) + 8h\left(\tfrac{1}{x}\right) + 2F_{11}(x)\Big] \qquad (4.120)$$

$$W_{12} = \left(C_2(R) - \frac{C(G)}{2}\right)\Big[2 + (9 - 8x)\ln x + (8x - 14)\ln(1-x)$$
$$+ (4 - 8x) f(0) + (12 - 16x) f\left(\tfrac{1}{x}\right) + (10 - 8x)\ln^2 x$$
$$+ (8x - 12)\ln x \ln(1-x) - 8x(1-x)\ln\left(\frac{1-x}{x}\right)\left(f\left(\tfrac{1}{x}\right) - f(0)\right)$$
$$- 12x(1-x)[@] - 4\ln\left(\frac{1-x}{x}\right)\ln\left(\frac{p^2}{q^2}\right) + 4F_{12}(x)\Big] \qquad (4.121)$$

$$W_{13} = \left(C_2(R) - \frac{C(G)}{2}\right)\Big[10 - \frac{10}{x} - \left(4 + \frac{8}{x}\right)\ln x - 4\ln^2 x$$
$$- 4\left(\frac{1-x}{x}\right)\ln\left(\frac{p^2}{q^2}\right)\Big] \qquad (4.122)$$

$$W_{14} = \frac{C(G)}{2}\Big[10 - 8x + (-6 + 8x)\ln(1-x) + (10 - 16)\ln x$$
$$+ (-24x + 8x^2) f(0) + (16 - 8x - 8x^2) f\left(\tfrac{1}{x}\right)$$
$$- 16x(1-x)[@] - 8x(1-x)\ln\left(\frac{1-x}{x}\right)\left(f\left(\tfrac{1}{x}\right) - f(0)\right) \qquad (4.123)$$
$$- 8(1-x)\ln x \ln\left(\frac{1-x}{x}\right)\Big]$$

$$W_{15} = \frac{C(G)}{2}\Big[\; 6\gamma + \frac{2}{x} + 13 + 10\ln x - 8\ln(1-x)$$

$$+4\ln^2 x - 4\ln x \ln(1-x) - 8f(0) - 4f\left(\tfrac{1}{x}\right)$$

$$+\left(-4+4\ln x - 4\ln(1-x)\right)\ln\left(\frac{p^2}{q^2}\right)\;\Big] \qquad (4.124)$$

These lead to a total contribution W

$$W = +e_i^2\left(\frac{g}{4\pi}\right)^4 C_2(R)\,4\pi p.q\,.$$

$$\Big[\;\left(\ln(4\pi)-\gamma_E\right)\left(\frac{37}{3}-\frac{2}{3}f\right)$$

$$-\left(11-\frac{2}{3}f-\frac{4}{3}-\frac{8}{3}\frac{1}{x}+\frac{8}{3}\ln x-\frac{16}{3}\ln(1-x)\right)\ln\left(\frac{Q^2}{\mu^2}\right)$$

$$+\left(-\frac{4}{3}-\frac{4}{3}-\frac{8}{3}\frac{1}{x}+\frac{8}{3}\ln x-\frac{16}{3}\ln(1-x)\right)\ln\left(-\frac{p^2}{\mu^2}\right)$$

$$+\frac{761}{12}-\frac{25}{9}f-\frac{4}{3}f(3)-\frac{43}{3}x+\left(\frac{2}{3}f-15\right)\frac{1}{x}$$

$$+\left(\frac{169}{6}-\frac{4}{3}f-\frac{43}{3}x-\frac{16}{3}\frac{1}{x}\right)\ln x$$

$$+\left(-11+\frac{2}{3}f+\frac{4}{3}f(0)\right)\ln(1-x)$$

$$+\left(-\frac{70}{3}-\frac{70}{3}x+\frac{43}{3}x^2\right)f(0)+\left(-\frac{16}{3}+\frac{34}{3}x-\frac{43}{3}x^2\right)f\left(\tfrac{1}{x}\right)$$

continued overleaf

$$+\frac{7}{3}\ln^2 x - \frac{16}{3}\ln x \ln(1-x) - \frac{4}{3}\ln x f\left(\frac{1}{x}\right)$$

$$-6x(1-x)\left[2\rho(3) \ln x \ln^2\left(\frac{x}{1-x}\right) + 2\ln\left(\frac{x}{1-x}\right) f\left(\frac{1}{x}\right) + g\left(\frac{1-x}{x}\right)\right]$$

$$-\frac{4}{3}h\left(\frac{1}{x}\right) - \frac{2}{3}F_{12}(x) - \frac{1}{3}F_{11}(x)\Bigg] \qquad (4.125)$$

F_{11} and F_{12} are the functions of x originating from the numerical integrals done in diagrams 11 and 12. Their value is known at 32 equally spaced points in the x range of 0 to 1, together with their first 10 moments which are given in Appendix A4. Their total contribution to the longitudinal coefficient function is small, being a maximum of 7% for n = 2.

In order to determine the longitudinal coefficient function $C_{L,n}^{NS}(1, \bar{g}^2)$ to $O(\bar{g}^4)$, we must expand the moments of the longitudinal structure function given by the operator product expansion, as a power series in g. Thus, from chapter 1,

$$M_L^{NS}(n,Q^2) \equiv \int_0^1 dx\, x^{n-2} F_L^{NS}(x,Q^2) = A_n^{NS}\left(\frac{p^2}{\mu^2}, g^2\right) C_{L,n}^{NS}\left(\frac{Q^2}{\mu^2}, g^2\right) \qquad (4.126)$$

The q^2 dependence of the coefficient functions is given by the renormalization group equation

$$C_{L,n}^{NS}\left(\frac{Q^2}{\mu^2}, g^2\right) = C_{L,n}^{NS}(1, \bar{g}^2) \exp\left[-\int_{\bar{g}(\mu^2)}^{\bar{g}(Q^2)} dg' \frac{\gamma_n^{NS}(g')}{\beta(g')}\right] \qquad (4.127)$$

if

$$C_{L,n}^{NS}(1, \bar{g}^2) = \delta_L^{NS}\left(0 + \left(\frac{\bar{g}}{4\pi}\right)^2 B_{L,n}^{1,NS} + \left(\frac{\bar{g}}{4\pi}\right)^4 B_{L,n}^{2,NS} + \cdots\right) \qquad (4.128)$$

Then, for deep inelastic scattering on a quark

$$C^{NS}_{L,n}\left(\frac{Q^2}{\mu^2}, g^2\right) = \delta^{NS}_L \left(\frac{g}{4\pi}\right)^2 \Bigg[B^{1,NS}_{L,n} + \left(\frac{g}{4\pi}\right)^2 \Bigg\{ B^{2,NS}_{L,n} - B^{1,NS}_{L,n}\left(\beta_0 + \frac{\gamma^{0,NS}_n}{2}\right) \ln\left(\frac{Q^2}{\mu^2}\right) \Bigg\} + O\left(\frac{g}{4\pi}\right)^4 \Bigg] \tag{4.129}$$

where $\delta^{NS}_L = e_i^2$ and

$$A^{NS}_n\left(\frac{p^2}{\mu^2}, g^2\right) = 1 + \left(\frac{g}{4\pi}\right)^2 \left(A^{2,NS}_n + \left(\frac{\gamma^{0,NS}_n}{2} - \gamma^0_F\right) \ln\left(\frac{-p^2}{\mu^2}\right) \right) + \cdots \tag{4.130}$$

With $A^{2,\,NS}_n$ being the finite parts obtained by calculating the diagrams of Fig 1.11 in a particular subtraction scheme. In the Feynman gauge $\alpha = 1$, and the MS scheme, the result is

$$A^{2,NS}_n = C_2(R) \Bigg[8 - \frac{4}{n} + \frac{2}{(n+1)} + \frac{2}{n^2} - \frac{4}{(n+1)^2} + \frac{2}{n(n+1)} \sum_{j=1}^{n} \frac{1}{j} - 4 \sum_{j=1}^{n} \frac{1}{j^2} - 4 \sum_{s=1}^{n} \frac{1}{s} \sum_{j=1}^{n} \frac{1}{j} + \left(\ln(4\pi) - \gamma_E\right)\left(\frac{2}{n(n+1)} - 4 \sum_{j=2}^{n} \frac{1}{j} \right) \Bigg] \tag{4.131}$$

Their numerical values in the $\overline{MS}$ scheme are given in Table 4.1 (where the last line of Eq 4.131 is neglected).

Table 4.1 $A_n^{2,\,NS}$ in the $\overline{MS}$ scheme

n	$A_n^{2,\,NS}$ $(\overline{MS})$
2	- 6.37037
3	- 9.92593
4	-12.86518
5	-15.40593
6	-17.65830
7	-19.68950
8	-21.54465
9	-23.25501
10	-24.84480

So combining Eqs (4.126), (4.128), (4.130) then we arrive at the result

$$M_L^{NS}(n,Q^2) = e_i^2\left(\frac{g}{4\pi}\right)^2 B_{L,n}^{1,NS} \cdot \left[1 + \left(\frac{g}{4\pi}\right)^2 \left\{ \left(\frac{\gamma_n^{0,NS}}{2} - \gamma_F^0\right) \ln\left(\frac{-p^2}{\mu^2}\right) - \left(\beta_0 + \frac{\gamma^{0,NS}}{2}\right) \ln\left(\frac{Q^2}{\mu^2}\right) + A_n^{2,NS} + R_{L,n}^{2,NS} \right\} + O\left(\frac{g}{4\pi}\right)^4 \right] \tag{4.132}$$

where

$$C_{L,n}(1,\bar{g}^2) = \delta_L^{NS} B_{L,n}^{1,NS}\left(\frac{\bar{g}}{4\pi}\right)^2\left[\ 1\ +\left(\frac{\bar{g}}{4\pi}\right)^2 R_{L,n}^{2,NS} + O(\bar{g}^4)\ \right] \qquad (4.133)$$

and

$$R_{L,n}^{2,NS} = \frac{B_{L,n}^{2,NS}}{B_{L,n}^{1,NS}} \qquad (4.134)$$

$$B_{L,n}^{1,NS} = C_2(R)\,\frac{4}{n+1} \qquad (4.135)$$

The above equations allow for the extraction of $R_{L,\,n}^{2,\,NS}$ from our diagram by diagram results. Since M_L^{NS} and $A_n^{2,\,NS}$ are separately both renormalisation prescription and gauge dependent, it is important that they both be calculated in the same schemes to extract $R_{L,\,n}^{2,\,NS}$ consistently. However, in the scheme in which the only existing calculations of the two loop anomalous dimensions have been performed (the MS scheme), then $\gamma_n^{NS}(\bar{g}^2)$ is gauge independent. This means that the gauge dependence of M_L^{NS} and $A_n^{2,\,NS}$ must cancel leaving $R_{L,\,n}^{2,\,NS}$ a gauge independent quantity. It is still renormalisation prescription dependent though. So

$$M_L^{NS}(n,Q^2) = \int_0^1 dx\, x^{n-2} F_L^{NS}(x,Q^2) = \frac{1}{\pi\nu}\int_0^1 dx\, x^n W(x,Q^2) \qquad (4.136)$$

leading to

$$R_{L,n}^{2,NS} = \frac{n+1}{e_i^2\left(\frac{g}{4\pi}\right)^4 C_2(R)\,4\pi\nu}\left(\int_0^1 dx\, x^n W(x,Q^2) - A_n^{2,NS} + \left(\beta_0+\frac{\gamma_n^{0,NS}}{2}\right)\ln\left(\frac{Q^2}{\mu^2}\right) - \left(\frac{\gamma_n^{0,NS}}{2}-\gamma_F^0\right)\ln\left(\frac{-p^2}{\mu^2}\right)\right) \qquad (4.137)$$

Numerical values of $R_{L,\,n}^{2,\,NS}$ determined in both $\overline{MS}$ and MS schemes are given in Tables 4.2, 4.3. The relation between them is

Table 4.2 $R_{L,\,n}^{2,\,NS}$ in the $\overline{MS}$ scheme (f = number of flavours)

n	f = 3	4	5	6
2	-16.0	-18.6	-21.1	-23.7
3	- 9.67	-12.6	-15.6	-18.5
4	- 4.57	- 7.77	-11.0	-14.2
5	- 0.303	- 3.69	- 7.08	-10.5
6	+ 3.37	- 0.159	- 3.71	- 7.23
7	+ 6.60	+ 2.94	- 0.719	- 3.21
8	+ 9.50	+ 5.73	+ 1.97	- 1.78
9	+ 12.1	+ 8.26	+ 4.41	+ 0.549
10	+14.5	+10.6	+ 6.65	+ 2.71

Table 4.3 $R_{L,\,n}^{2,\,NS}$ in the MS scheme (f = number of flavours)

n	f = 3	4	5	6
2	8.50	4.65	0.787	- 3.07
3	18.8	14.5	10.3	+ 6.02
4	26.6	22.1	17.6	12.9
5	33.1	28.4	23.7	19.0
6	38.5	33.7	28.9	24.0
7	43.3	38.3	33.3	29.6
8	47.5	42.4	37.4	32.3
9	51.3	46.1	41.0	35.8
10	54.8	49.5	44.3	39.0

$$R^{2,NS}_{L,n}(MS) = R^{2,NS}_{L,n}(\overline{MS}) + \left(\ln(4\pi) - \gamma_E\right)\left(\beta_0 + \frac{\gamma_n^{0,NS}}{2}\right) \qquad (4.138)$$

The numbers quoted are correct to three significant figures. The possible relevance of this result to the current experimental situation will be discussed in the next chapter.

Finally we mention the status of the agreement of this calculation with that of Duke et al [4.2] who utilise the dispersion relation technique and so obtain results for n even only. There is a substantial difference between our results for $R^{2,\ NS}_{L,\ n}$ and his (about + 40 for each n in the $\overline{MS}$ scheme) although the n dependence is roughly the same. A diagram by diagram comparison is complicated by the fact that the two calculations are performed using different infra-red regularisation schemes. We take initial quarks slightly off shell and space-like, whereas Duke et al use dimensional regularisation. Thus the infra-red divergent diagrams cannot be compared individually, but only as a whole. The result of a very careful diagram by diagram comparison reveals that the disagreement lies in only two infra-red finite diagrams (those of Fig 2.9(6) and 2.9(14))* together with the set of five which are infra-red divergent. We have thoroughly re-checked the calculational content of these diagrams and find no change in our previous results. We can therefore offer no explanation concerning the origin of this discrepancy. Clearly further work is needed in order to resolve this disagreement.

* These are diagrams which we have calculated totally analytically but for which Duke et al present numerical results only. We agree with all analytic results quoted by Duke et al.

CHAPTER FIVE

PHENOMENOLOGY OF σ_L TO FOURTH ORDER

In the last chapter we presented the results of a calculation of the fourth order longitudinal coefficient function. We can now use this result in an expansion of the moments of non-singlet structure functions in powers of the effective Q.C.D. coupling constant, $\bar{g}(Q^2)$. The problem then remains to invert these moment expressions and arrive at results for the experimentally measured structure functions themselves.

5.1 The moment inversion problem

Again, we start with the basic operator product expansion result for moments of non-singlet structure functions.

$$M_k^{NS}(n,Q^2) = A_n^{NS}\left(\frac{p^2}{\mu^2}, g^2\right) C_{k,n}^{NS}\left(\frac{Q^2}{\mu^2}, g^2\right) \tag{5.1}$$

and re-expand the coefficient functions, which govern the Q^2 depenedence of the moments, in terms of the effective coupling $\bar{g}(Q^2)$. We use the expression for $\bar{g}$ that satisfies the two loop beta function

$$\bar{g}(Q^2) = \bar{g}_0^2(Q^2) - \frac{\beta_1}{\beta_0}\frac{\bar{g}_0^4(Q^2)}{16\pi^2}\ln\ln\left(\frac{Q^2}{\Lambda^2}\right) \tag{5.2}$$

with

$$\bar{g}_0^2(Q^2) = \frac{16\pi^2}{\beta_0 \ln\left(\frac{Q^2}{\Lambda^2}\right)} \tag{5.3}$$

and Λ is chosen so that there are no more terms of $O(\bar{g}_o^4)$ in Eq. (5.2).

For the longitudinal structure function, straightforward expansion of Eq. (5.1) yields

$$M_L^{NS}(n,Q^2) = \bar{A}_n^{NS}\, \delta_L^{NS}\, B_{L,n}^{1,NS} \left(\frac{\bar{g}_o(Q^2)}{4\pi}\right)^2 \cdot \left(1 + \left(\frac{\bar{g}_o(Q^2)}{4\pi}\right)^2 \left\{ E_n^L + F_n + G_n(Q^2) \right\}\right) \left[\frac{\bar{g}_o^2(Q^2)}{\bar{g}_o^2(Q_o^2)}\right]^{\frac{\gamma_n^{0,NS}}{2\beta_o}} \qquad (5.4)$$

Where we have set, in Eq. (5.1), $\mu^2 = Q_o^2$ some reference value of 4-momentum transfer at which perturbation theory is still applicable. Clearly this results in no loss of generality since μ^2 is arbitrary. Now,

$$E_n^L = R_{L,n}^{2,NS} \qquad (5.6)$$

$$F_n = \frac{\gamma_n^{1,NS}}{2\beta_o} - \frac{\gamma_n^{0,NS}\beta_1}{2\beta_o^2} \qquad (5.7)$$

$$G_n(Q^2) = -\left(\frac{\gamma_n^{0,NS}\beta_1}{2\beta_o^2} + \frac{\beta_1}{\beta_o}\right) \ln\ln\left(\frac{Q^2}{\Lambda^2}\right) \qquad (5.8)$$

$\bar{A}_n^{NS}$ is an overall Q^2 independent normalisation constant whose evaluation lies outside the scope of perturbative Q.C.D. It can, however, be eliminated by measuring the moments of $F_2^{NS}(x, Q_o^2)$ at some Q_o^2 in the same process (i.e. ep scattering). F_2 is chosen as the data are the most accurate for this structure function. Thus we arrive at the result

$$M_L^{NS}(n,Q^2) = B_{L,n}^{1,NS}\left(\frac{g_0(Q^2)}{4\pi}\right)^2 \left(\frac{1+\left(\frac{g_0(Q^2)}{4\pi}\right)^2\left\{E_n^L + F_n + G_n(Q^2)\right\}}{1+\left(\frac{g_0(Q_0^2)}{4\pi}\right)^2\left\{E_n^2 + F_n + G_n'(Q_0^2)\right\}}\right) M_2^{NS}(n,Q_0^2)\left[\frac{\bar{g}_0^2(Q^2)}{\bar{g}_0^2(Q_0^2)}\right]^{\frac{\gamma_n^{0,NS}}{2\beta_0}} \qquad (5.9)$$

with

$$G_n'(Q_0^2) = -\frac{\gamma_n^{0,NS}\beta_1}{2\beta_0^2}\ln\ln\left(\frac{Q_0^2}{\Lambda^2}\right) \qquad (5.10)$$

and $E_n^2 = B_{2,n}^{1,NS}$ the previously calculated one loop coefficient function for the moments of the non-singlet structure function $F_2^{NS}(x,Q^2)$ specifically (in the MS scheme) [1.37].

$$B_{2,n}^{1,NS} = C_2(R)\left\{3\sum_{j=1}^{n}\frac{1}{j} - 4\sum_{j=1}^{n}\frac{1}{j^2} - \frac{2}{n(n+1)}\sum_{j=1}^{n}\frac{1}{j} + 4\sum_{j=1}^{n}\frac{1}{j}\sum_{k=1}^{j}\frac{1}{k} + \frac{3}{n} + \frac{4}{n+1} + \frac{2}{n^2} - 9\right\} + \frac{1}{2}\gamma_n^{0,NS}\left(\ln(4\pi) - \gamma_E\right) \qquad (5.11)$$

The n dependence of the salient quantities appearing in Eq. (5.9) is given in Table 5.1.

Table 5.1 The values of various quantities entering into Eq. (5.9). Renormalisation prescription dependent quantities are quoted in the MS scheme.

	$\frac{\gamma_n^{0,NS}}{2\beta_0}$	$\gamma_n^{1,NS}(MS)$	$F_n(MS)$	$E_n^2(MS)$	$E_n^L(MS,f=4)$
n=2	0.4267	71.37	1.6539	7.3914	4.65
3	0.6667	100.78	1.9401	14.0768	14.5
4	0.8373	120.14	2.0504	19.7000	22.1
5	0.9707	134.98	2.1195	24.5302	28.4
6	1.0805	147.00	2.1649	28.7673	33.7
7	1.1737	157.33	2.2097	32.5470	38.3
8	1.2550	166.39	2.2527	35.9633	42.4
9	1.3264	157.33	2.2940	39.0839	46.1
10	1.3911	181.78	2.3344	41.9589	49.5

Rewriting Eq. (5.9) as

$$M_L^{NS}(n,Q^2) = (\text{const}).\left[\bar{g}_o^2(Q^2)\right]^{\frac{\gamma_n^{o,NS}}{2\beta_o}}\left[1 + \left(\frac{\bar{g}_o(Q^2)}{4\pi}\right)^2 H_n^L(Q^2) + \cdots\right] \qquad (5.12)$$

where

$$H_n^L(Q^2) = E_n^L + F_n + G_n(Q^2) \qquad (5.13)$$

Then below in Table 5.2 are the values of $H_n^L(Q^2)$ for $Q^2 = 10$ Gev^2 and $\Lambda = 170$ MeV with the coupling constant $\bar{g}$ defined both in the MS and $\overline{MS}$ scheme. Thus

$$\left(\frac{\bar{g}\,(MS)}{4\pi}\right)^2 = \left(\frac{\bar{g}(\overline{MS})}{4\pi}\right)^2\left\{1 - 16{\cdot}28\left(\frac{\bar{g}(\overline{MS})}{4\pi}\right)^2 + \cdots\right\} \qquad (5.14)$$

Table 5.2 : Values of $H_n^L(Q^2)$, next to leading order corrections for longitudinal moments for coupling constants in different renormalisation schemes.

	$H_n^L(MS)$	$H_n^L(\overline{MS})$
n=2	- 9.22	- 16.2
3	- 1.67	- 12.5
4	+ 4.21	- 9.42
5	9.08	- 6.72
6	13.3	- 4.34
7	16.9	- 2.21
8	20.2	- 0.61
9	23.1	+ 1.54
10	25.8	+ 3.19

Note, to leading order in $\bar{g}(Q^2)$ the moments of the longitudinal structure function are given by

$$M_L^{NS}(n,Q^2) = \left(\frac{\bar{g}_0(Q^2)}{4\pi}\right)^2 B_{L,n}^{1,NS}\, M_2^{NS}(n,Q_0^2)\left[\frac{\bar{g}_0^2(Q^2)}{\bar{g}_0^2(Q_0^2)}\right]^{\frac{\gamma_n^{0,NS}}{2\beta_0}} \qquad (5.15)$$

A similar procedure may be followed to arrive at a next to leading order expression for the moments of non-singlet combinations of the structure function $F_2(x,Q^2)$.

$$M_2^{NS}(n,Q^2) = \frac{\left\{1+\left(\frac{\bar{g}_0(Q^2)}{4\pi}\right)^2\left(E_n^2+F_n+G_n'(Q^2)\right)\right\}}{\left\{1+\left(\frac{\bar{g}_0(Q_0^2)}{4\pi}\right)^2\left(E_n^2+F_n+G_n'(Q_0^2)\right)\right\}} M_2^{NS}(n,Q_0^2)\left[\frac{\bar{g}_0^2(Q^2)}{\bar{g}_0^2(Q_0^2)}\right]^{\frac{\gamma_n^{0,NS}}{2\beta_0}} \qquad (5.16)$$

With the corresponding leading order expression being simply

$$M_2^{NS}(n,Q^2) = M_2^{NS}(n,Q_0^2)\left[\frac{\bar{g}_0^2(Q^2)}{\bar{g}_0^2(Q_0^2)}\right]^{\frac{\gamma_n^{0,NS}}{2\beta_0}} \qquad (5.17)$$

We now have leading and next to leading order expressions from Q.C.D. that give the Q^2 evolution of the moments of non-singlet structure functions F_L^{NS} and F_2^{NS} from some fixed Q_0^2. The overall normalisation of the structure functions is taken from experiment at this chosen value of Q_0^2.

The problem that remains is to invert these moments and arrive at leading and next-to-leading order expressions for the structure functions themselves. Only then can we isolate the quantities relevant to a plot of $R(x,Q^2) = \frac{\sigma_L}{\sigma_T}$. An outline of one solution to this inversion problem is given in the next section.

5.2 The solution of Yndurain

There now exist a number of different solutions to the moment inversion problem, [5.1, 5.2] of various degrees of sophistication, designed specifically for the particle theorist. The formal solution, reconstructing the function exactly, requires knowledge of all its moments. This approach is usually abandoned by particle theorists who assume a definite form for the function depending on a finite number of parameters, and then determine these parameters by fitting moments of the function to the Q.C.D. expressions. This functional form is motivated by the phenomenological form of the structure functions.

$$F(x) = x^{\alpha}(1-x)^{\beta} \qquad \alpha,\beta > 0 \tag{5.18}$$

Because of its overall numerical simplicity, we chose the Yndurain [5.3] inversion technique. It has the disadvantage, though, that the Λ parameter is left undetermined and must be fed in as an input (more sophisticated numerical inversion techniques can determine Λ by fitting the overall normalisation of Q.C.D. scaling violations to those observed experimentally).

As with other practical methods of moment inversion, this technique avoids the problem of exact point-like reconstruction of the function. Instead, it solves the more tractable problem of supplying the weighted average of the function F around some point X. The optimal set of weight functions for the inversion of structure functions are the normalised Bernstein polynomials

$$b^{(N,k)}(x) = \frac{x^k(1-x)^{N-k}}{\int_0^1 dx\, x^k(1-x)^{N-k}} \tag{5.19}$$

$$b^{(N,k)}(X) = \frac{(N+1)!}{k!} \sum_{\ell=0}^{N-k} \frac{(-1)^{\ell}}{\ell!(N-k-\ell)!} X^{k+\ell} \tag{5.20}$$

where k takes on values

$$k = 0, 1, 2, \ldots\ldots N \tag{5.21}$$

if the first N moments $M_0, M_1, \ldots\ldots M_N$ are known.

These polynomials act as a suitable weight over the point $X_{N,k}$ where

$$X_{N,k} = \int_0^1 dX\ b^{(N,k)}(X).\ X = \frac{k+1}{N+2} \tag{5.22}$$

and give the average* of the function $F(X)$ around the point $X_{N,k}$ as

$$\tilde{F}(X_{N,k}) = \int_0^1 dX\ b^{(N,k)}(X)\ F(X) \tag{5.23}$$

or, equivalently

$$\tilde{F}(X_{N,k}) = \frac{(N+1)!}{k!} \sum_{\ell=0}^{N-k} \frac{(-1)^{\ell}}{\ell!(N-k-\ell)!} M_{k+\ell} \tag{5.24}$$

with

$$M_j = \int_0^1 dX\ X^j F(X) \tag{5.25}$$

Thus we can see that $\tilde{F}$ is immediately obtained from the moments of F. As the number of moments known increases, the width of the bins in X in which the average value of the function is given decreases.

(* this average is due to $b^{N,k}$ being peaked in the region of $X_{N,k}$).

A note on the practical use of the Yndurain formula Eq. (5.24) is in order. It may be thought that the width of the bins in X space can be made arbitrarily small by knowing an arbitrarily large number of the moments. This is true, but because of the oscillating sign in Eq. (5.24) the moments must be known to an increasing degree of accuracy for increasing N to allow for the differences of large factorials appearing in the sum. In fact we found a strong correlation between the number of bins chosen in X space and the number of significant figures needed in the moments for the reconstruction to work. Going from an $N=3$ to $N=6$ to $N=8$ reconstruction required the addition of a significant figure in the first N moments from 2 sig. fig. to 3 to 4 sig. figs. for the method to work. As we believe the longitudinal moments to be accurate to three significant figures, we chose $N=6$ to give the average of the structure function in X bins of width 0.125. Such a choice of N provided reconstructed test functions to an accuracy of typically better than 6% apart from the highest point in X space, $X = 0.875$, where the error was about twice this value.

Bearing such qualifying remarks in mind, it is then a relatively straightforward task to invert the Q.C.D. moment expressions.

5.3 Next to leading order results for $R(x,Q^2)$

In the abscence of target mass corrections, the experimentally measured structure functions $\nu W_k(x,Q^2)$ are equivalent to those considered in Q.C.D., $F_k(x,Q^2)$, whose Q^2 evolution is predicted in the limit of $Q^2 \to \infty$.

$$\nu W_k(X,Q^2) \equiv F_k(X,Q^2) \qquad k = L,2,3 \tag{5.26}$$

$$W_1(X,Q^2) \equiv F_1(X,Q^2) \tag{5.27}$$

Thus,

$$R(X,Q^2) = \frac{\sigma_L}{\sigma_T} = \frac{F_L(X,Q^2)}{2XF_1(X,Q^2)} \tag{5.28}$$

where

$$F_L(X,Q^2) = F_2(X,Q^2) - 2XF_1(X,Q^2) \tag{5.29}$$

So, in order to plot the ratio $R(X,Q^2)$ we need to invert both the structure functions F_L and F_2 consistently to leading and next to leading order. The relation Eq. (5.29) then allows both F_1 and hence R to be determined. Note that the ratio R is independent of the (X independent) normalisation of the structure function F_2 at $Q^2 = Q_o^2$.

This procedure was carried out using the Yndurain inversion technique at the fixed values of $Q^2 =$ 3.0, 6.0, 9.0, 12.0 and 15.0 $(\text{Gev})^2$ for which data on R currently exist. This allows a plot of both the Q^2 evolution at fixed values of X, and the X distribution for fixed Q^2 of the ratio R. For future experimental reference we repeated the program in the region of $Q^2 = 50 \rightarrow 250$ $(\text{Gev})^2$. In all cases, the input value of Λ was chosen to be 170 MeV, which is an average of the current values of Λ quoted by experimental groups as providing the best fit to the experimentally observed scaling violations.

The overall normalisation of F_2 was found by fitting a parameterised form of the structure function to the latest neutrino-nucleon scattering data of the C.D.H.S. group at CERN [5.4]. The fixed value of Q_0^2 was chosen as $Q_0^2 = 1.79\ (\text{Gev})^2$, and the parameterisation as

$$F_2(X, Q_0^2 = 1{\cdot}79\ \text{Gev}^2) = A_1 X^{A_2}(1-X)^{A_3} \tag{5.30}$$

Using a simple least-squares fitting routine, we found

$$\begin{aligned} A_1 &= 1{\cdot}382 \\ A_2 &= 0{\cdot}066 \\ A_3 &= 1{\cdot}329 \end{aligned} \tag{5.31}$$

As a test of this choice we compared the Q.C.D. evolved leading and next to leading order structure function $F_2(X,Q^2)$ with data at $Q^2 = 9.0\ \text{Gev}^2$ and concluded that the agreement was satisfactory (see Fig. 5.1(a)).

The results for the leading and next to leading order Q.C.D. predictions for the ratio $R(X,Q^2)$ are summarised in Figures 5.3, 5.2. The Q^2 evolution is shown only for values of $X > 0{\cdot}4$, where it is expected to be dominated by operators whose anomalous dimensions are equal to those of the non-singlet operators. At these values of X, the flavour singlet contribution to the structure function is negligible [2.7].

Although the errors are relatively large, we conclude in agreement with previous authors that the leading order $O[\bar{g}^2]$ Q.C.D. expression fails to give a satisfactory description of the ratio $R(X,Q^2) = \frac{\sigma_L}{\sigma_T}$ at large $X > 0{\cdot}5$. This theoretical prediction falls consistently below the data. This discrepancy is not explained by the inclusion of the next term in the perturbation expansion in $\bar{g}^2(MS)$ of $R(X,Q^2)$. Indeed, the agreement with data is made slightly worse. The inclusion of target mass corrections would have the effect of bringing both theoretical curves closer to the data, but only slightly so for large X .

From a theoretical viewpoint, the perturbation expansion in $\bar{g}^2$ of $R(X,Q^2)$ appears to be stable. The next to leading order $O[\bar{g}^4(MS)]$ correction is less than 12% for $X \gtrsim 0{\cdot}5$ and $Q^2 = 9{\cdot}0\ \text{Gev}^2$ and falls steadily as Q^2 increases. The small size of this correction must be partly due to the simultaneous increase in both the numerator and denominator with the inclusion of the next to leading order corrections to F_L and $2XF_1$ respectively. However, the moments of $F_L(X,Q^2)$ themselves appear to have a reliable perturbation expansion. The $O[\bar{g}^4(MS)]$ correction here is typically of the order of 10 - 40% for values of $Q^2 = 10\ \text{Gev}^2$ and Λ of 170 Mev. This result is itself due to a cancellation between the two dominant terms of E_n^L and $G_n(Q^2)$ which occur at fourth order.

All these facts point towards the reliability of the leading order Q.C.D. calculation and indicate that Q.C.D. perturbation theory is making sense. It is now therefore the responsibility of the experimentalists to attempt to reduce the error bars on the data in order to see whether the discrepancy persists.

Figure Captions

In all the following figures, leading order Q.C.D. results for the structure functions are shown in circles, whereas next to leading order predictions are given in triangles. The value of Λ is chosen throughout as Λ = 170 Mev.

Figure 5.1 (a) Comparison of Q.C.D. evolved $F_2(x,Q^2)$ to the data of ref. [5.4] at $Q^2 = 9.0\ Gev^2$.

(b) Q.C.D. evolved structure function $F_L(x,Q^2)$ at $Q^2 = 9.0\ Gev^2$.

(c) The ratio $R(x,Q^2)$ for $Q^2 = 9.0\ Gev^2$.

Figure 5.2 Comparison of the theoretical predictions for $R(x,Q^2)$ to the data of ref. [1.13], for fixed values of Q^2.

Figure 5.3 Comparison of the theoretical predictions for $R(x,Q^2)$ to the data of ref. [1.13] for fixed values of x.

Figure 5.4 Theoretical Q^2 evolution of $R(x,Q^2)$ at high values of Q^2.

Fig 5.1(a)

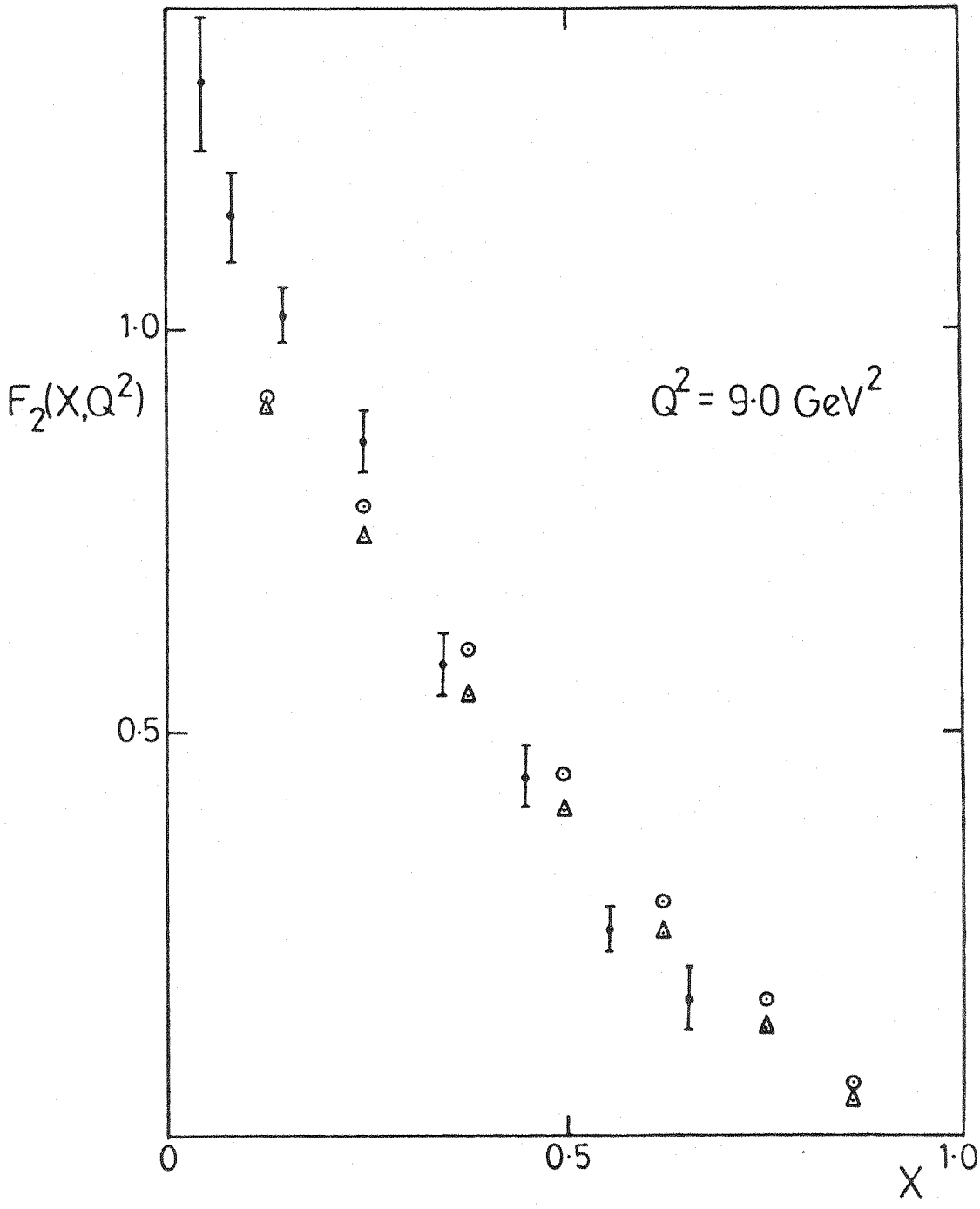

Fig 5.1(b)

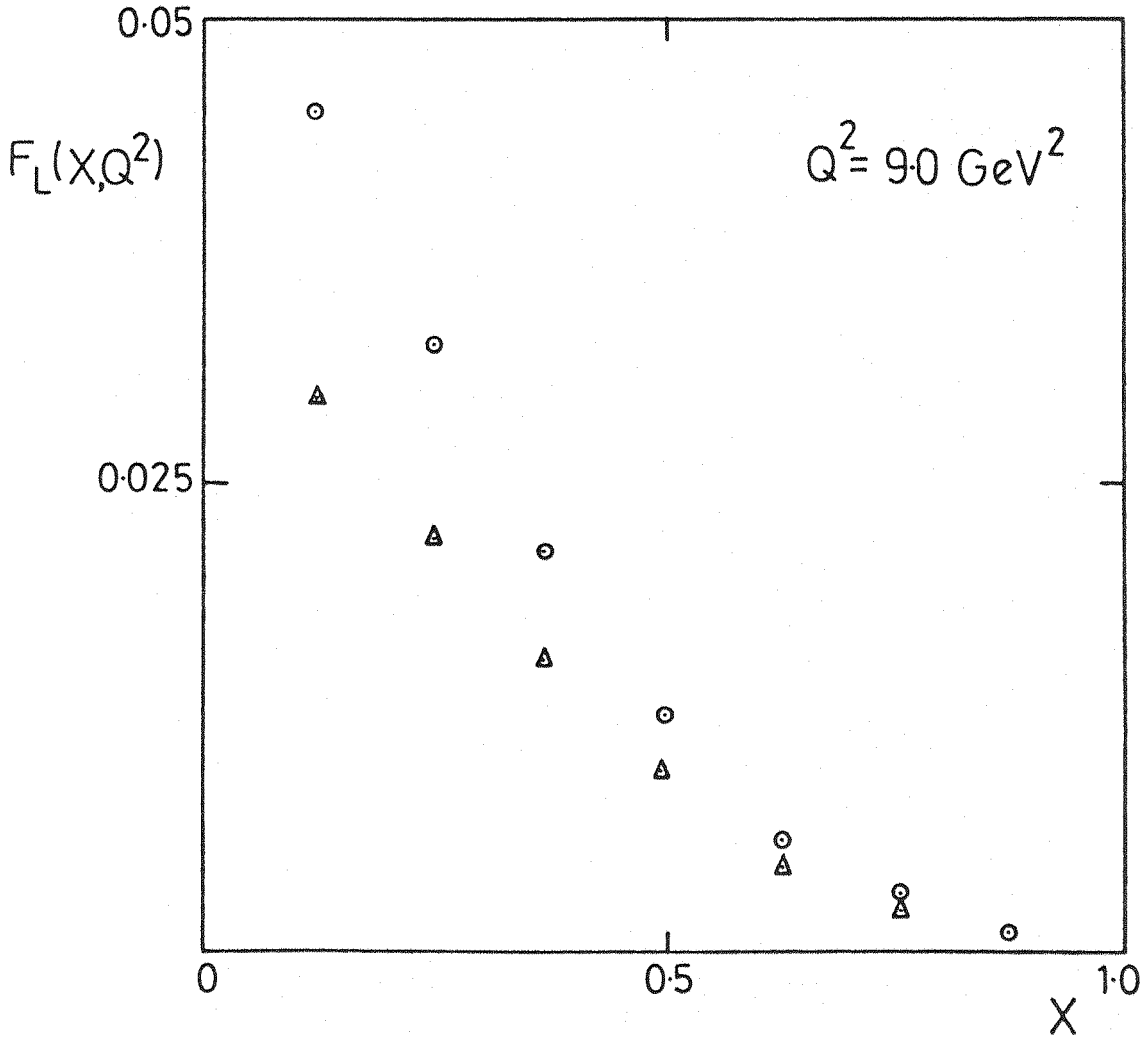

Fig 5.1(c)

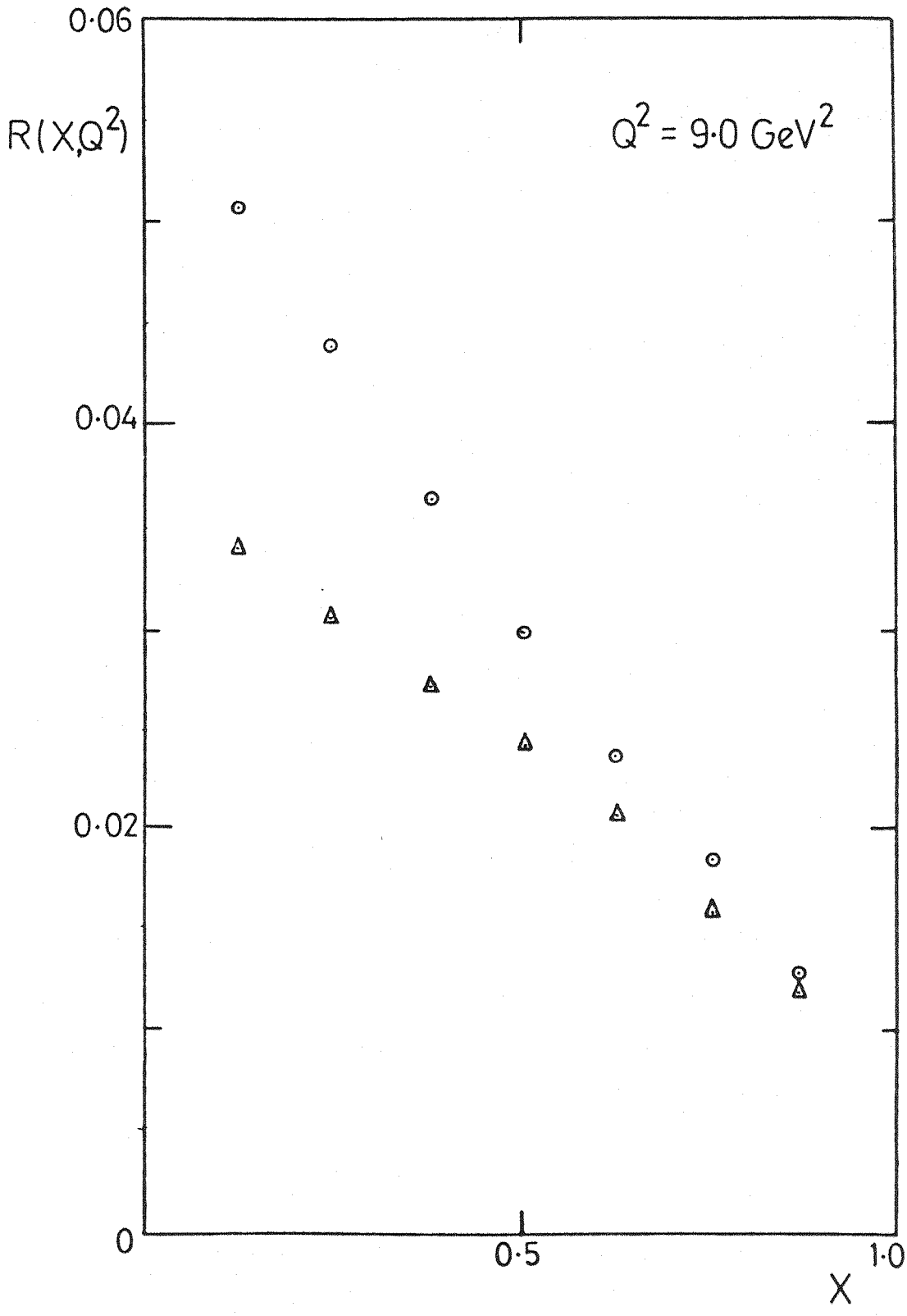

Fig 5.2(a)

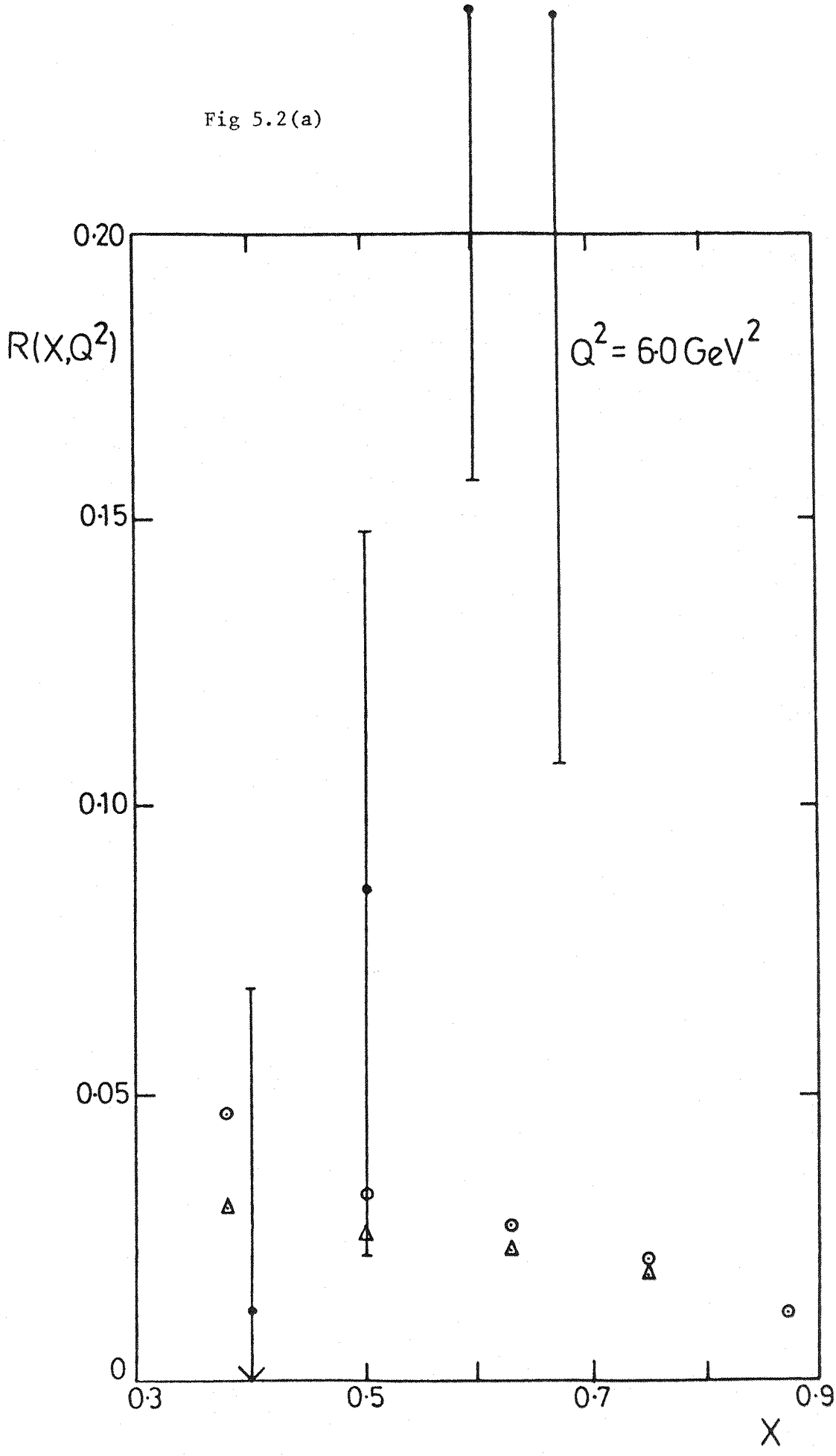

Fig 5.2(b)

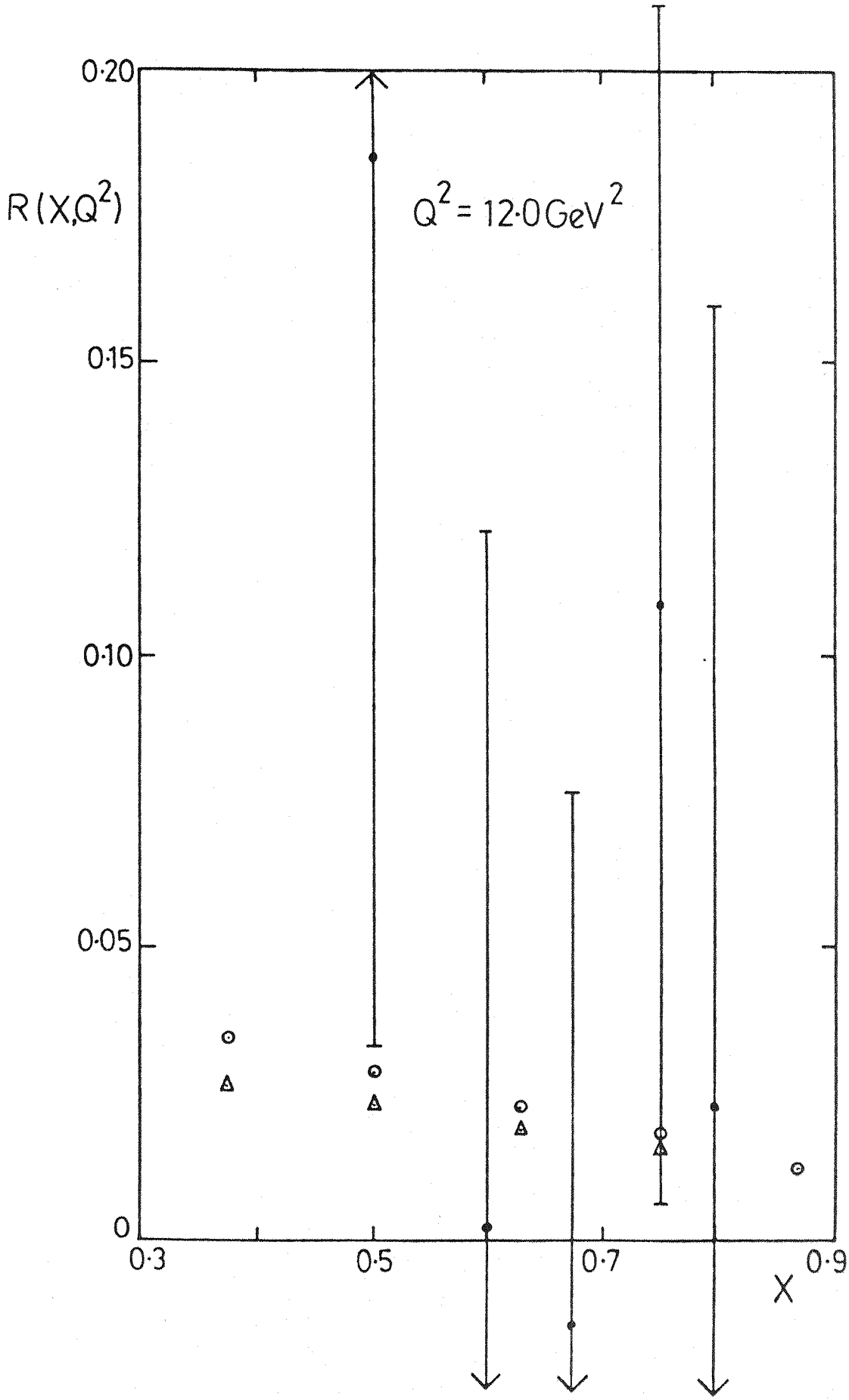

Fig 5.3(a)

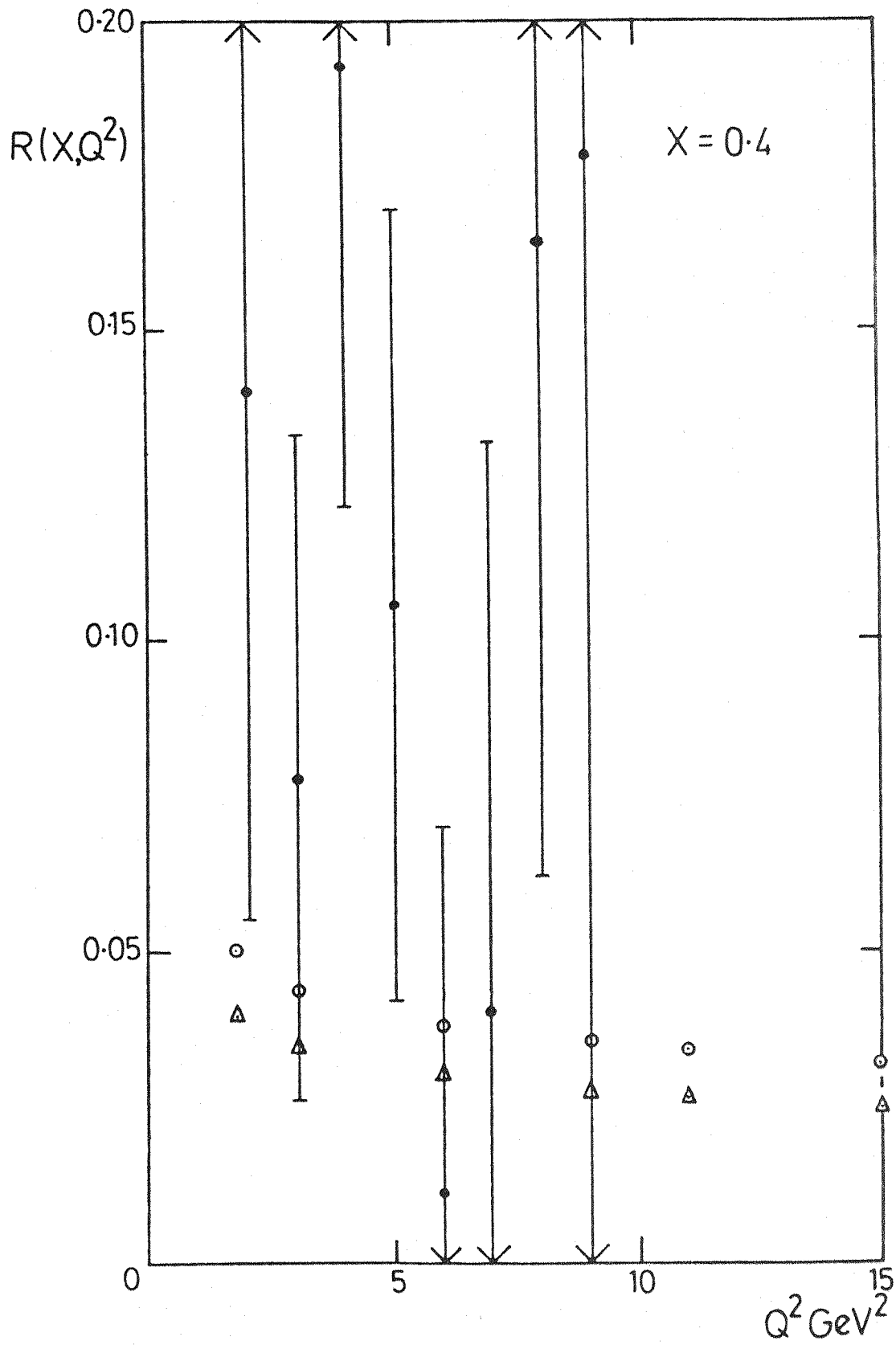

Fig 5.3(b)

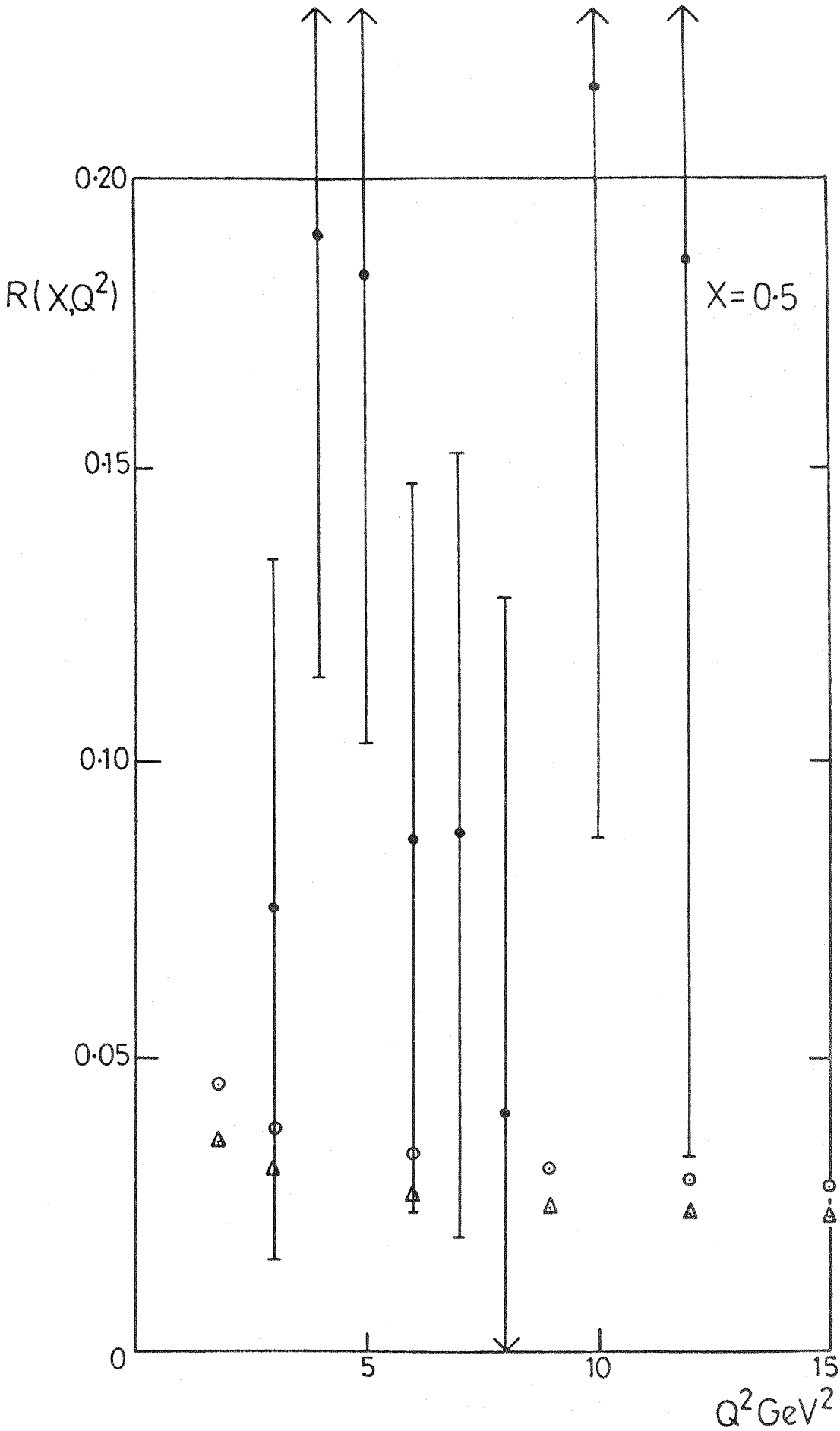

Fig 5.3(c)

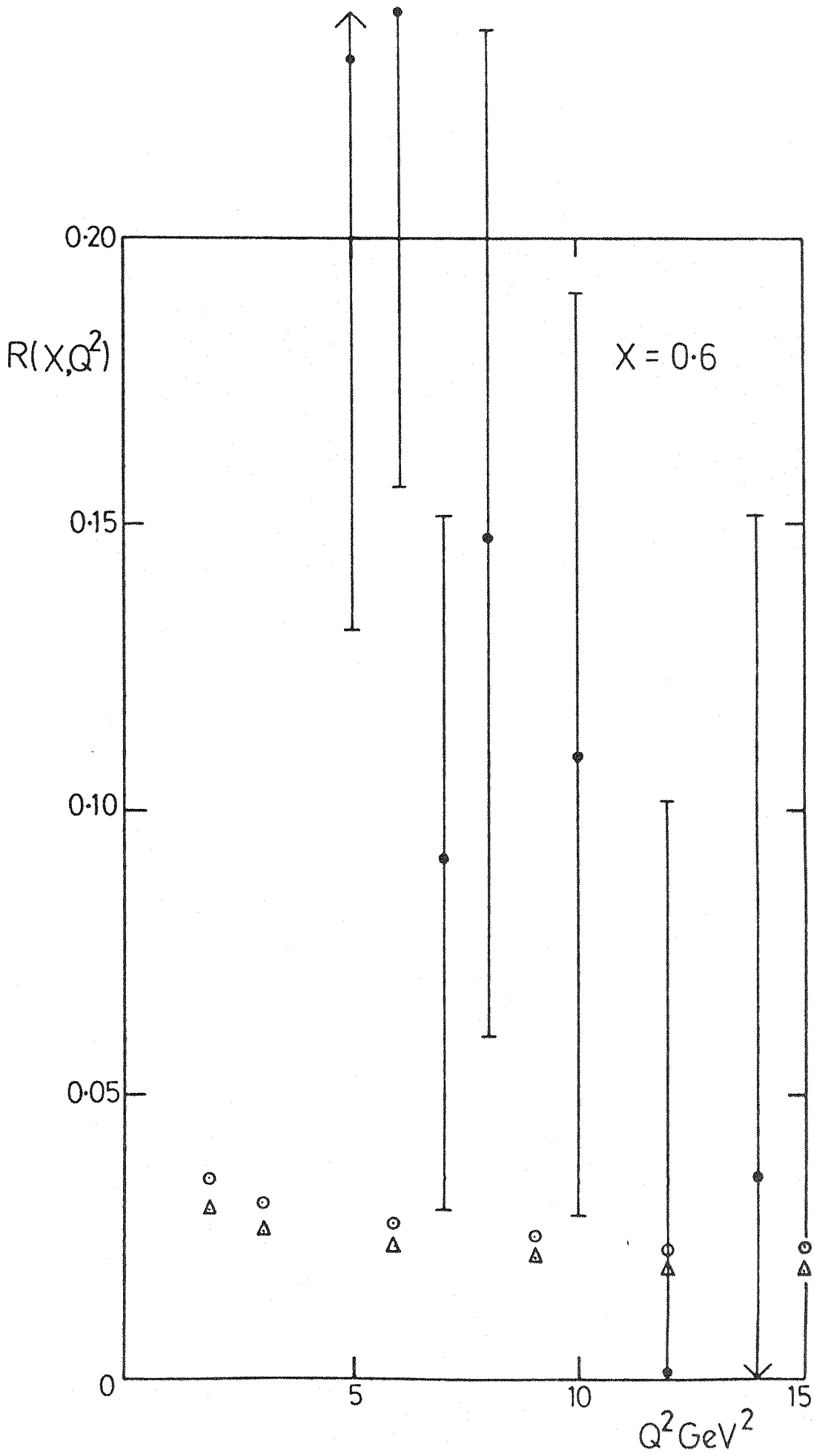

Fig 5.3(d)

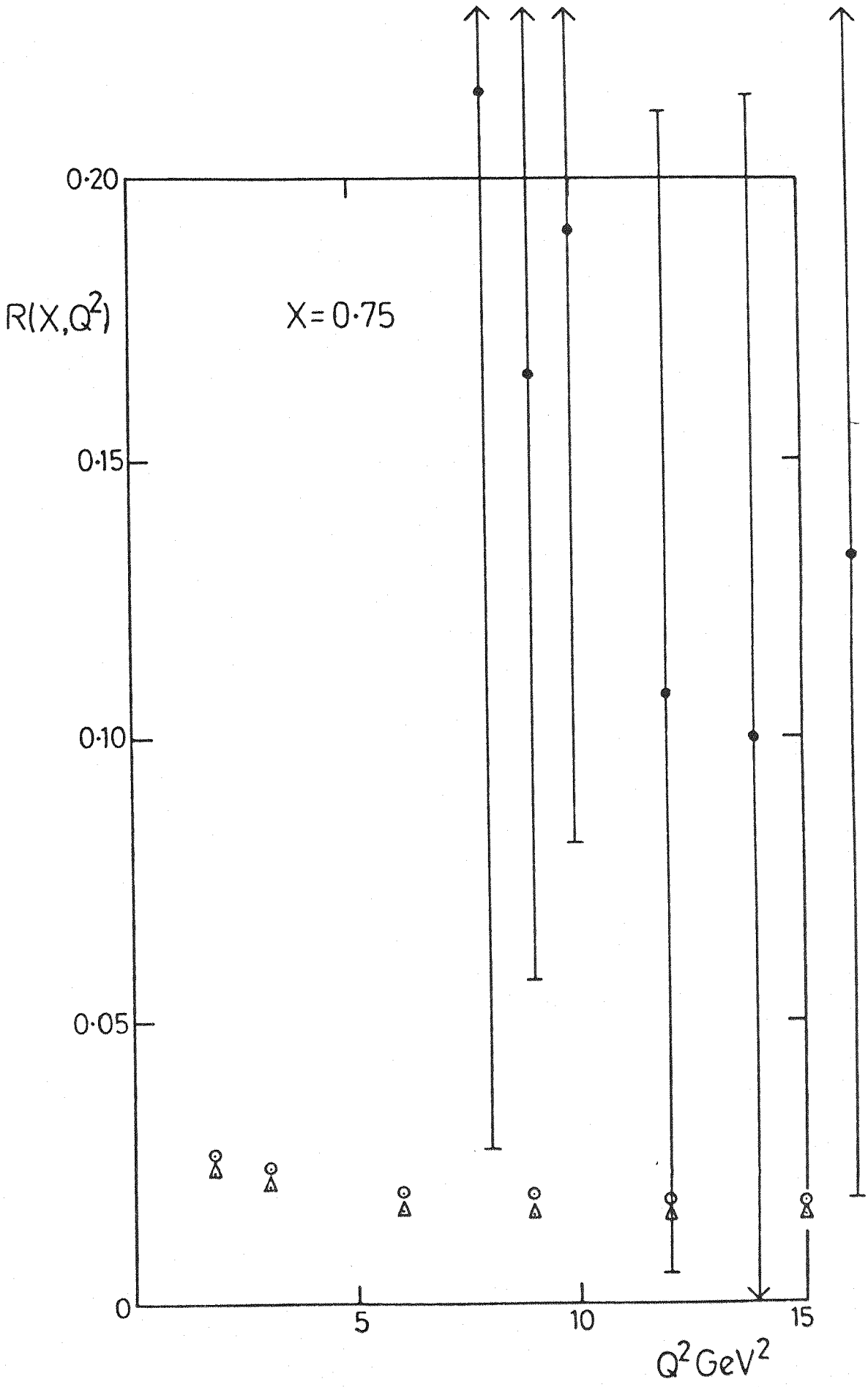

Fig 5.4

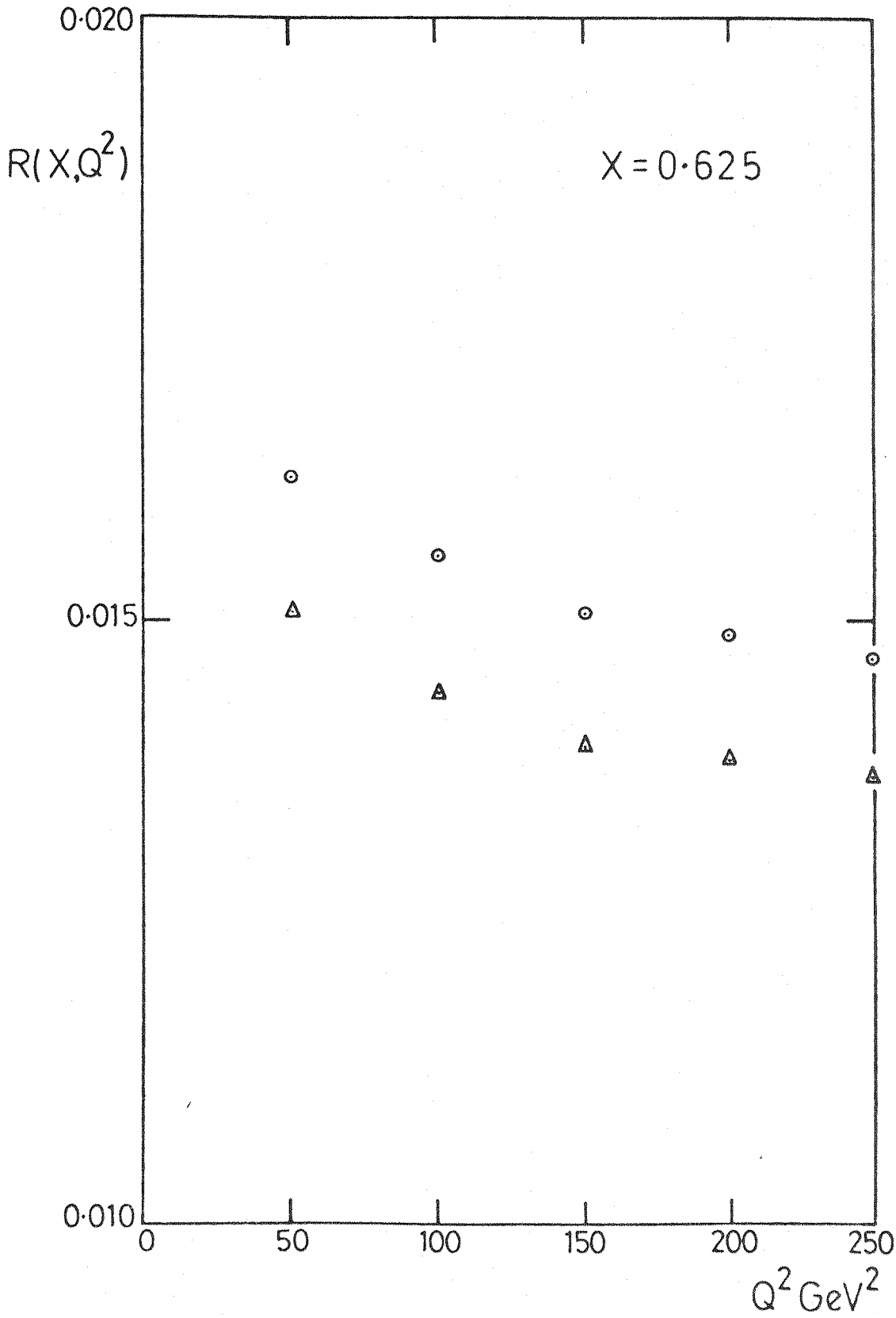

CHAPTER SIX

SUMMARY AND CONCLUSIONS

Nucleons exhibit a deviation from point-like behaviour. In contrast to electrons, they have large anomalous magnetic moments indicating considerable spatial structure. Inelastic lepton-nucleon scattering cross sections are parameterised by structure functions analagous to the electric and magnetic form factors introduced in the case of elastic scattering. These structure functions, nominally functions of the two independent kinematic invariants Q^2 and $\nu = p.q$ show a remarkable behaviour in the deep inelastic limit of both Q^2 and ν going to infinity, but their ratio $X = \frac{Q^2}{2\nu}$ remaining finite. In this limit, they are observed experimentally to approximate to functions of the scaling variable X only. This phenomenon, known as scaling, was predicted by Bjorken and served as the catalyst for the production of a simple model of nucleon structure.

In Feynman's naive parton model, the nucleon is seen as an assemblage of free, spin $\frac{1}{2}$, light on-shell partons. The consequences of such assumptions comprise exact Bjorken scaling and a value of the quantity $R = \frac{\sigma_L}{\sigma_T}$ equal to zero. Experimentally, a small but definite pattern of scaling violations is seen and the value of R is reported to be small but not equal to zero. Thus in order to satisfactorily explain the experimental data, it is necessary to go behond the simple parton model. Modifications can be introduced that fit the model to the data, but this seems to go against the spirit of simplicity in which the model was initially created. A far more interesting

approach is to take the view that the parton model is a first approximation to some underlying quantum field theory of the constituents of the nucleon.

The most promising choice for such a field theory is Quantum Chromodynamics (Q.C.D.); a non-abelian gauge theory describing the interactions of coloured spin $\frac{1}{2}$ quarks with the coloured massless vector gauge bosons called gluons. This leads to the natural identification of charged partons with the fundamental fields of Q.C.D., the quarks. An outstanding feature of this theory is the phenomenon known as Asymptotic Freedom. As in all renormalisable field theories, the quark-gluon coupling constant g , is not a constant at all but depends on some (arbitrary) momentum scale μ^2 at which the theory is renormalised. However, in Q.C.D. this momentum dependence can be approximately solved to reveal that as μ^2 approaches infinity, the effective coupling constant $\bar{g}(\mu^2)$ goes to zero as $\frac{1}{\ln \mu^2}$. It has been shown that this type of behaviour is admissible only to non-abelian gauge theories. Thus for processes that involve some large momentum transfer Q^2 , the quarks and gluons will interact as though effectively 'free' hence justifying the application of perturbation theory to the strong interaction; a task long thought to be impossible.

Deep inelastic lepton hadron scattering has since become a classic testing ground of pertubative Q.C.D. In the deep inelastic limit this process probes the light cone structure of products of hadronic electromagnetic currents. Thus one can reliably use the theoretical tools of the operator product expansion and renormalisation group to isolate and study those operators which dominate this process on the light cone. Q.C.D. predictions come most conveniently in the form

of moments of the inelastic structure functions. These moments are inverted usually using a parameterisation of the structure function motivated by parton model ideas, and compared directly to those experimentally measured. The leading order Q.C.D. contribution is found to be in agreement with the observed scaling violations; the only effect of the inclusion of the next to leading order correction being a change in Λ , the one free parameter of the theory that characterises the overall strength of these scaling violations. As a result of such agreement, approximate Bjorken scaling is thus interpreted as a consequence of asymptotic freedom.

The status for the current Q.C.D. prediction for the ratio of the cross sections $R = \frac{\sigma_L}{\sigma_T}$ observed in deep inelastic scattering is not as satisfactory though. Although the error bars on the data are large, several authors have already concluded that the leading order Q.C.D. contribution fails to give an adequate description of the data at large x . In this thesis we investigated the possibility that this discrepancy was due to the next term in the perturbation expansion. Knowledge of the magnitude of this term relative to that of the leading order contribution is desirable separately as a check on whether Q.C.D. is making any sense as a perturbative expansion. This is by no means clear in view of some of the recent perturbative calculations.

The novel quantity involved in the complete calculation the next to leading order correction to the moments of the flavour non-singlet longitudinal structure function, is the contribution coming from the corresponding two loop coefficient function appearing in the operator product expansion. This quantity we calculated directly by evaluating all possible s-channel cuts of the two loop forward elastic compton scattering amplitude. Following this procedure one is immediately

faced with the problem of spurious mass divergences encountered due to the production of collinear massless particles in the final state. A consistent regularisation scheme was introduced in chapter three and its use justified by exploiting the optical theorem. Many of the techniques involved in the general calculation including some aspects of renormalisation and three body phase space integration were discussed through the example calculation presented in chapter four. This chapter closed with a list of the diagrams by diagram results, together with the total contribution to the two loop flavour non-singlet longitudinal coefficient function. This total result is in disagreement with that of a recent calculation performed by Duke et al, who utilised different techniques to evaluate the imaginary parts of the same elastic amplitudes. After a very careful diagram by diagram comparison with this work, the disagreement lies in a small number of infra-red finite diagrams together with the set of five which are infra-red divergent. We have substantially checked the content of these diagrams and find that the discrepancy still remains. Clearly further work is needed in this direction.

In the final chapter, we employed a simple inversion technique to arrive at the next to leading order Q.C.D. corrections to the flavour non-singlet structure function, and thus the ratio $R = \frac{\sigma_L}{\sigma_T}$. A plot of the results show that this higher order Q.C.D. correction does not resolve the discrepancy between the theoretical prediction and the data at large X. At the moment, this is no disaster due to the large error bars on the data but, if the errors were to decrease and the data remain where it is, this may prove awkward for the theory of Q.C.D. We conclude then that the subsequent reduction of these errors should

be part of a main objective of experimentalists in the next few years. This is particularly so as from a theoretical standpoint the Q.C.D. perturbation expansion appears to be stable with the next to leading order correction being less than 12% for $X \geq 0.5$ and $Q^2 = 9.0\ \text{Gev}^2$, falling steadily with increasing Q^2.

APPENDIX

A.1 DIRAC ALGEBRA IN D DIMENSIONS
DIMENSIONAL REGULARISATION FORMULAE
SU(N) COLOUR FACTORS

$$g_{\mu\mu} = D \tag{A.1}$$

$$\{\gamma_\mu, \gamma_\nu\} = 2g_{\mu\nu}\hat{I} \tag{A.2}$$

$$\gamma^\mu\gamma^\mu = D\hat{I} \tag{A.3}$$

$$Tr(\gamma^\mu\gamma^\nu) = 4g^{\mu\nu} \tag{A.4}$$

$$Tr(\text{odd number of } \gamma\text{'s}) = 0 \tag{A.5}$$

$$Tr(\not{a}\not{b}\not{c}\not{d}) = 4[(a.b)(c.d) + (a.d)(c.b) - (a.c)(b.d)] \tag{A.6}$$

$$\gamma^\mu \not{a} \gamma^\mu = (2-D)\not{a} \tag{A.7}$$

$$\gamma^\mu \not{a}\not{b}\gamma^\mu = 4.a.b + (D-4)\not{a}\not{b} \tag{A.8}$$

$$\gamma^\mu \not{a}\not{b}\not{c}\gamma^\mu = -2\not{c}\not{b}\not{a} - (D-4)\not{a}\not{b}\not{c} \tag{A.9}$$

To combine propagators, use the Feynman parameter identity

$$\frac{1}{(a_1)^{\alpha_1}\cdots\cdots(a_n)^{\alpha_n}} = \frac{\Gamma(\Sigma\alpha_i)}{\prod_i \Gamma(\alpha_i)}\left\{\prod_{i=1}^{n}\int_0^1 dz_i\, z_i^{\alpha_i-1}\right\}\delta\left(1-\sum_{i=1}^{n} z_i\right)\left[\sum_i a_i z_i\right]^{-\sum_i \alpha_i} \tag{A.10}$$

which reduces for the case of two propagators to

$$\frac{1}{a_1^{\alpha_1}\, a_2^{\alpha_2}} = \frac{\Gamma(\alpha_1+\alpha_2)}{\Gamma(\alpha_1)\Gamma(\alpha_2)}\int_0^1 \frac{dz_1\, dz_2\, z_1^{\alpha_1-1} z_2^{\alpha_2-1}\,\delta(1-z_1-z_2)}{(a_1 z_1 + a_2 z_2)^{\alpha_1+\alpha_2}} \tag{A.11}$$

D dimensional loop integrals

$$\int d^D k \frac{1}{(k^2-M^2+i\varepsilon)^N} = \frac{i(-1)^N}{(4\pi)^{\frac{D}{2}}} \frac{\Gamma(N-\frac{D}{2})}{\Gamma(N)} \left[M^2-i\varepsilon\right]^{\frac{D}{2}-N} \tag{A.12}$$

$$\int d^D k \frac{k_\mu k_\nu}{(k^2-M^2+i\varepsilon)^N} = \frac{i(-1)^{N-1}}{(4\pi)^{\frac{D}{2}}} \frac{\Gamma(N-1-\frac{D}{2})}{\Gamma(N)} \frac{g_{\mu\nu}}{2} \left[M^2-i\varepsilon\right]^{\frac{D}{2}+1-N} \tag{A.13}$$

integrals containing an odd number of k_ρ in the numerator are zero by symmetry

$$\lim_{\varepsilon\to 0} \Gamma(\varepsilon) = \frac{1}{\varepsilon} - \gamma_E + O(\varepsilon) \tag{A.14}$$

Euler's constant

$$\gamma_E = 0.5772 \tag{A.15}$$

$$\Gamma(A+1) = A\Gamma(A) \tag{A.16}$$

Generators of $SU(n)$ symmetry are $\frac{\lambda^A}{2}$, where the Gell-Mann λ matrices satisfy

$$[\lambda^A, \lambda^B] = 2i f^{ABC} \lambda^C \tag{A.17}$$

$$\{\lambda^A, \lambda^B\} = \frac{4}{n}\delta^{AB}\hat{I} + 2 d^{ABC}\lambda^C \tag{A.18}$$

$$Tr(\lambda^A\lambda^B) = 2\delta^{AB} \tag{A.19}$$

with f^{ABC} the totally antisymmetric (real) group structure constants and d^{ABC} totally symmetric

$$(\lambda^A)_{il}(\lambda^B)_{lm} = \frac{2}{n}\delta^{AB}(\hat{I})_{im} + i f^{ABC}(\lambda^C)_{im} + d^{ABC}(\lambda^C)_{im} \tag{A.20}$$

$$\delta_{im} C_2(R) \equiv \left(\frac{\lambda^A}{2}\right)_{il}\left(\frac{\lambda^A}{2}\right)_{lm} \qquad C_2(R) = \frac{n^2-1}{2n} \tag{A.21}$$

$$\delta_{AB} C(G) \equiv f^{ACD} f^{BCD} \qquad C(G) = n \tag{A.22}$$

$$\delta_{AB} T(R) \equiv f\left(\frac{\lambda^A}{2}\right)_{ij}\left(\frac{\lambda^A}{2}\right)_{ji} \qquad T(R) = \frac{f}{2}, \quad f \text{ flavours} \tag{A.23}$$

A2 SAMPLE ANGULAR INTEGRALS OVER PROPAGATORS

All integrals are performed in the rest frame of K with

$$k_1^0 = |\underline{k}_1| = \frac{K^0}{2} \tag{A.24}$$

$$\int d\Omega = \int_0^{2\pi} d\phi \int_{-1}^{+1} d(\cos\theta) \tag{A.25}$$

$$\int d\Omega \frac{1}{(p+q-k_1)^2} = \frac{2\pi}{\sqrt{(K.(p+q))^2 - K^2(p+q)^2}} \ln\left(\frac{(p+q)^2 - K.(p+q) + \sqrt{(K.(p+q))^2 - K^2(p+q)^2}}{(p+q)^2 - K.(p+q) - \sqrt{(K.(p+q))^2 - K^2(p+q)^2}}\right) \tag{A.26}$$

$$\int d\Omega \frac{1}{(K-q-k_1)^2} = \frac{2\pi}{\sqrt{(K.q)^2 - K^2q^2}} \ln\left(\frac{q^2 - K.q + \sqrt{(K.q)^2 - K^2q^2}}{q^2 - K.q - \sqrt{(K.q)^2 - K^2q^2}}\right) \tag{A.27}$$

$$\int d\Omega \frac{1}{(p'+k_1)^2} = \frac{2\pi}{p'.K} \ln\left(\frac{2p'.K}{p'^2\left(1 + \frac{K^2}{2p'.K}\right)}\right) \tag{A.28}$$

$$\int d\Omega \frac{1}{(p-k_1)^2(p+q-k_1)^2} = \frac{-2\pi}{p.K(p+q)^2 - K^2 p.q}\left[\ln\left(\frac{-2p.K}{p^2\left(1-\frac{K^2}{2p.K}\right)} \right) + \ln\left(\frac{\left[(p+q)^2 - \frac{K^2}{p.K} p.q\right]^2}{(p+q)^2 p'^2} \right) \right] \tag{A.29}$$

$$\int d\Omega \frac{1}{(p-K+k_1)^2(p+q-k_1)^2} = \frac{-2\pi}{[(p+q)^2 - 2(p+q).K] + K^2 p.q}\left[\ln\left(\frac{-2p.K}{p^2\left(1-\frac{K^2}{2p.K}\right)} \right) + \ln\left(\frac{\left[(p+q)^2 - 2(p+q).K + \frac{K^2}{p.K} p.q\right]^2}{(p+q)^2 p'^2} \right) \right] \tag{A.30}$$

A3. SAMPLE FINAL INTEGRALS INVOLVED IN THREE BODY PHASE SPACE

The variable V is the ratio of the invariant mass squared of the gluon, quark or ghost pair produced, to the centre of mass energy $S=(p+q)^2$

$$a = \frac{2p.q}{S} \gg 1 \tag{A.31}$$

η is an infinitesimal regulator, $\eta = \frac{m^2}{S}$, where m^2 is a small mass given to the final state quark struck by the virtual photon of momentum q^μ.

$$\int_0^1 dv \frac{1}{(1-V)} \ln(1-V) \ln\left(\frac{V(a-1)}{a-V}\right) = \zeta(3) - \tfrac{1}{2}\ln^2(a-1)\ln\left(\frac{a}{a-1}\right) + \ln(a-1) f\left(\frac{a}{a-1}\right) + \tfrac{1}{2} g\left(\frac{1}{a-1}\right) \tag{A.32}$$

$$\equiv +\tfrac{1}{2}[\mathbb{O}]$$

$$\text{if } \ln_0 = \ln\left(\frac{u-\sqrt{u^2-4\eta}}{u+\sqrt{u^2-4\eta}}\right) \quad \text{with} \quad u = 1-v \tag{A.33}$$

$$\int_{2\sqrt{\eta}}^{1+\eta} du \, \frac{1}{\sqrt{u^2-4\eta}} \ln_0 = -\tfrac{1}{4}\ln^2\eta \tag{A.34}$$

$$\int_{2\sqrt{\eta}}^{1+\eta} du \, \frac{(1-u)}{\sqrt{u^2-4\eta}} \ln_0 = -\tfrac{1}{4}\ln^2\eta - \ln\eta - 2 \tag{A.35}$$

$$\int_{2\sqrt{\eta}}^{1+\eta} du \, \frac{(1-u)^2}{\sqrt{u^2-4\eta}} \ln_0 = -\tfrac{1}{4}\ln^2\eta - \tfrac{3}{2}\ln\eta - \tfrac{7}{2} \tag{A.36}$$

$$\int_{2\sqrt{\eta}}^{1+\eta} du \, \frac{1}{\sqrt{u^2-4\eta}} \ln_0 \ln\left(\frac{(1-u)(a-1)}{a-(1-u)}\right) = \left[f\left(\frac{a}{a-1}\right) - f(0)\right]\ln\eta - [0] \tag{A.37}$$

$$\int_{2\sqrt{\eta}}^{1+\eta} du \, \frac{(1-u)}{\sqrt{u^2-4\eta}} \ln_0 \ln\left(\frac{(1-u)(a-1)}{a-(1-u)}\right) = \left[f\left(\frac{a}{a-1}\right) - f(0) - a\ln\left(\frac{a-1}{a}\right)\right](\ln\eta + 2) \tag{A.38}$$
$$- 2a f\left(\frac{a}{a-1}\right) - [0]$$

$$\int_{2\sqrt{\eta}}^{1+\eta} du \, \frac{(1-u)^2}{\sqrt{u^2-4\eta}} \ln_0 \ln\left(\frac{(1-u)(a-1)}{a-(1-u)}\right) = \left[f\left(\frac{a}{a-1}\right) - f(0) - \frac{a}{2}(2+a)\ln\left(\frac{a-1}{a}\right) - \frac{a}{2}\right]\ln\eta \tag{A.39}$$
$$- (a+3)(a-1) f\left(\frac{a}{a-1}\right) - \frac{a}{2}(6+a)\ln\left(\frac{a-1}{a}\right) - \frac{3a}{2} - 3f(0) - [0]$$

where the dilogarithmn function $f(x)$ is defined by

$$f(x) = \int_1^x \frac{\ln t}{1-t}\, dt \quad , \quad f(0) = \frac{\pi^2}{6} \qquad f(1) = 0 \tag{A.40}$$

and the function $g(x)$ by

$$g(x) = \int_0^x \frac{\ln^2 t}{1+t}\, dt \quad , \quad g(0) = 0 \qquad g(1) = \tfrac{3}{2}\zeta(3) \tag{A.41}$$

Finally sample dilogarithmn integrals are

$$\int_0^1 dv\ f\left(\frac{a}{v}\right) = f(a) - f(0) + a f\left(\frac{1}{a}\right) \tag{A.42}$$

$$\int_0^1 dv\ f\left(\frac{a-v}{v(a-1)}\right) = f\left(\frac{a}{a-1}\right) - f(0) \tag{A.43}$$

$$\int_0^1 dv\ f\left(\frac{a(1-v)}{a-v}\right).(a-v) = -\tfrac{1}{2}(a-1)^2 f(0) - \tfrac{1}{2}a^2\left[f\left(\frac{a-1}{a}\right) - f(0)\right] + \tfrac{1}{2}a(a-1)\ln\left(\frac{a-1}{a}\right) \tag{A.44}$$

A4 RESULTS AND DEFINITIONS OF THE NUMERICAL INTEGRALS.

The integrals performed numerically in diagrams 11 and 12 are defined by

$$F_{11,12}(x) = \int d^4p'\, d^4k\ \delta^4(p+q-K-p')\,\delta(p'^2)\,\theta(p'^0)\left[F_{11,12}\right] \tag{A.46}$$

$$= \frac{4p.q}{8(2\pi)^2}(1-x)\int_0^1 dv(1-v)\int_0^1 dy\ \left[F_{11,12}\right] \tag{A.47}$$

where

$$(p+q)^2 = s \tag{A.48}$$

$$K^2 = sv \tag{A.49}$$

$$(p+q).K = \frac{s}{2}(1+v) \tag{A.50}$$

$$p'.K = \frac{s}{2}(1-v) \tag{A.51}$$

$$p.q = \frac{s}{2}\,\frac{1}{1-x} \tag{A.52}$$

$$p.K = \frac{s}{2}\,\frac{1}{1-x}\left(1-(1-v)y\right) \tag{A.53}$$

$$(p-K)^2 = s\left(v - \frac{1}{1-x}\left(1-(1-v)y\right)\right) \tag{A.54}$$

$$p.p' = \frac{s}{2}\,\frac{1}{(1-x)}\,(1-v)y \tag{A.55}$$

$$(p'-p).K = \frac{s}{2}\left(1-v-\frac{1}{1-x}+\frac{1}{1-x}(1-v)y\right) \tag{A.56}$$

$$C = K^2(p'-p).K + 2p.K(p'-p).K - 2K^2p.p' + 2K^2p.K \tag{A.57}$$

$$A = (p'-p).K\,p.K - K^2p.p' \tag{A.58}$$

$$R = \sqrt{\left((p'-p).K\right)^2 + 2p'.p\,K^2} \tag{A.59}$$

$$ln_6 = ln\left(\frac{2p.p' - (p'-p).K + R}{2p.p' - (p'-p).K - R}\right) \tag{A.60}$$

$$ln_7 = ln\left(\frac{\left[-2p.p'\,p.K + 2(p'-p).K\,p.K - K^2p.p'\right]^2}{(p.K)^2\,2p.p'\left(2p.p' - K^2 - 2(p'-p).K\right)}\right) \tag{A.61}$$

$$ln_8 = ln\left(\frac{4(p'.K)^2\,p.q\,x}{p.p'\left(2p'.K + K^2\right)}\right) \tag{A.62}$$

$$
\begin{aligned}
F_{12} = & -\frac{1}{2\pi}\frac{1}{(p-K)^2}\frac{\ell n_6}{R}\Big[-2p.K(p'-p).K + (p.K-p.p')(2p.K+K^2)\Big] \\
& + \frac{1}{2\pi}\frac{1}{(p-K)^2}\frac{1}{R^2}\Big[2A\Big(2p.K+\tfrac{1}{2}K^2-p'.K\Big) - 2K^2(p.K)^2 - p.K(p'-p).K\Big(\tfrac{3}{2}K^2-p.K\Big) \\
& \quad - \frac{\ell n_6}{R}\Big\{ G\Big(p.K(p'-p).K + p.p'\Big(2p.K+\tfrac{1}{2}K^2-p'.K\Big)\Big) \\
& \qquad + \tfrac{1}{4}(p'-p).K\, p.p'(p-K)^4\Big\} \\
& \quad + \frac{1}{R^2}\Big\{ -\tfrac{3}{2}(p'-p).K\, A G \\
& \qquad + \tfrac{3}{4}\frac{\ell n_6}{R}(p'-p).K\, p.p' G^2\Big\}\Big]
\end{aligned}
\tag{A.63}
$$

$$
\begin{aligned}
F_{11}^{(a)} = & \frac{1}{2\pi}\frac{1}{(p-K)^2}\frac{\ell n_6}{R}\Big(-2p.K\big(p.K+\tfrac{1}{2}K^2\big)\Big) \\
& + \frac{1}{2\pi}\frac{1}{(p-K)^2}\frac{1}{R^2}\Big[6K^2(p.K)^2 + \tfrac{5}{2}p.K\,K^2(p'-p).K + (p.K)^2(p'-p).K \\
& \quad + A(2p.K+K^2) - \tfrac{3}{2}p.K\,G \\
& \quad + \frac{\ell n_6}{R}\Big\{ -\tfrac{1}{4}p.p'(p'-p).K(p-K)^4 \\
& \qquad + \tfrac{1}{4}G\Big(4p.K(p'-p).K - 4p.p'p.K - 2K^2p.p'\Big)\Big\} \\
& \quad + \frac{1}{R^2}\Big\{ \tfrac{3}{2}p.p'G\Big(2K^2p.K + K^2(p'-p).K\Big) \\
& \qquad + \frac{\ell n_6}{R}\Big(\tfrac{3}{4}p.p'(p'-p).K G^2\Big)\Big\}\Big] \\
& + \frac{1}{2\pi}\frac{1}{(p-K)^2}\frac{2(p.K)^2}{p.p'}\Big(\ell n_7 + (p'-p).K\,\frac{\ell n_6}{R}\Big)
\end{aligned}
\tag{A.64}
$$

$$F_{11}^{(b)} = -\frac{1}{2\pi}\frac{1}{(p-K)^2}\frac{1}{R^2}\Bigg[\; p.p'(p'-p).K\big((p+q_1)^2-4p.K\big) + p.p'\Big(-2p.p'(p+q_1)^2+6p.p'p.K \\ -2(p.K)^2\Big)$$

$$+(p.p')^2\frac{\ln_6}{R}\Big\{\;(p'-p).K\Big(7p.K-\tfrac{1}{2}K^2-2(p+q_1)^2\Big) + \tfrac{3}{2}\hat{G} \\ +6(p.K)^2-6p.Kp.p'-2p.K(p+q_1)^2+2p.p'(p+q_1)^2\Big\}$$

$$+\frac{1}{R^2}\Big\{\;3(p.p')^2\hat{G}(p'-p).K + 6(p.p')^2\hat{G}p.K$$

$$+\frac{\ln_6}{R}(p.p')^2\Big(\tfrac{3}{2}\hat{G}(p'-p).K(-2p.p'+2p.K) - 2p.p'K^2 \\ -6\hat{G}p.p'p.K\Big)\Big\}\;\Bigg]$$

$$-\frac{1}{2\pi}\frac{p.p'}{K^2}\Big(2+\frac{(p'-p).K}{R^2}\big[2p.K-(p+q_1)^2\big]\Big)$$

$$-\frac{(p.p')^2}{2\pi}\frac{1}{K^2(p-K)^2}\Big[4\ln_8+\frac{\ln_6}{R}\Big\{2(p+q_1)^2-\frac{(p'-p).K(p-K)^2(2p.K-(p+q_1)^2)}{R^2}\Big\}\Big] \qquad \text{(A.65)}$$

$$F_{11} = F_{11}^{(a)} + F_{11}^{(b)} \qquad \text{(A.66)}$$

These three contributions correspond to the following S-channel cuts

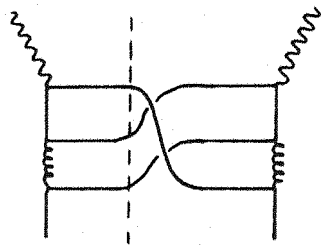

$= F_{12}$

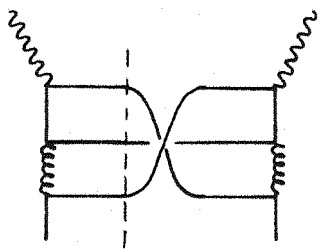

$= F_{11}^{(a)}$

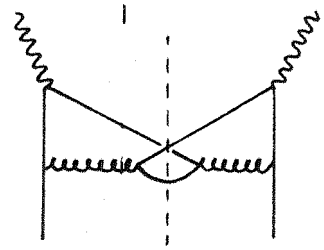

$= F_{11}^{(b)}$

It should be said that it is possible for R to vanish in the phase space integral, but one can show that in this region the numerator also vanishes to cancel this fake 'pole'.

The values of the first ten moments of the functions $F_{11,12}(x)$ are tabulated below. They are accurate to three significant figures

$$M^n_{11,12} = \int_0^1 dx\, x^n F_{11,12}(x) \tag{A.67}$$

Then

n	M^n_{12}	M^n_{11}
2	- 0.0390	- 0.248
3	- 0.0193	- 0.182
4	- 0.0113	- 0.143
5	- 0.00768	- 0.119
6	- 0.00530	- 0.102
7	- 0.00415	- 0.0893
8	- 0.00323	- 0.0792
9	- 0.00260	- 0.0703
10	- 0.00213	- 0.0648

These numbers represent a small contribution to $R^{2,NS}_{L,n}$ (the largest effect is $\sim$ 7% in the M5 scheme for n = 2)

LIST OF REFERENCES

INTRODUCTION

[0.1] T. Kinoshita and W.B. Linquist, CERN-TH 3093 (1981).

[0.2] R. Hofstadter, Ann.Rev. Nucleur Science 7 231 (1957)

[0.3] M.N. Rosenbluth, Phys. Rev. 79 615 (1950).

[0.4] W. Panofsky, Proceedings on Vienna Conference on High Energy Physics (1968).

[0.5] Bartel et. al, Phys. Lett 28B 148 (1968)

[0.6] S. Weinberg, Phys. Rev. Lett. 19 1264 (1967).

[0.7] A. Salam, Proceedings of the 8th Nobel Symposium (1968).

[0.8] S.L. Glashow, J. Iliopoulos and L. Maiani, Phys. Rev. D2 1285 (1970).

[0.9] J.D. Bjorken, Phys. Rev. 179 5 1547 (1969).

CHAPTER 1

[1.1] R.P. Feynman, in "Photon-Hadron Interactions", (pub. W.A. Benjamin 1972).

[1.2] J.D. Bjorken and E.A. Paschos, Phys. Rev. 185 1975 (1969).

[1.3] P. Roy, in "Theory of Lepton-Hadron Processes at High Energies", Clarendon Press, Oxford, (1975).

[1.4] C.G. Callan and D.J. Gross, Phys. Rev. Lett 22 156 (1969).

[1.5] O. Nachtmann, J. Phys. (Fr) 32 97 (1971).

[1.6] D.P. Majumdar, Phys. Rev. D3 2869 (1971).

[1.7] M.R. Sogard, in "Proceedings of XVI International Conference on High Energy Physics", (ed. Jackson and Roberts). Vol. 4, N.A.L. (1972).

[1.8] S.L. Adler and R.F. Dashen, in "Current Algebras". (pub. Benjamin, 1968).

[1.9] J.D. Bjorken, Phys. Rev. 163 1767 (1967).

[1.10] H. Kendall, in "Proceedings of 1971 International Symposium on Electron and Positron Interactions" (ed. Mistry). Lab. for Nucleur Studies, Cornell.

[1.11] D.H. Perkins, in Proceedings of XVI International Conference on High Energy Physics". (ed. Jackson and Roberts). Vol. 4, N.A.L. (1972).

[1.12] W.B. Atwood et al. Phys. Lett 64B 479 (1976).

[1.13] E.M. Riordan et al. SLAC-PUB 1634 (1975).

[1.14] A. Bodek et al. Phys. Rev. D20 1471 (1979).

[1.15] S.D. Drell and M. Chanowitz, Phys. Rev. Lett 30 807 (1973), and Phys. Rev. D9 2078 (1974).

[1.16] J.Ellis and C.T. Sachrajda, in "Quarks and Leptons", (ed. M. Lévy et al., pub. Plenum, 1979).

[1.17] W. Marciano and H. Pagels, Phys. Reports, 36C (1978).

[1.18] For a pedagogical review see: C. Itzykson and J.B. Zuber, "Quantum Field Theory" (pub. McGraw-Hill, 1980).

[1.19] G't Hooft and M. Veltman, Nucl. Phys. B44 189 (1972).

[1.20] W. Zimmerman, in "Lectures on Elementary Particles and Quantum Field Theory" 1970 Brandeis Summer Institute (MIT Press, Cambridge MASS. 1971).

[1.21] W. Clemester and D. Sivers, Argonne pre-print, ANL-HEP-PR-80-28.

[1.22] S. Weinberg, Phys. Rev. 118 838 (1960).

[1.23] D.J. Gross in 'Applications of the Renormalization Group to High Energy Physics' Les Houches Summer School, 1975. (North-Holland pub. 1976).

[1.24] D.J. Gross and F. Wilczek Phys. Rev. D8 (1973),3633
Phys. Rev. D9 986 (1974).

[1.25] H.D. Politzer, Phys. Reports 14 129, (1974).

[1.26] W. Caswell, D.R.T. Jones, Phys. Rev. Lett. 33 224 (1974). Nucl. Phys. B75 531 (1974).

[1.27] O.V. Tarasov, A.A. Vladimirov and A. Yu Zharkov, Phys. Lett. 93B 429 (1980).

[1.28] S. Coleman and D.J. Gross, Phys. Rev. Lett 33 244 (1974).

[1.29] For a complete review of Deep Inelastic Processes including discussions on higher order corrections and phenomenology see

A.J. Buras Rev. Mod. Phys. 52 199 (1980).

[1.30] For an heuristic account, see Ref. (2.1).

[1.31] K.G. Wilson, Phys. Rev. 178 1499 (1969).

[1.32] B.L. Ioffe, R.A. Brandt and G. Preparata, Y. Frishman, Phys. Lett. 30B 123 (1969). Nucl. Phys. B27, 541 (1971). Ann. of Phys. 66 237 (1973).

[1.33] O. Nachtman, Wandzura, Nucl. Phys. B63 237 (1973). Nucl. Phys. B122 412 (1977)

[1.34] H. Georgi and H.D. Politzer, R. Barbieri, M.K. Gaillard, J. Ellis and G.G. Ross Phys. Rev. D14 1829 (1976). Nucl. Phys. B117 50 (1976)

[1.35] A.J. Buras, E. Floratos, D.A. Ross and C.T. Sachrajda, Nucl. Phys. B131, 308 (1977).

[1.36] E. Floratos, D.A. Ross, and C.T. Sachrajda, and Erratum Nucl. Phys. B129 66 (1979). Nucl. Phys. B139 545 (1977).

[1.37] W.A. Bardeen, A.J. Buras, D.W. Duke and T. Muta, Phys. Rev. D18 3998 (1978).

[1.38] G. Altarelli, R.K. Ellis and G. Martinelli, and Erratum Nucl. Phys. B143 521 (1978). Nucl. Phys. B146 544 (1978).

[1.39] J.B. Kogut and L. Susskind, Phys. Rev. D9 697, 706, 3391 (1974).

[1.40] G. Altarelli and G. Parisi, Nucl. Phys. B126 298 (1977).

[1.41] Yu. L. Dokshitzer, D.I. Dyakonov and S.I. Troyan — Phys. Reports, 58, 269 (1980).

[1.42] Yu. L. Dokshitzer, — Sov. Phys. JETP 46 641 (1977).

CHAPTER 2

[2.1] J. Ellis — in 'Weak and Electromagnetic interactions at high energies' Les Houches Summer School, 1976. (North-Holland, Amsterdam 1977).

[2.2] J.E. Mandula, — Phys. Rev. D8, 328 (1973).

[2.3] P.V. Landshoff and J.C. Polkinghorne, — Phys. Reports 5C 1 (1972).

[2.4] R.E. Taylor — in - 'Proceedings of the 19th International Conference on High Energy Physics, Tokyo 1978'.

[2.5] R.P. Feynman — in 'Photon-Hadron Interactions' (pub. Benjamin 1972).

[2.6] A. Zee, F. Wilczek and S.B. Treiman, — Phys. Rev. D10 2881 (1974).

[2.7] A. De Rújula, H. Georgi and H.D. Politzer, — Annals of Phys. 103 3.5, (1977).

[2.8] A.J. Buras, E.G. Floratos, D.A. Ross and C.T. Sachrajda, — Nucl. Phys. B131 308 (1977)

[2.9] I.A. Schmidt and R. Blankenbecler, — Phys. Rev. D16 1318, 1977.

[2.10] For a review see C.H. Llewellyn Smith — in 'XX International Conference on Highe Energy Physics' Madison, 1980.

[2.11] M. Bacé — Phys. Lett 78B, 132 (1978).

CHAPTER 3

[3.1] J.M. Jauch and F. Rohrlich, — in "Theory of Photons and Electrons" (Addison-Wesley, Reading, Mass. 1955) Chapt. 17.

[3.2] W.J. Marciano — Phys. Rev. D15 3861 (1975).

[3.3] F. Bloch and A. Nordsieck, Phys. Rev. 52 54 (1937).

[3.4] D.R. Yennie, S.C. Frautschi and H. Suura, Ann. of Phys. 13 379 (1961).

[3.5] T. Kinoshita, J. Math. Phys. 3 650 (1962).

[3.6] T.D. Lee and M. Nauenberg, Phys. Rev. 133 1549 (196).

[3.7] B. Humpert and W.L. van Neervan, CERN preprint TH.2738 - CERN.

CHAPTER 4

[4.1] H. Abramowitz and I. Stegun, "Handbook of Mathematical Functions", (pub. Dover, New York 1970).

[4.2] D.W. Duke, J.D. Kimel, and G.A. Sowell, Tallahassee pre-print FSU-HEP-810812.

CHAPTER 5

[5.1] A.J. Buras and K. Gaemers, Phys. Lett. 71B, 186 (1977). and Nucl. Phys. B132 249 (1978).

[5.2] D.W. Duke and R.G. Roberts, Nucl. Phys. B166, 243 (1980).

[5.3] F.J. Ynduráin, Phys. Lett. 74B 68 (1978).

[5.4] R.G. Roberts, Private Communication.